

UNIVERSITY OF PRETORIA

DOCTORAL THESIS

**Fast temperature programmed gas
chromatography coupled to supercritical
fluid chromatography (SFCxGC)**

by

Daniel MALAN

Submitted in partial fulfilment of the requirements for the
degree

Doctor of Philosophy

In the Faculty of Natural & Agricultural Sciences
University of Pretoria
Pretoria

31 March 2020

Declaration of Authorship

I, Daniel MALAN, declare that the thesis, which I hereby submit for the degree Doctor of Philosophy at the University of Pretoria, is my own work and has not previously been submitted by me for a degree at this or any other tertiary institution.

SIGNATURE:

DATE:

Ethics statement

The author, whose name appears on the title page of this thesis, has obtained, for the research described in this work, the applicable research ethics approval.

The author declares that he/she has observed the ethical standards required in terms of the University of Pretoria's Code of ethics for researchers and the Policy guidelines for responsible research.

"Learning is a peculiar compound of memory, imagination, scientific habit, accurate observation, all concentrated, through a prolonged period, on the analysis of the remains of literature. The result of this sustained mental endeavour is not a book, but a man."

Mark Pattison

UNIVERSITY OF PRETORIA

Summary

Natural and Agricultural Sciences
Department of Chemistry

Doctor of Philosophy

Fast temperature programmed gas chromatography coupled to supercritical fluid chromatography (SFC \times GC)

by Daniel MALAN

The topic of this thesis is the development of comprehensively coupled (supercritical fluid \times gas) chromatography and its application to the chemical analysis of biodiesel and biodiesel blends. A future low-carbon economy might still have a need for large, high-efficiency diesel engines fuelled with a high-quality carbon-neutral fuel such as biodiesel. The quality of fuels are judged according to technical standards: documents that detail the requirements of compliance. Liquid fuels are complex mixtures that challenge the separation science used to ensure compliance. Chromatographic separations that use different separation mechanisms can be combined to meet those challenges, culminating in comprehensive coupling, where every fraction of a first separation is subjected to a second separation. The greater the difference between the separation mechanisms the more useful the comprehensive coupling. The difference between supercritical fluid chromatography (SFC) and gas chromatography (GC) separation mechanisms is great and their coupling is technically simple, but to make the coupling practical the GC separation must be fast and temperature-programmed. The construction of a coaxial resistive heater for short capillary columns with active cooling by liquid carbon dioxide allows for hundreds of consecutive fast temperature programmed GC separations which, if they are of fractions from an SFC separation, can be combined to construct a two-dimensional SFC \times GC chromatogram. When biodiesel and biodiesel blends are analysed by SFC \times GC, separation in the first dimension is by polarity and degree of unsaturation and in the second dimension by volatility. The resulting chromatograms contain powerful patterns of peaks, with the aromatic hydrocarbons separated from the alkanes, and the fatty acid methyl esters (FAMEs) of the biodiesel separated from the hydrocarbons of the petrodiesel. Because the flame ionization detector (FID) is used, quantification is straightforward and reliable. The FID remains compatible with SFC \times GC even when organic modifiers are added to the SFC mobile phase, because the modifiers elute on the GC as a solvent peak, separate from the analytes of interest. SFC \times GC can be used for research and quality control in the liquid fuels and vegetable oil industries.

Acknowledgements

I gratefully acknowledge my supervisor, Prof Egmont Rohwer, who had the faith in me to invite me to take on the project, and the patience to wait for me to respond and the patience to wait for me to finish.

Dok Fanie (Dr SJ van der Walt) my predecessor, showed me how to be bold in the lab. He was the giant on whose shoulders I stand.

I acknowledge my fellow students,

- Kobie Smit lent a kind ear to the laments, and helped me feel less alone.
- Marc Bouwer, whose youthful energy proved to be highly contagious. He spent hours in front of the whiteboard with me, helping to clarify thoughts and understand basic science.
- Elize Smit, who set me such a good example of academic performance. Thank goodness I didn't try to follow it.
- Linda Pretorius, whose PhD challenges made me grateful for the simplicity of my project.
- Nadine Broodryk, for all the conversations.
- My office mates, in no particular order: Sifiso Nsibande, Madelien Wooding, Kedibone Mashale, Portia Makhubela, Chiedza Munyeza, Amanda Mahlangu, Genna-Leigh Geldenhuys, Margaux Lim-a-Tock, Leandri van der Wat, Basil Mujanja, Olu Adegoke, Hanieh Montaseri. Arriving at work was always pleasant.

My father, Danie Malan, spent time and energy and time on instrument making. My mother, Retha Malan, ensured that I was fed and dressed.

Of course the project would not have been possible without the assistance from the technical team at the University of Pretoria:

- Our instrument maker, Nico van Vuuren, whose excellent work inspired me to create designs worthy of that quality of work.
- David Masemula, who maintained the supply of consumables.
- Yvette Naudé, a most kind and helpful lab manager.
- Naomi Steenkamp, the most quietly effective financial administrator known to man. Through her services purchasing supplies was a painless experience.
- Annetjie Kok and Ria Swart were the kindest administrators.
- Antoinette of the Centre for Microscopy and Microanalysis at the University of Pretoria, provided invaluable aid in collecting the SEM images.
- Dr Erna Gerryts, Faculty Academic Advisor, was my thesis writing manager. This is a unique role, and she was uniquely qualified to fill it. This thesis would not have been completed in time without her intervention.

I need to thank Dr Michael Denton and Therese Bron for reviewing and reading this thesis and offering invaluable advice.

Our commercial suppliers also need acknowledgement. Beyers at Chemetrix, who spent extra effort in keeping instrumentation running. Agilent supplied us with an excellent used instrument at nominal cost. Restek provided us with a set of HPLC columns at no cost. Reynard Heymans from FLIR recorded thermal videos of the coaxial heater in action without asking for money. Neil Frame of D.C. Wort supplied me with free samples and offered valuable advice.

Mathilda Mosterd of Precision Oils Laboratories Pty Ltd, provided me with prepared samples and their fatty acid profiles, which afforded valuable comparisons.

My mental health team kept me sane. Johan Erasmus, whose professional psychological help first guided me through clinical depression, and then was crucial in getting me unstuck. Maria Ramaahlo at the Disability Unit was the first person to offer concrete help with ADHD. Dr GP Grobler, my competent psychiatrist, always offered interesting conversations, despite his limited time. Dr Zuleikha Ahmed of Student Support treated me with the utmost kindness, even when I was extremely angry. And of course the innumerable staff members of Virgin Active Health Clubs always made visiting their gym a very pleasant experience.

Sasol Fuel and the NRF supported the laboratory through funding.

The financial assistance of the South African National Energy Research Institute towards this research is hereby acknowledged. Opinions expressed and conclusions arrived at, are those of the author and are not necessarily to be attributed to SANERI.

Sunil Patel, in true hacker spirit, made the L^AT_EXtemplate this document is based on freely available.

Preface

People learn from other people. In the academic environment, students formally learn from professors and from trusted authors of academic writing. Less formally, students also learn from other students and what other students wrote, including dissertations and theses.

In the South African academic environment, students often lack a wide base of knowledge: they survive a secondary education system that has the bare minimum of resources, and then enter a highly-focused tertiary degree programme. When they graduate, they are well-trained and knowledgeable in a narrow technical field. They rarely had the time to obtain knowledge extending beyond their formal academic programme.

This thesis was therefore written with the following audience in mind: A young South African who has successfully passed through the South African school system, has just obtained an Honours degree in chemistry at the University of Pretoria, and is now embarking on a postgraduate degree. The thesis starts by putting the scientific work strongly in context of history, society, and technology before elaborating on the theoretical and technical work and finally presenting the results obtained.

Contents

Title Page	i
Declaration of Authorship	iii
Ethics statement	v
Summary	ix
Acknowledgements	xi
Preface	xiii
Contents	xv
List of Figures	xxi
List of Tables	xxiii
List of Abbreviations	xxv
List of Symbols	xxvii
1 Introduction: Climate, fuel and biodiesel	1
1.1 Energy, fuel and the atmosphere	1
1.2 Carbon footprints and carbon neutrality	5
1.3 Internal combustion engines.	6
1.3.1 Scaling and efficiency	7
1.3.2 Engine design and thermodynamic cycles.	8
Otto engine and Otto cycle	9
Diesel cycle	10
Gas turbines and the Brayton cycle	11
1.3.3 Noxious pollution from internal combustion engines.	12
Unburnt fuel	12
Contaminants and additives.	13
Side-reactions	13
1.3.4 Mitigating pollution from internal-combustion engines.	13
Fuel formulation	14
Exhaust gas cleanup	14
Engine management	14
Efficiency implications	14
1.3.5 Avoiding pollution from internal-combustion engines	15
Electrification	15
Carbon-neutral fuels	16
1.4 Biofuels	16

1.4.1	Bio-gas	17
1.4.2	Bio-ethanol	17
	Brazilian ethanol	18
	US maize	18
1.4.3	Fischer-Tropsch fuel from biomass	18
1.4.4	Hydrotreated vegetable oil: "Green diesel"	19
1.4.5	Biodiesel	19
1.5	The significance of biodiesel	20
1.6	Conclusion: the role of chromatography	21
2	Introduction: Carbon dioxide and chromatography	23
2.1	The chemical industry	23
2.1.1	"Green chemistry"	25
2.1.2	Carbon dioxide as a green chemical	26
2.2	Extractions using carbon dioxide	27
2.2.1	Commercial extractions	27
	Plant oils	27
	Hops	27
	Coffee	27
2.2.2	Analytical extractions	28
2.2.3	Why carbon dioxide?	28
	Modifiers	30
	Practical extractions	30
2.3	Supercritical fluid chromatography	31
2.3.1	SFC and FID	33
2.3.2	SFC \times GC	35
3	Biodiesel standards	37
3.1	Introduction to standards	37
3.2	SANS 1935: An overview	39
3.3	SANS 1935: Properties, requirements and methods.	40
3.4	SANS 1935: Physical properties	40
3.4.1	Density	40
3.4.2	Kinematic viscosity	42
3.5	SANS 1935: Aggregate properties: Specialized instrumentation	42
3.5.1	Cetane number	42
3.5.2	Flash point	43
3.5.3	Oxidation stability	44
3.5.4	Cold filter plugging point	44
3.5.5	Copper strip corrosion	45
3.6	SANS 1935: Chemical properties: Classical determination	45
3.6.1	Sulfated ash	45
3.6.2	Carbon residue	46
3.6.3	Total contamination	46
3.6.4	Acid value	46
3.6.5	Iodine value	47
3.7	SANS 1935: Chemical properties: Electrochemical determination	47
3.7.1	Water content	47
3.8	SANS 1935: Chemical properties: Spectroscopic determination	48
3.8.1	Group I metals	48
3.8.2	Group II metals	48

3.8.3	Phosphorus	48
3.8.4	Sulfur	48
3.9	SANS 1935: Chemical properties: Chromatographic determination	49
3.9.1	Methanol content	49
3.9.2	Ester content	49
3.9.3	Glyceride content	49
3.9.4	Free glycerol	50
3.9.5	Polyunsaturated methyl esters	51
Linolenic acid methyl ester	51	
Highly unsaturated fatty acid methyl esters	51	
3.10	Comparison of SANS 1935 and SANS 342	51
3.10.1	Introduction	51
3.10.2	Comparison	51
PAHs	51	
FAMEs by IR	53	
Lubricity	53	
3.11	Conclusion: room for innovation.	53
4	Instrumentation: Supercritical Fluid Chromatography	55
4.1	SFC	55
4.2	Mobile phase	55
4.3	Pump	55
4.3.1	Pressure control system	57
4.3.2	Modifier Control	58
4.4	Sample injection	59
4.4.1	Column	59
4.4.2	Stopped-flow	61
4.5	Pressure Relief	61
4.6	Detector	64
5	Instrumentation: Fast GC	65
5.1	Speed of analysis	65
5.2	Fast gas chromatography theory	66
5.3	The General Elution Problem.	70
5.4	Temperature ramp rates	71
5.4.1	Resistive heating	73
5.5	Calibration	75
5.5.1	Temperature uniformity	76
Resistivity's dependence on temperature	76	
Thermal conduction	76	
Radiation	76	
Convection	76	
Examining thermal uniformity by imaging	77	
5.5.2	Temperature calibration	78
5.5.3	Thermocouple welding	80
5.5.4	Thermocouple probe construction	80
5.5.5	Thermocouple interfacing	82
5.5.6	Calibration procedure	82
5.5.7	Cold spots	84
5.5.8	Cold column	85
Cryogen supply	87	

5.5.9	Column mounting	87
5.5.10	Heating control	88
	Temperature monitoring	88
	PID tuning	88
	Heating rates	89
	Cooling rates	89
5.6	Detector	89
5.7	Data acquisition and control software	90
5.8	Data structure	90
5.9	Data visualization	91
6	Investigating biodiesel feedstock using SFC\timesGC	95
6.1	Introduction	95
6.2	SFC of FAMEs	95
6.3	Coaxial heater performance.	96
6.3.1	Column lifetime	96
	Mechanical degradation	96
	Stationary phase degradation	98
	Column bleed	98
6.3.2	Thermal shock	98
6.3.3	Thermal fatigue	99
6.3.4	Corrosion	99
6.3.5	GC retention time precision	99
6.3.6	Coolant consumption	100
6.4	Study of biodiesel feedstock by SFC \times GC	100
6.4.1	Samples	100
6.4.2	Sample preparation	100
	Method	101
6.4.3	SFC	101
6.4.4	Modulation	101
6.4.5	GC	101
6.4.6	Results and discussion	103
	Sunflower oil	104
	Coconut oil	104
	Flax seed oil	104
	Salmon oil	108
6.5	Conclusion	110
7	The determination of FAMEs and PAHs in diesel fuel by SFC\timesGC.	113
7.1	Introduction	113
7.1.1	FAMEs in diesel	113
7.1.2	PAHs in diesel	114
7.1.3	SFC \times GC of petrodiesel/biodiesel blends	115
7.2	Experimental	115
7.2.1	Samples	115
	Diesel/biodiesel blend	115
	Spiked diesel	115
7.2.2	SFC	115
7.2.3	Modulation	117
7.2.4	GC	117
7.3	Results and discussion	117

7.3.1	Aromatic hydrocarbons	117
7.3.2	FAMEs	124
7.3.3	Adjustable modulation	124
	SUSPENDING SFC fraction trapping	124
	Variable GC temperature programs	124
7.3.4	Application	125
7.4	Future work	125
7.5	Conclusion	126
8	Modified CO₂ as mobile phase for SFC×GC	127
8.1	Introduction	127
8.2	SFC×GC with modifier	128
8.2.1	Sample	128
8.2.2	SFC	129
8.2.3	Modulation	129
8.2.4	GC	129
8.2.5	Results and discussion	129
8.2.6	Conclusion	131
9	Conclusion	133
9.1	Synopsis	133
9.2	Contributions of this study	134
9.3	Special challenges	135
9.4	Design	135
9.4.1	Design weaknesses	136
	Energy efficiency	136
	Two-wire resistance measurement	136
	Cooling control	136
	Intertwined operation	136
	General-purpose computer operating system	137
9.4.2	Design strengths	137
	Metal protection for column	137
	Time decoupling	137
9.5	Aspects to be addressed	137
9.6	Future work	138
9.7	Concluding comments	138
A	Index	139
B	Published paper	143
C	Technical drawings	167
D	Fatty acid profiles	175
	Bibliography	179

List of Figures

1.1	The Otto cycle	9
1.2	The Diesel cycle	10
1.3	The Brayton cycle	12
1.4	Transesterification	19
2.1	Cyanocobalamin	24
2.2	The carbon dioxide phase diagram	29
2.3	SFE system diagram	31
2.4	SFC system diagram	32
2.5	Van Deemter	33
2.7	FID diagram	35
3.1	Discussion of SANS 1935	41
3.2	Cetane and isocetane	43
3.3	The peroxidation of lipids.	45
3.4	Derivitization	50
3.5	Overlap of requirements	52
4.1	Filling a CO ₂ pump.	56
4.2	A process control system	58
4.3	A cutaway diagram of the mixing chamber	59
4.4	Schematic diagram of the injection valve.	60
4.5	Schematic diagram of a continuous-flow valve.	61
4.6	A diagram of a integral restrictor.	62
4.7	A electron microscope photo of a restrictor orifice	63
4.8	A electron microscope photo of a blocked restrictor orifice	64
5.1	Schematic diagram of a the chromatographer's trilemma.	67
5.2	A plot of H vs. F	69
5.3	A temperature-rate table from the Agilent7890B data sheet	72
5.4	Suggested ramp rate	72
5.5	Coaxial heater resistance heater	74
5.6	A photograph of the setup used to record the thermal video	77
5.7	A thermograph of the coaxial heater at temperature	78
5.8	Welding process schematic	81
5.9	Fine-wire welder	81
5.10	A microphoto of a thermocouple twist ready to be welded.	82
5.11	A cartoon explaining how to construct a long, thin thermocouple probe.	83
5.12	Calibration curve of the coaxial heater	84
5.13	Measurement curve of the coaxial heater	85
5.14	Effect of controller tuning	89
5.15	Heating rate illustration	90
5.16	The main LabVIEW VI	91

5.17 A single fast GC chromatogram	92
5.18 A 2D SFC \times GC chromatogram	92
5.19 A 2D SFC \times GC chromatogram	93
6.1 Separation of FAMEs by GC	97
6.2 SFC \times GC of canola oil	102
6.3 SFC \times GC of sunflower oil	103
6.4 3D Bar chart of fatty acid profile	105
6.5 SFC \times GC of coconut oil	106
6.6 SFC \times GC of flax seed oil	107
6.7 SFC \times GC of salmon oil	108
6.8 3D Bar chart of salmon oil fatty acid profile	109
6.9 GC \times GC contour plot	110
7.1 The fidelity of a fast GC temperature program	118
7.2 Biodiesel separated from petrodiesel.	119
7.3 An example of a petrochemical fuel chromatogram.	120
7.4 Hydrocarbons in RME/diesel blend.	121
7.5 Comparing SFC-FID and virtual SFC.	122
7.6 Peak assignment in spiked diesel sample.	123
8.1 Modifiers in SFC	130
C.1 Manifold dimensions.	168
C.2 Manifold assembly.	169
C.3 Coolant reservoir	170
C.4 Technical drawing of coaxial heater mounting rails	171
C.5 Technical drawing of coaxial heater mounting.	172

List of Tables

3.1	A few well-known standards organizations	38
6.1	A summary of retention time repeatability of alkanes separated on the fast temperature programmed chromatograph.	99
6.2	Oils used for FAME analysis	100
7.1	Aromatic compounds added to a 1.2819 g low-sulfur diesel sample . .	116
D.1	The fatty acid profile of a sunflower oil sample as determined by a commercial oil analysis laboratory.	176
D.2	Fatty acid profile of coconut oil according to the Codex Alimentarius, a collection of internationally adopted food standards (Joint FAO/WHO Codex Alimentarius Commission 2019).	177
D.3	The fatty acid profile of salmon oil according to the Codex Alimentarius, a collection of internationally adopted food standards (Joint FAO/WHO Codex Alimentarius Commission 2017).	178

List of Abbreviations

ADC	Analog to Digital Converter
ATR	Attenuated Total Reflection
CCGT	Combined Cycle Gas Turbine
CFPP	Cold Filter Plugging Point
DIO	Digital Input/Output
ECD	Electron Capture Detector
EI	Electron Ionization
EOF	Efficiency-Optimized Flow
EOV	Efficiency-Optimized Velocity
EPC	Electronic Pneumatic Control
FAME	Fatty Acid Methyl Ester
FID	Flame Ionization Detector
GC	Gas Chromatography
GC\timesGC	Comprehensively coupled Gas Chromatography
GHG	Greenhouse Gases
HPLC	High-Performance Liquid Chromatography
IPCC	Intergovernmental Panel on Climate Change
IR	Infrared
IUPAC	International Union of Pure and Applied Chemistry
LCA	Life Cycle Analysis
LC\timesGC	Comprehensively coupled (Liquid Chromatography \times Gas Chromatography)
MS	Mass Spectrometry
MV	Manipulated Variable
NO_x	Nitrogen Oxides (NO, NO ₂ , NO ₃ and N ₂ O, and N ₂ O ₅)
PAH	Polycyclic Aromatic Hydrocarbons <i>or</i> Polynuclear Aromatic Hydrocarbons
PID	Proportional Integral Derivative
PLOT	Porous Layer Open Tubular
PUFA	Polyunsaturated fatty acid
PV	Photovoltaic
PV	Process Variable
PWM	Pulse-Width Modulation
RI	Refractive Index
RME	Rapeseed Metyl Ester
SEM	Scanning Electron Microscopy
SFC	Supercritical Fluid Chromatography
SFC\timesGC	Comprehensively coupled (Supercritical Fluid \times Gas Chromatography)
SFE	Supercritical Fluid Extraction
SIM	Single Ion Monitoring
SOF	Speed-Optimized Flow
SOV	Speed-Optimized Velocity
SPE	Solid Phase Extraction
SV	Set Value

TLC

Thin-Layer Chromatography

UHPLC

Ultra-high-performance Liquid Chromatography

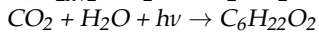
UNFCCC

United Nations Framework Convention on Climate Change

List of Symbols

Symbol	Name	Unit
α	selectivity	dimensionless
η	energy efficiency	dimensionless
η_C	Carnot energy efficiency	dimensionless
η_{CM}	Chambadal-Novikov energy efficiency	dimensionless
1D	first dimension	
2D	second dimension	
E	chromatographic efficiency	dimensionless
I	electrical current	A
k'	capacity factor	dimensionless
N	number of plates	dimensionless
P_M	modulation period	s
P	power	W
p_o	outlet pressure	Pa
Δp	pressure difference	Pa
T	temperature	K
t_r	retention time	s V
electrical potential difference	V	

Dedicated to the memory of Dr. Barbara Lotze



Hydrocarbons give heat and sunshine makes sugar

1

Introduction: Climate, fuel and biodiesel

1.1 Energy, fuel and the atmosphere

Industrialized societies depend on reliable sources of energy. For the purpose of this discussion, the main types of energy are considered to be electricity and fuels, although they are interconvertible. Fuels for industrialized societies are predominantly found as underground mineral deposits, from where they are extracted by mining or drilling. They are found as solids, liquids and gases, which the energy industry refers to as **coal**, **crude oil**, and **natural gas**. Because these fuels are of biological origin, deposited during previous geological eras, and then metamorphosed and preserved by geological processes, these fuels are commonly referred to as ‘fossil fuels’.

The large-scale exploitation of fossil fuels started in the middle of the 18th century, when the plentiful coal from the coalfields of Great Britain drove a development that is known to history as the Industrial Revolution. This development is closely associated with steam engines (Rosen 2012). The use of crude oil started in the middle of the 19th century, and is associated with the development of the automobile (Watts 2005, p. 42). The use of natural gas started in the middle of the 20th century and is associated with the introduction of gas-fired central heating for homes in cold climates (Hanmer and Abram 2017). Fossil fuels also serve as feedstock to the chemical industry, but that topic lies outside the scope of this discussion.

There is no doubt that the use of fossil fuels as an energy source greatly improved human circumstances. The mechanization of agriculture and the easy distribution of food by motorized transport have eliminated famine as a natural disaster (Angelis et al. 2007). The distribution of medical supplies by motorized transport and the rapid deployment of medical personnel have limited the impact and spread of epidemics (Ministere de la santé 2018). Heating and cooling of buildings have increased the habitable zone on earth. Artificial light has increased the hours available for mental activity, in particular extending the reach of entertainment, art and education.

However, in the context of chemistry, the uncontrolled use of fuels has at least two major problems: The first is that it is finite. There is only a finite amount of fossil fuel on earth. If all of it is extracted it will no longer be a reliable source of energy, and the existence of industrialized societies and the complex civilizations that depend on them will be in jeopardy. It is tempting to think that civilizations

would have the foresight to prepare for such an eventuality, but the historical record shows that societies can collapse when at the height of their powers (Diamond 2011).

The second problem with fuels is that they produce **pollution** wherever they are produced, processed, transported and used. Pollution is injurious to the health and well-being of individuals, societies and nature. When pollution becomes pervasive, it not only degrades society and the environment, but also negates the benefits brought by the application of energy: modern hospitals are possible through the intensive application of energy, but if they are filled with victims of pollution there is no nett benefit.

The first approach to pollution from fuels has been to ignore it. Pictures from the early industrial revolution shows English towns coated with soot and choked with smoke (Flick 1980), and rivers became toxic sewers (Halliday 2001).

The development of public health, social responsibility (Sreter 2003) and an embryonic environmental movement (Williams 1965) lead to political pressure for the implementation of pollution controls, which governments gradually introduced and increased in strictness. The first generation of pollution control offered essentially two options: concentrate or dilute.

These two options can be illustrated using the example of a typical South African coal-fired power station. In such a power station coal is burned to produce heat, which converts liquid water into high-pressure steam. The steam is allowed to expand through a turbine, which converts the energy in the steam into rotary motion that turns an alternator that produces an electric current by rotating a set of electrical conductors in a magnetic field. The furnaces of such a power station produce a flow of waste. This waste is an **aerosol**: finely divided solids suspended in a mixture of gases.

The solid part is typically separated from the gas-phase part by filter bags and electrostatic precipitators: the collected material is known as **fly ash**. The gas-phase part might be sent through scrubbers to remove some of the gas-phase pollutants, capturing it in a solid form. The solid part of the power station's furnace waste has now been concentrated. It is transported to a storage site, where it is stored indefinitely. It goes without saying that concentrated pollutants should be encapsulated during storage in some way, otherwise they just become additional sources of pollution.

The gas-phase part of the pollutant is handled by diluting it. The outlet for the gas-phase stream of waste is through a tall stack, which ends high above ground level¹. At this altitude the wind is strong and steady, which rapidly carries away and disperses the gases and remaining aerosols.

The dilution of pollutants might seem like an abdication of responsibility, but it is a reasonable response to pollution. Most pollutants that enter the biosphere at low enough concentration are broken down into harmless compounds by sunlight and microbes. This makes dilution a reasonable first attempt at controlling pollution.

The devil is, of course, in the detail. For example, mercury that finds its way into the environment is eventually converted by microbes to neurotoxic methyl mercury, which concentrates in aquatic animals. All rivers in the continental USA are now polluted by airborne mercury that originate from coal-fired power stations (Wentz et al. 2014). Some persistent organic pollutants, which also concentrate in the food chain, originate from fuel combustion. So while dilution was a reasonable first attempt at controlling pollution, it is certainly not the final solution.

¹The chimneys of those sooty Victorian towns were not there to disperse the smoke, but to create a 'draft', a flow of air created by the buoyancy of hot air. The better the draft, the more efficient the fire.

The majority of fuels provide their energy as heat, which can be converted into useful work. This heat is obtained by combining the chemical compounds found in the fuel with atmospheric oxygen to form compounds with lower internal energy. The maximum amount of work that can be extracted from a given fuel can be estimated by examining the Gibbs free energy equation:

$$\Delta G = \Delta H - T\Delta S$$

For a given fuel compound, ΔH is determined by the difference in enthalpy of formation of the product waste compounds and the enthalpy of formation of the reactant fuel compounds. Since the reactant fuel compounds are given, ΔH is maximized by having product compounds with very low enthalpies of formations.

To maximize ΔS , the products should be as disordered as possible. This implies that *gas-phase* products composed of *small molecules* will yield more work.

The temperature T should also be as high as possible.

Because the industrial machinery in economically competitive, capital-intensive industries is highly efficient, the maximum amount of energy is extracted from their fuels at the lowest cost. Following Gibbs, the major compounds left over after extracting the energy from a fuel should have very low enthalpies of formation and be in the gas phase at the temperature of the process.

Because all fuels contain carbon as a major component, the extraction of energy yields compounds containing carbon. Most fuels also contain hydrogen. Reacting these fuels with the oxygen in air to extract maximal work will therefore yield water (H_2O) and carbon dioxide (CO_2).

(Of course the argument is not that Victorian engineers designed steam engines using the Gibbs energy equation, but the variation-selection process (Vincenti 1990, Chapter 8) by which engineering improvements accrue would inevitably drive the development of heat engines fuelled by fossil fuels to emit large quantities of carbon dioxide gas.)

Water is of course not a pollutant at all, and carbon dioxide is only toxic at very high concentrations, and therefore, for most of the industrial era, carbon dioxide was easily dealt with by diluting it in the atmosphere, where it is also naturally present at low levels. To the extent that carbon dioxide was considered a pollutant it was assumed that it would be absorbed by the biosphere.

Photosynthesis, the process by which green plants capture the energy from sunlight to live and grow, does indeed remove carbon dioxide from the atmosphere, and an elementary model of the carbon cycle that assumes stability would seem to indicate that excess carbon dioxide in the atmosphere would be captured by photosynthesis and sequestered, leaving the carbon dioxide concentration in the atmosphere stable. Of course this model contains testable assumptions, which scientists could, and did, test.

The most famous of these tests is probably the “Keeling Curve” (Harris 2010). This is a continuous record of measurements of concentration of atmospheric carbon dioxide in the pristine air of the Pacific Ocean. This record starts in 1958 and shows that the carbon dioxide concentration of the atmosphere is increasing.

Paleoclimatologists have studied the hypothesis that the carbon dioxide concentration is stable over time. Not only have they found that the carbon dioxide concentration is *not* stable, they have also determined that the pre-industrial concentration of atmospheric carbon dioxide was lower than it was in 1958 (Petit et al. 1999).

So it is clear that the carbon dioxide concentration in the atmosphere is rising because the biosphere is not absorbing all the carbon dioxide produced by the combustion of fossil fuels. The projected concentration of carbon dioxide in the atmosphere is, however, still not at or even near toxic levels, which might make the continued dilution of carbon dioxide in the atmosphere seem a viable disposal method.

Emitted gases, however, do not only have chemical properties and biological impacts, they also have physical properties. Of concern for the current discussion is carbon dioxide's absorbance of electromagnetic radiation, in particular the radiation arriving from the sun, and the radiation from the earth's surface out to space, both of which must pass through the atmosphere. An atmospheric molecule can absorb parts of this radiation by having its electrons excited, or by changing its vibration state. Carbon dioxide is very stable, and therefore it is electronically excited only by extreme-ultraviolet radiation, just like the major gases in the atmosphere, molecular nitrogen and molecular oxygen. It poorly absorbs near-ultraviolet and visible light, which makes it also similar to the major gases. Because there are dipole moments between the carbon atom and the oxygen atoms of the carbon dioxide molecule, it is vibrationally excited by radiation in the infrared region of the electromagnetic spectrum. Oxygen and nitrogen molecules do not have dipole moments, and therefore these gases do not absorb infrared radiation strongly. This means that carbon dioxide will absorb infrared radiation in the atmosphere much more strongly than the major gases. The energy from the absorbed infrared radiation is of course turned into vibration, a form of kinetic energy, and this kinetic energy is randomly distributed among the gases of the atmosphere, appearing as an increase in temperature as the energy distribution moves towards equilibrium.

The most cursory understanding of the absorption of infrared radiation in the atmosphere by carbon dioxide therefore seems to say that an increase in the concentration of carbon dioxide in the atmosphere would lead to a higher average temperature in the atmosphere. This increase in temperature was first estimated by Svante Arrhenius in 1896 (Arrhenius 1897).

(The other major product of extracting energy from fuel is water. Its molecule also has a dipole moment, and it also absorbs infrared radiation strongly. However, its intermolecular properties set an upper limit to its concentration: at high enough concentrations it will either condense into water or crystallize into ice and precipitate from the atmosphere to end up as surface water.) Further research has only confirmed that the use of industrial processes that extract energy from fuel is increasing the amount of carbon dioxide in the atmosphere by gigatons every year (Xu et al. 2010), and that this increase is leading to higher temperatures in the atmosphere. It has also become increasingly certain that this increase in temperature is inevitable and significant: it will change the earth's climate². This projected increase in temperature and the accompanying change in global climate is bound to have impact on societies within the lifetime of people alive today, and a larger impact on future generations. Some of these projected changes are incompatible with the maintenance of the complex civilizations that are supported by industrialized societies (IPCC 2014).

Scientists do not inhabit ivory towers, and their research is funded by public money in the expectation that the resulting science will benefit their societies. As the understanding of carbon pollution grew, it became obvious to scientists that industrialized societies could not just continue diluting gigatons of carbon dioxide in the atmosphere, and they alerted policymakers. The iconic moment of this development

²The atmosphere is in contact with the hydrosphere, and the two exchange carbon dioxide. The carbon dioxide diluted in the atmosphere is therefore also diluted in the oceans. This leads to **ocean acidification**, a gigaton problem in its own right, but one that falls outside the scope of this discussion.

was the testimony of Dr James E. Hansen, at the time director of NASA's Goddard Institute of Space Studies, before the Senate of the US Congress in 1988 (Shabecoff 1988). In the same year the scientists of the world came together and established the Intergovernmental Panel on Climate Change (IPCC) to create a coherent body of knowledge to inform decision-making. The IPCC has so far produced a series of five Assessment Reports, which assess the science of climate change, its impacts, and ways to mitigate it (Allen et al. 2014).

(Carbon dioxide is not the only greenhouse gas and the IPCC reports consider each in detail, but because the other gases are not produced in significant quantities by fuels and the energy industry they fall outside the scope of this discussion.)

Industrialized societies require reliable supplies of energy to function. Currently that requirement is met through the use of fossil fuels. But the future health and well-being of humanity depends on ending the use of fossil fuels. Therefore, it is in the best interest of industrialized societies to create plans to reduce the dependence on energy from fossil fuels and exploit alternative energy sources. Industrialized societies, however, are also in economical competition with each other. This means that any society that spends resources on risky, expensive alternative sources of energy risks falling into a competitive disadvantage, and there is a surfeit of short-sighted politicians who will take advantage of this risk to create fear and so prevent planning for and investment in changes in energy production and use³.

Fortunately there are enough leaders who have vision, and based on the recommendations of the IPCC the governments of the world have come together to create the UNFCCC. The United Nations Framework Convention On Climate Change is an international agreement that structures the response of nations to limit their emissions of greenhouse gases. Two international treaties have been agreed to so far: the Kyoto Protocol in 1997 (*Kyoto Protocol to the United Nations Framework Convention on Climate Change*. 1997) and the Paris Agreement in 2015 (*Paris Agreement* 2015).

These agreements attempt to reduce the amount of carbon dioxide released into the atmosphere by dividing the cost of reducing emissions fairly. While the Kyoto Protocol invoked a complex carbon credit trading scheme, in the Paris Agreement nations pledge to reduce emissions of carbon dioxide into the atmosphere, and each is free to do so in a way that suits them best.

The Republic of South Africa is a signatory to the Paris Agreement, and therefore the country is legally bound to limit and reduce its emissions of carbon dioxide and other greenhouse gases. The country has so far promised to stop increasing emissions between 2020 and 2025 (*South Africa's Intended Nationally Determined Contribution (INDC)* 2016).

1.2 Carbon footprints and carbon neutrality

Ending the emission of carbon dioxide by industrialized societies is an exercise in balancing effort with consequences. Every reduction in carbon dioxide emissions must necessarily have an effect on the economy, and conversely, every change in economic activity will have an effect on carbon dioxide emissions.

A rational, discerning society in searching for ways to reduce carbon dioxide emissions will therefore attempt to change their economy in such a way that the emission of carbon dioxide is limited or reduced. But in most societies there are many ways to reduce carbon dioxide emissions, and decisions have to be made on which ones to implement. Such decisions must be based on sound information, and

³The impact of political corruption is not negligible but will not be discussed further.

one way to generate that information is a discipline called **life cycle analysis** (LCA). Life cycle analysis can yield rigorously-calculated data and comparisons, but it is a very general method. For analyses that are very similar and differ only in context, it is possible to develop simplified, standardized life-cycle analysis tools.

One such tool is the **carbon footprint**. Every economic activity in an industrialized society emits greenhouse gases. These emissions might be far removed from the activity in space and time. A familiar example of this is the use of electricity: At the moment I'm using an electronic computer to compose this paragraph and electric light illuminates the desk I'm working at here in my office in Pretoria. One can name the activity "academic writing." The electricity that powers the computer and the lamps are generated hundreds of kilometres from here, most of it on the Mpumalanga Highveld, in coal-fired power stations that emit carbon dioxide in the process. So my activity is far removed from the associated emissions **in space**. But even before the coal was burned, the machines that mined it and transported it to the power station emitted carbon dioxide, so my activity is also removed from the emissions **in time**. The sum of all these emissions connected with my activity constitutes the carbon footprint of my activity.

Although carbon footprinting is conceptually straightforward, it is analytically rigorous and computationally complex. But there are standard protocols (World Resource Institute 2004) that can be followed, so that carbon footprints from different activities and different organizations are transparent and comparable. Once an organization's activities have been footprinted, the organization can examine its operations and look at ways to change activities that will reduce that footprint. If my university, for example, decides to install solar panels on the roof of my building, and use the electricity to illuminate my office, the activity of academic writing will now most likely have a reduced carbon footprint, because solar electricity usually has a lower carbon footprint than coal-derived electricity.

To prevent a climate disaster, at some point industrialized societies will have to change all their activities until they no longer emit any greenhouse gases. Such activities will have carbon footprints of zero, and will be known as 'carbon neutral activities'. There are also activities that are nett removers of carbon from the atmosphere, which would be 'carbon negative'.

In reality, in industrialized societies there are very few carbon neutral activities. Even if I'm just sitting quietly in a pristine nature reserve, the food I am digesting and metabolizing has a positive carbon footprint: carbon was emitted to fix nitrogen from the air, which was used as fertilizer to help grow the food I ate, and is now in the proteins of my body. The very calcium and phosphorus in my bones were sourced from mines that were powered by fossil fuels.

1.3 Internal combustion engines.

An organization that calculates carbon footprints for its activities quickly learns that a major source of emissions is transport. Most transport in industrialized societies is powered by **internal-combustion engines**. (They are called 'internal-combustion' engines because the chemical transformation that extracts the energy from the fuel is internal to the engine. This is in contrast to the power station steam turbines mentioned earlier, where the extraction of the chemical energy from the fuel happens outside of the engine. The engine is the device that produces the mechanical energy.) These engines are usually powered by liquid fuels derived from crude oil, although

some designs run on gas, and of course in South Africa Sasol and PetroSA supply us with liquid fuels derived from coal and natural gas.

This discussion will use the term **noxious pollution** to describe pollution that is directly harmful to humans and **carbon pollution** to describe pollution that leads to climate disruption.

The simplest way to reduce an activity's carbon footprint is to use the fuel that drives that activity more efficiently. Fortunately market forces are aligned with this, because more efficient use of a fuel also reduces running costs. Discussing engine designs therefore almost always invokes **efficiency**. Efficiency of an engine is calculated by dividing the **output power** P_{out} by the **input power** P_{in} . The greek letter η is used as a symbol for efficiency:

$$\eta = \frac{P_{out}}{P_{in}}$$

Conservation of energy dictates that the output power cannot be more than the input power, and therefore $\eta \leq 1$. The power is 'lost' to two factors: firstly entropy, as dictated by the Second Law of Thermodynamics, and secondly losses, such as friction.

1.3.1 Scaling and efficiency

The larger an engine is, the more efficient it is, and the improvement is logarithmic. Three factors improve efficiency in larger engines (Brown, Menon, and Hagen 2015):

1. Longer residence time: In larger engines, the reacting fuel spends more time in the engine. This gives reactions more time to reach equilibrium, and hence more energy can be extracted.
2. Smaller surface area to volume ratio: The volume of an engine increases with the cube of its linear dimension, but the surface area increases with the square of its linear dimensions. This means that larger engines have a smaller surface-to-volume ratio than smaller engines. Since losses take place at the surface, the loss per unit volume is therefore larger for smaller engines than it would be for larger engines of the same type. If the losses in larger engines are comparatively smaller, we can expect larger engines to be more efficient than smaller ones.
3. Larger Reynolds number: The Reynolds number is a number that predicts the onset of turbulent flow, and is calculated from the viscosity, velocity and a characteristic linear dimension. The higher the Reynolds number, the higher the likelihood of turbulent flow. Turbulent flow promotes mixing, which leads to improved combustion and hence higher efficiency. The larger the engine, the larger the characteristic linear dimension, and therefore the higher the likelihood of turbulent flow.

From the viewpoint of reducing carbon pollution, one should therefore aim to use a few large engines rather than a multitude of small engines.

1.3.2 Engine design and thermodynamic cycles.

The final design of a successful internal combustion engine is determined by the variation-selection process described by Vincenti (Vincenti 1990). Such a design sufficiently satisfies a wide range of requirements. These requirements might be explicitly expressed in documentation or they may be implied or they may be practical. These requirements would include, but are not limited to, capital cost, running cost, maintenance cost, noise, sound⁴, ease of maintenance, power output, emissions, surface finish, weight, mounting method, size, supply chain capability, shape, colour, fuel availability, operating temperature, altitude tolerance and torque.

From designers' attempts to fulfil these requirements arise the myriad of different engine designs, delivering anything from milliwatts to megawatts of power to anything from model aircraft to oil tankers. Fortunately for researchers who study engine efficiency, there are only a few conceptual systems that explain how the internal combustion engines convert the chemical energy of the fuel into mechanical work.

The principles on which the different engines operate are named 'cycles', because the way they convert heat into work can be described in terms of a series of events that are repeated endlessly. The concept of a cycle is further entrenched because it is customary to explain the thermodynamic processes involved using a **PV diagram**, a research tool that shows the changes of state of the working fluid during engine operation.

Theoretical thermodynamic cycles are useful because they can predict the performance of heat engines, allowing for comparison. In particular, it allows for comparison with theoretical maxima. The maximum efficiency of a heat engine is delivered by an engine running on the Carnot cycle. This describes a hypothetical engine that uses only reversible processes to extract useful work from the temperature difference between two reservoirs of heat. It has been shown that the Carnot cycle offers the maximum possible heat extraction, and that the maximum efficiency (η_C) is determined solely by the temperature difference between the hot (T_h) and the cold (T_c) reservoirs.

$$\eta_C = 1 - \frac{T_c}{T_h}$$

The Carnot cycle, however, can only deliver an infinitesimal amount of work, because the heat transfer must be reversible, and therefore infinitesimal. A more realistic maximum efficiency is given by the Chambadal-Novikov efficiency (η_{CN}) (Hoffmann 2008):

$$\eta_{CN} = 1 - \sqrt{\frac{T_c}{T_h}}$$

This theoretical efficiency takes into account the irreversible processes that are inevitable in engines delivering finite amounts of power.

Barring revolutionary new discoveries and inventions, there will be only three thermodynamic cycles and their corresponding internal combustion engines on the market as we enter the low-carbon era.

⁴In 1994 the motorcycle manufacturer Harley-Davidson attempted to trademark the distinctive sound of the engines they install in their motorcycles (O'Dell 2000).



FIGURE 1.1: The pV diagram of the thermodynamic Otto cycle. The isochoric heat addition step (BC) corresponds to the burning of the homogeneous air-fuel mixture. Work is extracted from the engine during the adiabatic expansion CD (Wolfram | Alpha 2019a).

Otto engine and Otto cycle

The oldest of the internal combustion engines is the Otto engine. It is named after Nikolaus Otto, who developed the first working engine of this kind in 1876 (Cummins 1989, Chapter 9). In South Africa these engines are usually called ‘petrol engines’. In the Otto engine, a homogeneous mixture of atmospheric air and vaporized fuel is compressed. This mixture is then ignited by an electric spark. The energy released by the chemical reaction between the oxygen in the air and the fuel vapour causes the temperature of the compressed air to rise, and consequently also the pressure. If this — now hot — gas is allowed to expand in an expandable vessel, the motion of the vessel can be captured to perform useful work. Once the useful work is extracted, the vessel can be collapsed again to expel the exhausted air, and re-filled with a compressed air/fuel vapour mixture. This completes the cycle (See Figure 1.1). The expandable vessel is usually in the form of a cylinder and piston, with the piston connected to a crank that drives a shaft that transfers the work from the engine to the machine being powered.

(These legs of the cycle are only loosely related to the ‘strokes’ of a four-stroke engine, and should not be confused for them.)

The theoretical efficiency of the Otto cycle is given by

$$\eta = 1 - \left(\frac{1}{r^{\gamma-1}} \right) \quad (1.1)$$

where r is the **compression ratio**, $\frac{V_1}{V_2}$, and γ is the heat capacity ratio, which can be considered a constant for the purposes of this discussion (Wolfram | Alpha 2019a).



FIGURE 1.2: The pV diagram of the thermodynamic Diesel cycle. The isobaric process BC corresponds to the combustion of the finely divided fuel particles in air. Work is extracted from the engine both during this process and during the adiabatic process CD. (Wolfram | Alpha 2019b)

This means that the efficiency of an Otto engine can be improved by increasing the degree of compression of the intake air before combustion.

Diesel cycle

In the diesel engine, named after Rudolf Diesel who demonstrated the first engine of this type in 1897 (Cummins 1989, Chapter 14), air is compressed, and then a finely divided solid or liquid fuel is injected into the system. The fuel then reacts with the oxygen in the air. The energy released in the reaction appears as a higher temperature in the gas, and — following Gay-Lussac's Law — the pressure of the gas rises. If the gases expand in the confines of a collapsible vessel, useful work can be extracted from expansion of the vessel. Once the work has been extracted, the vessel can be collapsed again to remove the now inert ('exhausted') gas and prepare for receiving the next charge of air, completing the cycle. The theoretical cycle used to analyse the performance of the diesel engine is called the Diesel cycle. (See Figure 1.2)

The Diesel cycle differs from the Otto cycle in the heat addition step. In the Otto engine, the heat addition takes place when the homogeneous air/fuel mixture combusts. This combustion takes place in a short space of time during which the engine parts move only a negligible distance. Hence the pressure rises rapidly. In the diesel engine, the fuel is injected into a volume of compressed air, where it combusts. (There is no separate ignition source: the temperature of the adiabatically compressed air is higher than the fuel's **auto-ignition temperature**, so that the fuel ignites upon injection. While this is another difference between the two engines, it is of second-order importance when discussing thermodynamic cycles.) Because the

combustion takes place at the surface of fuel particles, the combustion rate is lower than the combustion rate of the homogeneous mixture in the Otto cycle. Hence the rising temperature is balanced by the motion of the engine, and the heat addition is essentially isobaric.

The theoretical efficiency of the Diesel cycle is given by Equation 1.2

$$\eta = 1 - \frac{1}{r(\gamma-1)} \left(\frac{\alpha^\gamma - 1}{\gamma(\alpha - 1)} \right) \quad (1.2)$$

where α is the **cut-off ratio** and γ is the compression ratio.

The term $\frac{\alpha^\gamma - 1}{\gamma(\alpha - 1)}$ is always larger than 1, and therefore, when we compare equation 1.2 with equation 1.1 it is clear that for a given compression ratio the Diesel cycle is always less thermally efficient than the Otto cycle.

However, at high compression ratios Otto engines start suffering from **knocking**. This is the phenomenon of the homogenous air/fuel mixture detonating instead of burning smoothly. The shock waves from this detonation will damage the engine and lead to faster wear. (The **octane number** of a fuel indicates the compression ratio it can accommodate.) Because Diesel engines do not suffer from this problem, they can, and usually are, designed to operate at higher compression ratios than Otto engines. Otto engines normally operate with a compression ration of up to 9:1, whereas diesel engines have compression ratios of up to 25:1. This makes Diesel engines significantly more efficient than Otto engines.

Gas turbines and the Brayton cycle

The third internal-combustion engine important to industrialized society is the **gas turbine**. Gas turbines are used rarely in road transport, more often in marine and stationary applications, but thousands take to the sky every day, propelling aircraft carrying billions of airline passengers every year (Morris 2017).

The first gas turbines were developed during wartime urgency to deliver pure jet thrust for military aircraft, but this proved to be an inefficient use of the available energy. Most modern turbine engines drive a shaft to extract rotational work. This shaft might drive a bypass fan (as used in airliner engines), a propeller (as used in smaller, low-speed aircraft), or a shaft which might drive a helicopter rotor or an electrical generator.

In operation, a gas turbine compresses air with one or more compressor stages. The compressed air passes through a combustion chamber, where fuel is added and combusted. As the now hot gases expand they pass through one or more turbine stages, which is connected to drive the compressor and the output shaft, which extracts work from the system. After the gas has passed through the turbine it returns to atmospheric pressure, optionally doing work on the engine in the form of thrust.

The theoretical thermodynamic cycle that is customarily used to analyse the gas turbine is called the **Brayton cycle**, named after George Brayton, who successfully manufactured a reciprocating engine based on this cycle. (See Figure 1.3) Such engines are no longer manufactured (Cummins 1989, Chapter 10).

The efficiency of the Brayton cycle is given by equation 1.3

$$\eta = 1 - \frac{T_1}{T_2} = 1 - \left(\frac{P_1}{P_2} \right)^{\frac{\gamma-1}{\gamma}} \quad (1.3)$$

where γ is the compression ratio (Wolfram | Alpha 2019c).

Because the fuel is continuously added to the compressed air and the combustion takes place in a heterogeneous mixture, gas turbines do not suffer from 'knocking'



FIGURE 1.3: The pV diagram of the thermodynamic Brayton cycle. In the gas turbine the continuous combustion of the injected fuel and free expansion of the air through a turbine means that the heat addition (BC) is isobaric. Work is extracted during the adiabatic expansion process CD (Wolfram | Alpha 2019c).

and therefore there is no upper limit to the compression ratio. The main figure determining the efficiency of the engine is the turbine inlet temperature, (*i.e.* the outlet temperature of the combustion chamber) which reaches 1600 °C in modern engines.

1.3.3 Noxious pollution from internal combustion engines.

Carbon pollution is not the only pollution emitted by internal combustion engines. There is also noxious pollution, which affects the societies in which they are used. There are ways to reduce or eliminate such pollution, but the implementation of such measures affect the efficiency of the engine. Noxious pollution from internal-combustion engines come from different sources and have different effects:

Unburnt fuel

The combustion reactions in internal-combustion engines are very fast, but they are never at equilibrium. This means that at the end of a cycle, the exhaust gases expelled from the engine contains, besides the carbon dioxide, also chemical intermediates and unreacted fuel molecules. Unreacted fuel is a noxious pollutant in its own right, but when it is released into the environment chemical reactions induced by sunlight produce **ozone**, a reactive oxygen species that cause respiratory problems in victims of pollution (Davidson 1998).

Some of the fuel-like pollutants from internal-combustion engines are not present in the fuel. These compounds are formed in a process that might be called **pyro-synthesis**. They are themselves more stable than the compounds from which they originate, but not as stable as the combustion end products, carbon dioxide and

water. Because they are themselves quite stable, they require high temperatures to combust, which might not be achieved before they leave the engine as waste. Notable pollutants from this source are the polycyclic aromatic hydrocarbons (PAH) and, if trace amounts of chlorinated substances are present in the fuel, dioxins.

One of the products of pyro-synthesis is particles of soot. These particles are agglomerations of nano-sized particles of pure, amorphous carbon. The agglomerations might include adsorbed PAHs and acids. Soot particles are very stable and only react at very high temperatures. Diesel engines in particular have a reputation for producing soot (Mohankumar and Senthilkumar 2017).

The final pollutant that can be classed as originating from partially combusted fuel is carbon monoxide. It forms readily when fuels are burned in oxygen-poor environments. Modern, well-maintained engines rarely cause acute carbon monoxide poisoning (Reumuth et al. 2018), but chronic exposure to low levels of environmental carbon monoxide has harmful effects (Wright 2002).

Contaminants and additives.

Crude oil and coal contains not only carbon and hydrogen, but also other elements, most notably sulfur and nitrogen. Depending on the refining process, these elements might find their way into fuels. Organic nitrogen and sulfur will easily oxidize and form stable oxides, yielding energy. Once outside the engine, however, the volatile oxides will dissolve in any atmospheric water and form acids (Duncan et al. 2016) that contribute to acid rain.

Fuel manufacturers add additives to fuels for various reasons, such as boosting octane rating or preventing corrosion. The prime example of additives as a source of noxious pollution was tetraethyllead, which was added to petrol as an octane booster. The emitted lead compounds were shown to be neurotoxic pollutants, and its use was phased out (Needleman 2000).

Side-reactions

Most internal combustion engines use atmospheric air as oxidant. This air consists of 21 % oxygen, and 78 % nitrogen. Nitrogen is very stable and inert at atmospheric temperatures and pressures, but at high temperatures and pressures it can react with oxygen. These reactions produce the oxides of nitrogen: NO, NO₂, NO₃, N₂O, and N₂O₅, collectively called NO_x. These oxides can participate in the cycle that causes a form of pollution called **photochemical smog**. They will also dissolve in atmospheric water and form acids: this might happen far from the point of emission, resulting in **acid rain**.

1.3.4 Mitigating pollution from internal-combustion engines.

Pollution from internal combustion engines is a social ill, and most governments have regulations in place to limit and reduce this pollution. Engine and fuel manufacturers are working hard to reduce this pollution.

The noxious pollution from internal combustion engines can be reduced by various improvements, but there are three complementary approaches: fuel formulation (Gertler et al. 1999), exhaust gas cleanup (Braun et al. 2018) and engine management (Reif 2015).

Fuel formulation

Adding oxygenates improves the octane rating of fuel and reduces NO_x formation.

Exhaust gas cleanup

Exhaust gases from internal combustion engines can be “cleaned”, and there are two approaches. The first is catalytic conversion, in which the exhaust gases that contain the pollutants are passed over a catalyst bed. The catalyst (a proprietary formulation of platinum, palladium and/or rhodium), adsorbs the uncombusted volatile organic carbons, and oxidizes them. It simultaneously catalytically decomposes NO_x to molecular nitrogen and oxygen. Secondly, filter systems can be used to remove particulate matter.

Engine management

As described above, the main source of noxious pollution from internal-combustion engines is uncompleted or undesired chemical reactions, and is not fundamental to the operation of the engine. By carefully managing the engine system, noxious pollution can be reduced.

The only mature engine management technology is the oxygen or ‘lambda’ sensor, which measures the oxygen in the exhaust gases. Such a sensor, coupled to an engine-management computer, allows the metering of the exact amount of fuel needed for optimum combustion (Frauhammer, Schweinsberg, and Winkler 2014).

A newer technology is known as **exhaust gas recirculation** (EGR). This mixes the intake air of the engine with exhaust gases, effectively diluting the oxygen. This reduces peak temperatures, and thereby NO_x formation.

In **stratified charge** engines the distribution of fuel in the volume of intake air is controlled by selective fuel injection. Carefully injecting the fuel at the right place at the right time can allow for higher compression ratios without inducing pinging. **Lean-burn** engines are Otto engines that use extremely high air to fuel ratios.

Electronic engine management systems result in much more efficient and less-polluting engines than non-managed ‘mechanical’ engines, but because engines for automotive applications endure such a wide range of operating conditions, they can at best achieve a compromise between power, efficiency and emissions. It was this unsatisfactory compromise that lead to the Volkswagen emissions scandal: manufacturers chose to cheat on emissions tests rather than admit to the relatively poor performance of a managed engine optimized for low emissions (Mansouri 2016).

Efficiency implications

Attempts to mitigate noxious pollution from internal-combustion engines mostly lead to losses in efficiency. For example:

- Exhaust gas flow through catalytic converters and filters dissipates energy that could have been used to perform work.
- The engines cannot approach their theoretical maximum efficiencies, because reducing NO_x emissions is handled by limiting maximum combustion temperatures.
- NO_x reduction catalysts require the presence of hydrocarbons, *i.e.* incomplete reactions, which implies that not all energy is extracted from the fuel.

- Every treatment system added to the engine adds weight to the vehicle, which reduces payload and hence the total efficiency.

Before carbon dioxide pollution was a concern, it made sense to accept lower efficiencies as a necessary cost of reducing noxious pollution, but in a low-carbon future we cannot just continue trading less noxious pollution for more carbon dioxide production.

1.3.5 Avoiding pollution from internal-combustion engines

The efficiency and cleanliness of internal-combustion engines have dramatically increased over the last century, and more improvements are being implemented. But these improvements have not been fundamental to the engines in any way, and have been driven mostly by government regulation, at the cost of increased complexity and a higher purchase price.

It would seem obvious that it would be a good idea to introduce alternative technologies.

Electrification

In principle, there is nothing special about internal-combustion engines: they are not an end in themselves. They merely deliver a source of torque, which can be coupled to machinery to do useful work. Before the industrial era such torque was available from windmills and waterwheels, and today an alternative is the electric motor.

Electric motors are engines that use the interaction between electric current and magnetic fields to deliver useful torque to drive machines. Because they use electricity as a source of energy, they have no noxious emissions where they operate. Because they are not heat engines, their efficiencies are not subject to the Carnot limit, and efficiencies exceeding 95% are standard (Li and Curiac 2012).

Electricity, of course, is not necessarily carbon-neutral. Most electricity is generated in power plants that use fossil fuels as a primary source of energy. But because these plants are huge, and efficiency scales logarithmically with size, the energy output by the electric motor has a similar or lower carbon footprint than an equivalent internal-combustion engine (Doucette and McCulloch 2011). Electricity grids are also increasingly being fed by solar and wind power, which are carbon-neutral at source. These renewable plants are also smaller and more flexible than their behemoth fossil-fuel counterparts, with lower capital costs and extremely low running costs. Hence, in a low-carbon future, there is every reason to support or mandate the use of electrical motors for stationary applications wherever possible.

In automotive applications, *i.e.* in cases where the engine is used to move itself in addition to some form of **payload**, the application of electric motors is more demanding. In this case it is not easy to bring the electricity to the motor, although electric trains and buses fed by overhead conductors are splendid examples of electrified transport. So for electric vehicles to use the existing road network, they need to carry a source of electricity with them.

This source of electricity can be either a chemical **storage battery**, or a **fuel cell**. In a chemical battery power from the grid is stored in the form of reversible electrochemical reaction, and in a fuel cell the chemical energy from a fuel is directly converted into electricity. There are fuel cells that can use hydrogen as a fuel, and fuel cells that can use methanol as a fuel. (It goes without saying that the hydrogen and the methanol need to be sourced from low-carbon sources for fuel cells to count as low-carbon energy sources.)

The storage and transport of hydrogen remain hurdles to the large-scale adoption of hydrogen-fuelled automobiles, although a market seems to be developing for hydrogen-fuelled electric trains (Agence France-Presse 2018). Hydrogen fuel cells emit no carbon or noxious pollution at point of use.

Direct methanol fuel cells can react methanol with atmospheric oxygen in an electrochemical cell to yield electricity, with carbon dioxide as a waste product. Little is known about possible noxious pollution.

At this time it seems that the electrification of road transport will be by chemical batteries. Lithium-ion batteries can now store enough energy and deliver enough power to make electric motor vehicles practical and attractive (Hayes et al. 2011), and some governments are considering plans to no longer allow the production of passenger vehicles propelled by internal-combustion engines (Burke-Kennedy 2018; Reuters 2018; Gabbatiss 2018).

Carbon-neutral fuels

Another way to avoid the carbon pollution associated with internal-combustion engines is to change the fuel. Not all fuels are fossil fuels, and it is possible to use fuels that are carbon neutral, and in some cases carbon negative.

Apart from using hydrogen in a fuel cell, as described above, **hydrogen** can also be used as a fuel in Otto engines, because it will combust in air to yield heat. The emissions are water and NO_x. Presently there are no hydrogen-fuelled Otto engines on the market.

Methanol is a common product of the fossil fuel industry, but work is underway to produce methanol by reducing carbon dioxide using solar energy. Such **solar methanol** might be used in direct conversion fuel cells, or in internal-combustion engines.

It is possible to harness the energy contained in the reduced carbon in biological materials and use it as fuel. These fuels are known as **biofuels**.

1.4 Biofuels

Biological processes are an integral part of the carbon cycle, because photosynthesis in plants reduces carbon dioxide in the atmosphere to sugars, which are converted by plant physiology into structural cellulose and other metabolites. The prototypical biofuel is wood, used in all societies for cooking and heating. This familiarity makes biofuels seem an obvious and viable source of energy, but details matter, and switching from fossil fuels to biofuels to reduce carbon footprints of human activities is not a simple choice.

Firstly, the efficiency of photosynthesis is notoriously low: not above a few per cent (Simkin, López-Calcagno, and Raines 2019), whereas the efficiency of a modern, mass-produced silicon-based solar **photovoltaic** (PV) panel can exceed 20 % (Green et al. 2019). In general, if mechanical power is required it will be much more efficient to capture solar energy in a PV panel and use it to power an electric motor than to produce a biofuel and use it to fuel an internal-combustion engine.

Secondly, increased biofuel production has numerous impacts on the environment and society which cannot be ignored. Discussing all the factors that need to be studied to make such a decision is outside the scope of this work, but as an example a report prepared for stakeholders in the Netherlands (Smeets et al. 2006) uses the following criteria:

- *GHG [greenhouse gas] emissions – the use of biofuels should cause reductions of GHG emissions. The comparison should be done regarding the average use of fossil fuels, considering the life cycle of fossil and biofuels (i.e., well-to-wheel basis) and in case of biofuels reduction should be at least 30%*
- *Impacts over food supply – the production of biomass for energy must not endanger the food supply and other local biomass applications. The analysis should be developed considering possible changes of land use in the region of biomass production.*
- *Biodiversity – Biomass production must not affect protected or vulnerable biodiversity.*
- *The basic criteria are that violation of national laws and regulations are unacceptable.*
- *Local environmental effects – Principles include (a) soil and soil quality, that must be retained or even improved, (b) ground and surface water supply, that must not be polluted.*
- *Local economic effects – The production of biomass must contribute towards local prosperity.*
- *Social well-being – The production of biomass must not decrease the well-being of local societies.*

Nevertheless, there are cases where using biofuels is an option that reduces the impact of energy use on the environment.

1.4.1 Bio-gas

Anaerobic bacteria can convert carbon compounds of biological origin to methane. This methane is identical to the methane obtained from natural gas, and can be used for the same applications, including fuelling Otto engines and gas turbines. This technology has been applied since the industrial revolution, when some streetlamps in England were fuelled with bio-gas (Klass 1998, p. 448).

An excellent application for the use of bio-gas is waste remediation. Waste material from the agri-food industry can be highly polluting if not handled responsibly, emitting noxious chemicals into water and the potent greenhouse gas methane into the atmosphere. When used as feedstock for bio-gas production it reduces carbon pollution by capturing methane and displacing natural gas and also prevents water pollution (Venter 2014).

1.4.2 Bio-ethanol

The technology to convert sugars or starch from plant materials into ethanol by microbial fermentation is as old as civilization. The products of this process are beer and wine. Beer and wine can best be described chemically as aqueous solutions of sugars, ethanol, flavourants and colourants, with or without suspended solids, and are of no use as fuels. It was not until the 8th century CE that Persian and Arab scientists mastered the art of distillation and purified ethanol (Modanlou 2008), and it was not until Pasteur that yeast was seen as a living organism and it was understood that ethanol is a product of its metabolism (Barnett 2000). It is unclear when ethanol was first used as a fuel, but its flammability must have been noticed by the first distillers. By 1838 pure ethanol was common enough to be used in alcohol lamps as a source of heat in the chemical laboratory (Griffin 1838), and by the 1850s it was a major component of lamp oil used for illumination in the USA (Abebe 2008). Ethanol as

a fuel for internal combustion engines has a clear start date: in 1826 Samuel Morley was granted a patent for an engine designed to use ethanol as fuel (Cummins 1989, p.79).

The industrial production of ethanol as a fuel is a technologically advanced process and an active research field. A paper (Cardona and Sánchez 2007) reviewing the process technology of producing bio-ethanol written in 2007 had garnered 644 citations by January 2019. The industrial production of ethanol consists of three steps:

1. Fermentation
2. Distillation
3. Dehydration

The fermentation step is the biological process by which the yeast organism *Saccharomyces cerevisiae* converts the sugar and starch in the biological material to ethanol and carbon dioxide. This needs to be done in a sterile environment to prevent contamination by other micro-organisms.

The distillation step is the physical process of separating the produced alcohol from the aqueous mixture in which it is produced. This generally produces an **azeotropic mixture** that contains 95.6 % ethanol (Kumar, Singh, and Prasad 2010).

While the processes of fermentation and distillation of ethanol for fuel are in principle the same as that of producing alcoholic beverages, the emphasis of the processes are very different. In the beverage industry the emphasis is on the development of complex flavours and a consistent, recognizable drinking experience. In the fuel industry the emphasis is on efficiency and throughput.

To produce fuel-grade ethanol from the distilled azeotrope, dehydration is a necessary third step. This step can be implemented by various distillation processes that add a third compound, but in most modern plants the water is removed by adsorption onto molecular sieves (Kumar, Singh, and Prasad 2010).

Brazilian ethanol

Brazilian sugar-cane ethanol is an integral part of the country's energy network. In that country most Otto-engine vehicles have 'flex-fuel' engines, which can be fuelled with any blend of ethanol and petrol. The industry is regarded as sustainable (Smeets et al. 2006).

US maize

US maize ethanol is primarily blended with petrol to meet legislative requirements of oxygenates in fuels. The production of maize is water-intensive and the fermentation process is carbon-intensive. The US ethanol from maize has a poorer energy balance and larger carbon footprint than Brazilian ethanol from sugar cane, but has a smaller water footprint (Mekonnen et al. 2018).

Ethanol can fuel Otto engines and gas turbines.

1.4.3 Fischer-Tropsch fuel from biomass

It is possible to heat woody biomass with steam in a low-oxygen environment to produce synthesis gas, which can be converted to a mix of fuel products in the well-known Fischer-Tropsch catalytic process. Such a fuel could be called a bio-fuel, but its production would be difficult to reconcile with the principles of **green chemistry**, described in Section 2.1.1.

1.4.4 Hydrotreated vegetable oil: "Green diesel"

The petroleum industry has developed a collection of chemical processes, such as hydrogenation, oxygenation and cracking. This collection of processes can be applied to vegetable oils to produce a fuel for diesel engines and gas turbines. This path is being followed by the aviation industry (Chiaramonti et al. 2014).

1.4.5 Biodiesel

Oils and fats have been used as fuels since antiquity, most obviously as a fuel for lamps: olive oil has been identified as the fuel used in lamps dating from around 600 CE (Kimpe, Jacobs, and Waelkens 2001), and at the Paris World Fair in 1900 Rudolf Diesel demonstrated an engine that ran on peanut oil (Knothe 2010).

During the energy crisis of the 1970s which caused high prices and shortages of crude oil, the South African government looked at alternative sources of fuel. Experiments were done with sunflower oil as a fuel for agricultural tractors, but the formation of carbon deposits injector nozzles was an intractable problem. Seeing that the clogging of the injectors might be caused by the high viscosity of the sunflower oil as a fuel, the **transesterification** of the oil was implemented, replacing the glycerol in the sunflower oil with methanol (See Figure 1.4). This created an oily liquid with a lower viscosity, which proved to be a trouble-free alternative to diesel fuel (Van Niekerk 1980). With the easing of the energy crisis the interest in this technology waned.

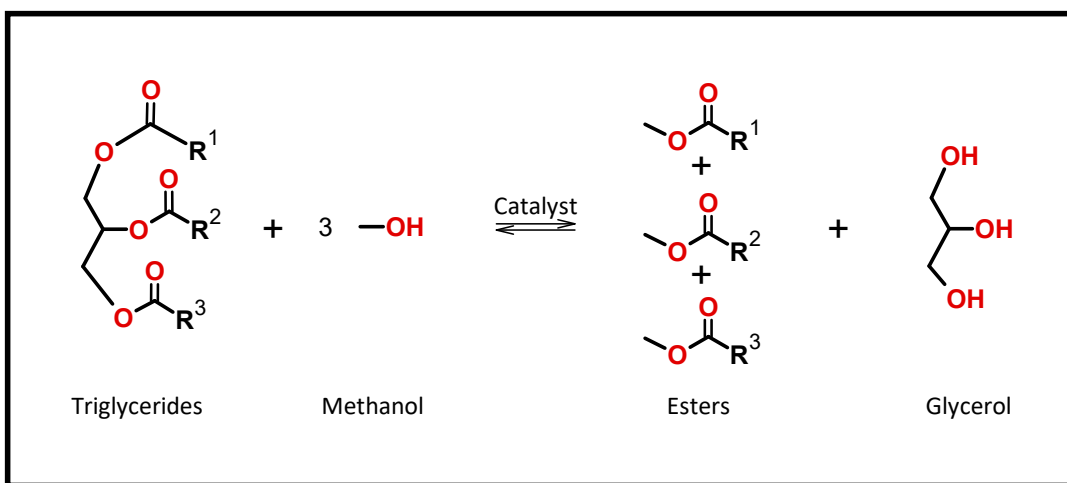


FIGURE 1.4: Transesterification: the chemical reaction that converts vegetable oils into biodiesel

Such a transformed oil is termed **biodiesel**. It consists primarily of a mixture of fatty acid methyl esters, often abbreviated into the acronym FAMEs. Compared to ethanol, biodiesel production is relatively simple, the main method sharing much with the ancient technology of making soap. This simplicity makes the production of biodiesel attractive to small and decentralized manufacturing, and consequently governments consider biodiesel production an attractive proposition: it can create job opportunities in rural populations and it can create a stable market for farmers who produce vegetable oil crops.

Biodiesel is not yet carbon neutral: the methanol used to create the methyl esters is a product of the petroleum industry, and therefore biodiesel emissions contribute

to global warming. But replacing fossil diesel fuel with biodiesel results in a nett reduction of carbon emissions, with the future possibility of replacing fossil-derived methanol with carbon-neutral bio-methanol (Shamsul et al. 2014).

1.5 Conclusion: the significance of biodiesel and its quality control.

In a complex technical, economic and social environment it is likely that there will always be a need that can be best met by internal combustion engines. The decision on the type of engine and the decision on the fuel for that engine are not independent, as Cummins reminds us (Cummins 1989):

“Our generation faces a similar challenge in a real liquid fuel energy shortage that will come within the lifetime now living. As we plunge into the seeking of solutions to our dilemma, we must never forget that *an engine and the fuel it consumes are inseparable partners*; the one cannot progress without the full cooperation of the other. This precept is vital to the planning of future powerplants, since an engine’s design determines its fuel and binds us to our future resource requirements.”

The variation-selection process by which real engineering progress is ‘blind’: the combination of factors that make a design successful is not known at the start of a development (Vincenti 1990). But scientific knowledge provides guidance to engineering design in the form of insight into processes and theoretically achievable targets for performance. Using the scientific knowledge we have today, we can risk a forecast: if society is determined that its carbon footprint should be reduced with minimal noxious pollution, then the application of internal combustion engines would tend towards the following:

1. Larger: Because larger engines are more efficient than smaller engines, larger engines would be preferred. (See section 1.3.1)
2. Low-carbon: The preferred engine would be fuelled by carbon-neutral fuels. (Section 1.3.5)
3. Constant speed: Engines are most efficient when they can work at constant load. (Section 1.3.4)
4. Efficient: Engines with high efficiency should be preferred, which implies engines with high compression or pressure ratios. (Section 1.3.2)
5. Cleanup: The exhaust should be amenable to cleanup, *i.e.* the exhaust gases of the fuel-engine system should not contain compounds that are incompatible with available converter or filter technologies. (Section 1.3.4)

From this it should be clear that the optimal engine of the future will not be an Otto engine, because it will always have a limited compression ratio and its catalytic exhaust cleanup will always require stoichiometric air:fuel ratios, which puts bounds to efficiency increases.

Because it is the most efficient engine, the gas turbine will play an important role. However, its exhaust temperature is very high, which begs for energy recovery to increase the efficiency of the system. Such systems are already seen in the **combined**

cycle gas turbine (CCGT). But energy recovery systems are not light and small, so their best application outside aerospace (where the excess heat is utilized as thrust) appears to be stationary electricity generation.

To reduce the carbon footprint of automotive applications, the best engine may be a large diesel engine with exhaust cleanup to remove NO_x and soot, fuelled with a carbon-neutral fuel.

In choosing between hydrotreated vegetable oil and biodiesel as a fuel, it is most likely that biodiesel will have a lower carbon footprint. Refinery operations are energy intensive, which might add to the carbon footprint of the fuel. Refineries are not usually near the point of use, so that transport will also add to its carbon footprint. The carbon emissions of locally-produced biodiesel are comparatively low, which means that its carbon footprint will tend to be smaller. (At this point it is important to note that these observations are not definitive: carbon footprints are not predicted, they must be calculated.)

Buying large, highly efficient diesel engines with sophisticated management systems and exhaust cleanup require high capital investment. In an economically competitive environment they therefore need to bring reliable returns, which implies high availability, as measured by frequency of breakdown and length of time between maintenance stops. Such high reliability can only be achieved if the engine builder understands the fuel-engine system well and it behaves predictably.

In a low-carbon future, therefore, well-characterized biodiesel might be expected to play a central role in non-electric ground transport and other industrial applications where electrification is not possible.

1.6 Conclusion: the role of chromatography.

The development of the fuel-engine systems depends heavily on the chemical characterization of fuels and engine emissions, and chromatography has always played a central role: some of the earliest researchers developing gas chromatography were employees of a petrochemical company (Keulemans, Kwantes, and Zaal 1955).

This thesis explores the possibility of applying comprehensive two-dimensional (supercritical fluid \times gas) chromatography (SFC \times GC) to the chemical analysis of biodiesel for characterization and quality control.

The next chapter (Chapter 2) focuses on the use of supercritical carbon dioxide as extractant and chromatographic mobile phase. Chapter 3 explores the technical standards applicable to biodiesel offered for sale in South Africa, and then focuses on the prescribed chromatographic methods. Chapter 4 and Chapter 5 focus on the chromatographic instrumentation developed for SFC \times GC, and Chapters 6 and 7 show the results obtained when biodiesel and biodiesel blends are analysed using the developed SFC \times GC instrumentation. Chapter 8 shows a chromatogram that illustrates the promise of SFC \times GC-FID when the carbon dioxide mobile phase is modified by the addition of organic solvents.

$PV \neq nRT$

The ideal gas law does not apply to supercritical fluids.

2

Introduction: Carbon dioxide and chromatography

2.1 The chemical industry

Industrialized societies depend on chemicals. (In this discussion I define chemicals as pure substances that are produced by industry for industry.) Chemicals might be used in the processing of products, or blended with other chemicals in formulations that might be sold to users as products. In a familiar example, Sucrose is a chemical produced by the sugar industry from sugar cane or sugar beet. It is a pure substance that is mostly used in the industry as an ingredient for processed food. Other uses of sugar include coatings for medication, and feedstock for engineered micro-organisms that produce pharmaceuticals. (Sucrose is a rare example of a chemical that is also sold to consumers.)

The chemical industry produces a huge variety of products, from compounds as simple as hydrochloric acid to compounds as sophisticated as cyanocobalamin (Figure 2.1). All of these chemicals help produce the products indispensable to industrialized societies. Nevertheless, the chemical industry is not held in high regard by people outside the industry. A part of this negative perception comes from the chemical industry's reputation for fatal accidents and pollution (Gumm 2015).

The list of incidents is long and examples easily spring to mind: In 1984 a leak at a chemical plant in Bhopal, India, caused the death of thousands of people and the injury of thousands more (Varma and Varma 2005). Stratospheric ozone is struggling to recover from depletion caused by the reckless emissions of chlorofluorocarbons (Ball et al. 2018). Plastic microparticles are now found everywhere in the oceans (Woodall et al. 2014), and the pesticide DDT (dichlorodiphenyltrichloroethane or 1-chloro-4-[2,2,2-trichloro-1-(4-chlorophenyl)ethyl]benzene) is found in the breast milk of Inuit mothers (Gibson et al. 2016) who live in polar regions, very far from the tropical areas where it was once sprayed for pest control.

The chemical industry is also a prodigious producer of greenhouse gases. Apart from the carbon dioxide emitted by the production of the energy that powers chemical production processes, some chemical processes emit carbon dioxide as a waste product. Most notable of these is the reduction of atmospheric nitrogen as the first step in the production of nitrogen fertilizers. Of all the greenhouse gases monitored

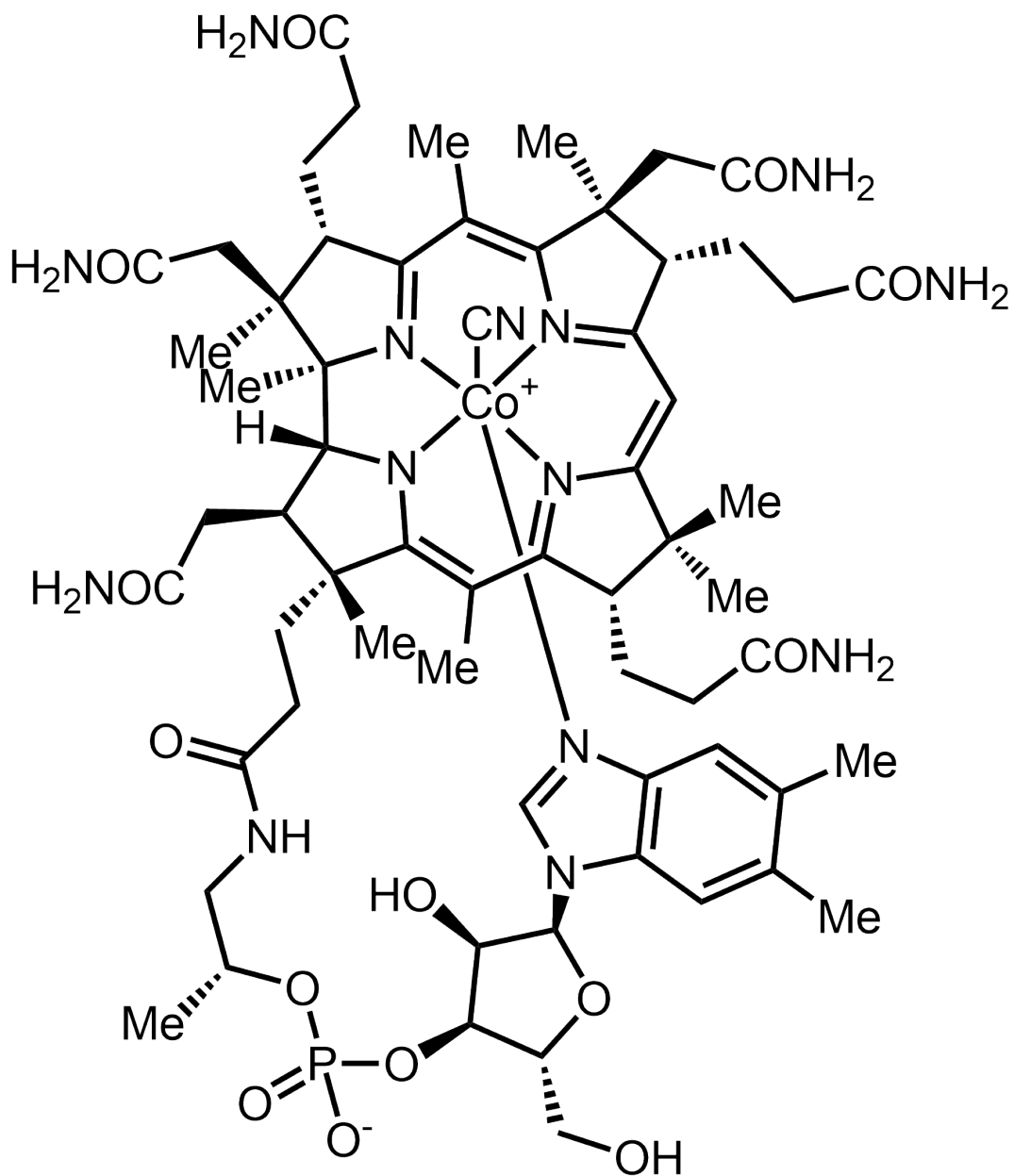


FIGURE 2.1: The chemical structure of cyanocobalamin, a form of vitamin B12. This compound is produced on the tonne scale by the chemical industry.

by the Intergovernmental Panel on Climate Change (IPCC), only carbon dioxide, methane and nitrous oxide are found in nature: the others are exclusively products of the chemical industry (IPCC 2014).

No chemical has ever jumped out of a lab, multiplied uncontrollably, and spread into the environment to poison or pollute: they have all been introduced into the environment by human ignorance, negligence or recklessness. All chemicals behave well when used in properly controlled environments, but human actions can let them escape to damage and pollute. But while we try to solve the intractable problem of human behaviour, we as chemists cannot just lay blame: we must pay attention to the intrinsic safety of chemicals and chemical processes.

2.1.1 “Green chemistry”

The date of birth of the environmental movement is conventionally set to 1962, when the biologist Rachel Carson published the book *Silent Spring*, which pointed out the destruction of nature by the unrestricted use of pesticides and the dangers of their overuse (Carson 2003). This was a direct imputation of the chemical industry, because the pesticide products contained many chemicals.

Chemists are human, and the realization that uncontrolled chemicals can have detrimental effects led at least some chemists to reflect on their own work. This has given rise to the concept of **green chemistry**. Although the term has no rigorous definition or quantitative measure (Linthorst 2010), a set of 12 principles or guidelines are proposed (Anastas and Warner 1998):

1. *It is better to prevent waste than to treat or clean up waste after it is formed.*
2. *Synthetic methods should be designed to maximize the incorporation of all materials used in the process into the final product.*
3. *Wherever practicable, synthetic methodologies should be designed to use and generate substances that possess little or no toxicity to human health and the environment.*
4. *Chemical products should be designed to preserve efficacy of function while reducing toxicity.*
5. *The use of auxiliary substances (e.g. solvents, separation agents, etc.) should be made unnecessary wherever possible and innocuous when used.*
6. *Energy requirements should be recognized for their environmental and economic impacts and should be minimized. Synthetic methods should be conducted at ambient temperature and pressure.*
7. *A raw material or feedstock should be renewable rather than depleting wherever technically and economically practicable.*
8. *Unnecessary derivatization (blocking group, protection/deprotection, temporary modification of physical/chemical processes) should be avoided whenever possible.*
9. *Catalytic reagents (as selective as possible) are superior to stoichiometric reagents.*
10. *Chemical products should be designed so that at the end of their function they break down into innocuous degradation products and do not persist in the environment.*
11. *Analytical methodologies need to be further developed to allow for real-time, in-process monitoring and control prior to the formation of hazardous substances.*

12. *Substances and the form of a substance used in a chemical process should be chosen so as to minimize the potential for chemical accidents, including releases, explosions, and fires.*

While these guidelines are clearly written with synthetic chemistry in mind, it does not mean that they do not apply to analytical chemistry. For example, Principle 7 suggests that, when possible, one should use hydrogen rather than helium as mobile phase in capillary gas chromatography: hydrogen is renewable, whereas helium is a finite resource and from time to time there are reports of shortages (Kornblut 2019).

One large area of the greening of chemistry is changing the use of solvents. Principle 5 recommends that solvent use be avoided, as most solvents used in chemistry are ultimately derived from petroleum and are toxic to some degree. But solvents play a large role in many kinds of chemistry, and eliminating their use in the near future seems unlikely. Searching for and characterizing bio-derived, non-toxic, non-persistent solvents is an active field of research (Clarke et al. 2018). Fortunately there are a few solvents already in use that are inherently “green”, such as water or ethanol. One such naturally green solvent is carbon dioxide.

2.1.2 Carbon dioxide as a green chemical

Carbon dioxide as a chemical is used in industry in a few key areas.

- Carbon dioxide is often used in firefighting, in the form of portable fire extinguishers or room flooding systems. In this last use it is displacing the ozone-depleting halomethane ‘Halon’ formulations.
- When liquid water is supersaturated with carbon dioxide, the gas desolvates slowly in the form of streams of tiny bubbles. This phenomenon makes beverages prepared from water supersaturated with carbon dioxide (or **carbonated water**) interesting to drink, and a large, international beverage industry is based on carbonated water.
- Carbon dioxide has a freezing point of -77°C , and the solid can be conveniently obtained by evaporating liquid carbon dioxide at atmospheric pressure. The evaporating liquid rapidly cools the stream of carbon dioxide, lowering the temperature of the stream to below freezing point, and the gas crystallizes. The resulting ‘snow’ can be compressed into blocks, which only slowly sublimates into gaseous carbon dioxide, keeping the temperature at the freezing point. Packing frozen food products together with this ‘dry ice’ allows for it to be transported cold without mechanical refrigeration.
- Pellets of dry ice can be entrained in a jet of air, and used to abrade surfaces for cleaning (Spur, Uhlmann, and Elbing 1999). This use of carbon dioxide can displace toxic solvents or abate the noxious dust produced by blasting operations.
- Carbon dioxide is a ‘natural refrigerant’ (Pearson 2005) and can be used to displace hydrofluorocarbon refrigerants, which are potent, long-lived greenhouse gases.

- Carbon dioxide can be used as a preservative and anti-oxidant in packaged food. If air in a packaged food is removed by purging the headspace with carbon dioxide, the growth of microbes can be discouraged, extending the shelf life of the product (Jacobsen and Bertelsen 2002).
- Carbon dioxide can be used to extract compounds from natural products.

Of these uses, extractions are economically the most important, where it replaces hydrocarbon solvents.

2.2 Extractions using carbon dioxide

2.2.1 Commercial extractions

There are several commercial processes that use carbon dioxide to extract valuable products from plant material.

Plant oils

Vegetable oils are obtained from various crops, and can be extracted from the plant material by pressing, heating or extraction. High-pressure carbon dioxide has been used to extract vegetable oils from various plants, although it seems that this process has only found niche applications so far (Eisenmenger et al. 2006; Grażyna and Anna 2018).

Hops

Hops is an essential component in the brewing of beer. It imparts a desired bitter flavour, stabilizes the beer during storage, and assists with foam formation (Schönberger and Kostelecky 2011). Hops is a seasonal crop with a limited growing range, but the demand for beer is not limited to certain areas or seasons. The creation of hops extract makes it possible for brewers to benefit from hops without owning a hops plantation or storing and transporting dried hops over long distances. All hops extracts produced today are extracted by carbon dioxide (Hunt et al. 2010).

Coffee

Coffee is an international industry, with coffee drunk in many cultures and in many forms. One of the attractions of coffee is the effects of the psychoactive substance found in the coffee bean, **caffeine**. Caffeine is a mild stimulant and promotes wakefulness. A small proportion of coffee drinkers enjoy drinking coffee, but prefer to avoid the stimulant effect, which might induce insomnia or irritability. For these coffee drinkers the market supplies **decaffeinated coffee**.

Given the large amount of coffee traded (an estimated 167.47 million bags of coffee in the 2018-2019 coffee year (*Coffee Market Report December 2018 2018*))¹, if only a small percentage of coffee needs to be decaffeinated, it will be a large amount of coffee to process, and industrial processes will be necessary to supply the demand.

Decaffeination of coffee is achieved by selectively extracting the caffeine from green (*i.e.* unroasted) coffee beans using carbon dioxide. This is the largest use

¹The factoid that “coffee is the second-most traded commodity after oil” has been proven to be untrue (Greenberg 2017).

of carbon dioxide for extraction (Ramalakshmi and Raghavan 1999). The extracted caffeine is sold for use in medication and ‘energy’ drinks.

2.2.2 Analytical extractions

Extraction is not only an industrial process: is an essential part of many procedures used in analytical chemistry. Industrial extraction processes using supercritical fluids were converted into analytical techniques (Taylor 2013). Extractions using high-pressure gases for analytical purposes is usually called **supercritical fluid extraction** (SFE).

2.2.3 Why carbon dioxide?

What makes carbon dioxide a suitable solvent for extraction?

There are two aspects to this question. The first is about the *greenness* of carbon dioxide. It is non-toxic, non-persistent, non-flammable, non-corrosive, inexpensive, commercially available, and a waste product. (It goes without saying that this carbon dioxide is sourced from a carbon-neutral source, perhaps the brewing industry.) The second aspect of the desirability of carbon dioxide lies in its physical properties and the conditions under which it is used.

Chemists will intuitively understand that gaseous carbon dioxide has no solvating properties, and that liquid carbon dioxide should not behave much differently than any other solvent. Both these statements are true under ‘normal’ circumstances.

But consider the case of an isobaric cooling of a volume of gas. The gas-liquid transition takes place because energy is removed from the system: at some point the kinetic energy of some of the molecules becomes less than the energy of the intermolecular forces, and the molecules prefer to “clump together”, *i.e.* it **condenses**. The remaining gas molecules receive the excess energy, and therefore stay in the gas state, until more energy is removed, leading to more of the gas condensing. During this process the temperature remains constant, and the value of this temperature is known as the **boiling point** of the compound.

Now consider a solid or liquid solute dispersed in the same volume of gas being cooled. In this case, as the gas cools, the gas-solute intermolecular forces can become stronger than than the gas-gas intermolecular forces at a temperature which is higher than the boiling point. In such a case the gas molecules will “clump” around solute molecules, while the gas molecules will not “clump together”. Now the gas has obtained solvating properties and the solute is truly dissolved in the gas, without any condensation of the gas itself. The same effect can be imagined to happen during the isothermal compression of a gas.

If there is more than one solute in a volume of gas at a given temperature and pressure, some might dissolve in the gas, while others might not. This means that the solvating gas can be **selective**. It can also be seen that the solvating power of the gas will depend on the temperature and the pressure of the gas. This means that the solvent’s solvating power becomes **tunable**.

While the dense gas has solvating properties, it still has the physical properties of a gas:

Diffusivity The solvating gas maintains its high diffusion coefficients, which means that it can easily diffuse into porous material, and that solutes will rapidly diffuse through it.

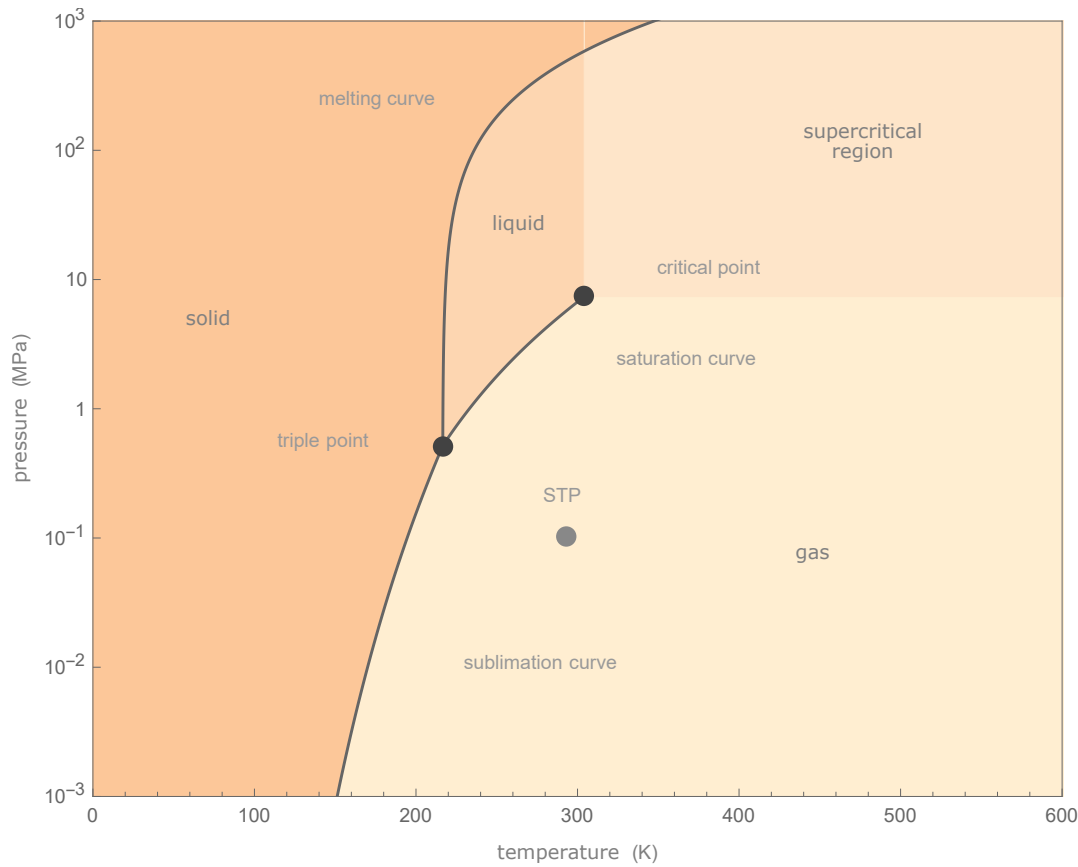


FIGURE 2.2: The phase diagram of carbon dioxide (Wolfram | Alpha 2019d).

Surface tension The solvating gas has a low surface tension, which means that it will readily ‘wet’ surfaces and penetrate porous material.

Viscosity The solvating gas has a low viscosity, which means that it takes little energy to pump it.

For historical reasons such solvating gases are known as ‘supercritical fluids’, because they were first obtained by heating a liquid at high pressure (Berche, Henkel, and Kenna 2009), so that the temperature and pressure of the substance is higher than its **critical point**. The critical pressure of a substance is the pressure above which it is impossible to create a gas-liquid phase transition by isobaric cooling, and the critical temperature is the temperature above which it is impossible to create a gas-liquid phase transition by isothermal compression. When the gas is at its critical temperature and critical pressure, it is at its critical point. The critical point is very different from the **triple point**: there is no equilibrium involved (See Figure 2.2). The terms ‘supercritical fluid’ and ‘dense gas’ are synonyms (Randall 1982) — the adjective ‘dense’ in ‘dense gas’ of course implies that the gas behaviour is far from that of an ideal gas. There are no discontinuities in binary diffusivity when temperature is changed from above to below the critical temperature (Lauer, McManigill, and Board 1983). Hence extractions are often done under conditions which are not technically ‘supercritical’ but still yields its benefits.

The critical temperature of carbon dioxide is 304.12 K (31.10 °C), and the critical pressure is 7.39 MPa (72.9 bar). This temperature and pressure are easy to achieve in

the laboratory with standard chromatographic instrumentation, or in an industrial plant with standard process engineering technologies.

Carbon dioxide is gaseous at ambient conditions. This means that once it has been used in its role as extractant and is exposed to the atmosphere, it will rapidly evaporate without added heat, leaving no residues.

Any pure compound will have a supercritical point. Compounds with technologically feasible supercritical points and useful chemical properties include ammonia, methanol, CFCs/Freon, hydrocarbons (propane, butane), water and sulfur hexafluoride. All of these lack green attributes: hydrocarbons pollute, the CFCs deplete ozone, sulfur hexafluoride is a potent greenhouse gas, and methanol and water are liquid at ambient conditions. For these reasons the term supercritical fluid extraction is practically synonymous with extraction using high-pressure carbon dioxide².

Modifiers

The carbon dioxide molecule has zero dipole moment and the bulk fluid a low dielectric constant, so supercritical carbon dioxide is expected to be a non-polar solvent. (Although in practice the solvent behaviour is more complex, partly explained by the high quadrupole moment of the carbon dioxide molecule (Raveendran, Ikushima, and Wallen 2005).)

While the solvating power of a supercritical fluid is certainly ‘tunable’ by adjusting its pressure and/or temperature, the range in solubility might be quite limited in practice. Just as with other solvents, it is possible to add a co-solvent or **modifier** to the supercritical carbon dioxide. This makes it possible to increase the solubility of polar compounds in the supercritical fluid. Methanol, ethanol, formic acid, and water are examples of suitable green modifiers for carbon dioxide (Herrero et al. 2010). When modifiers are used the carbon dioxide, modifier and solute form a system with four degrees of freedom (modifier fraction, solute fraction, pressure, and temperature), which can become difficult to model. While this is a challenge for process engineers who need to design efficient industrial systems, analytical chemists can afford to be pragmatic and use heuristics to find suitable conditions (Wells, Zhou, and Parcher 2003).

Practical extractions

Figure 2.3 shows a schematic diagram of a system set up for supercritical fluid extractions. Carbon dioxide (a) is readily available from suppliers of industrial gases and high-purity grades are available. Chromatography-grade solvents are usually used as modifiers (d). High-pressure pumps (HPLC type) are used to compress the carbon dioxide (b) and the modifier (c), which are mixed together at the appropriate ratio. The mixture gets pumped into the (optionally heated (f)) extraction cell (e), which contains the material that needs to be extracted. Having extracted the target compounds from the material, the supercritical fluid passes through a pressure-control mechanism (g). This allows the pressure of the supercritical fluid to drop to ambient, turning it into a low-density non-solvating gas. The extract becomes desolvated and precipitates in the collection vessel (h). The operation of the system might be either static or dynamic: in static operation the supercritical fluid is pumped into the system, the flow is stopped, the matrix/fluid mixture is given time to approach

²It is also possible to use supercritical fluids as reactants. For example, treating vegetable oils with supercritical methanol yields biodiesel in an uncatalyzed reaction. This topics falls outside the scope of this discussion.

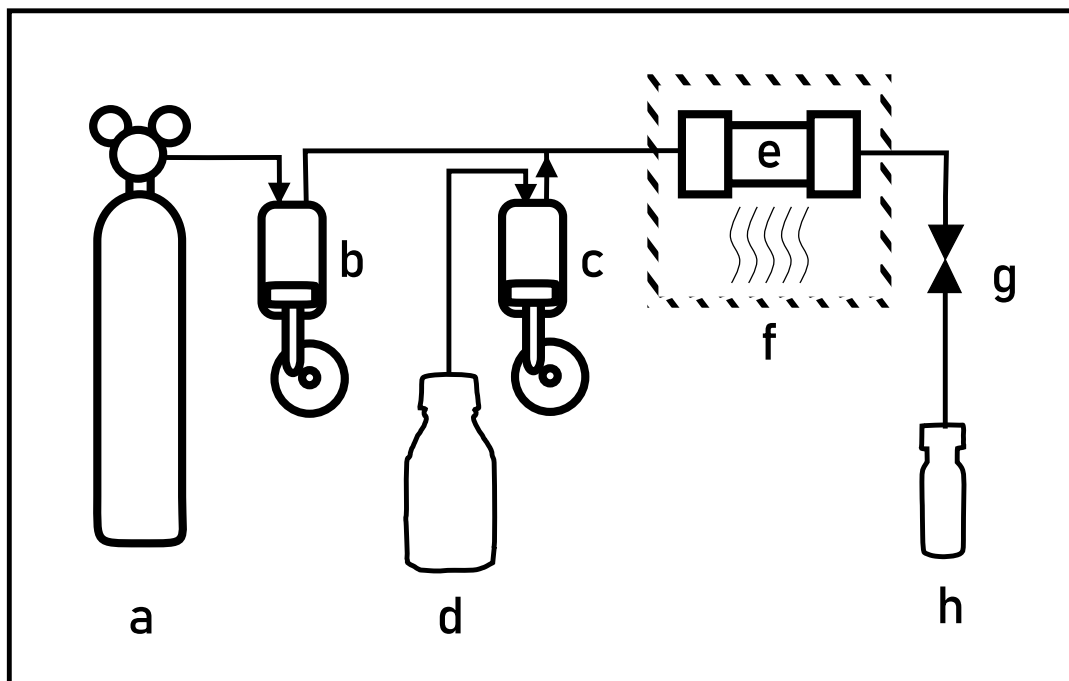


FIGURE 2.3: A diagram of an SFE system. (a) CO₂ supply (b) High-pressure SF pump (c) High-pressure modifier pump (d) Modifier reservoir (e) Extraction cell (f) Temperature control (g) Pressure control (h) Collection vessel

equilibrium, and then the fluid is expelled and the extract collected. In dynamic operation the supercritical fluid is pumped through the extraction cell and the extract collected continuously.

2.3 Supercritical fluid chromatography

An analyte will extract out of a matrix into a given solvent with a certain efficiency and at a certain rate. While this is important when finding an optimum extraction method, its relevance is otherwise limited.

However, *different* analytes will extract out of a matrix with *different* efficiencies and at *different* rates. In a 1906 paper the Russian botanist Mikhail Semyonovich Tsvet³ applied this observation to the dynamic extraction of a bed of calcium carbonate that had mixture of plant pigments applied at the inlet end, using petrochemical solvents. The different extraction efficiencies and rates of adsorption and desorption on the calcium carbonate surface lead to the **separation** of the compounds in the mixture. Tsvet called this method of separation **chromatography** (Ettre and Sakodynskii 1993a; Ettre and Sakodynskii 1993b). With time this method became generalized, and today chromatography is a major, established scientific field with many ramifications and a myriad of applications.

The effectiveness of a chromatographic system is firstly judged by how well it separates two compounds of interest. The separation is quantified by the **resolution R**, which is calculated as the ratio of the distance by which the two compounds of interest have been separated to the width to which they have spread during the

³Also transliterated from Russian as Tsvett, Tswett, Tswet, Zwet, or Cvet

separation. Because these distances are rarely measured directly in modern instruments, the proxy of **retention times** t_r are normally used for the distance travelled. To compare the retention of different compounds, a normalized measure is used to remove the effect of the time they would have spent in the column if they were unretained, the **hold-up time** t_m . This is the **retention factor**, $k = \frac{t_r - t_m}{t_m}$, and is related to the relative amounts of the analyte in the mobile and stationary phases respectively. The relative retention of two compounds can then be quantified by the **separation factor** $\alpha = \frac{k_2}{k_1}$. The values of k and α are determined by thermodynamic and chemical factors, respectively, but these only address the difference in retention of the two compounds used to calculate separation.

$$R = \sqrt{N} \left(\frac{k}{k-1} \right) \left(\frac{\alpha-1}{\alpha} \right)$$

Rigorous derivations of this equation can be found in the literature (Sandra 1989b; Sandra 1989a) and precise definitions of the factors are provided by IUPAC (Ettre 1993).

Because of the different technologies used in its applications, chromatography is conventionally classed by the state of its mobile phase as either **gas chromatography** (GC) or **liquid chromatography** (LC). However, as we have seen, solvating gases can also extract analytes from solid stationary phases, and hence the term **supercritical fluid chromatography** (SFC) was created for these kinds of separations.

Supercritical fluid chromatography as practised today bears a great resemblance to **high performance liquid chromatography** (HPLC) (See Figure 2.4). The main reason for this is that there is a large overlap between the technology used for HPLC and the technology needed for SFC. In particular, both use high-pressure pumps and columns packed with particles of very small diameter and use optical detectors. Manufacturers supplying HPLC instrumentation often also supply SFC instrumentation.

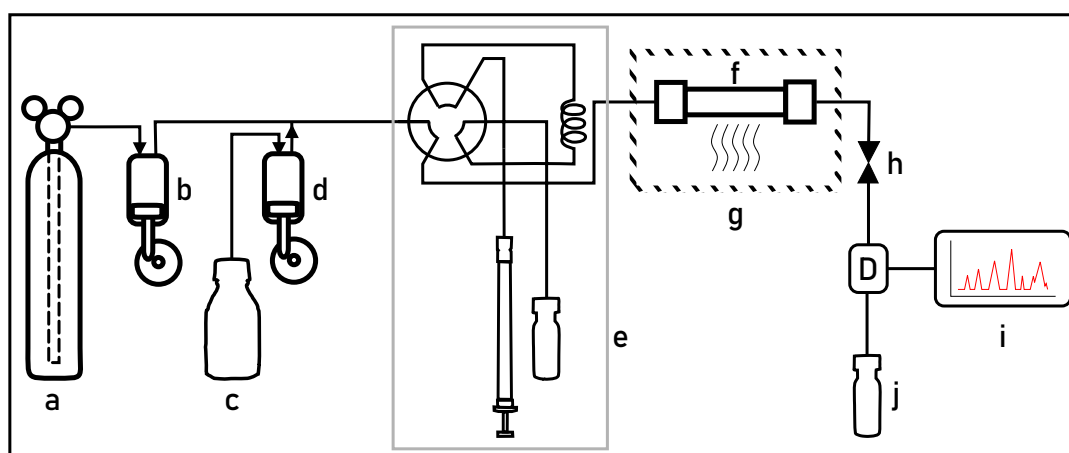


FIGURE 2.4: A diagram of an SFC system. (a) CO₂ supply (b) High-pressure SF pump (c) Modifier reservoir (d) High-pressure modifier pump (e) Injection system (f) Column (g) Optional heating (h) Back-pressure control (D) Detector (i) Data system (j) Optional fraction collection.

A full discussion of the differences between SFC and HPLC is beyond the scope

of this thesis, but the kinetic advantages of SFC are considerable. In a study comparing SFC and LC methods for the analytical separation of pharmaceutical compounds (Perrenoud, Veuthey, and Guillarme 2012), the flow at minimum plate height H , was found to be five times higher for SFC than for LC when using columns packed with $3.5\text{ }\mu\text{m}$ particles, and four times higher for columns packed with $1.7\text{ }\mu\text{m}$ particles. (See Figure 2.5). This difference in speed is attributed to the higher diffusivity of supercritical carbon dioxide, which increases the rate of mass transfer between the stationary and mobile phases.

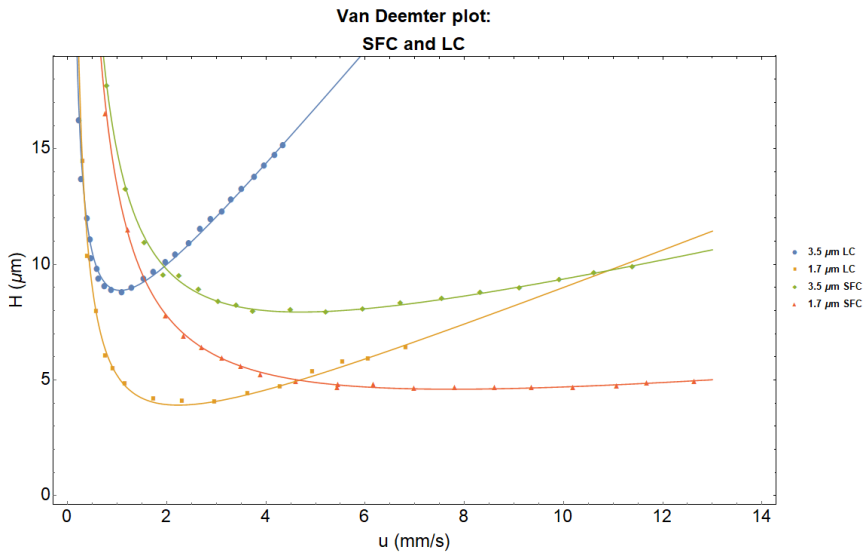


FIGURE 2.5: Kinetic performance as a function of linear velocity for 1.7 and 3.5 m particles in LC and SFC. Van Deemter curves for butyl-paraben on 2 systems equipped with 1.7 or 3.5 m particles columns. LC conditions: $\text{H}_2\text{O}/\text{ACN}$ ($60/40$, v/v), 30°C , $1\text{ }\mu\text{l}$ injected. SFC conditions: CO_2/MeOH ($96/4$, v/v), 40°C , 150 bar backpressure, $1\text{ }\mu\text{l}$ injected. Adapted from (Perrenoud, Veuthey, and Guillarme 2012).

These high speeds can be achieved at much lower pressure drops per length of column than in LC, as shown in Figure 2.6. This can be attributed to the low viscosity of supercritical carbon dioxide, because less energy is required to pump the lower-viscosity supercritical fluid at the same flow rate as a liquid, all else being equal.

This low pressure drop can be exploited by using very long columns to generate a large number of plates.

2.3.1 SFC and FID

But SFC was not always a technique based on HPLC technology. In the 1980s SFC was practised using open tubular columns and flame detectors, so the instrument designs looked more like GC instruments than HPLC instruments, and SFC was promoted as a replacement for GC (Poole 2003). During this era the detectors used for SFC were the flame-based detectors developed for GC, in particular the flame ionization detector (FID). The **flame ionization detector** was invented near-simultaneously in South Africa and New Zealand (Ettre 2008). The core of the system is a flame of hydrogen gas burning in pure air (See Figure 2.7). The measured signal is the electrical conductivity of the flame plasma, which is measured by applying a -100 V potential difference between electrodes at the tip and the base of the flame. There

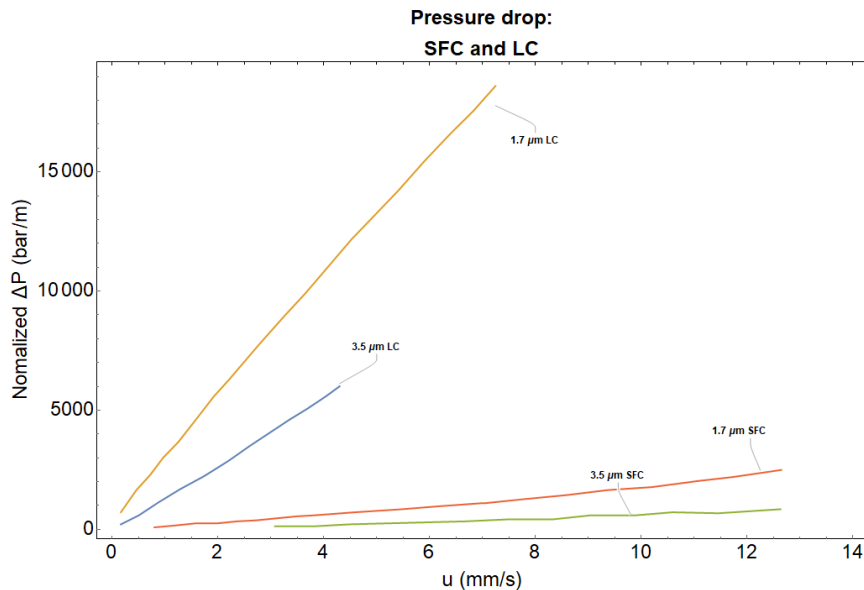


FIGURE 2.6: Normalized generated pressure drop as a function of linear velocity for 1.7 and 3.5 m particles in LC and SFC. Each curve represents the pressure drop required to generate the linear velocity of the corresponding curve in Figure 2.5, normalized to 1 m of column to avoid influence of column geometry variations. Adapted from (Perrenoud, Veuthey, and Guillarme 2012).

are very few free ions in the hydrogen flame, so the conductivity is normally low. But if organic compounds are introduced into the flame free ions are created during their combustion, which increases the conductivity of the flame gases. The change in conductivity is measured by measuring the small current between the two electrodes with an **electrometer**.

As a first approximation the signal produced by the FID is proportional to the number of carbon atoms in the analyte. The mechanism that explains this surprising result is fairly simple: at high temperature in the hydrogen-rich core of the flame, all the carbon atoms in the analyte are reduced to methane (Holm and Madsen 1996). Once it gets into contact with the hot oxygen in the outer layers of the flame there is a chemi-ionization reaction. The electric field acting on the ions creates a flow of ions, which can be measured as an electric current. The current is proportional to the number of ions, which is proportional to the number of methane molecules, which is proportional to the number of carbon atoms in the analyte.

The FID's shining strength as a detector is its tremendous linear dynamic range of 10^7 . Combining the linear dynamic range with its carbon sensitivity makes it an excellent detector for quantifying organic compounds. During the period of history when SFC was seen as a variant of GC, the FID was the detector of choice. But when SFC started resembling HPLC, and the selectivity of the chromatography started being manipulated by adding modifiers (see Section 2.2.3), the FID lost its utility. The quantity of modifier added to the carbon dioxide mobile phase swamps the FID, rendering it useless as a detector. In contrast, if the chosen modifiers are transparent at the relevant wavelengths, optical detectors are more useful in SFC using modified carbon dioxide as a mobile phase.

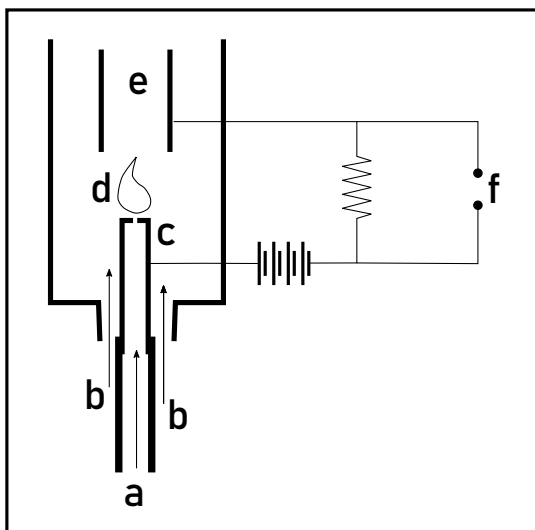


FIGURE 2.7: A schematic diagram of the flame ionization detector. (a) Mixture of column eluate and hydrogen gas (b) Clean air (c) Metallic flame tip electrode (d) Collector electrode (e) Flame (f) Conductivity signal

2.3.2 SFCxGC

In chromatography, the analyte in the eluate can be detected to yield information about the sample, or fractions of eluate can be collected for further purification or characterization, or both. If fractions are collected, there is nothing that prevents the chromatographer from subjecting a collected fraction to another chromatographic separation. For example, a synthetic chemist might use column chromatography to separate their target compound from side-reaction compounds, collecting fractions of the eluate. If the compounds are colourless, the chemist might use **thin-layer chromatography** (TLC) to examine the fractions for presence and purity of the relevant compounds. If the product and the side-product were co-eluting it would not help to use the same chromatographic system (*i.e.* combination of stationary phase and mobile phase) for the TLC examination, because the co-elution would not become apparent. If, however, the chemist changed the mobile phase, or switched to a different stationary phase for the TLC examination, it is quite likely that the two compounds would be separated. For example, if a synthesis involving sugars were being attempted, two sugar enantiomers would likely co-elute on a silica clean-up column. Investigating the sugar fraction using a TLC plate with a chiral stationary phase would reveal the presence of stereoisomers. The second (chiral) separation (on TLC) is said to be **orthogonal** to the first (packed column) separation. Such a separation is an example of a two-dimensional (2D) separation. In analytical chromatography, 2D separations is a powerful tool. The simplest 2D chromatography is called **heart-cutting**. In such a case a fraction of interest is collected from the **first dimension** (¹D) separation, and subjected to a **second dimension** (²D) separation. For example, a fraction collected from an HPLC separation could be injected into a gas chromatograph. The separation on the GC dimension would obviously be very different from the separation on the HPLC dimension, and therefore we can say that the orthogonality is high.

Heart-cutting is a useful way to get detailed information from a sample, but it is technically demanding and labour-intensive. It is usually employed for challenging

separations in well-understood samples, because peaks of interest in the first dimension must be captured for injection on the second dimension. This requires precise timing under supervision of an expert chromatographer.

If, however, one collects the eluate in equal fractions and does identical separations of each of the fractions, then one enters the domain of **comprehensively coupled chromatography**. The comprehensive coupling of orthogonal chromatographies does not demand a previous understanding of the sample, and doing exactly the same separation for each fraction allows the process to be automated.

A 2D separation can be called comprehensive if the following three criteria are met (Giddings 1987):

1. Every part of the sample is separated by two distinct chromatographic processes.
2. Equal percentages of all sample fractions are separated by the second process. (Ideally 100 % of each fraction would be subjected to the second process, but sometimes it might be necessary to reduce the transferred percentage, for example to prevent column overloading.)
3. Compounds resolved by the first dimension separation remain resolved.

To effectively distinguish between heart-cut and comprehensive 2D couplings, a terse nomenclature was developed Marriott2012. Simple coupling between systems is designated by a hyphen ("‐"), for example "HPLC-GC". This corresponds to the usual notation of a coupled detector coupled to a chromatograph, for example GC-FID or GC-MS. Comprehensive coupling is denoted by a multiplex sign ("×"), for example GC×GC. If it is not clear from the context, the detector can be specified using a hyphen, as in GC×GC-MS. Of the comprehensive coupled chromatography techniques, GC×GC is the most mature, with a selection of powerful instruments on the market.

This thesis further explores the implementation of SFC×GC, first demonstrated by Venter and Rohwer (Venter and Rohwer 2004; Venter, Makgwane, and Rohwer 2006). In the implementation of SFC×GC described in this thesis, fractions of the eluate from the SFC are transferred to the GC. The mobile phase is changed from carbon dioxide to hydrogen in the modulating interface, and the GC dimension is a conventional open-tubular capillary separation with FID detection. Any volatile modifiers or additives added to the SFC mobile phase will be separated from the analytes by the GC dimension. This makes it possible to still use the FID as a detector in an SFC×GC chromatograph where the SFC is based on HPLC technology.

The ²D separations are **fast** chromatographic separations, *i.e.* separations optimized for speed, sacrificing resolution. This is achieved using fast temperature programming of the GC separation. The high orthogonality of the SFC and the GC separations enables novel comprehensive 2D chromatography, which was applied to the chemical analysis of biodiesel.

The nice thing about standards is that you have so many to choose from.

Andrew S. Tanenbaum

3

Biodiesel, technical standards and chemical analysis

3.1 Introduction to standards

The fact that vegetable oil can be used to fuel diesel engines has been known since the earliest days. Rudolf Diesel himself had exhibited an engine at the Paris Exhibition in 1900 (Knothe 2010) that ran on peanut oil. But the development of the petroleum industry late in the 19th century ensured an ample supply of fossil fuel for these engines, and it was only with the energy crisis of the 1970s and the growing climate crisis that attention was again given to vegetable oils as fuels.

The development of the diesel engine happened in parallel with its fuel, for, as Cummins said "...we must never forget that *an engine and the fuel it consumes are inseparable partners*; the one cannot progress without the full cooperation of the other" (Cummins 1989). The first invention of an engine presupposes a supply of fuel, but the variation-selection process that searches for lower costs and higher efficiency then opens up the quest for more fuels. If new fuels are proposed, meticulous engine builders would then have to test each new fuel in their engines and approve it. But fuel suppliers would like to see their fuels used in as many engines as possible. This convergence of interests gives rise to the establishment of **technical standards**. Technical standards allow engine builders to develop engines that will run on any fuel with certain agreed-upon standard qualities, and fuel producers can produce fuels knowing that they will work on any engine designed for that fuel.

A technical standard or just **standard** is a "document, established by consensus and approved by a recognized body, that provides, for common and repeated use, rules, guidelines or characteristics for activities or their results, aimed at the achievement of the optimum degree of order in a given context" (Hatto 2010). Standards are used in many aspects of industrialized societies, from implantable medical devices (ISO 2019) to coffins and caskets (SABS 1993). Standards are often associated with products, but also apply to procedures (ISO 2015) and systems (ISO 2017).

Standards are not mandatory, nor do they provide the 'best' way of doing something. The great strength of standards is their reliability. "Standards exist principally to provide a reliable basis on which common expectations can be shared regarding specific characteristics of a product, service or process" (BSI 2016).

TABLE 3.1: A few well-known standards organizations

Abbreviation	Name	Country of origin
SABS	South African Bureau of Standards	South Africa
ISO	International Organization for Standardization	International
CEN	European Committee for Standardization	Europe
ASTM	ASTM International	USA
BSI	British Standards Institution	UK
IEC	International Electrotechnical Commission	International
DIN	German Institute for Standardization	Germany
ANSI	American National Standards Institute	USA
UL	Underwriter's Laboratory	USA
ITU	International Telecommunication Union	International

Standards are published by **standards organizations**, which might be national or international in character, or might be established to serve a certain industry. Standards organizations are often known by their abbreviations, and a few of them are listed in Table 3.1. The authors of these standards documents are usually **technical committees**, comprised of individuals from a wide variety of stakeholder organizations, who work towards consensus.

Standards have a unique publication system. They are not published by publishing houses, but by the standards organizations themselves, who sell the documents directly to end users. Each standard is usually also better known by its number than by its title. For example, few people would know that “Quality management systems — Requirements” is the title of the well-known quality system standard usually referred to as ISO 9001. To distinguish between standards bodies and their documents, in this thesis the numbers of technical standards will be rendered in **SMALL CAPS**, e.g. SANS 1935.

The South African national standards body is the South African Bureau of Standards (SABS), which was established by an act of parliament, Standards Act, 1945 (Act No. 24 of 1945), as amended by the Standards Act, Act No. 8 of 2008 (South African Government 2008). The SABS issues South African National Standards.

Standards organizations not only write standards, they might also **adopt** them. Adoption happens when a suitable standard has already been issued by another standards organization. Standards very often refer to other standards, and standards are often based on published academic research. While standards are not mandatory, some legislation might refer to standards.

The desire for engine designers for access to a reliable fuel and for fuel suppliers to have the largest possible market, lead them to cooperate in the development of standards for fuels. In South Africa the relevant standard for petroleum-based diesel fuel is SANS 342, in the USA the equivalent is ASTM D975, and in the European Union it is EN 590. According to the Petroleum Products Act of 1977, as amended, diesel fuel sold to an end-consumer must conform to SANS 342.

Biodiesel is chemically very different from **petrodiesel** (diesel derived from fossil sources), and therefore the technical standards of biodiesel need to be different from the standards for petrodiesel.

3.2 SANS 1935: An overview

The current South African standard applicable to biodiesel is “South African National Standard 1935 Automotive biodiesel — Fatty Acid Methyl Esters (FAME) for diesel engines — Requirements and test methods” (SABS 2008). This is an adoption of the European Committee for Standardization’s (CEN) standard EN 14214 (CEN 2008). In the USA the equivalent standard is ASTM D7651, which is largely similar but of different heritage.

SANS 1935 consists of 18 pages. The first two pages are unnumbered: for the purposes of this discussion they will be numbered in small Roman numerals.

- p(i) The first page is a title page, following the usual format for SABS standards. The top line of the page contains the ISBN (978-0-626-26349-2), and in large type the standard number (SANS 1935:2011). Then follows in capital letters “South African National Standards”, and below that the title “Automotive biodiesel — Fatty Acid Methyl Esters (FAME) for diesel engines — Requirements and test methods”. At the bottom edge of the page we find the SABS logo and some contact information.
- p(ii) The second page is an informational page. It starts with a table of changes, which was still empty at the time of writing. Then follows a foreword in which the technical committee who approved the standard is acknowledged (National Committee SABS SC 1018A). It also gives the date of publication (December 2011) and states that it supersedes SANS 1935:2004. Then there is a very significant line, which states that the standard is referenced in the Petroleum Products Act (South African Government 1977).

p1 Contains the table of contents.

p2 Is left blank.

p3 Paragraph 1: This paragraph describes the scope of the standard, which is that it applies to biodiesel as an automotive fuel.

p3 Paragraph 2: This paragraph lists all the normative standards required to comply with SANS 1935. Thirty-five standards are listed.

p4 Continues the list of normative references.

p5 Paragraph 3: This paragraph contains a list of definitions. The most important one is this: “biodiesel [is a] fuel comprised of methyl esters of long chain fatty acids derived from vegetable oils.” This is a very specific description of biodiesel. It excludes animal fats as a source of fatty acids and it excludes *ethyl* esters. But a note reads “Consideration for the inclusion of ethyl esters, animal fats and C8 – C12 carbon chains should be taken later.” The significance of ethyl esters is that methyl esters are not usually “carbon neutral”, that is, the methanol used in the transesterification reaction is usually obtained from the petrochemical industry, whereas ethanol from fermentation (See Section 1.4.2) could be carbon neutral. The definition also rules out hydrotreated vegetable oil (see Section 1.4.4) or biomass-derived Fischer-Tropsch diesel (see Section 1.4.3).

p5 Paragraph 4: This paragraph lists requirements.

- p5** Paragraph 4.1 discusses general requirements. According to these requirements biodiesel is a homogeneous liquid, free of adulterants or contaminants, to which additives might be added. It provides details regarding testing for oxidative stability and cold-flow properties.
- p6** Paragraph 4.2: This paragraph is about physical and chemical properties and states that biodiesel shall comply to the requirements of Table 1
- p7** Paragraph 4.3: This paragraph concerns methods of testing. It states that test methods shall be one of the test methods listed in Table 1.
- p7-p8** These pages contain Table 1.
- p9** Paragraph 5 describes a few simple rules for packing and marking biodiesel.
- p10-p11** Annex A describes a method for the calculation of iodine value from chromatographic data. This calculation might be used instead of a direct measurement of the iodine value.
- p12** Annex B prescribes how samples for testing must be taken.
- p13** Annex C gives a list of values for calculating precision.
- p14** Annex D provides an approved method for correcting density measurements. The prescribed test requires density to be measured at 15 °C, which might be inconvenient. Instead, a different test may be made at a more convenient temperature and a correction applied.
- p15** Annex E is informative and recommends the implementation of quality management systems. It is followed by a bibliography.
- p16** The final page contains information about the SABS and its services.

3.3 SANS 1935: Properties, requirements and methods.

On studying SANS 1935, it quickly becomes clear that the core of the document is Table 1. This table has three columns. The first column lists a **property**, the second column specifies a numerical value the property has to conform to, the **requirement**, and the third column prescribes the **test method** that must be used to obtain the value.

In the following discussion each of the requirements will be discussed in order of increasing relevance to this thesis, grouped by method of determination (See Figure 3.1).

3.4 SANS 1935: Physical properties

3.4.1 Density

A diesel engine can only deliver work proportional to the heat of combustion of the fuel, and for a given chemical composition the energy will be proportional to the

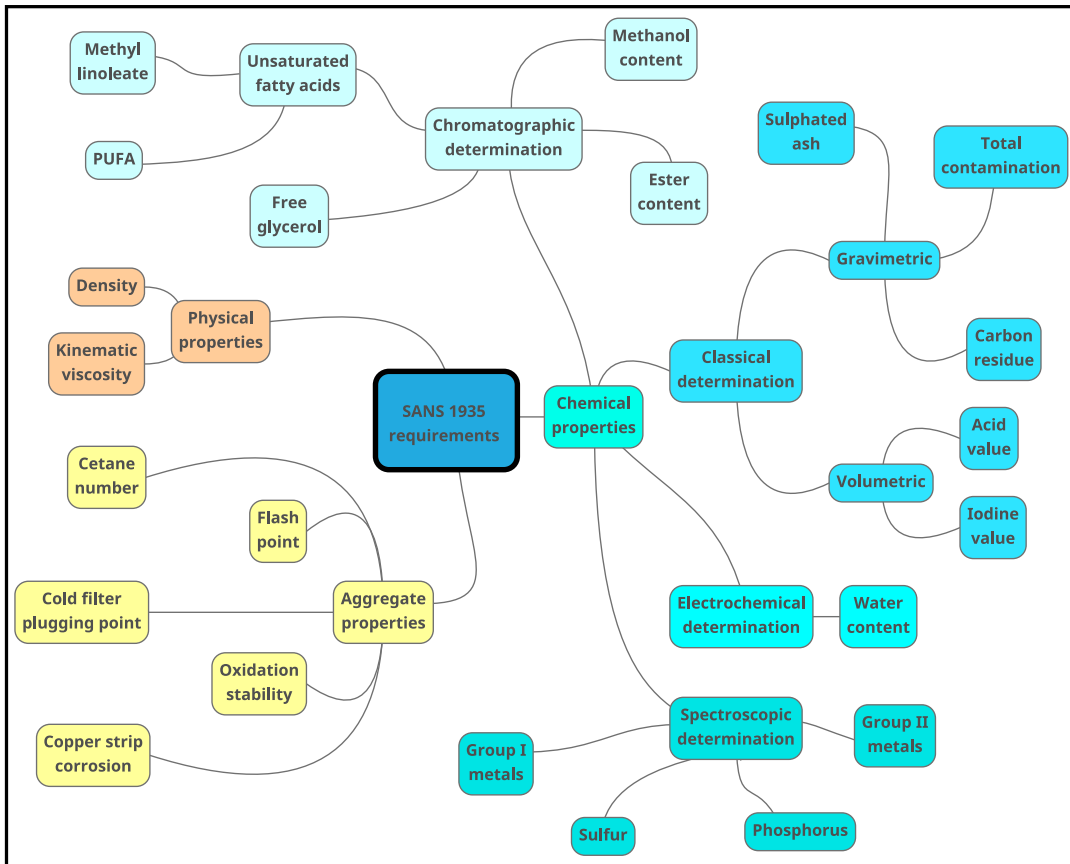


FIGURE 3.1: A mind map showing how the properties of biodiesel assessed by SANS 1935 is grouped for the purpose of discussion in this chapter.

mass of the fuel. But diesel engines inject measured volumes of fuel, not measured masses. (Fuel is also sold by volume, not mass.) Therefore, the stated power output of an engine depends on a specified fuel density.

According to SANS 1935 the density of biodiesel is required to be 860 kg m^{-3} to 900 kg m^{-3} at a temperature of 15°C . The testing methods that can be used are described in ISO 3675 and ISO 12185.

ISO 12185 prescribes the measurement of density by using an electronic instrument known as the oscillating tube density meter. This measures the density of a liquid by measuring the frequency of a freely-oscillating tube filled with the liquid under test. The frequency depends on the mass of the filled tube, and therefore on the density of the liquid. These devices are easy to use and very accurate. The temperature of the liquid is controlled electronically.

ISO 3675 prescribes the use of a hydrometer, which is an instrument that measures density by measuring the buoyant force on a floating indicator. According to the law of Archimedes, the buoyant force on a body immersed in a liquid is equal to the weight of the displaced liquid. If the liquid is denser, the force is greater. Therefore, in a denser liquid a floating indicator will float with more of the indicator above the surface of the liquid. Hydrometer technology is mature, and the devices are simple and robust. If ISO 3675 is used at a temperature other than the specified one, a temperature correction is applied, as described in Annex D.

3.4.2 Kinematic viscosity

The viscosity of a fluid is a measure of its resistance to flow when a force is applied to it. Kinematic viscosity is the resistance to flow of a liquid when it experiences the force of gravity. Flow under gravity of course depends on the density of the liquid, so that kinematic viscosity is determined by measuring the liquid's viscosity and dividing it by its density. The viscosity of a diesel fuel is important, because the fuel must be finely divided for rapid combustion. In the diesel engine this division is achieved by the **injector**, which produces a spray of fuel into the cylinder. The fuel droplet size distribution in the spray is strongly influenced by the fuel's viscosity.

SANS 1935 requires that kinematic viscosity be $3.5 \text{ mm}^2 \text{ s}^{-1}$ to $5.0 \text{ mm}^2 \text{ s}^{-1}$. The measurement method is specified by ISO 3104, which uses a capillary viscometer: the time taken for a fixed volume of liquid to flow through a capillary. This time is then multiplied by an instrument-specific factor to yield the kinematic viscosity.

3.5 SANS 1935: Aggregate properties: Specialized instrumentation

Some of the requirements specified in SANS 1935 are not values that have direct correspondence to physical or chemical quantities usually used in science, but are measures that have proved useful in engineering practice.

3.5.1 Cetane number

For a diesel engine to operate according to design the fuel must combust in a reliable manner. The **cetane number** is a number that indicates the ease of ignition of a fuel in a diesel engine. A higher number indicates easier ignition. Cetane is a synonym for hexadecane, and is a liquid compound that auto-ignites easily when injected into a diesel engine cylinder at high compression and temperature. In contrast, its

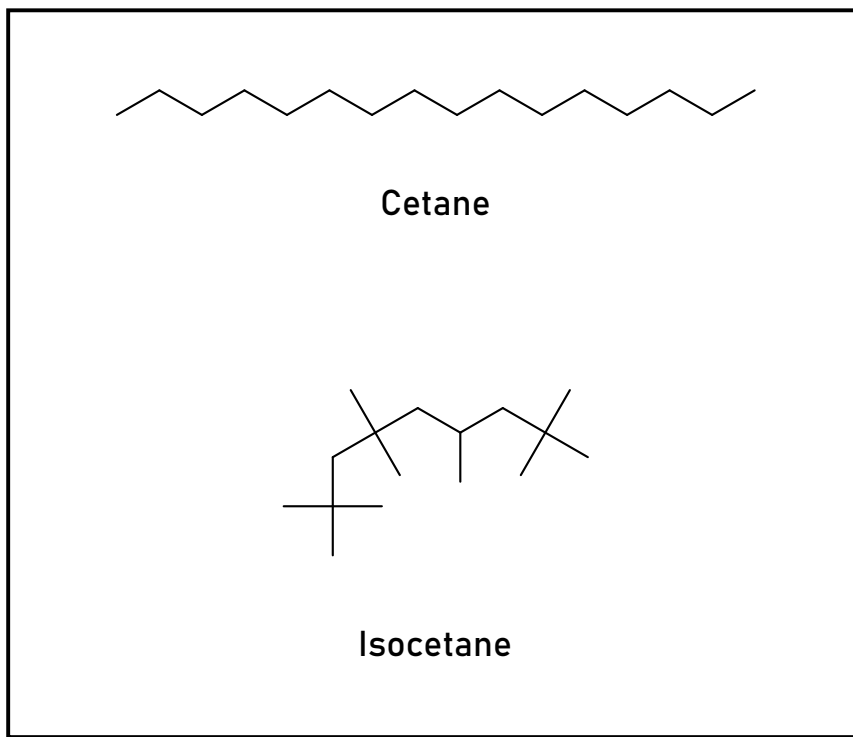


FIGURE 3.2: The chemical structures of the C16 hydrocarbon isomers cetane and isocetane.

highly branched isomer 2,2,4,4,6,8,8-heptamethylnonane (also called isocetane, see Figure 3.2) ignites less easily. The intuitively-understood “ease of combustion” can be quantified as the **ignition delay**, the time between the moment the fuel is injected in to the engine and the moment the ignition starts. A mixture of the two compounds will have an ignition delay somewhere between that of the two compounds.

SANS 1935 prescribes the test method of ISO 5165. The cetane number is obtained by measuring the ignition delay in a highly specialized test engine. The engine is equipped with the necessary instrumentation to measure ignition delay. It is a single-piston, four-stroke engine that has a combustion chamber of variable volume, which gives it a variable compression ratio. While running on the fuel under test, the compression ratio is changed until a prescribed ignition delay is achieved. Then the cetane/isocetane mixture that will give the same ignition delay at that compression ratio is found. If pure cetane will give the prescribed ignition delay, then the cetane number 100 is assigned. If pure isocetane gives the prescribed ignition delay, then the cetane number 0 is assigned. If it is found that a 50:50 cetane:isocetane mixture produces the prescribed ignition delay, then the cetane number 50 is assigned.

Cetane number gives limited insight into the chemical properties of the fuel or the performance of an engine using the fuel, but it is a trusted measure of the suitability of a fuel for use in a diesel engine and is therefore included in the standard. Biodiesel from common feedstocks usually easily meets the cetane specifications.

3.5.2 Flash point

Fuels are, naturally, flammable and different fuels are flammable to different degrees. A fuel’s **flash point** can be used to quantify its degree of flammability. The flash point is the temperature at which a fuel’s vapour at atmospheric pressure will

ignite when it comes in contact with a flame. The inclusion of flash point in fuel technical standards is not primarily concerned with the performance of the fuel inside the engine, but is important to know because it determines how the fuel can safely be handled during transport and storage (Worldwide Fuel Charter Committee 2009).

SANS 1935 specifies that either ISO 2719 (Procedure A) or ISO 3679 be used to determine the flash point of biodiesel. It seems that this aspect of SANS 1935 is out of date, because ISO 2719:2002 has been withdrawn and revised by ISO 2719:2016, which adds a Procedure C, specifically for FAMEs. ISO 2719 specifies the use of a Pensky-Martin closed-cup test, an automated device in which a temperature ramp heats an enclosed amount of liquid, while an ignition source is periodically introduced. The temperature at which the vapour ignites is the flash point. In ISO 3679 the test procedure is similar, but the prescribed device uses a smaller volume of liquid and the liquid and its vapour are considered to be in thermal equilibrium.

3.5.3 Oxidation stability

Fossil fuels for diesel engines are largely composed of alkanes, which are chemically very inert. This means that they can be stored for long periods without significant degradation. Biodiesel, in contrast, is by definition (SABS 2008, Paragraph 4.1.1) mostly composed of fatty acids, which are less inert than alkanes. That fatty acids are liable to oxidation has been known since antiquity: oils and other fatty foods stored for long periods can go **rancid**. In particular, double bonds in the fatty acids will react with atmospheric oxygen (Velasco, Dobarganes, and Márquez-Ruiz 2010) in a series of free radical reactions, illustrated in Figure 3.3. The hydroperoxides that form are highly reactive and can react with other fuel compounds to form polymers, soaps and acids.

The oxidative stability is measured by the Rancimat, an automated instrument. In operation it bubbles a stream of hot air through a sample of biodiesel and then through a conductivity cell filled with deionized water. This air starts oxidizing the sample. Some of the oxidation products are volatile organic acids, which dissolve in the water and increase its electrical conductivity. At the beginning of the test period very few acids are swept into the water, so the conductivity remains low. As the sample oxidizes and produces acids, the conductivity of the water slowly increases. But the oxidation reaction is **autocatalytic**, which means that the products of the oxidation reaction accelerates the oxidation. The result of the autocatalysis is that there is a sudden increase in the slope of the conductivity/time curve. The time taken until this point is reached is called the **induction period**.

SANS 1935 requires a minimum induction period of 6 min at 110 °C. Paragraph 4.1.2 permits the addition of antioxidants, compounds that prevent oxidation.

3.5.4 Cold filter plugging point

The flow of a liquid depends on its temperature. Most obviously, its viscosity depends on the temperature. But a liquid can freeze, which will also influence its flow. The operating temperature of a diesel engine is so high that the temperature of the fuel in the engine will be high enough to guarantee adequate flow for injection, but the biodiesel needs to be pumped from the fuel tank, through a fuel filter, to the engine. If crystals of fuel form at low ambient temperatures, these crystals might plug the pores in the filter, which could lead to fuel starvation in the engine. It is therefore important that the biodiesel can be pumped through the engine's fuel filter at all expected temperatures.

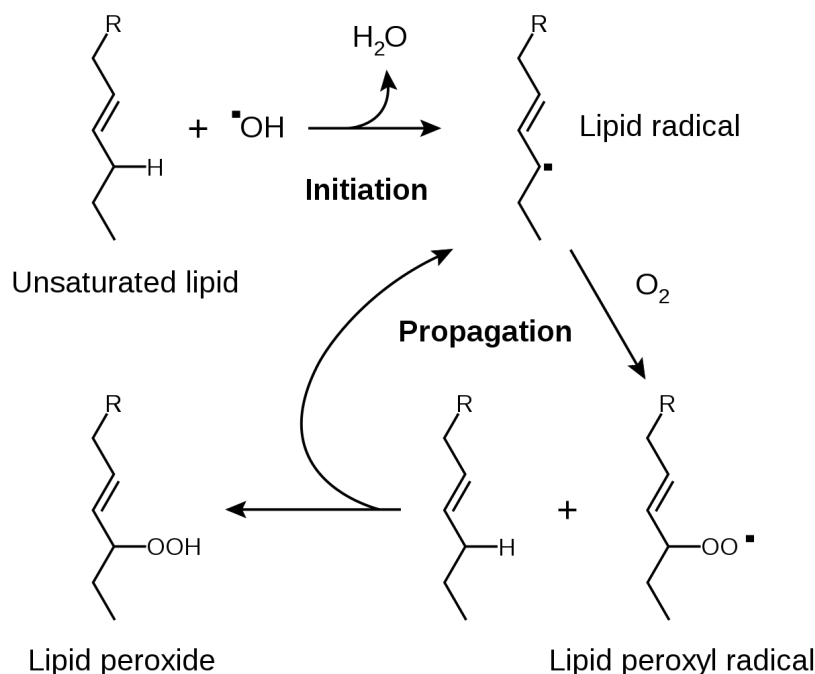


FIGURE 3.3: The peroxidation of lipids. By Tim Vickers, after (Young and McEneny 2001). Public Domain, <https://commons.wikimedia.org/w/index.php?curid=1728531>

For this purpose SANS 1935 specifies a **cold filter plugging point**, measured according to SANS 50116. It is the lowest temperature at which a given volume of biodiesel still passes through a standardized filtration device in a specified time when cooled under certain conditions.

3.5.5 Copper strip corrosion

Many fuel storage and transfer systems parts and engines parts are made of metals, and under adverse conditions those parts are susceptible to corrosion. Corrosion accelerates in chemical environments that include, *inter alia*, acids, water and oxygen, but corrosion is a complex process, so it is very difficult to predict which combination of factors will result in unacceptable corrosion.

SANS 1935 prescribes ISO 2160 as the test for corrosiveness. In this test a strip of pure copper metal is polished and then immersed in a sample of the biodiesel at 50 °C for 3 h. The degree of corrosion is judged by visually comparing it to a standard card and then assigning it to a corrosion class.

3.6 SANS 1935: Chemical properties: Classical determination

3.6.1 Sulfated ash

Ash is the solids remaining after the complete combustion of a fuel. This is measure of the solids that will remain after use. Ash might originate from suspended solids,

soluble metallic soaps, and residual catalyst that form refractory oxides during combustion. In addition to wear and deposits in the fuel system associated with ash, it also impairs modern diesel particulate filters.

SANS 1935 specifies ISO 3987 for the determination of sulfated ash. For the determination of ash it would not be practical to actually combust the sample and weigh the residue, because the ash might be carried away, either as volatile species or as a finely divided aerosol. Therefore the sample is oxidized using sulphuric acid, and then heated to drive off the sulphuric acid. The requirement specifies the mass of the metal oxides that remain.

3.6.2 Carbon residue

When a mixture of organic compounds is heated under conditions of low oxygen, it can form coke. Coke is a solid material composed of practically pure carbon. Pure, solid carbon will combust, but the reaction is kinetically limited, so it will only combust slowly under conditions of high temperature and a large excess of oxygen. If a fuel tends to form coke inside an engine, it can cause problems in operation. When neat vegetable oil is used as diesel fuel, for example, coke tends to form on the engine's injectors (Van der Walt and Hugo 1982). This coking can cause problems with fuel injection, which would affect engine performance. Carbon residue is not a specification based on academic research: from long experience it has been found to correlate with coking tendencies of oils in the petroleum industry, and so found its way into the biodiesel standard.

The test method prescribed for testing for carbon residue is ISO 10370. This involves heating a sample of biodiesel to high temperature in a crucible in air, using standardized apparatus. Most of the sample burns off, leaving a residue. The mass of the residue is determined and reported.

3.6.3 Total contamination

Ideally, biodiesel should be a homogeneous liquid. Some undissolved material can be tolerated, but too much can plug filters. The amount of undissolved solids is termed **total contamination**.

The test of total contamination specified by SANS 1935 is contained in SANS 52662, which is synonymous with EN 12662. In this test total contamination is determined by obtaining the mass of material retained on a glass-fibre filter after passage of the biodiesel sample.

3.6.4 Acid value

The end products of oxidative degradation of biodiesel include free organic acids, so the acidity of biodiesel is a good indicator of its quality. Measuring the acidity gives an indication of how much the biodiesel has already oxidized, whereas the oxidation stability (measured by Rancimat, see Section 6.4.6) indicates how well the biodiesel will withstand oxidation on storage.

SANS 1935 specifies the test described in SANS 54104, which is equivalent to EN 14104. This test is a titration with alcoholic KOH of a sample of biodiesel dissolved in a mixture of solvents. A glass pH electrode connected to an electronic pH meter is used to follow the titration.

3.6.5 Iodine value

As discussed above (see Section 6.4.6) the oxidation of biodiesel is a major quality concern. The tendency of biodiesel to oxidize correlates with the number of double bonds in the fatty acids, or their **degree of unsaturation**.

The degree of unsaturation of oils and fats have long been measured by the **iodine value**, dating from 1884 (Knothe 2007). Halogens will rapidly add to double bonds, so that when a mixture of fatty acids is treated with a known excess of iodinating reagent, the remaining iodine can be titrated to determine the amount of iodine absorbed by the fatty acids. The iodine value is the mass of iodine absorbed by 100 mass units of fat or oil.

The relevance of including iodine value in biodiesel standards has been questioned (Knothe 2002), because all the information regarding unsaturation of the fatty acids in biodiesel is contained in chromatographic data which need to be obtained in other requirements. SANS 1935 seems to acknowledge this, because Annex A allows that the iodine value can be calculated from chromatographic results (see Section 3.9.5).

Because determining iodine value is a mature technology and therefore relatively simple, it is tempting to think of it as a test that might be useful to small biodiesel producers. Unfortunately the iodine value is determined by the feedstock, so that for a feedstock from a certain vegetable oil crop there is unlikely to be any significant variation in iodine value, no matter the production process. Iodine value might be useful as a simple indicator of feedstock quality when the biodiesel is produced from waste vegetable oil, which might contain a variety of oils from different origins.

The prescribed method for the requirement is SANS 54111 (or, equivalently, EN 14111). In this method a known excess of Wijs's reagent (iodine chloride in acetic acid) is added to a weighed sample. The reaction mixture is then treated with potassium iodide, which converts the excess ICl to I_2 , which is then titrated with potassium thiosulfate. The titration is followed potentiometrically and the equivalence point determined from the titration curve.

3.7 SANS 1935: Chemical properties: Electrochemical determination

3.7.1 Water content.

The compounds that comprise biodiesel are much more polar than those of petrodiesel. Therefore, much more water can dissolve in biodiesel than in petrodiesel. This water has several deleterious effects on the quality of biodiesel: it encourages the growth of micro-organisms, allows hydrolysis, and accelerates corrosion. The permitted mass fraction of water specified in the requirements of SANS 1935 is lower than the solubility of water in biodiesel, and therefore refers to dissolved water. Free, visible water is excluded by paragraph 4.1.4.

The method specified by SANS 1935 for the determination of water in biodiesel is ISO 12937. This standard prescribes the well-known Karl Fischer titration used for the determination of water in solvents. This is a **coulometric** titration, which means that electricity is used as titrant. The titration curve is a plot of oxidation potential of a platinum electrode against the amount of charge (current integrated over time).

3.8 SANS 1935: Chemical properties: Spectroscopic determination

3.8.1 Group I metals

The most common catalysts in biodiesel production are sodium or potassium hydroxides (NaOH and KOH) or alkoxides (CH_3ONa and CH_3OK). These catalysts are polar and will dissolve in the glycerol byproduct of biodiesel production. But some may remain in the biodiesel itself and need to be removed. This cleanup can be done by washing with water, adsorbent columns, or selective membranes (Atadashi et al. 2011).

SANS 54108 is the method specified for the determination of sodium, and SANS 54109 the method specified for potassium. Both are flame atomic absorption spectroscopy methods: a sample of the biodiesel is aspirated into a gas flame, where the sodium and potassium are atomized. The atoms will absorb light at certain wavelengths and measuring the amount of light absorbed will give an indication of the amount. Alternatively, EN 14538 may be used to determine sodium and potassium simultaneously with calcium and magnesium (see Section 3.8.2).

3.8.2 Group II metals

Fatty acids neutralized by alkali and alkaline earth metal hydroxides form **soaps**. If these metals are present in the feedstock, as catalyst, or in washing water they can form soaps with the fatty acids in the biodiesel. These soaps can form deposits in engines that can affect operation. For example, deposits of calcium soaps have been reported to cause injectors to stick (Pischinger, Schlag, and Mittelbach 2000).

SANS 1935 prescribes EN 14538 as the method for determining Group II metals. This is an optical emission spectroscopy method: a sample of the biodiesel is diluted in kerosene, and injected into a inductively coupled argon plasma. The emission intensities at certain wavelengths are compared to the emission intensities of solvents containing known concentrations of the metals.

3.8.3 Phosphorus

Phosphorus expected in biodiesel should not affect a diesel engine's performance, but it can have a detrimental effect on the exhaust treatment system by forming ash that can clog filters and reactive species that can reduce catalyst effectiveness. Trace levels of phosphorus will be expected in biodiesel in the bound form of phospholipids found in the feedstock. Normal biodiesel feedstock and production methods should yield biodiesel with acceptable phosphorus concentration, but inorganic phosphorus might be present in biodiesel produced from used cooking oil.

SANS 54107 is the prescribed method for determining phosphorus in biodiesel. A sample of biodiesel is dissolved in xylene, and the solution introduced in aerosol form into an inductively coupled argon plasma. The high temperature of the plasma causes phosphorus atoms and/or ions to emit radiation. This emission is measured at a certain wavelength and compared to emissions from solutions with known concentrations.

3.8.4 Sulfur

The amount of sulfur in biodiesel is limited not because it affects the fuel's performance, but because the fuel must be compatible with emission control systems and

must not emit more sulfur than petrodiesel. Most biodiesel feedstocks are naturally low in sulfur and are therefore unlikely to exceed the limits.

SANS 1935 offers two alternative tests for sulfur. ISO 20846 is a UV fluorescence method, while ISO 20884 is an X-ray fluorescence methods. The quantum-mechanical mechanism is the same for both methods: a chemical species absorbs energy from a photon which puts it in an activated state. The species then returns to a state of lower energy, emitting a photon of different energy. In the case of ISO 20846 the species is gaseous SO₂ (obtained by combusting the sample), and the activating photons are from the ultraviolet part of the electromagnetic spectrum. In the case of ISO 20884 the chemical species are the bound forms of sulfur as found in the biodiesel, and the activating photons are from the X-ray region of the electromagnetic spectrum.

3.9 SANS 1935: Chemical properties: Chromatographic determination

3.9.1 Methanol content

Methanol in biodiesel increases its flash point and is an indicator of poor production process control.

SANS 1935 requires a maximum mass fraction of 0.2 % of methanol in biodiesel. The prescribed test method is contained in SANS 54110, and involves heating a sealed vial partly filled with biodiesel to 80 °C. A portion of the headspace vapour is taken and injected into a gas chromatograph. The amount of methanol is quantified by comparing the methanol peak to either an internal or external standard.

3.9.2 Ester content

As prescribed in Paragraph 3 of SANS 1935, biodiesel must consist of fatty acid methyl esters. The first line of Table 1 quantifies this requirement as a minimum of 96.5 % mass fraction.

The specified method is SANS 54103. This document refers to ISO 5508:1990, which has been withdrawn and superseded by ISO 12966-4:2015. ISO 5508 and ISO 12966 describe gas chromatographic methods for the determination of FAMEs. ISO 5508 is obsolete: it gives conditions for packed GC columns and thermal conductivity detectors, two technologies which are now rarely found in the chromatography laboratory. Both methods, however, require polar stationary phases. The quantity of esters is determined by integrating all the peaks in a certain retention time window and comparing it to the peak area of an internal standard.

3.9.3 Glyceride content

Glycerol (propane-1,2,3-triol) is the “backbone” of the oil molecules that constitute the feedstock for biodiesel production. Each hydroxyl group can form an ester bond with a fatty acid, and when each of the three have a fatty acid bound to it the compound is an ‘oil molecule’. IUPAC recommends that such a molecule be called a tri-O-acylglycerol (Nič et al. 2009), but by long-established custom they are called triglycerides. The conversion of a triglyceride to FAMEs is a stepwise process, with one ester bond at a time being methanolized. This means that during the reaction process, there will also be di- and monoglycerides (di- and mono-O-acylglycerols)

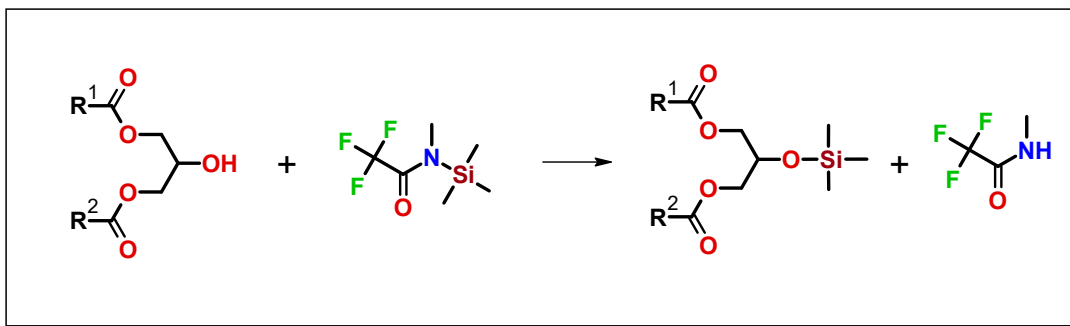


FIGURE 3.4: The derivitization of a diglyceride with N-methyl-N-(trimethylsilyl)-trifluoroacetamide (MSTFA). During GC the inert trimethylsilyl group does not interact with the stationary support, and the volatile trifluoroacetamide elutes with the solvent front.

in the reaction mixture. If the reaction is not controlled to ensure that the reaction goes to completion, these glycerides will be found in the final product. Apart from being an indicator of an incomplete transesterification reaction, the presence of glycerides has further negative effects: during cold weather or in blends with petrodiesel, some dissolved impurities might precipitate, in particular the mono-glycerides (Dunn 2009; Plata, Gauthier-Maradei, and Kafarov 2015). This precipitate might block filters or otherwise interfere with engine performance.

SANS 1935 specifies that the mono-, di- and triglyceride content of biodiesel must be determined by a procedure compliant with SANS 54105 (or, equivalently, EN 14105). In this method, the biodiesel sample is treated with MSTFA (2,2,2-Tri-fluoro-N-methyl-N-(trimethylsilyl)acetamide) before separation by GC. MSTFA is a **derivatization reagent**: It reacts with the hydroxyl groups in the glycerides to form trimethylsilyl derivatives, as shown in Figure 3.4. The molecule is then much more inert and will not interact with the stationary phase support, yielding peaks with better shapes.

The trifluoroacetamide group is a good leaving group, and upon nucleophilic attack by the hydroxyl oxygen its bond with the trimethylsilyl (TMS) group is cleaved, leaving the TMS bound to the oxygen. The labile hydrogen atom is now replaced by the TMS group, which is inert and will not interact with polar entities in the stationary phase or column, which will lead to improved peak shapes.

3.9.4 Free glycerol

Free glycerol is one of the products of the transesterification of plant oils to produce biodiesel. It is a polar compound, which naturally separates from the non-polar biodiesel, and any excess remaining dissolved in the biodiesel is removed during the washing step. Inappropriate processing may leave excess free glycerol in the biodiesel. Free glycerol contributes to injector coking, therefore determining free glycerol is an important quality-control step.

Free glycerol can be determined by the same chromatographic procedure prescribed for the determination of the other glycerides in SANS 54105 (see Section 3.9.3), but SANS 1935 also offers the option of SANS 54016. This standard uses a liquid-liquid extraction of biodiesel with a mixture of ethanol, water, and hexane. The free glycerol transfers quantitatively to the bottom layer, which is then analysed with a gas chromatographic method. The benefit of this method is that the resulting

chromatogram has only one peak, that of glycerol, so quantification is straightforward. The column specified in SANS 54106 method is a **porous layer open tubular** (PLOT) column, *i.e.* a capillary lined on the inside with a layer of particles coated with the stationary phase, in this case a polar polyethylene glycol.

3.9.5 Polyunsaturated methyl esters

The degree of unsaturation of the constituent fatty acids is the main determinant of the oxidative stability of biodiesel. SANS 1935 limits the amount of highly unsaturated FAMEs by two lines in Table 1. In particular, the amount of methyl linoleate is limited to less than 12 % mass fraction, and the amount of polyunsaturated fatty acid methyl esters with four or more double bonds is limited to less than 1 % mass fraction.

Linolenic acid methyl ester

The prescribed method for the determination of methyl linolenate (C18:3) is SANS 54103, the same method as prescribed for total esters (see Section 3.9.2).

Highly unsaturated fatty acid methyl esters

Polyunsaturated fatty acids (PUFAs) with more than four double bonds are not commonly found in plant oils, but are found in algae. Fish that feed on algae accumulate these oils, so that they are also found in fish oils, but fish oil is not a sustainable resource and should not be used for fuel (Kitessa et al. 2014). PUFAs are also highly oxidatively unstable, and therefore undesirable in biodiesel.

The method prescribed for the determination of PUFA FAMEs is EN 15779. This method uses a capillary column with a polyethylene glycol stationary phase.

3.10 Comparison of SANS 1935 and SANS 342

3.10.1 Introduction

SANS 1935 sets the standard for neat biodiesel or biodiesel blendstock in South Africa and SANS 342 sets the standard for petrodiesel. As can be expected, there is considerable overlap of the requirements of petrodiesel and biodiesel, summarized in Figure 3.5.

3.10.2 Comparison

There are 5 requirements for petrodiesel in SANS 342 that have no equivalents in SANS 1935. The first two, labelled “Distillation” and “Recovery” are borrowed from petroleum engineering tests, and are intended to ensure an appropriate volatility range. These two tests fall outside the scope of this discussion.

PAHs

The amount of **polycyclic aromatic hydrocarbons** (PAHs) in petrodiesel is limited by SANS 342 to help control their levels in the environment. PAHs have many sources, including uncombusted petrodiesel.

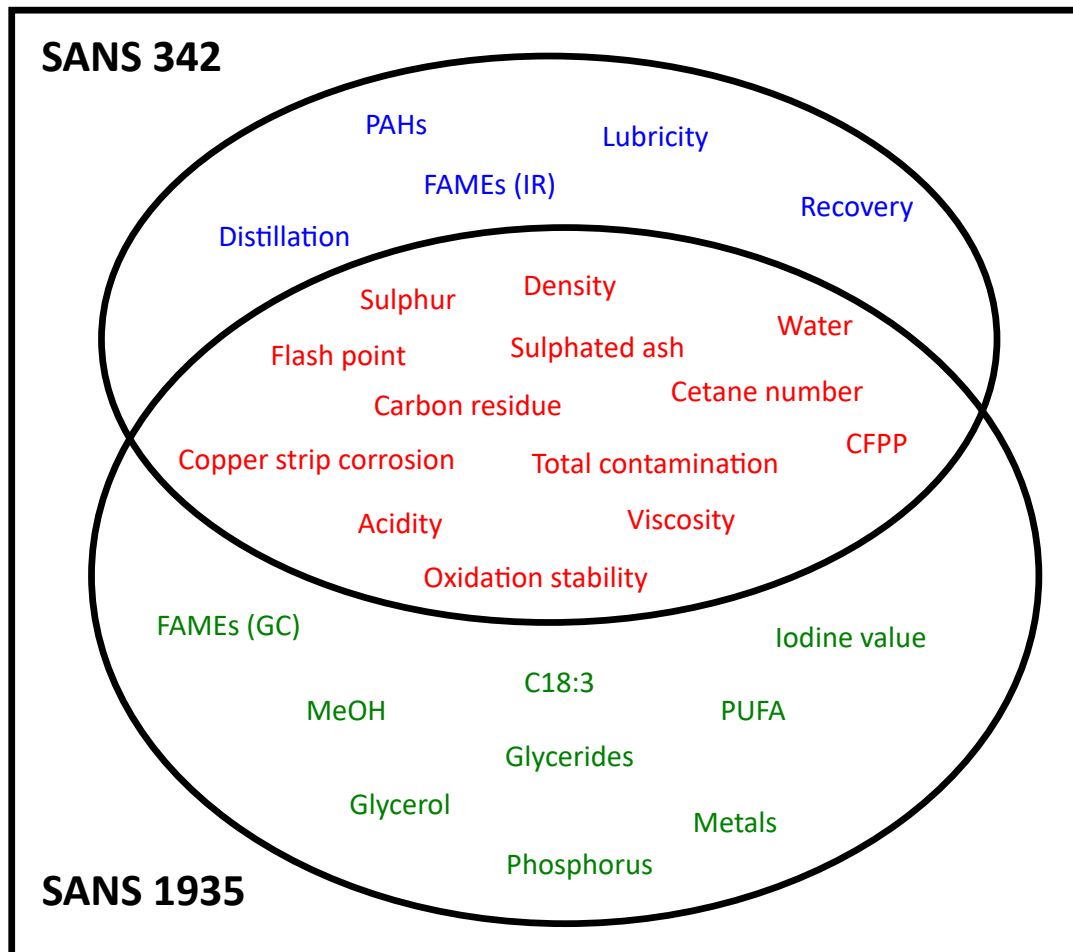


FIGURE 3.5: The overlap of requirements of SANS 1935 for biodiesel and SANS 342 for petrodiesel. PAHs: Polycyclic Aromatic Hydrocarbons, IR: Infrared, GC: Gas chromatography, PUFA: Polyunsaturated fatty acids, C18:3: Methyl linolenate, FAMEs: Fatty Acid Methyl Esters, CFPP: Cold filter plugging point.

Determining FAMES in blends by IR

The Petroleum Products Act allows the blending of up to 5 % of biodiesel with petrodiesel without the need to label it explicitly as a biodiesel blend. The method prescribed by SANS 342 for determining the FAMEs in petrodiesel is EN 14078. This is an infrared (IR) spectrophotometry method: the amount of infrared radiation absorbed by a sample of diesel is compared to the radiation absorbed by solutions containing known amounts of FAMEs. This method is based on the strong absorption of IR the carbonyl group at 1745 cm^{-1} ; of course every fatty acid contains a carbonyl group. Petrodiesel exhibits low absorbance at this wavelength, because petrodiesel contains only trace levels of compounds with carbonyl groups. While this spectroscopic test method can be made very simple, its accuracy depends on certain assumptions about the sample, which might not be valid (Pinho et al. 2014).

Lubricity

The pumps in modern diesel engines generate pressures of up to 2500 bar, which imply that the mechanical parts exert large forces on each other. Metal parts that transmit large forces need to be lubricated to limit wear to acceptable rates. Some of these pump parts are immersed in the fuel, and can therefore not be conventionally lubricated: the circulating fuel will rapidly dissolve and sweep away any grease or lubricating oil. Therefore, the lubrication depends on the lubricating properties of the fuel itself. **Lubricity** is a measure of the lubricating properties of a fuel. It is an aggregate property, and it is quantified by the **wear scar** caused when two metal test parts of specified shape are rubbed against each other with a specified force for a specified duration, while being lubricated by the liquid under test. Such tests are done using special-purpose test machines.

SANS 1935 contains no lubricity requirement, because it has been found that biodiesel always provides adequate lubricity. Also, biodiesel can be used as a lubricity improver in ultra-low-sulphur petrodiesel that might not meet the requirement. This lubricity is not provided by the FAMEs, but by polar impurities in the biodiesel, such as free fatty acids and monoglycerides (Knothe and Steidley 2005).

3.11 Conclusion: room for innovation.

The diversity of chromatographic biodiesel quality control methods implies that the compliance with SANS 1935 can be expensive. To comply, a biodiesel producer will have to submit samples of biodiesel to at least four different kinds of chromatographic analysis:

- EN 14105 for free and total glycerol
- EN 14103 for FAME and methyl linoleate content
- EN 14110 for residual methanol
- EN 15779 for highly unsaturated FAMEs
- (Optionally) EN 14106 for free glycerol

This might prove costly, and there has been at least one innovation to reduce the number of instruments required (McCurry and Norman 2009).

As was emphasized in the introduction to this chapter (see Section 3.1), standards are not ‘the best’ way of determining a certain desirable property of biodiesel, they are merely trusted methods. As improved methods are developed and become trustworthy, they can be adopted as alternatives. As far as biodiesel is concerned, it seems that there is ample room for chromatographers to innovate and develop improved methods and instrumentation. This was the motivation for selecting biodiesel as a practical challenge for developing SFC \times GC.

304.1 K, 7.38 MPa, 0.469 g cm⁻³

The critical temperature, pressure, and density of carbon dioxide.

4

Instrumentation: Supercritical Fluid Chromatography

In this thesis the development of a comprehensively coupled (supercritical fluid × gas) chromatograph and its application to the analysis of biodiesel is discussed. The discussion on the experimental work divides naturally into two parts: this chapter discusses the supercritical fluid chromatography (SFC) and the next chapter discusses the gas chromatography (GC).

4.1 SFC

As discussed in Chapter 2, an SFC chromatograph consists of a supply of mobile phase, a pump, a pressure control system, a modifier control system, a column, a pressure relief system and a detector. These subsystems are discussed below.

4.2 Mobile phase

The benefits of carbon dioxide as a solvent and mobile phase is discussed in Chapter 2. For the research presented in this thesis 99.995 % pure carbon dioxide supplied by Air Products was used. Our colleagues in industry also use food grade or technical grade carbon dioxide and they have not reported any significant impurities.

Methanol was used as a modifier, specifically the LiChrosolv® brand from Merck. This is an 'HPLC-grade' solvent, of which the purification is optimized for the removal of impurities that absorb ultraviolet radiation. Using this grade of solvent is important when using optical absorbance or fluorescence detectors, because lowering the concentration of these impurities improves the limits of detection. It is quite likely that a less expensive grade of modifier would also be suitable for SFC, because optical detectors weren't used.

4.3 Pump

The robust, reliable Varian 8500 HPLC pump was used because it was available. This pump had its control electronics removed and was controlled from a computer. The

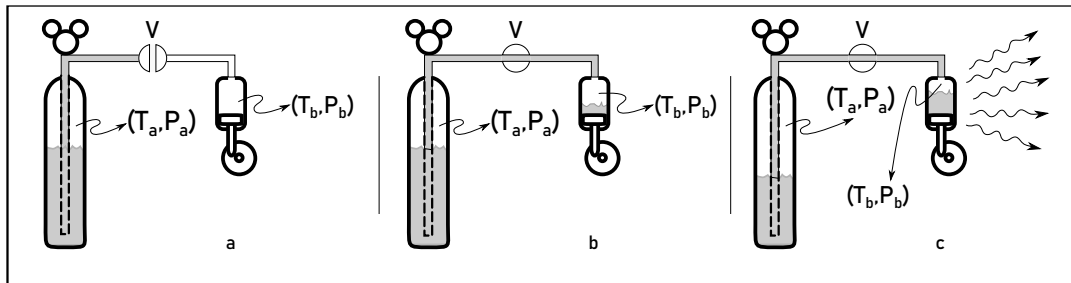


FIGURE 4.1: A schematic diagram of the process of the filling of the carbon dioxide pump. (a) The pressure in the reservoir P_a is much higher than the pressure in the receptacle P_b . The valve is closed, so there is no flow. (b) The valve is open and some carbon dioxide has flowed from the reservoir to the receptacle. But $P_b = P_a$, so there is no flow. (c) When the temperature in the receptacle $T_b < T_a$, then $P_b < P_a$, following Gay-Lussac's law. Flow will continue until all the vapour in the receptacle has condensed.

Varian 8500 pump is driven by a stepper motor. This kind of motor turns in discrete steps instead of at a constant rate. It is driven by pulses of electric current, rather than a continuous current, and therefore the speed of the motor can be controlled by varying the rate of the pulses. This makes it relatively simple to control the speed of the motor from a computer. The Varian 8500 pump has a built-in pressure transducer that provides an electronic signal proportional to the pressure at the pump outlet.

The Varian 8500 pump is a single-piston pump with a 250 ml capacity that needs to be refilled between strokes. Chromatography is not possible during refilling, so to prevent the interruption of chromatographic runs it is necessary to fill the pump to full capacity. It also means that the pump needs to be filled with carbon dioxide in the liquid phase rather than the vapour phase: compressing either phase creates the desired mobile phase, but compressing a vapour leaves a much smaller volume of high-pressure carbon dioxide in the pump than compressing a liquid does.

However, filling a piston pump with liquid carbon dioxide can be a challenge. Imagine a reservoir of liquid carbon dioxide, equipped with a dip tube, connected to an empty receptacle via a valve (V). (See Figure 4.1) One can assume that the receptacle is empty and contains only carbon dioxide vapour at atmospheric pressure, say 1 bar. The vapour pressure of the vapour above the liquid in the reservoir is about 55.3 bar (5.6 MPa). When the valve (V) is opened the high-pressure vapour in the reservoir will expel the liquid carbon dioxide through the dip tube and through the valve, into the receptacle. In the low-pressure environment of the receptacle the carbon dioxide will boil. Soon there will be some liquid carbon dioxide in the receptacle, with the rest of the receptacle volume filled with gaseous carbon dioxide. When the system comes to equilibrium the pressure in the receptacle (P_b) will equal the pressure in the reservoir (P_a), and there will be no flow of liquid carbon dioxide. One can attempt to now increase the flow by increasing the volume of the receptacle (for example by withdrawing a pump piston), and hence decreasing the vapour pressure there. But any flow from the reservoir will lead to expansion of the headspace of the reservoir. This will lead to cooling of the vapour, and therefore lower pressure and therefore lower flow. The final result of this process is that the receptacle is never filled to capacity with liquid.

The only way to restore the flow from the reservoir to the receptacle is to create a pressure difference $P_a - P_b$. While it is possible to create an overpressure in the

reservoir by adding a headspace gas, it is technically challenging and expensive. It is simpler to use the Gay-Lussac gas law. According to this law the ratio of the pressure to the temperature of a gas is constant so that $\frac{P_b}{T_b} = k$. This means that a decrease in temperature will lead to a decrease in pressure. The way to fill the reservoir to capacity is to ensure that the temperature of headspace vapour T_a is higher than the temperature of the headspace vapour T_b . Because safety regulations prohibit the heating of a cylinder of pressurized gas, the way to ensure $T_a < T_b$ is to cool the receptacle. This cools the headspace vapour, and following the Gay-Lussac law the pressure P_b decreases, the difference $P_a - P_b$ increases and the liquid flows until the receptacle is filled to capacity.

In the case of the Varian 8500 pump the cooling of the pump was achieved by pumping a chilled heat-exchange fluid through a coil of copper tubing wrapped around the cylinder. A chiller with a mechanically cooled tank with a 20 l capacity was filled with a solution of 5.01 of diethyl glycerol in about 10 l of water. This mixture has a freezing point of -15°C , which can be cooled by the chiller without freezing. (If the coolant freezes a layer of ice forms on the cooling plate of the chiller, which isolates the remaining liquid from the cooling plate and limits the minimum temperature of the coolant.) An inexpensive submersible water pump (designed for decorative water fountains) was used to pump the coolant through the circuit. This pump can deliver 800 l of water per hour against a hydraulic head of 1.2 m.

For some experiments an SFT-10 pump from Supercritical Fluid Technologies (Newark, Delaware, USA) was used. This is a purpose-built two-piston pump with sapphire valve seats and a Peltier-cooled head. This is much better technology than the HPLC pump. It takes up less space and does not need refilling, since it feeds directly from the cylinder. This pump had its own microprocessor controllers on board so that flow and pressure could simply be commanded from the computer through a USB cable.

4.3.1 Pressure control system

The aim of chromatography is to separate compounds in distance. But the days of separating coloured compounds in glass packed columns are long past and the direct measurement of distances are now relegated to thin-layer chromatography. Instead, proxies for distance such as **retention volumes** or **retention times** are used.

Retention times are particularly convenient today, because they can easily be measured by computer systems. Retention times, however, depend on a known flow rate of the mobile phase through the column. The flow rate need not be constant, although for the sake of simplicity a constant flow rate is preferred. Ideally, the flow rate should also be adjustable. The need for an adjustable, constant flow rate can be met by using a control system. Control systems are well understood by engineers, among whom it is a major field of study (Koenig 2009).

Figure 4.2 shows a diagram of a simple process control system. Some aspect of the process under control is measured, which yields the **process variable** (PV). The PV is compared to the **set value** (SV), and the **error** (e) is obtained by finding the difference. The error is provided to the controller, which calculates the **manipulated variable** (MV). The MV is used to drive the final control element, which adjusts the process with the aim of producing a smaller error.

Chromatographic systems conventionally work under pressure control or flow control regimes. Either is suitable: constant pressure systems usually yield constant flow if other parameters are held constant. Because flow measurement is more complex than pressure measurement, pressure control is the older, simpler and less

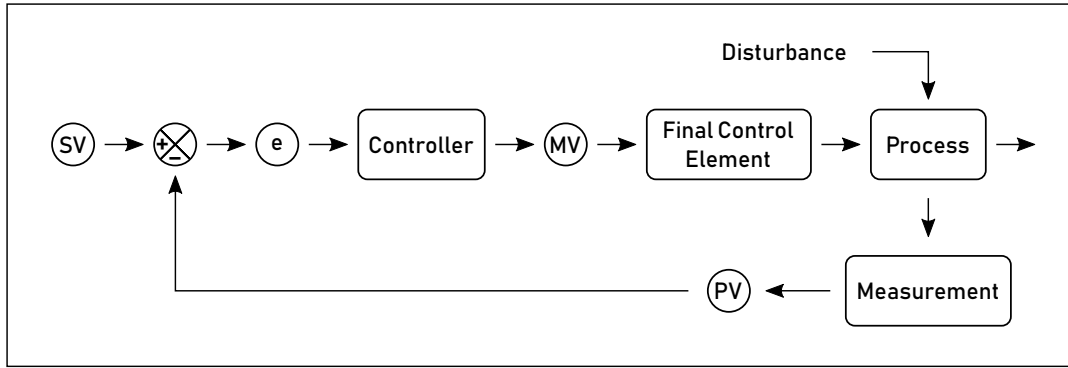


FIGURE 4.2: Schematic diagram of a closed-loop control system. (SV) Set Value, (PV) Process Variable, (e) Error, (MV) Manipulated Variable

expensive control method. Also, in SFC the solvent strength of the mobile phase is pressure/density dependent. Pressure control was therefore used as the control regime.

In our system the pressure measured by the on-pump sensor was the process variable (PV). This was compared to the set value (SV) set on the computer console. The controller was a software algorithm, implemented as a virtual instrument in the programming environment LabVIEW. The controller computed an output value for the manipulated variable (MV), which was the rate at which pulses were sent to the pump, in hertz. The digital input/output (DIO) interface of a National Instruments PCI-6014 multifunction data acquisition board created those pulses and sent them to the pump's electronic interface.

The software used a PID (Proportional-Integral-Derivative) controller module, with the Integral and Derivative contributions disabled. The simpler proportional control was found totally adequate for our purpose, and it can be improved in future by finding an appropriate tuning method and applying it with the integral and/or derivative activated.

4.3.2 Modifier Control

The modifier needs to be present in the mobile phase at a known and controlled concentration. There are various SFC-modifier mobile phase supply units on the market. They tend to be expensive and complex because they require the use of two controlled, high-pressure pumps. Given that our needs were rather modest, we elected to use a simpler system. Instead of accurately pumping the supercritical fluid and the modifier, only the supercritical carbon dioxide was pumped and controlled and measured volumes of modifier was added.

The modifier control unit consisted of a six-port valve, a fixed-volume measuring loop, and a mixing chamber. The unit operates by filling the measuring loop with modifier and then switching the measuring loop into the flowing mobile phase. The modifier is washed into the mixing chamber, where it is intimately mixed with and dissolved in the supercritical carbon dioxide. The concentration of modifier in the mobile phase is determined by the switching rate of the sampling valve. The highest concentration of modifier that can be added in this manner is about 25% because about 3 volumes of supercritical carbon dioxide is needed to wash the modifier out of the loop.

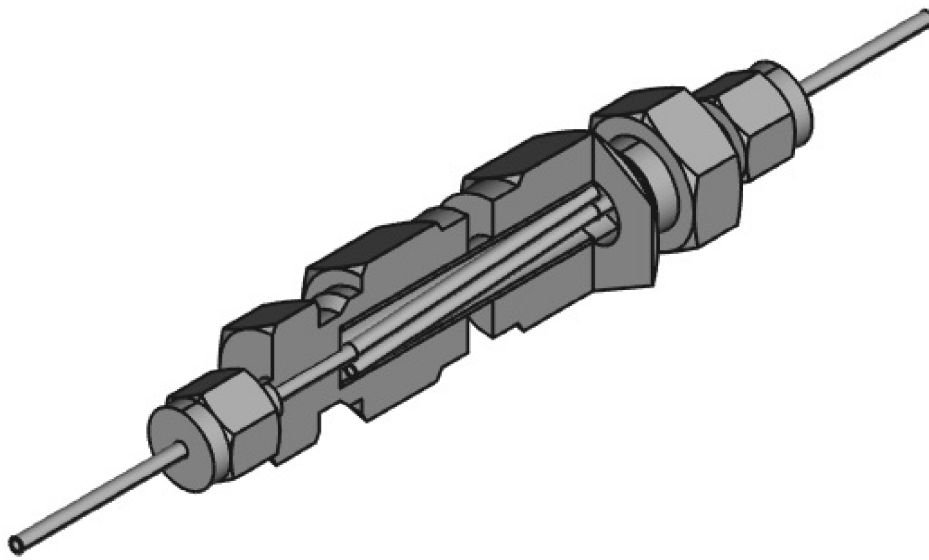


FIGURE 4.3: A cutaway diagram of the mixing chamber design. The chamber is designed for the mixing of the modifier and the supercritical carbon dioxide.

Figure 4.3 shows the chosen design of the mixing chamber. The inlet and outlet pipes of the mixing chamber extend far into the chamber, to break up plug flow and encourage rapid mixing.

The modifier injection valve position was commanded from the controlling computer by electronic voltage pulses.

4.4 Sample injection

The sample inlet was a two-position rotary valve with an internal sampling groove (Figure 4.4). In one position the sampling volume is filled with a syringe. When the valve is commanded to switch to the other position the valve rotates to a position where the carrier stream flows through the sample groove and the sample is swept out of the valve. The sample volume was $0.5 \mu\text{l}$. The injection valve position was commanded from the controlling computer by electronic voltage pulses.

The six-port valve with an external sample loop is an alternative injection system. The benefit of the internal groove injection valve is that it allows a much smaller volume to be injected. Using this small volume makes it possible to inject samples without dilution, which simplifies sample preparation. A drawback of the internal groove design is that it is not possible to vary the volume of sample injected.

4.4.1 Column

The separation power of a chromatographic system can be modelled by the equation

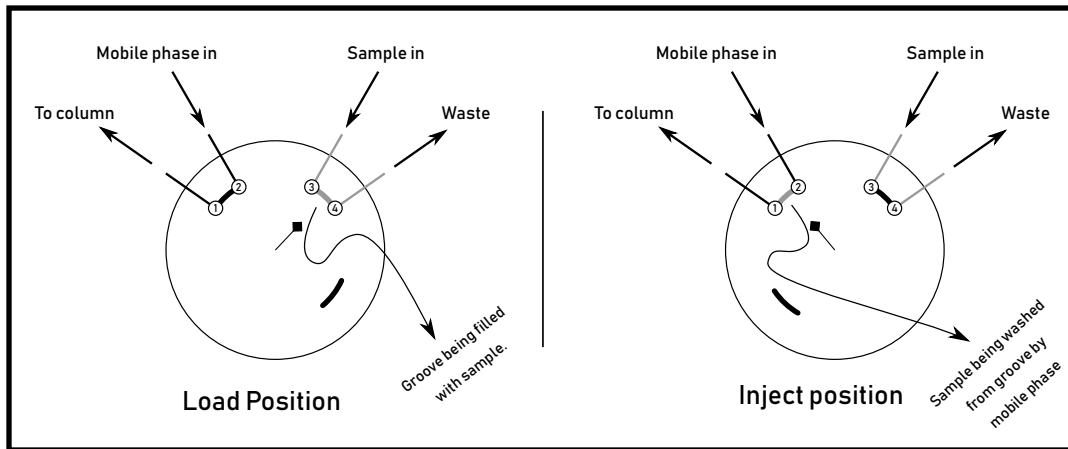


FIGURE 4.4: A schematic diagram of the sampling valve.

$$R_s = \left(\frac{\sqrt{N}}{4} \right) \left(\frac{\alpha - 1}{\alpha} \right) \left(\frac{k'}{1 + k'} \right)$$

where R_s is the **peak resolution**, N is the **number of plates**, α is the **selectivity**, and k' is the **retention factor**.

The number of plates N can be increased simply by making the column longer at the cost of increasing the time of the run. The maximum length of the column is determined by the pressure drop available that will still yield adequate flow. In capillary gas chromatography the openness of the column and the low viscosity of the gas-phase mobile phase routinely allows columns 100 m long at inlet pressures of a few atmospheres. In HPLC the high viscosity of the mobile phase and the narrow, tortuous pathways between the small particles of the packing material means that the columns are typically 100 mm to 200 mm long, requiring hundreds of atmospheres of inlet pressure for adequate flow.

The low viscosity of an SFC mobile phase allows the use of packed columns much longer than those usually found in HPLC. This provides a much higher number of plates in the chromatographic system than HPLC. The SFC column used in the SFCxGC system was a set of five HPLC columns (150 mm × 4.6 mm, 3 µm particles) (Restek, Pinnacle DB Silica) connected in series.

The stationary phase in this column is 'bare silica', which is usually considered 'polar'. This means that the packing of the column consists of porous silica particles with no organic phase covering its surface, and hence one that will interact strongly with polar molecules. In contrast, the ubiquitous 'C18' stationary phase used in reverse-phase HPLC is 'non-polar'. The particles of such a stationary phase are coated with octadecyl chains bonded to its surface, and hence will tend to interact strongly with non-polar molecules. The base material of the particles is usually silica, but that is only because manufacturing uniform particles of a given size from silica is a mature technology and not because silica is important to the separation mechanism. (In fact, some care has to be taken to deactivate the silica so that it does not contribute to the retention. Such a mixed retention mechanism can lead to **peak tailing**.)

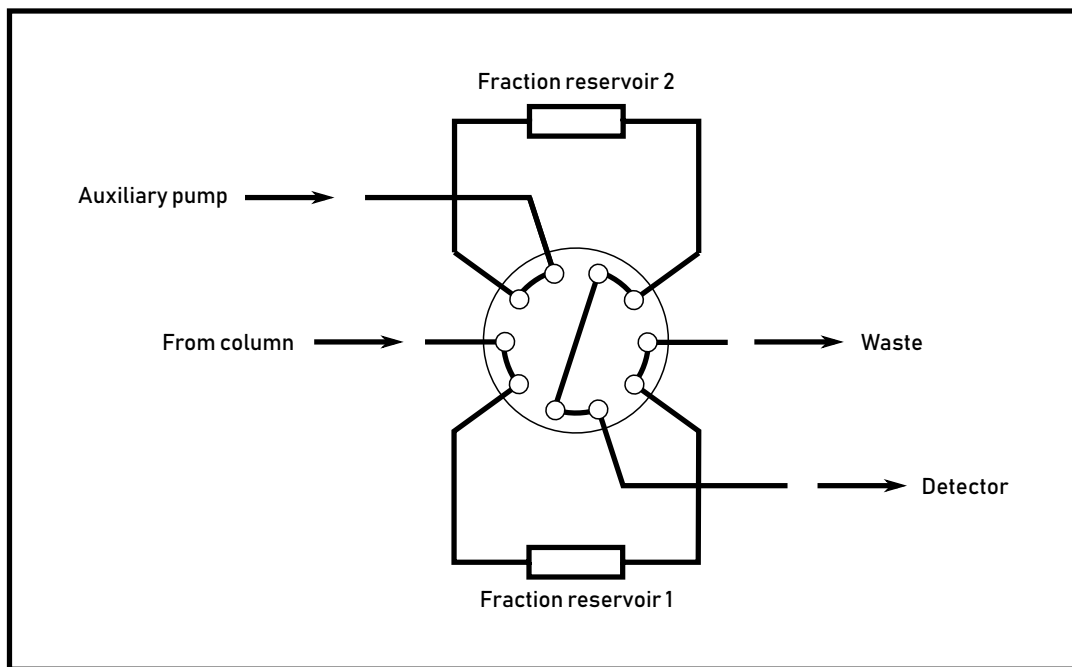


FIGURE 4.5: A schematic diagram of a valve configured to allow continuous-flow fraction collection.

4.4.2 Stopped-flow

Among analytical chemists it is the convention that chromatographic runs are done without interruptions. The SFC \times GC chromatograph collected fractions of SFC eluate and separated them by GC. It is possible to collect, store and inject fractions of SFC eluate while maintaining continuous flow, for example using a dual storage loop system like the one depicted in Figure 4.5. But such systems require careful selection of volumes, fraction collection reservoirs with matching volumes, and an auxiliary pump.

Instead of such a system, a more versatile and simpler stopped-flow system was chosen. In this system a fraction of the SFC eluate is collected, and then the flow through the column is stopped. While the flow is stopped the collected fraction is subjected to separation by GC. The flow was stopped by a six-port rotary valve using three of the ports, directing flow either to a blocked-off port or to the depressurizer, in effect making it an on-off controller.

In packed columns, "eddy diffusion is always the main cause for peak broadening at any temperature and at high velocities" (Gritti and Guiochon 2006). During the period that the flow is stopped only longitudinal diffusion contributes to peak broadening, which is small compared to eddy diffusion in dense mobile phases. Using the simple stopped-flow technique of sample collection will therefore not have a major effect on the resolution of the ^1D chromatography.

4.5 Pressure Relief

No matter the kind of SFC system one uses, at some point the eluate needs to be depressurized. This can be before or after the detector. If depressurization happens

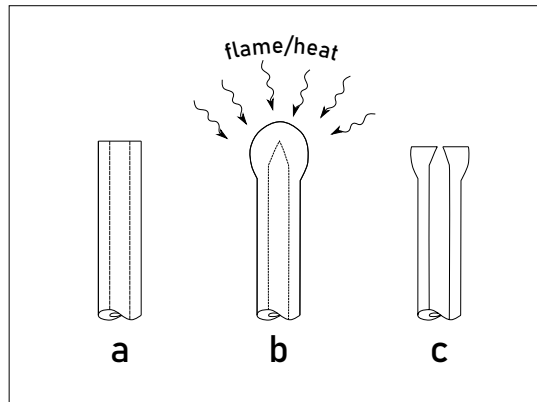


FIGURE 4.6: The steps of making a Guthrie restrictor. (a) Cut length of quartz capillary (b) Heat with flame to soften glass and create internal cone (c) Grind down end to expose orifice of the appropriate size.

after the detector, the details of the mechanism don't matter much, because the information has been obtained and the eluate can be discarded. If, as in our case, the depressurized eluate needs to still pass the detector, it is important to not lose the resolution achieved by the column. This means that the design of the depressurizer requires some care.

The main concern in depressurizer design is premature desolvation of analytes. This causes **discrimination**, which is the differential treatment of substances where identical treatments are required. In particular, compounds of higher molecular weight tend to desolve first from the supercritical fluid, and might precipitate in the wrong place if the depressurizer is not designed to prevent it.

Depressurization can be done either statically or dynamically. In a dynamic system there is an active element that controls the flow of the eluate in such a way as to maintain the pressure upstream of the active element of the controller. Such a device is often called a **back pressure regulator**, and is usually an electromechanical device with digital control. They tend to be complex and expensive.

In static depressurization there is no active pressure control. A simple **restrictor** is used to limit the flow between the high pressure of the SFC and the low-pressure outlet. Textbooks often discuss different restrictor designs. (The book by Luque de Castro, Valcárcel, and Tena 1994, provides an example.). Our preferred depressurizer was the 'integral' or Guthrie design (Guthrie and Schwartz 1986). Figure 4.6 shows the steps in manufacturing the Guthrie restrictor.

This restrictor design is robust and fairly simple to manufacture. It was possible to adjust the flow to a given flow rate. This design of restrictor should eliminate discrimination, because the decompression takes place in a very short space.

However, the Guthrie restrictor design proved prone to blockage. Blockages are usually attributed to particles, but incorporating a $0.5\text{ }\mu\text{m}$ filter before the restrictor did not eliminate or reduce the blockages. This prompted a structured investigation into the cause of blockages. To rule out the possibility that it was particles that caused the Guthrie restrictor to become blocked, the diameter of the orifice had to be determined. This proved to be harder than expected: optical microscopy was not able to give a simple, unambiguous measure of the orifice diameter. Scanning electron microscopy (SEM) showed that the orifice diameter of a Guthrie restrictor is about $10\text{ }\mu\text{m}$, as shown in Figure 4.7. This makes it very unlikely that particles with

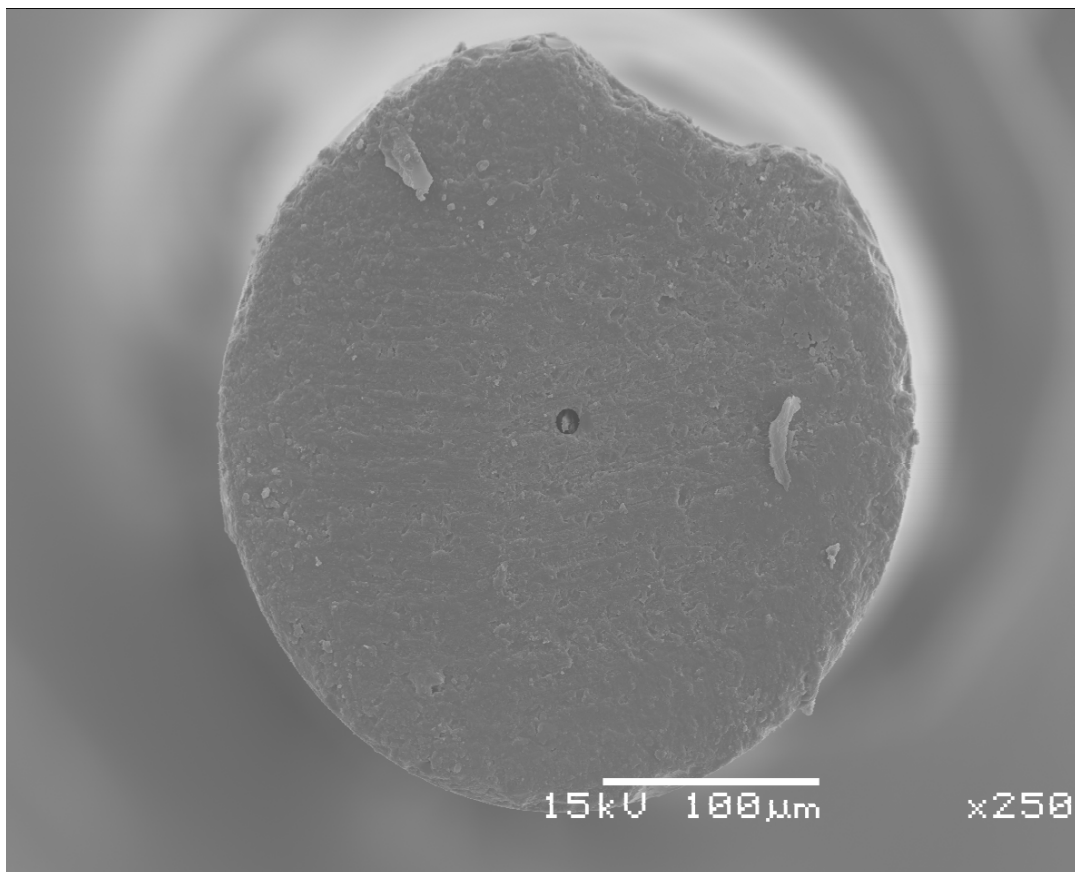


FIGURE 4.7: An electron micrograph of a restrictor tip, showing the size of the orifice.

an origin in the SFC system blocked the restrictor: even the $3\text{ }\mu\text{m}$ particles from the column packing material should not block this restrictor.

Experience had taught us that the restrictor did not block if the flow was continuous. It was only when the pressure in the restrictor cycled that blockages occurred. To eliminate the possibility that it was material from the stop valve (see Section 4.4.2) that caused the blockages, the pressure was cycled by switching the pump on and off, allowing the pressure to bleed off through the restrictor. This way of cycling the pressure did not prevent blockages.

Examining the blocked restrictors with an electron microscope revealed that the restrictors became blocked by a soft material. Backscatter SEM mode allows the energy of X-rays to be measured by energy-dispersive spectrometry, which yields information about elemental composition. While much care must be taken before this information can be used for quantitation, it revealed that the deposited material contained significant quantities of carbon and oxygen, and possibly some chlorine. This points to the probability that the material blocking the column is organic in nature and possibly polymeric. See Figure 4.8.

The origin of the material was not identified, but it seems likely to be the column, because cycling the pressure without a column did not cause a blockage. The blockages did not have an origin in the modifier, because no modifiers were used. The possibility of blockage by sample material was eliminated by using a brand new column. The suspicion is that the blocking material might be remnants of surfactants used in the synthesis of the silica gel stationary phase. These surfactants are

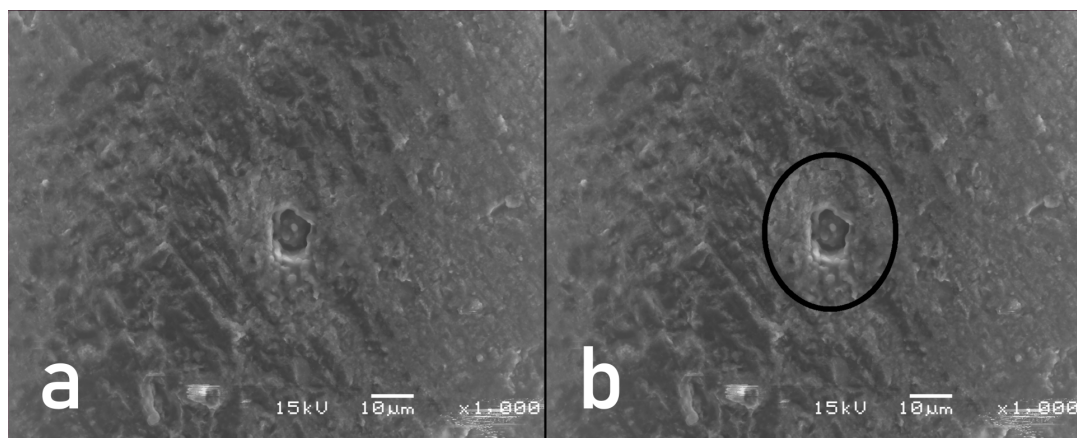


FIGURE 4.8: An electron micrograph of a blocked restrictor orifice. (a) Original image (b) Image with black circle showing estimated original orifice location

leached out of the column packing by the highly diffusive supercritical fluid mobile phase, and they then precipitate in the restrictor when the pressure drops and the compounds desolvate. Repetitive pressure cycles causes a build-up of material which gradually blocks the orifice.

The smallness of the orifice contributes to the plugging problem. With a diameter of 50 μm, a solid sphere that fits in this capillary will have a volume of 0.065 nl, or 65 pl. This means that nanogram quantities of material can easily block the restrictor.

Being satisfied that an unfortunate combination of restrictor design and column packing was the likely cause of the blockages, a different restrictor design was chosen. The choice was a simple linear restrictor, and the heat of the hot GC inlet was trusted to prevent discrimination. The final linear restrictor was a 800 mm long fused silica capillary with an internal diameter of 0.050 mm.

4.6 Detector

When SFC was first developed, a capillary column was the usual column and an FID was the usual detector. In current use, however, packed columns used with mobile phase modifiers predominate and flame detectors have lost their place: the high concentration of modifiers in the mobile phase would swamp the signal from analytes or saturate the detector. Therefore modern SFC predominantly uses UV/Vis optical detectors.

In the supercritical fluid chromatograph described in this chapter there was no dedicated detector: the role of the detector was taken by a gas chromatograph. This gas chromatograph collected fractions from the SFC and separated them in fast chromatographic runs, detecting the analytes with an FID, yielding comprehensive 2D chromatograms. This chromatograph-as-a-detector is described in Chapter 5.

There are no significant technical limitations to column temperature programming in the order of a few hundred degrees per minute and equally rapid cool-down rates.

Wolfgang Bertsch, 1997

5

Instrumentation: Fast temperature programmed gas chromatography

The topic of this thesis is the development of a comprehensively coupled (supercritical fluid \times gas) chromatograph and its application to the analysis of biodiesel. The discussion on the experimental work divides naturally into two parts: the topic of the previous chapter is supercritical fluid chromatography (SFC) and of this chapter it is gas chromatography (GC).

5.1 Speed of analysis

The coupling between two chromatographs can be called **comprehensive** if it meets the following criteria (as discussed in Section 2.3.2):

1. Every part of the sample is separated by two distinct chromatographic processes.
2. Equal percentages of all sample fractions are separated by the second process.
3. Compounds resolved by the first dimension separation remain resolved.

In principle, such a coupling could be implemented by manually or mechanically collecting equal-sized fractions from a first ^1D chromatograph, and then injecting a portion of each fraction into a different (^2D) chromatograph. In practice, such an approach would be slow, labour-intensive, expensive, and error-prone. But reliable devices that can repeatedly collect and re-inject fractions of eluate were invented. These devices became known as **modulators** and made comprehensively coupled chromatography practical. In continuous flow coupling, such as that found in GC \times GC, the fraction collection and ^2D injection happens during the uninterrupted ^1D separation. In stopped-flow coupling as used in the SFC \times GC chromatography described here, the ^1D SFC separation is stopped after a fraction has been collected. This fraction is separated on the ^2D GC column. After the ^2D run is complete the SFC run is resumed and the next fraction is collected.

Fractions of the ^1D separation are collected at a rate which is determined by the peak width on the ^1D chromatogram. To get adequate peak detection in the ^1D

chromatogram, at least 3 fractions of each ^1D peak should be collected (Murphy, Schure, and Foley 1998), but more would be better. For example, if the peaks are 3 s wide the collection rate should not be less than 1 Hz. The rate of fractions collection is known as the **modulation rate** and its inverse is the **modulation period** (P_M). In continuous-flow coupling (e.g. as found in GC \times GC), the ^2D separation should be completed in a time less than the modulation period. Evidently, this means that the ^2D separation should be faster than the ^1D separation.

In stopped-flow coupling, the duration of the ^2D separation is largely decoupled from the peak width of the ^1D separation and, by implication, the ^1D modulation period. In terms of the third criterion of comprehensive coupling listed at the start of this section, as long as the resolution obtained in the ^1D separation is not lost during the stopped-flow period, the duration of the ^2D separation can be as long as it needs to be. In SFC the longitudinal diffusion is low, so that in principle the ^2D GC runs in SFC \times GC need not be remarkably fast. In practice, however, **sample throughput** of a chromatographic method needs to be acceptable. One of the major determinants of sample throughput is **run time**, the time it takes from when the sample is injected until the final compound has eluted. The judgement of what is acceptable depends strongly on context: for finding the proverbial biomarker for Alzheimer's disease very long run times might be acceptable, but for routine analysis of a commodity biodiesel acceptable run times would probably be short. Therefore, when developing a practical SFC \times GC chromatograph the aim should be to make run times as short as possible.

The time it takes for a stopped-flow SFC \times GC run can be calculated from

$$t_T = t_{1D} \left(1 + \frac{t_{stopped}}{P_M}\right)$$

where t_T is the total time, t_{1D} is the run time the unmodulated ^1D run would take, P_M is the **modulation period**, and $t_{stopped}$ is the duration of the SFC stopped-flow state, during which the ^2D run is completed. With continuous-flow coupling (as in GC \times GC) $t_{stopped} = 0$, so that $t_T = t_{1D}$.

Examining the expression shows that we can decrease t_T by increasing P_M , but there is limit to this: as the modulation period becomes longer the separation obtained in the ^1D separation is decreased when fractions start including first portions of two adjacent peaks and then more than one peak. So, the only way to decrease the total run time is to reduce $t_{stopped}$, the GC run time. For example, if a typical SFC run takes 20 min and fractions are collected for every 5 s of SFC run, it means there will be $20 \times 60 / 5 = 240$ fractions collected. Each of these fractions must be injected into a GC chromatograph. If each GC run took 1 min, the SFC \times GC run would last $240 \text{ min} = 4 \text{ h}$. This is a very long run time, and in the context of commodity biodiesel analysis the sample throughput of such a chromatograph would probably be judged unacceptable.

Reducing the run time of the ^2D GC chromatography in SFC \times GC means applying the concepts of **fast chromatography**. Fast chromatography is the discipline that studies the theories, experiments, and technologies that shorten chromatographic run times.

5.2 Fast gas chromatography theory

Improving the speed of chromatographic separations is an aspect of **optimization**. Optimization can be defined as "the action of making the best or most effective use of

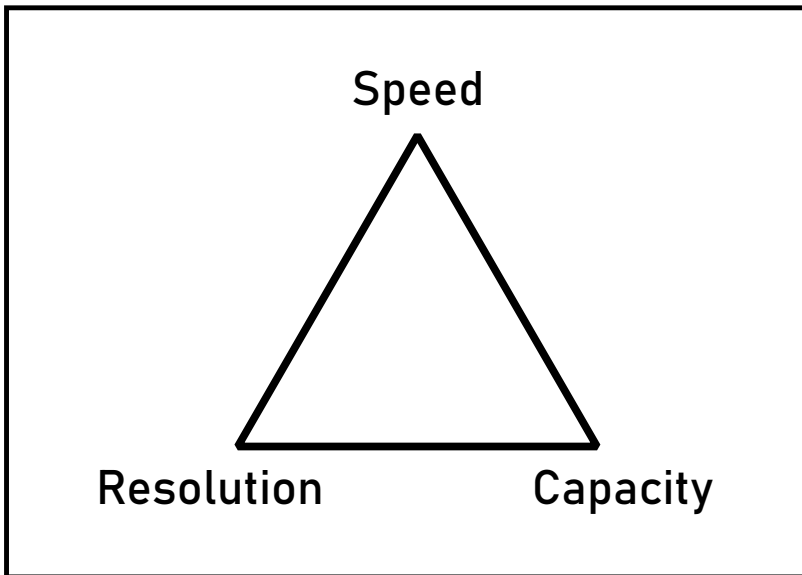


FIGURE 5.1: The chromatographer's trilemma.

a situation or resource" (Oxford University Press 2019). "Making the most effective use" means that optimization has a **goal**, which can be characterized by a numerical **criterion** while subject to some **constraints**. The relative and variable amount of "resources" used are **optimizing parameters**.

There are two kinds of optimization in chromatography: selectivity and kinetics. The difference between them is not the goal of the optimization, but how the optimizing parameters are selected. **Selectivity optimization** is the process of selecting the best combination of stationary phase and analyte. The optimization parameters are the different stationary phases and derivitization methods available. **Kinetics optimization** is the process of selecting the best combination of carrier gas, temperature, flow rate, column length, column diameter, and stationary phase thickness. This differentiation between selectivity optimization and kinetics optimization is not made on theoretical grounds, but for practical reasons: selectivity optimization often involves the discrete and expensive parameter of selecting a column, whereas the parameters involved in kinetics optimization can often be adjusted continuously and inexpensively. Selectivity optimization is guided by chemical thermodynamic knowledge; kinetics optimization is guided by **chromatographic rate theory**.

Every chromatographer involved in a kinetics optimization has met the chromatographer's trilemma (See Figure 5.1): Any chromatographic method that involves decisions about speed, resolution, and capacity can optimize only one at a time¹. The fastest chromatography will have low capacity and low resolution, the chromatography giving the highest resolution will be slow with low capacity, and the chromatography of a sample with a large amount of analyte will be slow and have low resolution (Klee and Blumberg 2002). One way the chromatographer can ease the grip of the trilemma is to decide what factor is least important for the current problem, pick a value that is likely to satisfy most conditions, keep it fixed, and then find an acceptable compromise between the other two. In the development of the SFC \times GC it was decided to work with a fixed sample capacity: a capillary column

¹This trilemma applies only to capillary chromatography. When using packed columns, the capacity can be readily increased by using a column with a larger diameter and a larger amount of packing.

with a 0.25 mm internal diameter and a 0.25 µm stationary phase was chosen. With the sample capacity held constant, it is now possible to optimize the system so that it gives adequate resolution in the shortest possible time.

The **efficiency** of a column is given by the relationship $E = \frac{t_R}{\sigma}$, where t_R is the **retention time** of a peak, and σ is its standard deviation, related to the **peak width** (Blumberg 2018). The efficiency is a measure of how much the peak spread during its transport through the column relative to distance it travelled, using time as a proxy for distance. Efficiency is related to the more traditional but less intuitive **number of plates** N through the expression $N = E^2$. The length of the column (L), divided by the square of the efficiency gives the **plate height** (H). Plate height is a measure of how much each unit of length of the column contributes to the separation: a lower H means that the separation is more effective. The value of H in chromatographic theory is that equations can be developed that express H as functions of the adjustable parameters of kinetics optimization. Such functions help predict suitable chromatographic conditions and set limits to the expected performance of the separation.

Any chromatographic optimization goal must contain resolution as part of the criteria. After all, the purpose of the activity is the separation of chemical compounds. Traditionally, the first optimization taught is the optimization of H as criterion, with the rate at which the carrier gas passes through the column as the variable parameter. The rate can be characterized by either the average gas velocity (\bar{u}) or the gas volume flow rate (F). Traditionally \bar{u} has been used, because it can be conveniently calculated from simple measurements: $\bar{u} = L/t_m$, where t_m is the **void time**, which is easily determined by measuring the retention time of an unretained compound. In modern gas chromatographs F can be continuously controlled by electronic pneumatic control (EPC) systems, and has become a more convenient parameter.

Blumberg has developed the theory of optimized flow rate (Blumberg 1999). He found that the function that describes plate height in terms of flow rate can be simplified to two cases: a high-pressure drop and a low-pressure drop. (A high pressure drop is defined as the case when the difference in pressure between the inlet and outlet is much greater than the outlet pressure, $\Delta p \gg p_o$). When the pressure drop is low

$$H = \frac{b}{F} + (c_1 + c_2)F$$

and when the pressure drop is high

$$H = \frac{9}{8} \left(\frac{b}{F} + c_1 F \right) + C_2 \sqrt{F}$$

where c_1 , c_2 and C_2 are constants independent of F .

When the layer of stationary phase is thin, also known as the **thin-film case**, then $c_2 = 0$ and $C_2 = 0$, and

$$H = \frac{b}{F} + c_1 F$$

for the low pressure drop case and

$$H = \frac{9}{8} \left(\frac{b}{F} + c_1 F \right)$$

for the high pressure drop case. The low pressure drop case will be immediately recognized as the **van Deemter equation**, and the high-pressure drop case differs from it only by a factor of 1.125 (See Figure 5.2).

It is clear that the function has a minimum. The flow rate at this minimum H can be called $F_{H\min}$. This flow is called **efficiency-optimized flow**, EOF. A remarkable feature of this theoretical result is that it is independent of column length (Blumberg

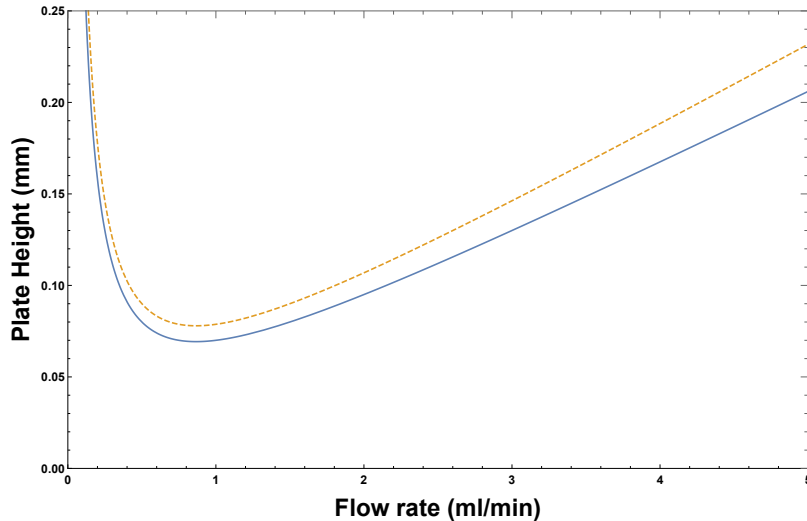


FIGURE 5.2: A plot of H vs. F . The solid line represents the low pressure drop case, and the dashed line the high pressure drop case.

1999) even at appreciable pressure drops. In contrast, the **efficiency optimized velocity** (EOF) depends on the column length when the pressure drop is high (Blumberg 1997). Because $E = \sqrt{\frac{L}{H}}$ it means that any necessary resolution can be obtained by making the column as long as necessary. This theoretical result is supported by experiment: the world record for the longest capillary column is 1300 m. “This column produced excellent resolution of a petroleum sample, but took 3 hours to elute methane and 3 days to elute the last peak” (Ferguson 2013). Reducing the column length while keeping EOF will reduce the column efficiency, although the plate height will remain constant.

In this study the aim is to reduce the time it takes to complete a run, and therefore the question is not what the best possible efficiency is, but what the shortest time is in which a specified efficiency can be maintained. The remarkably simple theoretical result is that under **speed-optimized flow** (SOF), $F = \sqrt{2}F_{H\min}$ (Blumberg 1997). Because this flow is higher than the EOF, H is larger, but this can be compensated for by increasing N , which is implemented by using a longer column. For a given solute, column diameter, stationary phase and carrier gas there is no flow that will yield a faster separation without reducing the efficiency of the separation.

The remaining parameters that can be manipulated during kinetics optimization for speed are column diameter and carrier gas diffusivity. The theoretical details will not be discussed here, but it will be clear that optimizing for separation speed tends towards the selection of narrow-bore capillary columns and using hydrogen as a carrier gas. The theoretical study of optimization gives great insight into which parameters to choose, but the actual calculation can be tedious, so for practical purposes the use of online method translation calculators is recommended (Restek Corporation 2014).

SOF improves the speed of analysis by finding the combination of parameters F and L that will give the fastest separation under the constraint of constant H . If the constraint on H is relaxed, a faster separation can be achieved. Assuming that it is not possible to optimize the selectivity further (for example because the stationary phase cannot be changed), there are only two ways to relax the plate height constraint: **selective detection** and **sample cleanup**. In selective detection a detector is

chosen that only responds to the analytes, and not to any interfering compounds. For example, an **electron capture detector** (ECD) responds strongly to halides, so a GC-ECD chromatogram of a soil extract will be much simpler than the equivalent GC-FID chromatogram, which means that the GC-ECD analysis of chlorinated pesticides in soil can be much faster than the equivalent GC-FID analysis. GC-MS using **single ion monitoring** (SIM) also enables faster chromatography by simplifying the chromatogram. In sample cleanup the efficiency constraint can be relaxed because the sample becomes chemically simpler. For example, a sample might be passed through a **solid phase extraction** (SPE) cartridge before it is injected into the chromatograph. Interfering compounds are retained in the cartridge, which simplifies the sample. A simpler sample requires lower efficiency, so the SOF can be higher.

The high speed chromatography that is used in GC \times GC is possible because any fraction collected from the ^1D separation is considerably simpler than the original sample, and therefore the efficiency constraint is relaxed, which allows a much higher SOF, and therefore a very fast ^2D separation. Even at SOF, there might still be excess efficiency, which could be traded for higher speed. Since $E^2 = \frac{H}{L}$, this higher speed can be obtained by increasing the flow beyond SOF (increasing H), or by using a shorter column (decreasing L). Studies of optimization with the goal of the best speed/efficiency ratio using column length and flow as optimizing parameters revealed, theoretically and experimentally, that flow nearer the SOF combined with shorter columns gives better performance than flow much faster than SOF combined with longer columns (Klee and Blumberg 2002; Reed 1999).

5.3 The General Elution Problem.

The theory developed above is for kinetics optimization: it assumes a single **retention factor**, k' . This means that the optimization is focused on the kinetic conditions required to optimally separate two compounds eluting after each other, and have similar retention behaviours. If a sample were to contain only these two compounds, then all would be well. But if another pair of compounds, with similar relative retention behaviour but absolute retention behaviour very different from the first pair were to be separated, the optimum conditions will be very different. So not all the compounds in complex mixture can be optimally separated with a single set of conditions. This is known as the **general elution problem** (Skoog, Holler, and Crouch 2007, p. 779). The general elution problem makes speed and resolution mutually exclusive: a fast chromatogram will not satisfy resolution constraints, and a fully resolved chromatogram will not satisfy speed constraints.

The solution to the general elution problem is to adjust the thermodynamic conditions during the run so that the retention factors k' stay constant during the run. This strategy is implemented in LC by **gradient elution**, and in GC by **temperature programming**. In isothermal GC less volatile compounds exhibit higher k' than more volatile compounds. If kinetic conditions are optimized for the more volatile compounds, they will elute optimally, but the heavier compounds will elute well-resolved and after a long time. If — after the elution of the more volatile compounds — the temperature of the column is increased, then k' of the less volatile compounds will decrease, so that the selectivity conditions will now match the optimized kinetic conditions, and their elution will be optimal. With a precise control system the temperature can be continuously adjusted so that the selectivity conditions always

match the kinetic conditions, and all the compounds elute optimally. The technology for **temperature programming** in GC is mature, and every column manufacturer specifies temperature limits for isothermal and ramped temperature programs for every stationary phase.

In GC \times GC the general elution problem appears in the form of **wrap-around**, defined as “the occurrence of second dimension peaks in subsequent modulation sequences, caused by second-dimension retention times that exceed the modulation period of a comprehensive two-dimensional system” (Marriott, Schoenmakers, and Wu 2012). In GC \times GC the ^2D separation is isothermal, but because GC separations are predominantly determined by volatility, in the ^2D separation the retention factors have similar values and wrap-around is a nuisance which can be readily be addressed by a slight increase of the ^2D column temperature above that of the ^1D column. In SFC \times GC, where the group-type separation on the ^1D column yields fractions that contain compounds with a wide range of volatilities (Venter, Rohwer, and Laubscher 1999), isothermal GC will have unacceptable wrap-around. Therefore, temperature programming is necessary for successful SFC \times GC. This exemplifies the true orthogonality between the two chromatographic methods.

Guided by the theory described above, the fast GC used as the ^2D separation in the SFC \times GC chromatograph was designed to use a short GC column (1 m long) with flow higher than SOF and a correspondingly fast temperature program.

5.4 Temperature ramp rates

Early experimenters understood the importance of temperature control in GC, and used vapour baths (Desty and Whyman 1957) or oil baths (Eggertsen, Knight, and Groennings 1956) for temperature control in their experiments, but they quickly learned that leaks or cracks could allow oil into the column. Oil that entered the column would then contaminate the stationary phase, rendering it useless. If air is used to transfer heat to the column, the gas pressure inside the column is higher than the atmospheric air pressure outside the column, so leaks let carrier gas escape but does not allow contaminants to enter. Therefore, in the modern gas chromatograph the convention is to control the temperature of GC columns by keeping them immersed in an air bath with a precisely controlled temperature.

A temperature program is traditionally described using a series of **ramps** and **holds**. A ramp is a period of time during which the temperature changes, almost always increasing. The **ramp rate** is the rate at which the temperature changes. A hold is a period of time during which the temperature is kept constant.

When developing a chromatographic method, at what rate must the temperature of a column increase so that the conditions for optimal selectivity match the conditions for optimal kinetics? Blumberg and Klee (Blumberg and Klee 2000) recommend that a good initial temperature ramp rate is $10\text{ }^\circ\text{C}$ per void time (t_m). For long columns the void times are long and the ramp rates can be low. As an illustration, Figure 5.3 shows the temperature ramp rates of a state-of-the-art chromatograph. By contrast, for short, narrow-bore columns, the ramp rate needs to be thousands of $^\circ\text{C min}^{-1}$, because the suggested ramp rate is inversely proportional to the void time: as the void time gets smaller the suggested ramp rate increases rapidly (See Figure 5.4).

The ramp rate of conventional air baths is limited by three factors:

- The low heat capacity of air

Table 1. Typical 7890B GC Oven Ramp Rates

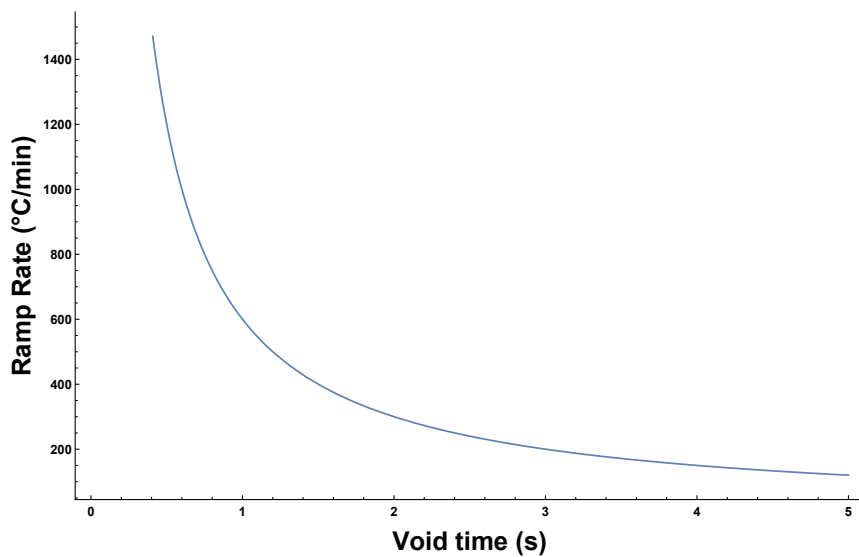
Temperature range (°C)	120 V Oven* rates (°C/min)	Fast ramp rates** (°C/min) Dual-Channel	Fast ramp rates** (°C/min) Single-Channel***
50 to 70	75	120	120
70 to 115	45	95	120
115 to 175	40	65	110
175 to 300	30	45	80
300 to 450	20	35	65

* Results obtained with line voltage maintained at 120V

** Fast ramp rates require power > 200 volts at > 15 Amps.

***Requires G2646-60500 oven insert accessory.

FIGURE 5.3: The ramp-rate table from the Agilent 7890B chromatograph data sheet. (Agilent Technologies 2019).

FIGURE 5.4: The ramp rate for temperature-programmed gas chromatography as a function of void time (10°C per void time (t_m)).

- The poor thermal conductivity of air
- The mass of the oven that needs to be heated.

There is very little that can be done about these matters. Attempts by instrument manufacturers to create air baths with faster ramp rates include decreasing the size of the oven and increasing the air flow rate, which yields modest improvements.

5.4.1 Resistive heating

Fortunately, the heating rate problem has a technologically simple solution, namely **resistive heating**². When a constant electric field is applied to a metal, the free electrons in the metal will be accelerated by the electric field. But the electrons are within the crystal lattice of the metal, where their mean free path is very short. The electrons will therefore collide with atoms in the crystal lattice, scattering inelastically. The energy lost in the inelastic collisions will increase the vibrational energy of atoms, and this energy will appear as heat.

The number of electrons and their average (drift) speed in combination is described by a measure called the **current** (I), and the electric field can be described by the applied **voltage** (V). The current I is proportional to the applied voltage, and the ratio $\frac{V}{I}$ defines a proportionality constant R , called the **resistance**, which is a function of the conductor's material and dimensions. The total **power** dissipated to heat (P) is given by $P = IV$ or, equivalently, $P = I^2R$ or $P = \frac{R}{V^2}$.

Applying a voltage V to a metal element close to a chromatographic column will heat the metal, and therefore the column in contact with it. The rate at which the piece of metal heats up depends on the power dissipated, the mass of the metal, and its heat capacity. If the volume of the metal is small enough, and the current high enough, the temperature of the metal element (and with it the temperature of the column) will increase at a rate high enough to be useful in fast chromatography. By suitable manipulation of V , then, the temperature of the column can then be changed at any desirable rate.

This technology has been reviewed (Wang, Tolley, and Lee 2012; Jacobs, Hilder, and Shellie 2013; Miranda 2010), and a few technologies for resistive heating of capillary columns have emerged:

- Direct heating of a metal column or a column coated with a metal layer
- Collinear heating
- Coaxial heating

The first SFC \times GC work done (Venter and Rohwer 2004) used a directly heated metal column. While this approach proved the concept, experience showed two shortcomings. Firstly, metallic columns are usually designed with specific high-temperature applications in mind. This means that metal columns are not available with all the stationary phases available in fused-silica columns. Secondly, it was harder than expected to control the temperature accurately. The temperature was determined by a thermocouple glued to the column, which was sensitive to local variations.

An example of collinear resistive heating is Agilent™'s 'low thermal mass' column, which includes collinear heating wire and a collinear sensing element bundled

²Alternative methods of heating by electromagnetic fields are **radiative heating**, **inductive heating** and **dielectric heating**.

with a short fused silica column. This approach requires that the collinear heating element be wrapped in close contact with the column as part of the manufacturing process.

For the work presented in this thesis, a coaxial heater was used. This heater is in the form of a thin-walled stainless-steel tube that carries the electric current. It was made of a 940 mm length of a standard stainless steel alloy (SAE 304) with an outside diameter of 1.06 mm and an inside diameter of 0.80 mm, obtained from Mifam (Milanówek, Poland). The column was threaded inside the stainless steel tube, which put it in close contact with the heater for reliable heat transfer. The coaxial heater can be coiled to fit inside a conventional GC oven.

This coaxial design has the advantage that the column can be changed without changing the resistive heater. This means that there is no need to re-calibrate the heater when columns are changed.

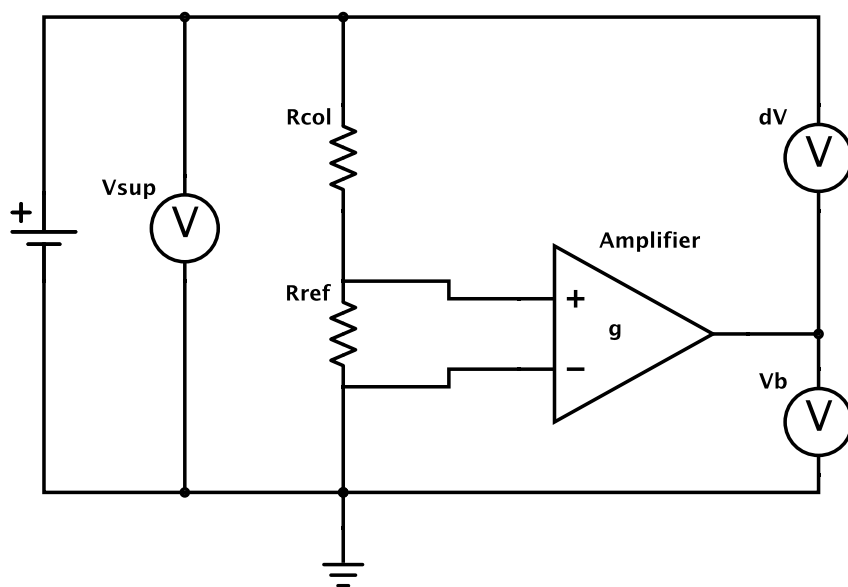


FIGURE 5.5: Electric circuit diagram of the coaxial heater.

The electrical resistance of a conductor is determined by its dimensions, the material it is made of, and the temperature of that material. In a conductor of given dimensions, therefore, a knowledge of the resistance implies a knowledge of the temperature. By following changes in the resistance, one can determine changes in the temperature, and by comparing resistance at certain temperatures with known temperatures, one can get a calibrated temperature from a given resistance.

High-powered resistive heating at safe, convenient voltages implies low resistance. Measuring the *absolute value* of low resistance is technologically challenging (Dyos 2012). But a simple electronic circuit can be used to *compare* the resistance of the coaxial heater with that of a reference resistor (Figure 5.5). The circuit is supplied by a voltage V_{sup} , in general an unknown value. V_{col} and V_{ref} represent the voltage drops over the respective resistors. Because the current I through the circuit is the same for both R_{col} and R_{ref} , it is true that $\frac{R_{col}}{V_{col}} = \frac{R_{ref}}{V_{ref}}$, and therefore

$$R_{col} = R_{ref} \frac{V_{col}}{V_{ref}}$$

The voltage drop across R_{ref} is too small to be directly digitized, therefore it is amplified by an amplifier with gain g , so that $V_b = gV_{ref}$. V_b is measured, as is dV ,

the potential difference between the supply and the amplifier output. We can show that the coaxial heater resistance R_{col} is a function of the voltage ratio $\frac{dV}{V_b}$.

First,

$$V_{sup} = V_{col} + V_{ref}$$

but also

$$V_{sup} = dV + V_b$$

Therefore,

$$V_{col} + V_{ref} = dV + V_b$$

But $V_b = gV_{ref}$, so

$$V_{col} + V_{ref} = dV + gV_{ref}$$

$$V_{col} = dV + gV_{ref} - V_{ref}$$

$$V_{col} = dV + V_{ref}(g - 1)$$

$$\frac{V_{col}}{gV_{ref}} = dV/gV_{ref} + V_{ref}(g - 1)/gV_{ref}$$

$$\frac{V_{col}}{V_{ref}} = gdV/gV_{ref} + gV_{ref}(g - 1)/gV_{ref}$$

$$\frac{V_{col}}{V_{ref}} = g \frac{dV}{V_b} + (g - 1)$$

This proves that $\frac{V_{col}}{V_{ref}}$ is a linear function of dV/V_b . A quick check for correctness of the expression: for a unity-gain amplifier $g = 1$, and $\frac{V_{col}}{V_{ref}} = dV/V_b$.

Therefore

$$R_{col} = R_{ref} \left(\frac{gdV}{V_b} + (g - 1) \right)$$

In practice the gain g is not completely constant, but shows a slight dependence on dV , so a general expression might be

$$R_{col} = f \left(\frac{dV}{V_b} \right)$$

5.5 Calibration

The assumption is that the temperature is a function of the resistance of the coaxial heater, or $T = g(R_{col})$. Because $R_{col} = f(\frac{dV}{V_b})$, we can see that $T = g(f(\frac{dV}{V_b}))$, or, because a function g of a function f is a function h ($f \circ g = h$), $T = h(\frac{dV}{V_b})$. Through a calibration procedure h can be approximated by a polynomial or lookup table.

5.5.1 Temperature uniformity

It is highly desirable that the coaxial heater should give uniform heating, but there is no obvious guarantee an electrically heated tube will heat uniformly. The problem was not analysed theoretically, but the following factors will play a role:

Resistivity's dependence on temperature

The resistance of a metal increases with temperature. This means that if one section of the coaxial heater gets hotter than the rest, its resistance will increase. If the current were to remain constant, more power would be dissipated in this section ($P = I^2R$). If more power is dissipated, the temperature will increase, leading to a higher resistivity, leading to higher power dissipation, leading to a higher temperature, in a runaway cycle. In contrast, if the coaxial heater was made of a material of which the resistivity decreases with an increase in temperature, the temperature along the length of the heater would be stabilized by negative feedback. In the case of the supply voltage being held constant a higher resistance in one section would mean a lower current overall, but still a higher power dissipation in the section with higher temperature.

Thermal conduction

Each section of the coaxial heater is in thermal contact with its neighbours. If it were to get hotter, the heat will flow from the hotter section to the cooler neighbouring sections. This will tend to even out any temperature differences. This longitudinal equilibrium process is inefficient for a long, thin-walled tube.

Radiation

An object radiates heat, which can be approximated by the Stefan-Boltzmann law:

$$P = A\epsilon\sigma T^4 \quad (5.1)$$

where A is the surface area of the object, ϵ is the **emissivity** of the surface, σ is the Stefan-Boltzmann constant, and T is the absolute temperature of the object.

If a section of the coaxial heater were to become hotter than the other sections, it would therefore radiate more heat. The increased power dissipation by the higher resistance will therefore be partially offset by a higher radiation. This will tend to moderate temperature differences.

Convection

When a part of the coaxial heater is hot, it will heat the air around it through radiation and conduction. This air might then move, through buoyancy or any other force, past another part of the coaxial heater. This second part could then be heated up by the transported air. For example, a vertically mounted coaxial heater can be expected to develop a temperature gradient from bottom to top, as natural convection lets hot air transfer heat from the lower end of the heater to the upper end. In this way temperature gradients could be established and maintained.



FIGURE 5.6: This photograph shows the setup used to record the thermal video.

Examining thermal uniformity by imaging

The effect of the combination of resistivity’s temperature dependence, thermal conduction, radiation, and convection on the temperature uniformity of the coaxial heater could be mathematically or numerically modelled, but such an endeavour would fall outside the scope of this project. Experience had not led us to expect any significant temperature non-uniformity, but the opportunity to get empirical confirmation was welcomed.

Thermal imaging is the process by which infrared radiation from objects can be captured in a photographic process. At near-ambient temperatures objects emit copious amounts of infrared radiation, and the higher the temperature, the more is emitted. (See Equation 5.1.) Cameras designed using specialized optics and sensors allow the capture of that radiation as an image of a scene that shows objects based on their surface temperature. The technological capability of thermal imaging has improved markedly over the past years.

A FLIR™ T660 thermal imaging camera was used to obtain a video of the coaxial heater executing three consecutive temperature ramps. This camera uses a 640×480 focal plane uncooled bolometer array as a detector, which is sensitive to radiation in the range $7.5\text{ }\mu\text{m}$ to $14\text{ }\mu\text{m}$. Figure 5.6 shows the setup used to record the thermal video. To get reliable temperature information from a thermal image requires calibration or a precise knowledge of the material’s **emissivity**. In the absence of such calibration, the obtained temperature measurement is more useful if seen as relative rather than absolute.

The video showed that the three consecutive temperature runs heated the coaxial

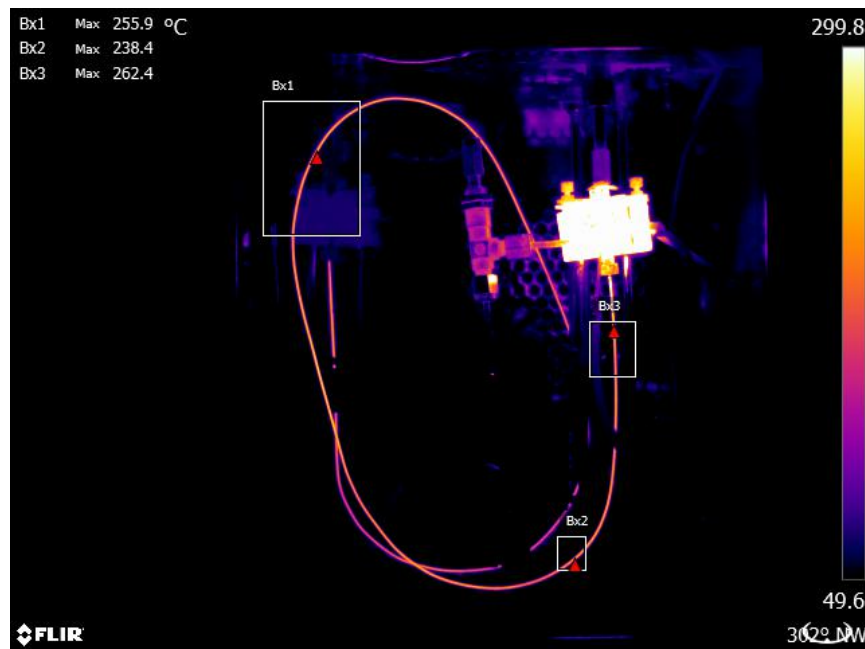


FIGURE 5.7: A thermograph of the coaxial heater at high temperature. It shows that there are no runaway hot spots.

heater identically. Figure 5.7 is a frame from the video, analysed to give estimates of the temperatures on spots on the coaxial heater. The maximum temperature difference between any two points is 17.5 °C, and there are no marked gradients.

This examination of the uniformity of the coaxial heater helped to dispel fears that unexpected temperature gradients would interfere with the fast gas chromatography.

5.5.2 Temperature calibration

When doing temperature-programmed gas chromatography it is desirable to have an absolute measurement of the column temperatures. This makes it possible to translate and compare methods between instruments. It was therefore necessary to calibrate the temperature of the coaxial heater. Calibration is the comparison of measurement values from a device under test with those of a calibration standard of known accuracy. In the case of the temperature calibration of the coaxial heater, it means comparing the results of the temperature as measured by the coaxial heater with a standard temperature.

The problems of measuring a temperature inside a tube with a bore of 0.8 mm are not trivial, and to solve them the available technologies were examined to find the optimum solution.

The following temperature measurement technologies exist:

- Liquid-in-glass thermometers
- Sealed liquid or gas sensing instruments and bimetallic sensors
- Electrical resistance temperature measurement using metallic sensors
- Thermistors and semiconductors

- Thermoelectric temperature measurement
- Disappearing filament optical pyrometer
- Photoelectric optical pyrometers
- Total radiation pyrometers

Liquid-in-glass thermometry would not be applicable because of the size of the devices, and because they don't give a desirable electrical signal. Bimetallic and sealed liquid or gas sensing elements are also too bulky and are best used where only an on/off electric signal is required.

In recent years **pyrometry**, the technology of measuring temperature by radiant energy methods, have improved markedly and has become affordable, in the form of thermal cameras. However, at lower temperatures the accuracy of the recorded temperature depends heavily on the emissivity of the measured material. Thermal imaging will also only measure the outside wall surface temperature of the heater, and not the temperature on the inside of the coaxial heater. So, while thermal imaging settled questions about heater uniformity (Section 5.5.1), it was not considered ready to serve as a calibration standard.

The remaining options are resistance temperature measurement with metallic sensors, thermistors and semiconductors, and thermoelectric temperature measurement.

Electrical resistance measurement using metallic sensors might have been feasible, if sensing elements of the appropriate dimensions were commercially available. A further difficulty with this method of temperature measurement is that long, thin conductors would be needed to connect the sensing element to the electronics. These conductors would add to the resistance measured by the sensing element, requiring complex correction or multi-wire measuring methods.

Thermistor and semiconductor devices could be made small enough, but all commercially available packages are too large. Besides, the temperature range used in GC (-50°C to 400°C) does not fall inside the operating temperature range specified by manufacturers of semiconductor devices (-55°C to 125°C for military applications) (Department of Defence 1996).

Thermoelectric temperature measurement was the only remaining alternative, and was used to calibrate the coaxial heater. In particular, the **Seebeck effect** was exploited, which is the observation that a temperature gradient imposed on a metallic conductor will generate an electrical potential along the gradient. Therefore, a circuit of two dissimilar metallic conductors will generate a voltage when there is a temperature gradient along the conductors. The voltage generated is a function of the temperature difference between the hot junction of the two metals and their cold junctions at the voltmeter input. Such a pair of dissimilar conductors used to generate a voltage is known as a **thermocouple**, and this technology is mature and widely used in industry. Standard thermocouples are constructed from well-characterized alloys that generate predictable voltages for given junction temperatures. Pairs of thermocouple standardized alloys are known as 'types', of which the general-purpose Type K suited our purpose best. Thermocouple wire can be purchased in a range of gauges, down to $25\ \mu\text{m}$ in diameter, and the signal processing for thermocouple signals have been standardized. Thermocouple junctions can be made by welding, crimping, soft soldering, hard soldering, bolting, or simply twisting the wires together (McGee 1988). Because the temperature range to be measured was (-50°C to 400°C) soft soldering is not a viable choice, because soft solders have

melting points around 200 °C. The possibility of corrosion and mechanical vibration suggests that twisting the wires together will not form a reliable joint, and of course there are no sub-millimetre bolts on the market.

This leaves welding, crimping and hard soldering as methods for making thermocouple junctions. Tools for crimping hair-fine wire are rare and it is likely that a practical crimped connection will have a diameter many times the diameter of the wire, possibly making it too large to fit.

Hard soldering is usually done with a high-temperature flame, and on contact the flame will rapidly burn the fine wires and destroy them. The temperature required for hard soldering is still lower than the melting point of the wires, so that hard soldering is not excluded, but the knowledge or the technology to solve the associated problems was not available.

Welding was found to be an accessible technology for forming small, reliable joints in fine thermocouple wire.

5.5.3 Thermocouple welding

Welding is the process of joining two metal parts by melting a portion of each part, allowing the molten metals first to mix, and then to solidify. This creates a permanent joint between the two metals. Welding is widely practised as an industrial process in applications ranging from shipbuilding to microelectronics. Previous work in our laboratories used capacitive discharge spot welding to melt the spot where two wires crossed. These thermocouples were found to be too fragile for the intended application, so a method was developed to yield a more robust thermocouple.

In the laboratory, electricity is the most convenient source of heat. A 24 V direct current, adjustable bench power supply was used to supply the current. The two wires of the thermocouple were twisted together and the twisted pair was connected to one pole of the power supply. A carbon electrode was connected to the other pole. The carbon electrode was carefully brought closer to the thermocouple pair until a spark jumped across the air gap. When the spark turned into an arc the heat of the arc melted the end of the twisted pair. The molten metal would then contract into a spherical globule, which grew as the arc added more heat. As more of the metal of the wire melted, the globule would move away from the carbon electrode, until the gap became too large to sustain the arc. The current would then stop, leaving a spherical welded bead at the end of the wires. (See Figure 5.8.) The process could be repeated as often as necessary to obtain a bead of the desired size.

It is worth noting that it is necessary to form an arc: if the carbon electrode happens to touch the wire so that a current flows directly from the wire to the carbon electrode the wire rapidly heats up over its length and melts. It is also seems necessary to have a roughly broken carbon electrode surface: a polished surface would not generate an arc, or even make electrical contact with the wires. This might be because the graphite used for the electrode was formulated for use in pencils.

The apparatus used to do the welding is depicted in Figure 5.9, and Figure 5.10 shows the image seen through the microscope during welding.

5.5.4 Thermocouple probe construction

To measure the temperature inside the coaxial heater required the thermocouple to be inserted into the coaxial heater. For this a fused silica capillary with an inside diameter of 0.25 mm and an outside diameter of 0.4 mm was used to construct a probe. (These capillaries were readily available, in the form of discarded chromatographic

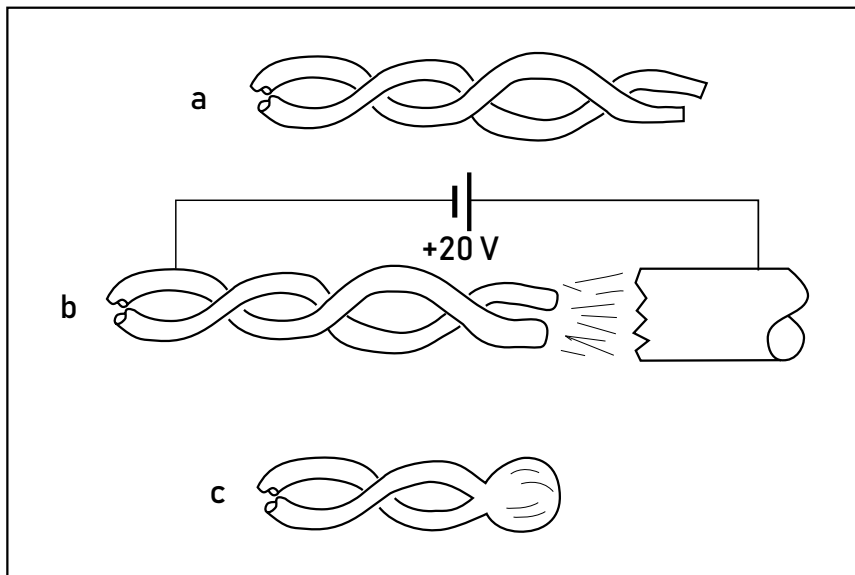


FIGURE 5.8: The process of welding fine wires to make thermocouples (a) Wires twisted together (b) Electric arc heating up the wires (c) Wires welded with a well-formed bead.

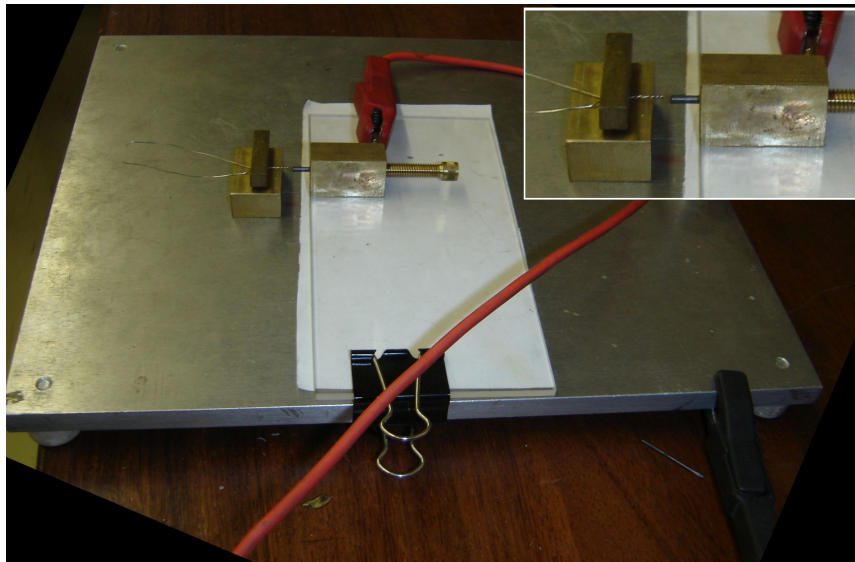


FIGURE 5.9: A view of the fine-wire thermocouple welder, as set up on a microscope base plate. The wire shown in the photograph is much thicker the one actually used. It is shown clamped between the clamping bar and the clamping weight. A thin sheet of acrylic serves to isolate the positive electrode from the negative base. The carbon electrode can be advanced towards the thermocouple twist using the screw. The black clamp at the bottom right-hand corner attached to the base plate and the red clamp attached to the screw housing provide a potential difference of approximately 20 V between the carbon electrode and the thermocouple. *To do (??)*

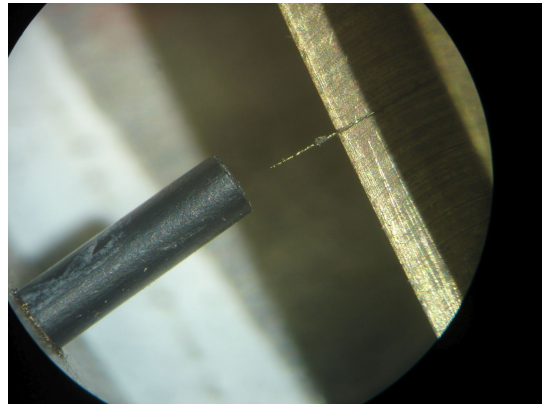


FIGURE 5.10: A microphoto of a pair of twisted thermocouple wires ready to be welded. The black carbon electrode is 2 mm in diameter.

columns.) A narrower capillary was used to draw the wires through the probe capillary, in a process described in Figure 5.11. The wires could then be welded to form a thermocouple and positioned at the desired position in the probe capillary.

5.5.5 Thermocouple interfacing

The Type K thermocouple has a sensitivity of approximately $41 \mu\text{V}^{\circ}\text{C}^{-1}$. This means the voltage generated at the temperature range of interest is too small to be conveniently digitized and therefore must be amplified. Because the Type K thermocouple is so commonly used in industry, amplifiers have been developed specifically for thermocouple signal conditioning. The AD595 integrated circuit amplifier was chosen. The component's data sheet explains its application concisely: "The AD595 is a complete instrumentation amplifier and thermocouple cold junction compensator on a monolithic chip. It combines an ice point reference with a pre-calibrated amplifier to produce a high level (10 mV/ $^{\circ}\text{C}$) output directly from a thermocouple signal" (Analog Devices 1999). The output signal of the AD595 can be directly digitized for computer recording.

5.5.6 Calibration procedure

The International Vocabulary of Metrology (*International vocabulary of metrology – Basic and general concepts and associated terms (VIM)* 2019) defines **calibration** as "[an] operation that, under specified conditions, in a first step, establishes a relation between the **quantity values** with **measurement uncertainties** provided by **measurement standards** and corresponding **indications** with associated measurement uncertainties and, in a second step, uses this information to establish a relation for obtaining a **measurement result** from an indication."

In the first step of calibration, the **quantity values** used in the calibration were the temperature value of the thermocouple probe as provided by the thermocouple voltage, the AD595 amplifier, the digitization and the subsequent calculations according to the AD595 data sheet. The **measurement standards** were the known responses of the thermocouple (Ripple 1995), the amplifier and the digitization system. The **indication** was the voltage ratio $\frac{dV}{V_b}$. As this was a first attempt at calibration, **measurement uncertainties** were assumed to be negligible.

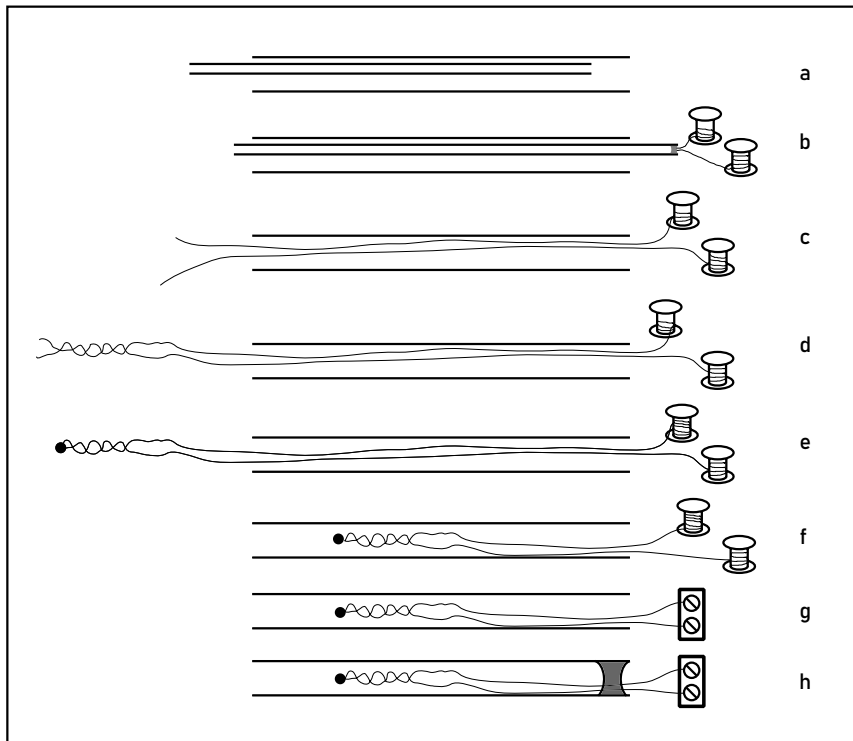


FIGURE 5.11: (a) A narrow capillary is threaded inside a wider one
(b) The ends of a pair of thermocouple wires are fitted inside the end of the narrow capillary and anchored with cyanoacrylate adhesive.
(c) The wires are pulled through the wider capillary using the narrow capillary.
(d) The ends of the wires are twisted together, creating a mutual mechanical anchor.
(e) The ends of the wires are welded together.
(f) The wires are pulled back into the thick capillary, locating the junction at the desired position in the capillary.
(g) The wires are trimmed and connected to a terminal block.
(h) A drop of cyanoacrylate adhesive is used to anchor the wires permanently in the capillary.

In preparation for calibration the coaxial heater was installed in the oven of the Varian 3300 GC as it would be when in use. The detector was removed and the thermocouple probe was threaded through the detector stem, through the heated T-piece block, and into the coaxial heater until the thermocouple junction was about half-way between the inlet end and the detector end of the coaxial heater. When the system was set up as it would be during use, the coaxial heater was cooled down before a power ramp was applied. As the power increased the temperature rose, and the temperature of the thermocouple was recorded together with the voltages dV and V_b . A curve could then be plotted of thermocouple temperature T_{TC} against the voltage ratio $\frac{dV}{V_b}$ (Figure 5.12). This revealed the shape of the function $T(\frac{dV}{V_b})$ and completed the first step of the calibration.

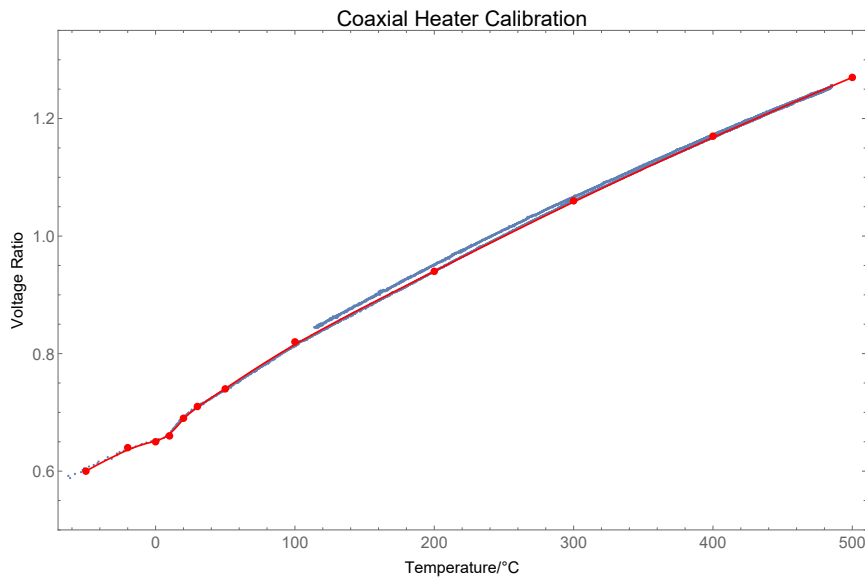


FIGURE 5.12: Calibration curve for the coaxial heater.

The second step of a calibration is to establish a **measurement result** from an **indication**. It would be traditional to fit a mathematical function such as a polynomial to the curve, but a numerical method was chosen instead. A B-spline was fitted to the data and coordinates on the B-spline was extracted. (See Figure 5.13). An interpolation function was then used to obtain the measurement result T from the indication dV/V_b .

The calibration could be checked by setting the current through the coaxial heater to a minimum, at which not enough heat is generated to affect its temperature. Then the oven of the Varian 3300 GC could be set to a range of different temperatures. Once equilibrium was reached the reported temperature of the coaxial heater and the air bath temperature could be compared and the calibration adjusted.

The technique of constructing a long, thin thermocouple probe allowed the calibration of the coaxial heater, which makes it possible to translate chromatographic methods. The probe has also proven useful in other applications, for example providing overheating in a GC-MS transfer line.

5.5.7 Cold spots

For the fastest temperature programming with resistive heating, the heating element should be as light as possible and carry the largest necessary current. The current

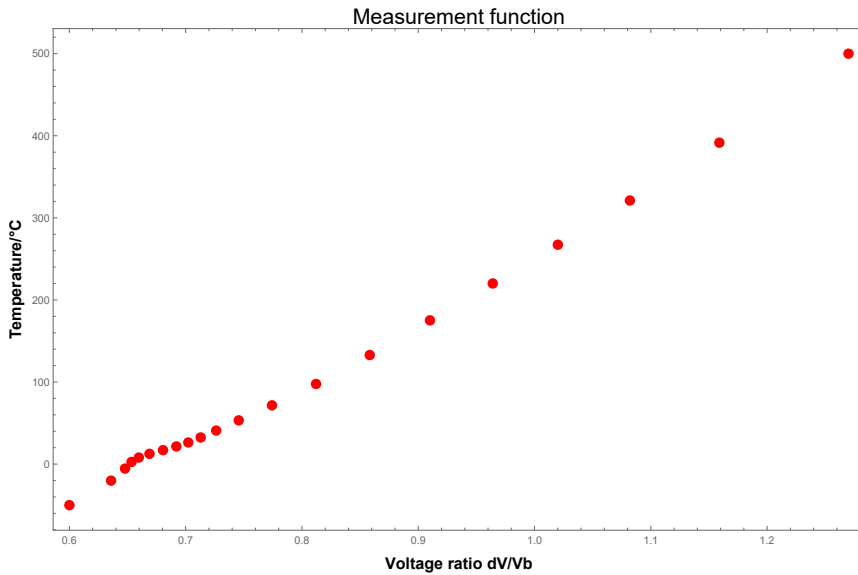


FIGURE 5.13: Measurement curve for the coaxial heater.

doing the heating must be carried to the coaxial heater using a feed conductor. To prevent the feed conductor from heating up it must have a low resistance, and this is achieved by making the conductor as 'thick' or as 'heavy' as necessary, meaning that it is constructed of a material with a high mass per unit length.

Good electrical metallic conductors are invariably also good thermal conductors. Therefore the area around the junction of the feed conductor to the coaxial heater will always have a lower temperature than the nominal temperature of the heater. In capillary GC this is undesirable: a cold spot in a column can wreak havoc with retention times and peak shapes.

Conversely, if an attempt is made to reduce the contact area between the feed conductor and the thin material of the coaxial heater, a hot spot might develop, which could burn a hole in the coaxial heater tube or damage the column.

The electrical connection between the feed conductor and the coaxial heater was therefore designed in the form of an externally heated block. This block was kept at a higher temperature than the highest expected temperature of the chromatographic temperature program. This prevented the formation of cold spots in the coaxial heater, which might lead to cold spots in the column, while also providing a large contact area so that hot spots do not develop. Each end of the coaxial heater was fitted into one of two heated blocks, where it was brazed in place. Each block had a brass tail, to which an electric feed-wire was soft-soldered. Each block was heated by four 100 W Hotset™ electrical cartridge heaters, with dimensions of 6.5 mm × 40 mm. The cartridge heaters were switched on and off by solid state relays controlled from the computer. The temperature of the block was monitored through a thermocouple mounted in a blind hole in the block and the amount of power to the heaters was controlled by **pulse width modulation** (PWM) implemented in software.

5.5.8 Cold column

In a cold GC stationary phase, the retention factor k' of a particular compound can be very high. This means that the analytes migrate slowly relative to the mobile

phase. The lower the temperature, the higher k' becomes, so that for very low temperatures the migration of the analyte becomes negligible. In effect, the analytes are 'trapped'. This trapping, also called **cryo-trapping** or **cryo-focusing** is useful in various aspects of gas chromatography, such as two-stage thermal desorption or thermal modulation in GC \times GC.

In the SFC \times GC instrument described here, cryo-trapping was used as the second stage of a two-stage modulator. (The stop valve described in Section 4.4.2 represents the first stage.) The column was cooled down to very low temperatures, which trapped any analytes eluting from the first dimension in a narrow band on the GC column. Once the required amount of fraction had been collected, the eluate flow from the first dimension was stopped by closing the stop valve. Then the temperature ramp of the fast GC would start. As the coaxial heater warmed up the column the values of k' would decrease, and the narrow analyte band would start migrating.

The first SFC \times GC chromatograph cooled the column by using the oven cryo-cooling capability of the Varian 3300 GC (Venter and Rohwer 2004; Venter 2003). The purpose is to cool the GC column to sub-ambient temperatures, normally needed when analysing volatile compounds. In such cases the k' values at or near room temperature are too low to provide adequate retention, and the cryo-cooling function permits temperature programs to start at sub-ambient temperatures.

The Varian 3300 cryo-cools its oven by injecting liquid carbon dioxide into the oven's air circulation fan. The evaporating liquid carbon dioxide absorbs energy from the air, which lowers the temperature of the air in the oven. A control system controls the amount of carbon dioxide admitted and the amount of heat added through the oven heaters, thereby keeping the oven at the required temperature.

The cryo-cooling function can cool down the oven to cryo-trap analytes, but there are two reasons why it is not suitable for practical trapping in SFC \times GC. The first reason is the quantity of coolant required: doing SFC \times GC runs revealed that about 15 kg of carbon dioxide was consumed per run. A standard cylinder of carbon dioxide contains 33 kg, which implies that a new cylinder would be required every two runs. Such a rate of use is much too high for the intended application of the instrument. The second reason is that it is much too slow. The time spent on cooling the oven and the column is time that cannot be spent doing separations, and cooling a conventional GC oven takes a lot of time: the Varian 3300's cryo-cooling function took 30 s to cool the column down to a low starting temperature. A commercial forced-convection system ("GC Chaser" supplied by Zip Scientific) improves the cool down time of an Agilent 6890 GC oven, taking 7 minutes instead of 16, cooling down the oven from 350 °C to 30 °C. Cooling the column in an air bath has the same drawbacks of low conductivity and low heat capacity as air-bath heating has (see Section 5.4).

A system was therefore developed that injected liquid carbon dioxide into one end of the space between the column and its coaxial heater, with the other end open to the atmosphere. When the valve opens the space rapidly fills with liquid carbon dioxide, while the pressure drops from 55 atm in the cylinder to 1 atm at the outlet. The liquid boils, absorbing large quantities of heat from the column and coaxial heater in the process, so that their temperatures decrease rapidly. This system solves the speed and coolant consumption problems: because the coolant is in direct contact with the parts that need to be cooled, the cooling is rapid, and because the coolant is applied where it is needed, only a small quantity is required.

The carbon dioxide for cooling the coaxial heater was introduced through the same heated block that provided the electrical connection (see Section 5.5.7). A T-piece design allowed the liquid carbon dioxide to be admitted to the end of the

coaxial heater, which was brazed to the block. A micro-union brazed to the block sealed the column's exit port, and the liquid carbon dioxide entered along the side of the T (Figure C.1 and Figure C.2). A metering valve allowed the flow rate of the coolant to be adjusted, and a computer-controlled solenoid valve switched the flow on or off.

Cryogen supply

The carbon dioxide for cooling was supplied by Afrox in high-pressure cylinders each containing 33kg of technical grade carbon dioxide. Each cylinder was internally equipped with a **dip tube**, a tube that extends from the valve at the top of the cylinder to the bottom of the cylinder. This ensures that when the valve is opened, liquid carbon dioxide is delivered.

Experience taught that for repeatable cooling, the source of liquid carbon dioxide had to be near the solenoid valve. If this was not the case, when the valve was opened initially only carbon dioxide gas would be admitted, followed by a mixture of gas and liquid, and only finally liquid. (This is similar to the common experience of opening a water tap after a municipal water supply interruption: a lot of gurgling and spitting before a reliable stream of water flows from the tap.) Such unreliable coolant flow gives unreliable cooling. To solve this problem a reservoir for liquid carbon dioxide was installed on top of the GC. The problem of filling a receptacle with liquid carbon dioxide was described in Section 4.3, so the final design of the reservoir took the form of a coil of copper tube immersed in a circulating coolant (Figure C.3). Mounting the reservoir above the cut-off valve allows the liquid to collect at the bottom and allow gas to collect at the top, so that when the valve opens the flow into the coaxial heater contains only liquid.

5.5.9 Column mounting

The T-piece blocks described in Section 5.5.7 and Section 5.5.8 above and also depicted in Figure C.2 acted as electrical connections for the coaxial heater and as injection point for coolant. The block is heavy compared to the coaxial heater and column, and also has to absorb the forces of the coolant inlet tube and the electrical connections. The column runs from the heated inlet/detector to a heated T-piece block, and in between it should not be exposed to any low-temperature cold spots, therefore the gap between the T-piece block and the inlet/detector should be quite small, but the gap cannot be zero, because electrical isolation needs to be maintained. Also, fused-silica capillary columns are fragile and misalignment causes them to break. Therefore, mechanically stiff and accurate mounting was needed for the T-piece blocks to allow the precise but adjustable alignment of the T-piece blocks with the inlet/detector.

The final design for mounting the T-piece blocks was a pair of parallel rails. These rails were held in place in the Varian 3300 oven by friction, so that they could be adjusted and removed as necessary, yet were stiff enough to transfer the necessary forces without deflecting. The pointed ends of the rails pressed against a solid aluminium plate used as the floor of the oven, and at the top adjustable points pressed against pressure plates which pressed against the roof of the oven. Figure C.4 shows a technical drawing of the rails as designed.

The T-piece blocks were the electrical connections for the resistive coaxial heater, which meant they needed to be electrically isolated, but they were also heated,

which meant that the insulation had to be resistant to heat. A commercially available material that met these requirements was found in the form of **silicon mica**, a composite material of mica and a silicone resin. This material has a continuous operating temperature of at least 500 °C, making it ideally suited to GC applications. The silicon mica is also machinable and can easily be shaped to the required design.

The T-piece blocks were mounted on a pair of cars riding on the round-bar rails. Each car was designed as a sandwich of plates of stainless steel and silicon mica around a pair of brass bushes. Once assembled, the cars offered a set of studs on to which the user could fit and bolt down the T-piece blocks. The positions of the cars were determined by a locking collar on one of the rails. Figure C.5 shows technical drawings of the cars that explain the design.

5.5.10 Heating control

The amount of electrical power supplied to the coaxial heater was controlled by a bank of six PNP 2N2955 transistors, connected in parallel to distribute their heat dissipation. The final control signal was a voltage set either by a potentiometer from the front panel, or by the computer. An operational amplifier adjusted the current through the coaxial heater circuit so that a portion of the voltage applied to the coaxial heater was equal to the set-point voltage. By varying the set-point voltage the current through the coaxial heater can be controlled to provide any desired amount of heat ($P = I^2R$).

Temperature monitoring

Independent of the amount of power dissipated in the coaxial heater, the current through the reference resistor was compared to the current through the column. This ratio corresponds to the resistance of the coaxial heater. This resistance is a function of the temperature of the heater. Through the calibration procedure described in 5.5.6 the temperature of the coaxial heater can be calculated. The computer can do this fast enough to continuously provide temperature as a process variable to the control system.

PID tuning

A proportional-integral-derivative (PID) controller was used to calculate the amount of power necessary to keep the temperature of the coaxial heater as close to the temperature set-point as possible. The temperature set-point, in turn, was given by the desired chromatographic temperature ramp.

The process of determining the best calculation by the PID is called **tuning**, and usually consists of determining the optimum values of a few parameters. Tuning PID controllers is a complex sub-discipline of process engineering, and outside the scope of this project, but for practical purposes a privately published tuning method was used (Peacock 2008). This is a step-by-step implementation of the Cohen-Coon tuning method.

Figure 5.14 shows the effect of an improved loop tuning.

A properly tuned heater helps to improve the repeatability of the chromatography through reliable temperature programs and prevents damage to the column due to overheating during set point overshoots.

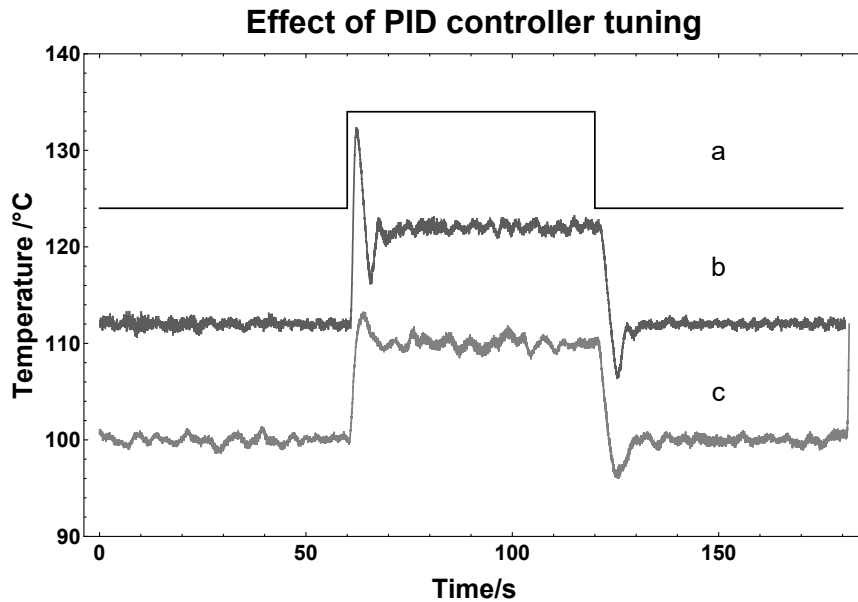


FIGURE 5.14: An illustration of effective PID controller tuning. The trace (a) represents the set point change over time and includes a step change. (b) Before tuning the temperature overshoots and then undershoots the step change in the set point. (c) After the controller has been tuned the overshoot in response to a step change in the set point is minimized.

Heating rates

As discussed in Section 5.4, for fast temperature-programmed gas chromatography the ramp rate needs to be in the order of thousands of degrees Celsius per minute.

Figure 5.15 contains heating ramps executed by the coaxial heater. The heating rate was $4000\text{ }^{\circ}\text{C min}^{-1}$, and there are no significant differences between the 9 consecutive ramps.

Cooling rates

The project did not demand a precise knowledge of, or control over, the cooling rate of the coaxial heater. The only requirement was that cooling should be as fast as possible. The cooling rate could be adjusted through the metering valve, and an optimum cooling rate of $5100\text{ }^{\circ}\text{C min}^{-1}$ was achieved with a carbon dioxide flow rate of around 30 g min^{-1} . This allowed the column to be cooled down from $350\text{ }^{\circ}\text{C}$ to $-20\text{ }^{\circ}\text{C}$ in about 2 s. At this rate the portion of the chromatographic cycle that is not used for separation is dominated by fraction collection, and further cooling rate increases will not significantly reduce sample throughput.

To do (??)

5.6 Detector

The detector used in this fast GC was an unmodified VarianTM 3300 flame ionization detector (FID). The detector bias voltage was supplied by the original electronics, but a stand-alone high-speed electrometer (V.G. Micromass Ltd, Model M406-H)

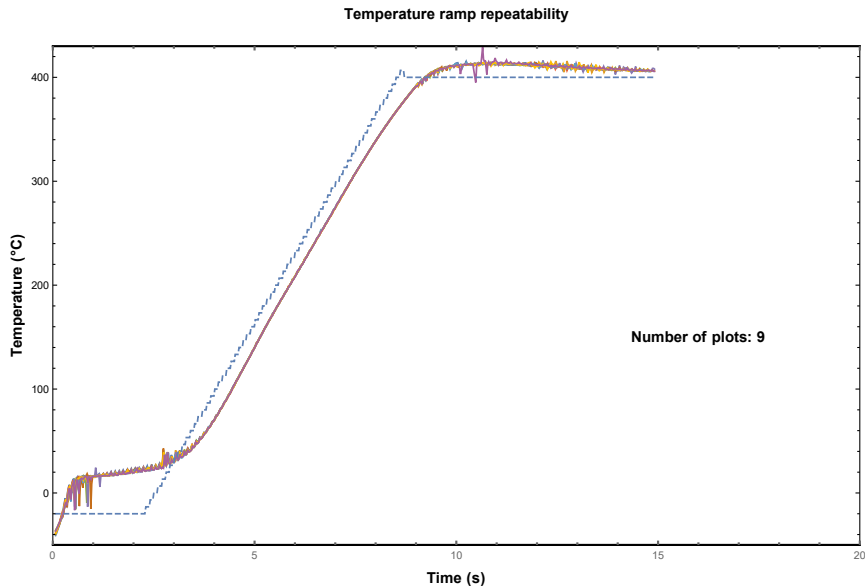


FIGURE 5.15: A graph of 9 identical, consecutive temperature ramps overlaid. The heating rate is $4000\text{ }^{\circ}\text{C min}^{-1}$. The temperature follows (with some lag) the set point up to $350\text{ }^{\circ}\text{C}$ before deviating noticeably.

captured the signal, which was then conditioned by a bench-top amplifier (V.G. Micromass Ltd, Model M406) before it was sent to the computer. This electrometer and amplifier were fast enough to detect and amplify the signals generated by the fast GC.

5.7 Data acquisition and control software

The whole SFC \times GC instrument was controlled from a single PC, running a single program. The program was written in LabVIEW 7.1TM (National Instruments). This software was designed to interact very easily with the National Instruments PCI-6014 multifunction data acquisition board. LabVIEW is a **visual programming language**, so called because programs are created by manipulating icons and wires on a screen, instead of typing text. This visual aspect of it makes it very easy to develop user interfaces as **virtual instruments** and get quick results. Figure 5.16 shows the interface of the program used to control the SFC \times GC instrument.

5.8 Data structure

In GC \times GC, 2D data is recorded as a continuous FID output stream — as if it is a 1D GC chromatogram — and later converted into a 2D chromatogram using knowledge of the modulation period. For two reasons this approach could not be used. Firstly, in this instrument the first (SFC) dimension runs in a stop-flow mode making continuous data recording inappropriate. Secondly, the duration of the cooling cycle varies, which would introduce unacceptable variation in ${}^2\text{D}$ retention times.

The 2D chromatograms were therefore constructed by recording a GC run for each SFC fraction injected. The ${}^1\text{D}$ retention times were recorded as the start times of each individual GC run. The ${}^2\text{D}$ retention times were measured from the time the GC fast temperature program started.

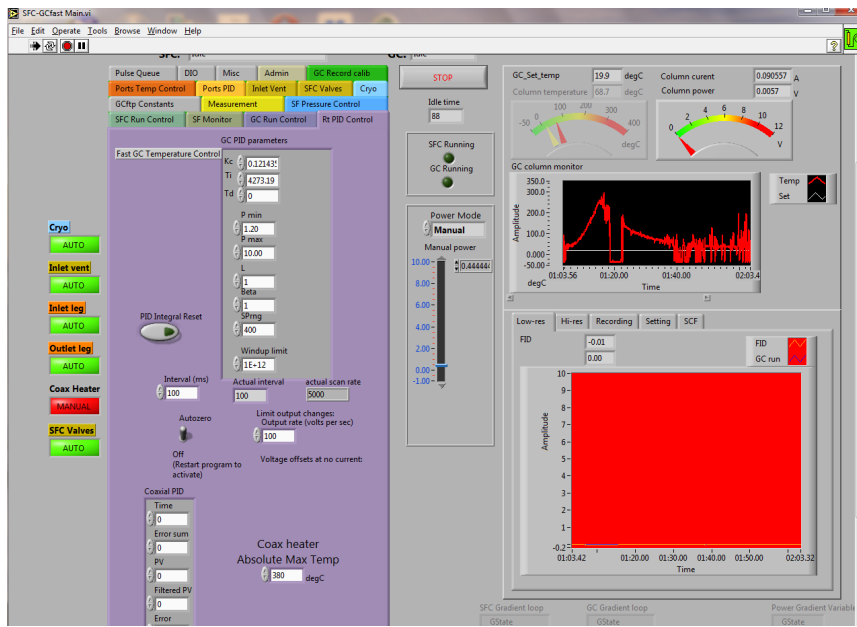


FIGURE 5.16: A screenshot of the LabVIEW virtual instrument used to control the SFC \times GC instrument.

5.9 Data visualization

To visualize the data the technical computing system Wolfram Mathematica 11.3TM was used. Mathematica is an extremely powerful and broad system, and its data manipulation and visualization tools were exploited.

The collected data could be handled in different ways. One way was to split it up into separate GC runs. Each individual GC run and its associated data could then be examined using the `Manipulate[]` function (Figure 5.17).

Then the data could be re-arranged into a list of three-element lists, with ¹D retention time, ²D retention time, and detector signal as the elements of the inner lists. The Mathematica functions `List3DPlot[]` and `ContourPlot[]` could then be used to plot 3D chromatograms (Figure 5.18) or contour plots (Figure 5.19) respectively.

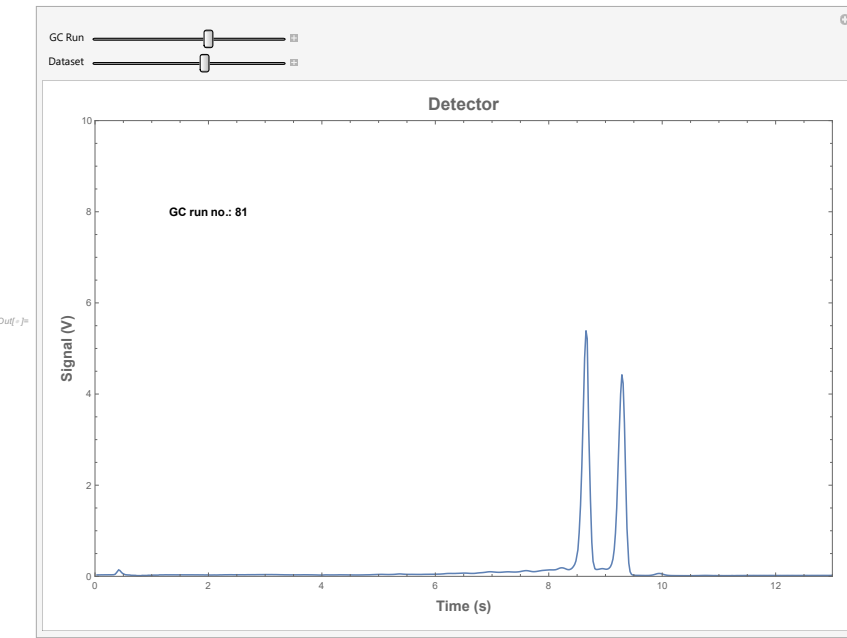


FIGURE 5.17: A single fast GC chromatogram, in a Mathematica Manipulate[] environment. The sliders can be used to select which GC run to view, and which data of that run.

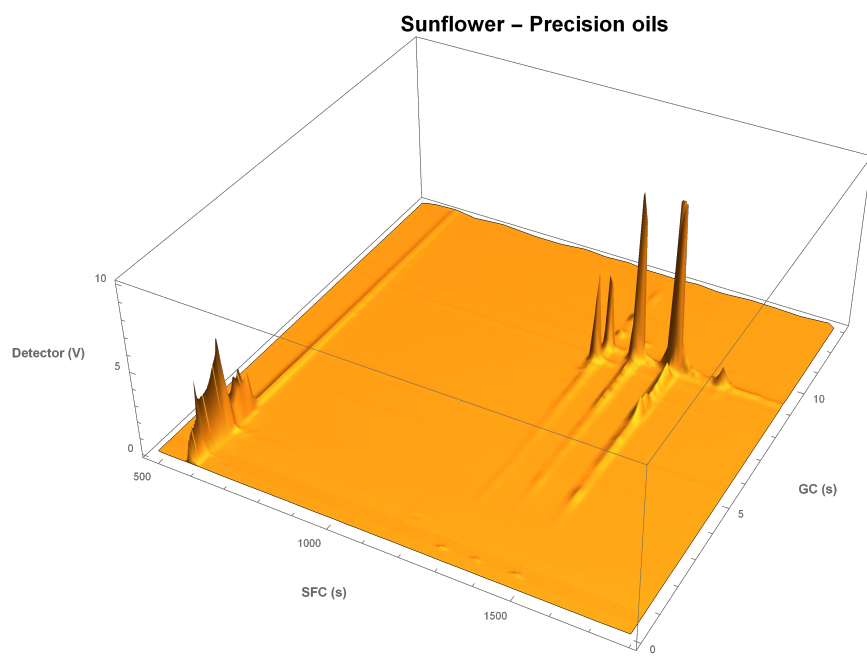


FIGURE 5.18: A 2D SFC \times GC chromatogram of fatty acid methyl esters of sunflower oil

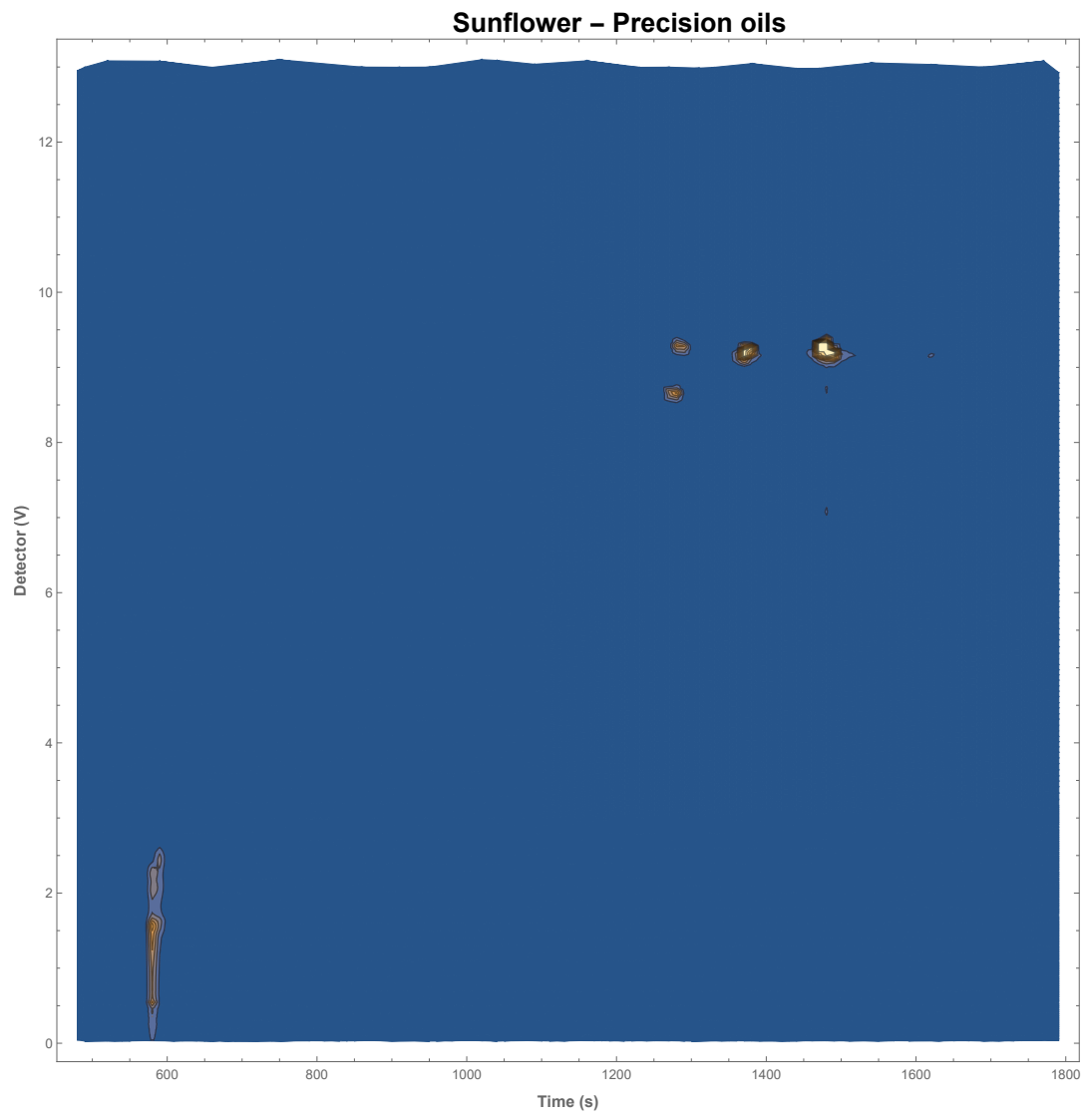


FIGURE 5.19: The SFC \times GC contour plot representation of the 2D chromatogram shown in Figure 5.18.

I'm really into coconut oil for everything. I cook it, eat it, put it in my hair, and use it as body lotion. I put it on my face, too - day cream, night cream, whatever. I love the smell. It reminds me of the beach. I'm not particular on what brand as long as it's organic.

Actress Juliette Lewis, observing the oxidative stability of coconut oil.

6

Investigating biodiesel feedstock using SFC \times GC

6.1 Introduction

Biodiesel consists mostly of a mixture of methyl esters of fatty acids obtained from plant oils. To comply with the relevant technical standard, SANS 1935, (SABS 2008) (see Chapter 3), it must consist of a mass fraction of 96.5 % or more of fatty acid methyl esters (FAME), but not more than 12 % linolenic acid methyl ester, and not more than 1 % of FAMEs with more than 4 double bonds. The prescribed methods for determining the quantities of these compounds are chromatographic, but the method for determining the *total amount* of FAMEs differs completely from the method for determining the amount of *unsaturated* FAMEs. Both these methods generate complex chromatograms that need highly skilled and experienced chromatographers to interpret. There is no doubt that the use of artificial intelligence and other technological innovations for interpreting chromatograms will grow, but the paradox of automation¹ predicts that as biodiesel production grows, feedstocks proliferate, and complexity increase, the analytical chemist will need better tools, methods, and instruments to understand the problems that arise when automation fails. Comprehensively coupled chromatography offers a way to better exploit chemistry for improved analytical separations, adding another tool to the analytical chemist's toolbox. It does this in three ways: the first is by increasing the peak capacity of the system, the second is by improved sensitivity, and the third is by generating patterns in the data.

6.2 SFC of FAMEs

The power of comprehensive chromatography is unlocked by orthogonality. Orthogonality is the difference in separation mechanism between the two dimensions (Marriott, Schoenmakers, and Wu 2012). When FAMES are chromatographically separated by SFC using neat carbon dioxide as a mobile phase and unmodified silica as a stationary phase, the separation is according to the number of double bonds,

¹Automation helps you least when you need it most (Strauch 2018; Bainbridge 1983).

independent of chain length (Robertson et al. 1991; Smith and Cocks 1994; Smith, Hyytiänen, et al. 2001). This stands in strong contrast to the separation of FAMEs by GC, where the major separation is according to volatility, which can be adjusted — but not overridden — by changing the polarity (or other chemical aspect) of the stationary phase (See Figure 6.1).

Silver ions are often used in stationary phases to separate unsaturated compounds, and this includes stationary phases for SFC (Sandra et al. 2002; Potgieter et al. 2013). The retention mechanism is quite complex (Nikolova-Damyanova 2019), but it offers a powerful technique for the elucidation of lipid structures, as reviewed as early as 1966 (Morris 1966). Nevertheless, in this chapter the use of stationary phases modified with silver ions was neither necessary nor attempted.

The utterly different retention behaviours of FAMEs on silica with a carbon dioxide mobile phase and on GC offers high orthogonality, which promises to make comprehensive coupling worthwhile.

6.3 Performance of the coaxial heater.

Practical SFC \times GC depends on reliably repeating fast temperature programs on a capillary gas chromatography column. The effect of these conditions on the column will be discussed in the following sections.

6.3.1 Column lifetime

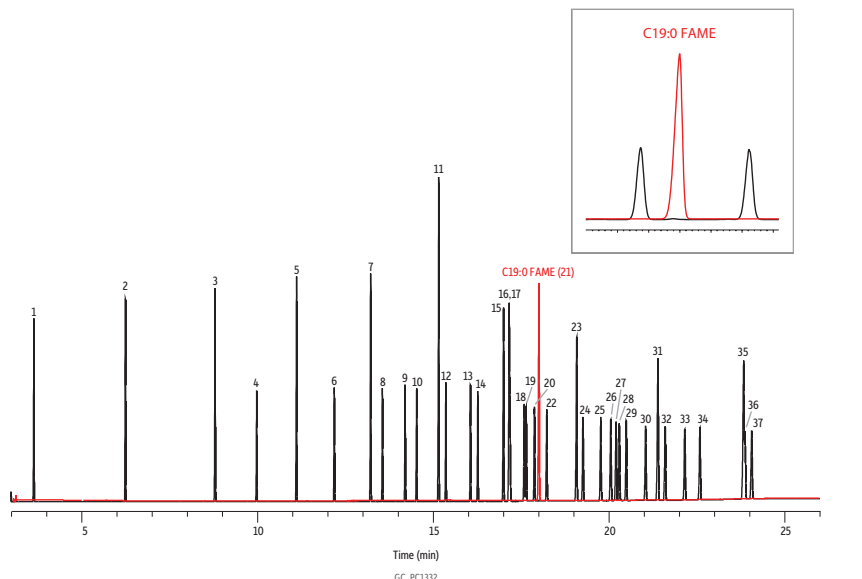
As discussed in Section 3.9, FAMEs can be separated by gas chromatography using relatively non-polar columns with high-temperature programs. For this purpose column manufacturers supply special 'high temperature' columns, which address two aspects of column lifetime: mechanical degradation and stationary phase degradation. The SFC \times GC chromatograph did not use such columns, and the following discussion explains why their use could be avoided.

Mechanical degradation

Fused silica has a high **tensile strength**, but also a low **fracture toughness**. This means that it is strong enough to resist the forces involved in its use as a column, but very liable to fracture if it gets damaged. Very small flaws, less than a micron in depth, will cause fused silica (or any other glass) to fracture under loads far under what would be expected from its tensile strength. Such flaws can be caused by mechanical scratches or reaction with atmospheric water. To prevent this the outside of the fused silica capillary is coated with a protective layer of **polyimide resin**. The strength of the a capillary column therefore depends on the integrity of the polyimide coating. Like all resins and polymers, the polyimide coating degrades faster at higher temperatures, so the longer the column spends at high temperature the sooner the polyimide will degrade to the point where it fails to protect the fused silica, and the shorter the overall mechanical lifetime of the column will be.

Traditionally, chromatographers are advised to use temperature programs that minimize the time spent at high temperature, which will contribute to longer column lifetimes. The usual way to do it is to use a temperature program with a maximum temperature no higher than necessary, but the same cumulative time at high temperature can be obtained by using higher temperatures but for shorter periods. Fast temperature programs expose the columns to high temperatures for only very brief periods.

Food Industry FAME on FAMEWAX by EN14103 (2011)



Peaks	<i>t_x</i> (min)	Conc. (mg/mL)	Structural Nomenclature
1. Methyl capronate	3.629	1.2	C6:0
2. Methyl caprylate	6.237	1.2	C8:0
3. Methyl caprate	8.787	1.2	C10:0
4. Methyl undecanoate	9.971	0.6	C11:0
5. Methyl laurate	11.105	1.2	C12:0
6. Methyl tridecanoate	12.179	0.6	C13:0
7. Methyl myristate	13.215	1.2	C14:0
8. Methyl myristoleate	13.549	0.6	C14:1 (<i>cis</i> -9)
9. Methyl pentadecanoate	14.196	0.6	C15:0
10. Methyl pentadecenoate	14.524	0.6	C15:1 (<i>cis</i> -10)
11. Methyl palmitate	15.152	1.8	C16:0
12. Methyl palmitoleate	15.355	0.6	C16:1 (<i>cis</i> -9)
13. Methyl margarate	16.052	0.6	C17:0
14. Methyl heptadecenoate	16.261	0.6	C17:1 (<i>cis</i> -10)
15. Methyl stearate	16.995	1.2	C18:0
16. Methyl oleate	17.156	1.2	C18:1 (<i>cis</i> -9)
17. Methyl elaidate	17.168	1.2	C18:1 (<i>trans</i> -9)
18. Methyl linoleate	17.583	0.6	C18:2 (<i>all-cis</i> -9,12)
19. Methyl linoleinolate	17.641	0.6	C18:2 (<i>all-trans</i> -9,12)
20. Methyl γ-linolenate	17.874	0.6	C18:3 (<i>all-cis</i> -6,9,12)
21. Methyl nonadecanoate	18.052	2.0	C19:0
22. Methyl o-heneicosate	18.223	0.6	C18:3 (<i>all-cis</i> -9,12,15)
23. Methyl arachidonate	19.075	1.2	C20:0
24. Methyl (2 <i>Z</i>)-11-eicosenoate	19.255	0.6	C20:1 (<i>cis</i> -11)
25. Methyl 11,14,17-eicosatrienoate	19.763	0.6	C20:2 (<i>all-cis</i> -11,14)
26. Methyl eicos-8,11,14-trienoate	20.046	0.6	C20:3 (<i>all-cis</i> -8,11,14)
27. Methyl hexadecanoate	20.197	0.6	C16:0
28. Methyl arachidonate	20.290	0.6	C20:4 (<i>all-cis</i> -5,8,11,14)
29. Methyl 11,14,17-eicosatrienoate	20.488	0.6	C20:3 (<i>all-cis</i> -11,14,17)
30. Methyl 5,8,11,14,17-eicosapentaenoate	21.036	0.6	C20:5 (<i>all-cis</i> -5,8,11,14,17)
31. Methyl behenate	21.39	1.2	C22:0
32. Methyl erucate	21.595	0.6	C22:1 (<i>cis</i> -13)
33. Methyl decosadipenoate	22.150	0.6	C22:2 (<i>all-cis</i> -13,16)
34. Methyl tricosanoate	22.584	0.6	C23:0
35. Methyl lignocerate	23.826	1.2	C24:0
36. Methyl docosahexaenoate	23.863	0.6	C22:6 (<i>all-cis</i> -4,7,10,13,16,19)
37. Methyl nervonate	24.055	0.6	C24:1 (<i>cis</i> -15)

Column Sample FAMEWAX, 30 m, 0.25 mm ID, 0.25 μ m (cat.# 12497)
Food industry FAME mix (cat.# 35077)
Methyl nonadecanoate (cat.# 35055)
Standard cat.# 35055 was dissolved in toluene.

Diluent: 1 μ L split (split ratio 100:1)

Injection Inj. Vol.: 24.0 μ L

Liner: Topaz 4.0 mm ID Precision inlet liner w/wool (cat.# 23305)

Oven Inj. Temp.: 240 °C

Oven Temp.: 60 °C (hold 2 min) to 200 °C at 10 °C/min to 240 °C at 5 °C/min (hold 7 min)

Carrier Gas He, constant flow

Flow Rate: 1.7 mL/min

Detector FID @ 250 °C

Instrument Agilent 7890B GC

Notes This chromatogram is an overlay of two injections: food industry FAME standard (black) and C19:0 methyl ester in toluene (red). An excellent separation of C19:0 (used in EN14103 as an internal standard) and the most prevalent FAMEs found in biodiesel blends was achieved. Note that C4:0 from the food industry FAME standard elutes in the solvent front.



© 2018 Restek Corporation. All rights reserved.
www.restek.com

Restek patents and trademarks are the property of Restek Corporation. (See www.restek.com/Patents-Trademarks for full list.) Other trademarks in Restek literature or on its website are the property of their respective owners. Restek registered trademarks are registered in the U.S. and may also be registered in other countries.

FIGURE 6.1: This figure shows that when separating FAMEs by GC, using a specialized column, separation is primarily by fatty acid chain length, and secondarily by number of double bonds. Reproduced with permission of Restek Corporation.

(Column mechanical lifetime can also be improved by using metal capillaries. Metals are not afflicted by brittle fracture the way fused silica is, but they don't offer the chemical inertness of fused silica. To exploit the fracture toughness of metal, technologies have been developed to deactivate metal surfaces (Rohwer, Pretorius, and Hulse 1986; Smith 2002), which makes metal columns a modern possibility. Column manufacturers offer metal columns specifically designed for biodiesel analysis.)

Another durability benefit of the stainless steel coaxial heater is that the outer surface of the capillary column is protected from mechanical damage by its encasement in the stainless steel tube of the coaxial heater. During development of the coaxial heater there were occasions where the column was accidentally overheated by poorly-controlled resistive heating. Even though the polyimide coating had been completely charred away and the capillary was left fragile, the column was intact and still provided separations.

Using carbon dioxide as a between-program coolant also protects the polyimide coating from oxidative damage by purging the column environment of oxygen.

Stationary phase degradation

The stationary phases inside the GC columns face degradation similar to that of the polyimide. Column manufacturers minimize stationary phase degradation by using improved technologies like cross-linked resins, or polymers with backbones resistant to certain degradation mechanisms (Day et al. 2003). Fast temperature programs help extend stationary phase lifetime by minimizing the cumulative time the column spends at high temperature.

Column bleed

Short columns and fast temperature programs have another beneficial side effect: reduced **column bleed**. Any resin- or polymer-based stationary phase degrades over time, and this degradation is faster at higher temperatures (McNair, Miller, and Snow 2019, p. 66). It is observed as a rise in baseline during the high temperature part of a temperature program. Various stationary phase technologies can be employed to reduce column bleed, but because the amount of column bleed depends on the amount of stationary phase it is clear that a 1 m column will have 1/30th of the column bleed of a 30 m column with the same stationary phase. Despite using temperature programs that went up to the temperature limit recommended by the column manufacturer, column bleed was not a significant feature in the obtained chromatograms.

6.3.2 Thermal shock

An aspect of fast temperature programming with such a temperature range as used in this study (-30°C to 400°C) is **thermal shock**. Thermal shock occurs when an object is subjected to a rapid change in temperature. Under such non-equilibrium conditions different parts of the object will have different temperatures. The material that the object is made of has a certain **coefficient of thermal expansion**, which means that the relative sizes of the parts of the object at different temperatures will change at different rates. This will cause stress between the parts, and if the stress exceeds the strength of the material, the material will fracture. Fused silica has a low

coefficient of expansion², and therefore experiences low thermal shock. The amount of material in a capillary is also relatively small, which keeps temperature gradients small and therefore stresses low. No column failures that could be ascribed to thermal shock were observed.

6.3.3 Thermal fatigue

Another cause of material failure due to temperature is **thermal fatigue**. "Thermal fatigue (TF) is the gradual deterioration and eventual cracking of a material by alternate heating and cooling during which free thermal expansion is partially or completely constrained" (Rao and Raj 2001). The expansion of the portion of the fused silica column subjected to alternate heating and cooling is not constrained, and the part of the fused silica column that is constrained (in the sealing ferrules) is not subjected to alternate heating and cooling (it is held at constant temperature in the heated T-piece block), therefore thermal fatigue is not expected. No explicit test for thermal fatigue was performed, but no column failure that could be attributed to thermal fatigue was observed.

6.3.4 Corrosion

One failure of the coaxial heater could be attributed to corrosion. The joint between the coaxial heater and the heated T-piece block is brazed, and there was a failure of the thin-walled stainless steel tube near that joint in the portion heated during the brazing operation. Visual inspection seemed to indicate thinning caused by corrosion. An acid flux was used during the brazing, which might have contributed to the corrosion, especially in the presence of water condensed from the atmosphere during the cooling of the column.

6.3.5 GC retention time precision

During the development of the resistive heater it was shown that the measured temperature ramps are highly repeatable. But the retention times of compounds being separated by GC are highly sensitive to temperature, so it was necessary to obtain a measure of the retention time repeatability.

To estimate the retention time variance, two alkanes (dodecane and hexadecane) were added to the SFC mobile phase at a concentration of about 0.6 %. These compounds are not retained on the silica at all, and are therefore present in all the GC runs at the same concentration and all the peaks should be identical. Variance in retention time, peak area, and peak height therefore indicate the repeatability of the fast GC system. Variability of retention time is summarized in Table 6.1.

TABLE 6.1: A summary of retention time repeatability of alkanes separated on the fast temperature programmed chromatograph.

Compound	n	t _r (s)	S.D. of t _r (s)	R.S.D. of t _r (%)
Dodecane	73	5.07	0.023	0.46
Hexadecane	73	6.58	0.052	0.78

² $0.55 \times 10^{-6} \text{ K}^{-1}$, compared to the $9.0 \times 10^{-6} \text{ K}^{-1}$ of soda lime glass or the $4.0 \times 10^{-6} \text{ K}^{-1}$ of borosilicate glass

The peak widths were about 500 ms, so the 20 ms standard deviation for hexadecane means that the variation in retention time is only about 10 % of the peak width. The relative standard deviations (RSD) of retention times were similar to those obtained in GC \times GC (Shellie, Xie, and Marriott 2002), and much smaller than those of our original “proof of concept” instrument , for which standard deviations of 0.080 s and 0.087 s were reported for dodecane and hexadecane respectively (Venter 2003; Venter and Rohwer 2004).

6.3.6 Coolant consumption

In Section 5.5.8 it was mentioned that the first SFC \times GC instrument consumed many kilograms of carbon dioxide coolant for each run. With coaxial cooling, if a typical SFC \times GC run consists of 200 GC runs which each requires 7 s of coolant flow at a rate of 30 g min⁻¹, then 700 g of carbon dioxide coolant would be consumed per run, an order-of-magnitude improvement.

6.4 Study of potential biodiesel feedstock by SFC \times GC

Biodiesel can be produced from any combination of a variety of vegetable oils³. Indeed, to ensure conformance to standards it might be necessary to produce biodiesel from blends or combinations of oils. But as an introduction it is instructive to start by analysing the FAMEs obtained from neat oils.

6.4.1 Samples

Various samples of edible oil were obtained from supermarkets. (See Table 6.2)

TABLE 6.2: Oils used for FAME analysis

Oil	Brand	Species
Canola	Spar	<i>Brassica napus</i>
Sunflower oil	Pick n Pay	<i>Helianthus annuus</i>
Coconut oil	Lemcke	<i>Cocos nucifera</i>
Flax seed oil	Lemcke	<i>Linum usitatissimum</i>
Salmon oil	Dis-Chem Gold	Family <i>Salmonidae</i>

6.4.2 Sample preparation

Fatty acids in oils might be either free or bound to glycerol. To quantitatively convert them to FAMEs therefore requires that the bound fatty acid be transesterified, and the free fatty acids esterified. Both transesterification and esterification can be achieved by acid catalyst, but this reaction is quite slow. Basic catalysts can rapidly transesterify acyl glycerols, but will not esterify free fatty acids.

The method used involved first treating the oil sample with sodium hydroxide dissolved in dry methanol. The methanol acts as a solvent but also provides an excess of methanol so that the transesterification reaction is driven to completion.

³At this time SANS 1935 excludes animal fats, but they might be included in future. All of the following discussion also applies to animal fats.

On completion of the reaction an excess of acid is added, which neutralizes the base and esterifies any free fatty acids. Then an organic solvent and water are added, which provides two phases: the non-polar FAMEs dissolve in the organic layer, and the polar glycerol and salts dissolve in the water layer.

Method

This method is based on an official method (AOCS 2017), modified in two respects. Firstly, the acidic catalyst boron trifluoride is replaced by sulphuric acid, and secondly, hexane is used instead of heptane.

1. Transfer 4 drops of melted sample to a 20 ml glass stoppered test tube. Add a few boiling stones.
2. Add 2 ml NaOH/methanol solution (0.5N) and boil for 11 min under reflux.
3. Add 2 ml 10% H₂SO₄/methanol solution via the condenser and boil for 2 min.
4. Add 2 ml hexane via the condenser and boil for 1 min.
5. Remove the test tube from the heat source and leave to cool.
6. Add 4 ml saturated NaCl solution and mix gently.
7. Allow the phases to separate. Transfer the hexane layer to a vial and use for injection.

6.4.3 SFC

A 0.5 μ l volume of the hexane layer was injected into the neat carbon dioxide mobile phase as described in Section 4.4. The column was five HPLC columns (150 mm \times 4.6 mm, 3 μ m particles) (Restek, Pinnacle DB Silica) connected in series.

6.4.4 Modulation

The modulation period was 10 s, during which the fractions of the SFC eluate were transferred to the GC inlet via a linear restrictor. In the hot (350 °C) inlet the fractions evaporated instantly and were swept onto the cold (-20 °C) column where they were trapped in the stationary phase. 3 s after the collection period ended the vent valve opened for 1 s to vent excess pressure from the GC inlet.

6.4.5 GC

The fast temperature program ramped the GC column temperature from -20 °C to 350 °C in 10 s (2220 °C min⁻¹), maintaining 350 °C for 2 s. Then the cooling system activated and cooled the column to -20 °C or below, ready to trap the next SFC fraction. The FID detector was kept at 350 °C.

In this way a series of GC chromatograms of SFC fractions were recorded, which were assembled into a 2D chromatogram. Figure 6.2 shows a 2D chromatogram of a sample of FAMEs prepared from canola oil. This 2D chromatogram consists of 132 fast GC chromatograms collected in approximately 90 minutes.

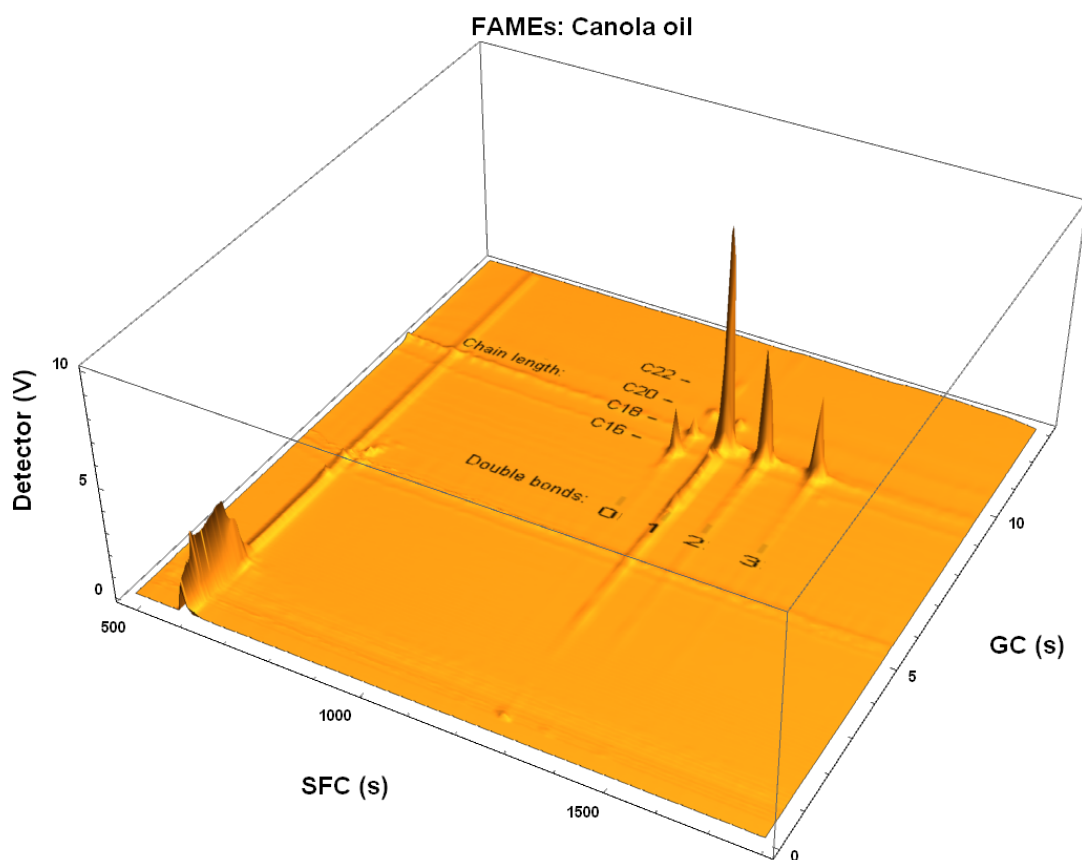


FIGURE 6.2: A 2D chromatogram of FAMEs derived from canola oil.
It is clear that the oil consists mostly of unsaturated fatty acids.

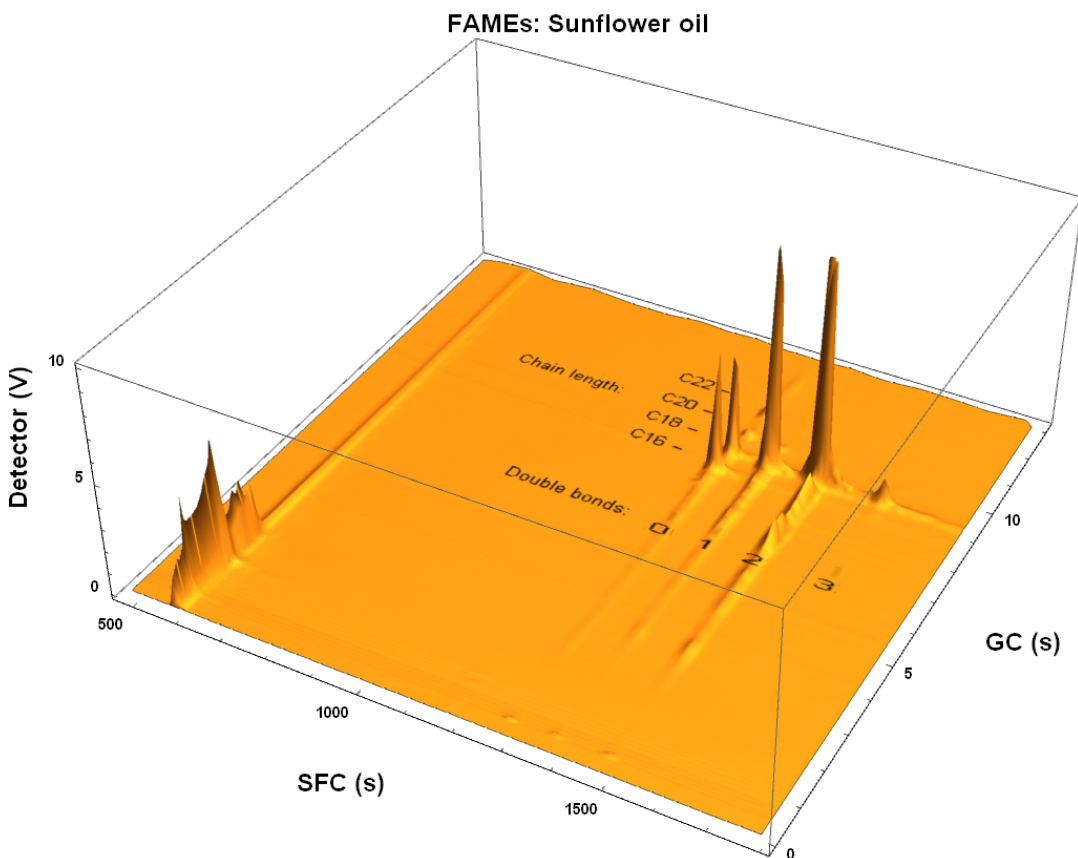


FIGURE 6.3: A 2D chromatogram of FAMEs derived from sunflower oil. It is clear that the oil consists mostly of unsaturated fatty acids, with a high proportion of linoleic acid (C18:2).

6.4.6 Results and discussion

The chromatogram shown in Figure 6.2 is very simple to interpret. In the SFC dimension, separation is by number of double bonds. This means that FAMEs without double bonds elute first in this dimension, followed by FAMEs with one, two and three double bonds respectively. There is good resolution between the peaks in the SFC dimension.

The volatility of a FAME depends primarily on the length of the carbon atom chain, therefore the separation in the GC dimension is by chain length. Because these FAMEs are of biological origin, we expect their chains to have an even number of carbon atoms. From the literature we know that oleic acid (C18:1) is the most common fatty acid in canola oil (Joint FAO/WHO Codex Alimentarius Commission 2019), and that therefore the major peak in the chromatogram is a C18 FAME. This allows us to easily identify the peaks for C16, C18, C20, and C22 in the GC dimension.

The information provided by this chromatogram confirms that canola oil is a viable biodiesel feedstock: The unsaturated compounds have mostly a single double bond, which should make it oxidatively stable (), and the quantities of unsaturated FAMEs are low, which means that it will most likely have suitable cold-flow properties (see Section 3.5.4), because the naturally occurring *cis* isomers of unsaturated FAMEs have higher freezing points than their saturated analogues.

Sunflower oil

Figure 6.3 shows an SFC \times GC chromatogram of FAMEs obtained from sunflower oil. The biggest peak in the chromatogram corresponds to linoleic acid methyl ester (C18:2). This agrees with the literature, which indicates that the main, traditional cultivar of sunflower produced in South Africa is of the high-linoleic type, with a fatty acid profile of 69 % linoleic acid, 20 % oleic acid, and 11 % saturated fats (Joint FAO/WHO Codex Alimentarius Commission 2019).

This sunflower oil chromatogram was compared to a fatty acid profile obtained by an accredited oil analysis laboratory⁴. (See Table D.1.) The fatty acid profile data was plotted on a 3D bar chart (See Figure 6.4). The axes of the bar chart were chosen to plot the fatty acid profile information in a similar space and scale as the chromatogram (Figure 6.3). It can be seen that the bar chart shows the same information as the chromatogram. The information in the bar chart has been obtained from a 1D chromatogram by integrating peaks, calculating amounts of FAMEs from peak areas, and then plotting those amounts in the bar chart, whereas the SFC \times GC chromatogram is a plot of FID response and involves no quantification.

This chromatogram suggests that sunflower oil is a suitable feedstock for producing biodiesel: the relatively high amount of unsaturated FAs would seem to imply suitable cold flow properties (see Section 3.5.4). The relatively high degree of unsaturation does suggest caution regarding oxidative stability (see Section 6.4.6).

Coconut oil

Figure 6.5 shows the SFC \times GC chromatogram of FAMES from coconut oil (*Cocos nucifera L.*). It is clear that the dominant FAMEs in coconut oil are saturated.

The high saturation of coconut oil makes it oxidatively stable (see Section sec:Rancimat), but the high melting point of the saturated FAMEs also means that it might not meet cold flow requirements (see Section 3.5.4).

The high oxidative stability of coconut oil makes it resistant to going rancid, which means it has been used as a natural ingredient for cosmetics since antiquity (Berdick 1972).

Flax seed oil

Figure 6.6 shows an SFC \times GC chromatogram of FAMEs obtained from flax seed oil. This oil is obtained from the seeds of the annual plant *Linum usitatissimum*, and was sold as an edible oil.

The chromatogram shows that the major fatty acid component of flax seed oil is linolenic acid (C18:3). This will immediately inform a producer that flax seed oil would not be a suitable feedstock for biodiesel: SANS 1935 limits the linolenic acid fraction to less than 12 % (See section 3.9.5).

Flax seed oil only recently became considered a food or a food supplement: the 1911 edition of the Encyclopaedia Britannica only mentions it as a food by saying "The oil is to some extent used as food in Russia and in parts of Poland and Hungary" (*Linseed* 1911), and remarks that the oil is edible when it is cold pressed. This is not surprising, because the oil goes rancid very quickly, leaving it unpalatable. Historically the more common name for the oil has been **linseed oil** and it was mainly used for industrial purposes, particularly in paint and varnish formulations. As the

⁴Precision Oil Laboratories, info@precisionoils.co.za, +27 15 307 7208, SANAS Testing Laboratory T0802

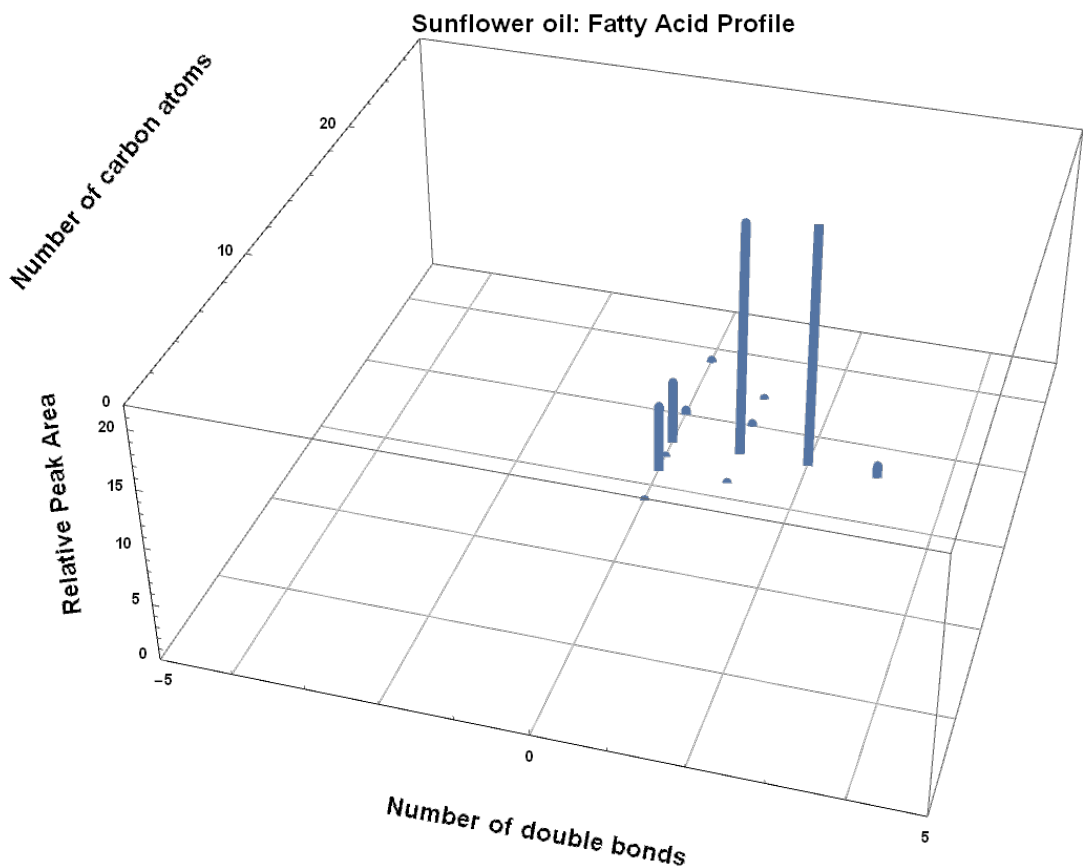


FIGURE 6.4: The fatty acid profile of a sunflower oil, when plotted on a suitably-scaled bar chart, shows how well the SFC \times GC chromatogram of the same oil (Figure 6.3) represents the same data without any processing.

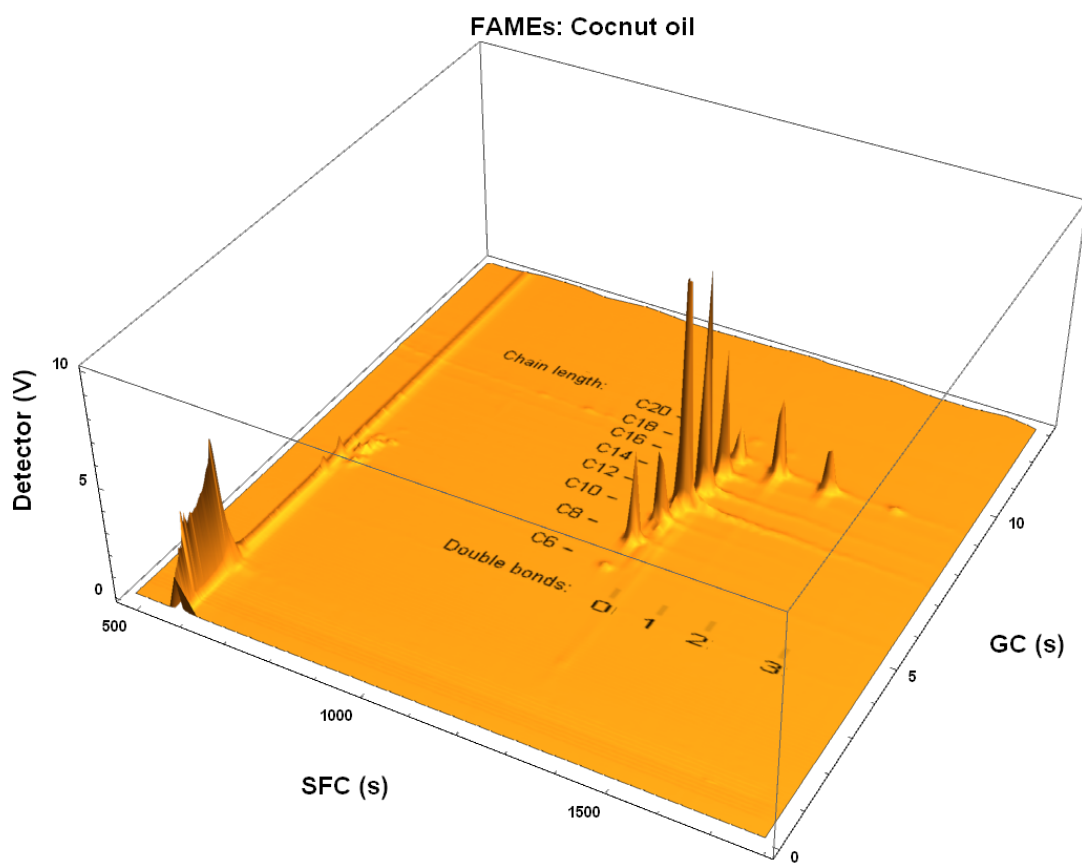


FIGURE 6.5: A 2D chromatogram of FAMEs derived from coconut oil.
It is clear that the oil consists mostly of saturated fatty acids.

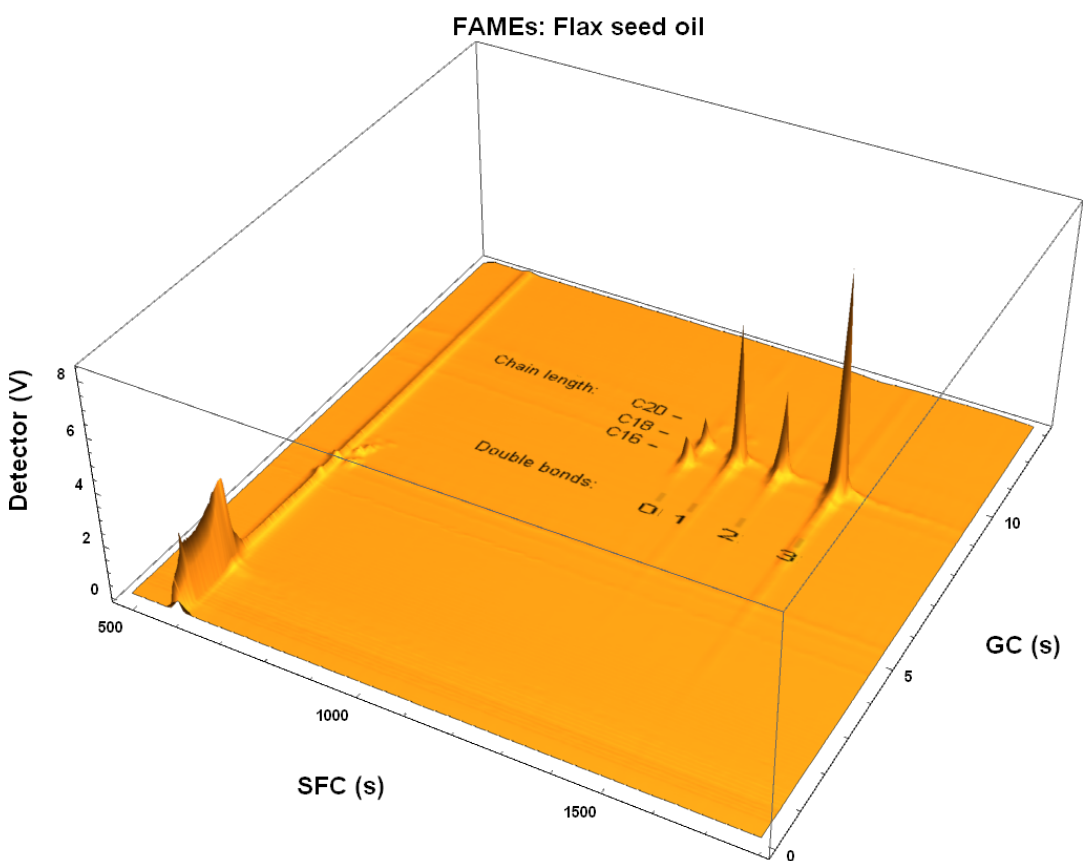


FIGURE 6.6: A 2D chromatogram of FAMEs derived from flax seed oil. It is clear that the oil consists mostly of highly unsaturated fatty acids.

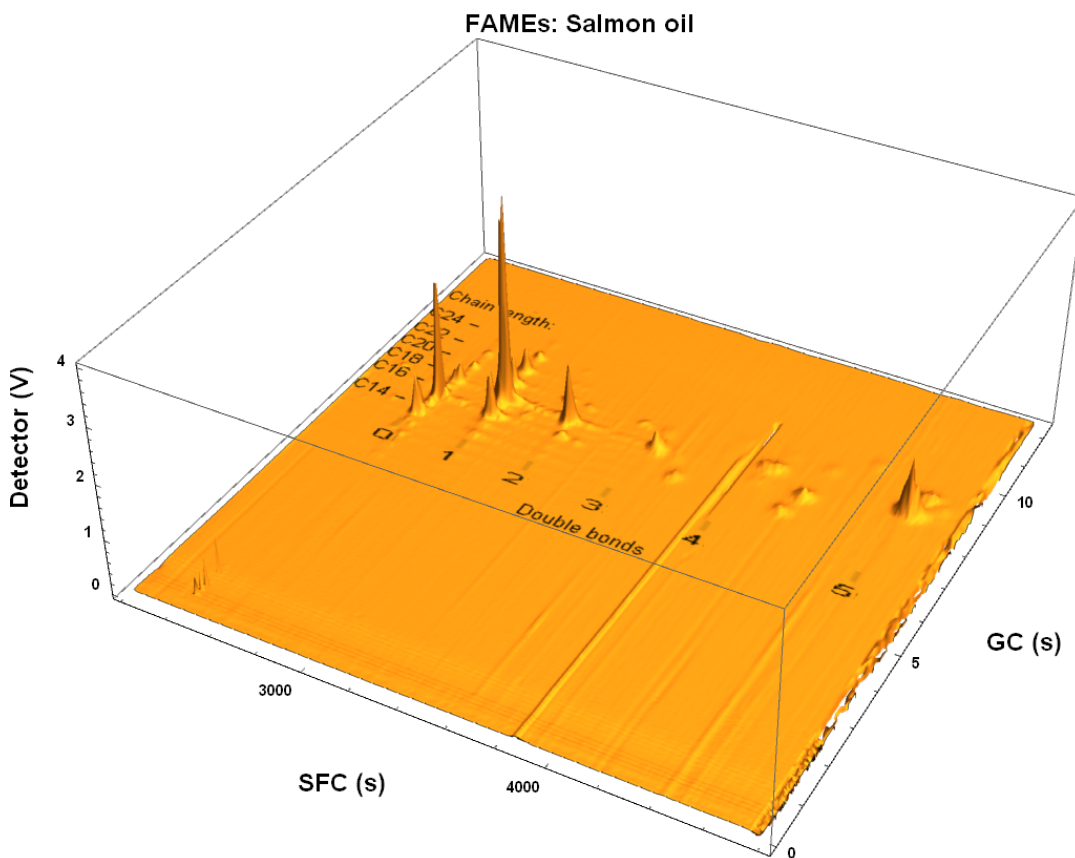


FIGURE 6.7: A 2D chromatogram of FAMEs derived from salmon oil. It is clear that the oil contains significant quantities of polyunsaturated fatty acids.

encyclopedia puts it: “Commercial linseed oil has a peculiar, rather disagreeable sharp taste and smell.” The oil used in artists’ oil paints is most commonly refined and prepared linseed oil. This oil is classed as a **drying oil**, because a layer of this oil exposed to air becomes solid, or “dry”. This is the result of the high degree of unsaturation of the oil, which rapidly causes oxygen-mediated polymerization. On exposure to air the oil gradually turns more viscous and eventually solid, making it a suitable base for paint, particularly if the oil has been pre-treated. In biodiesel such polymerization could cause clogging or the formation of objectionable sludge.

Salmon oil

Figure 6.7 shows an SFC \times GC chromatogram of FAMEs obtained from salmon oil. This oil is obtained from a variety of fish species of the family *Salmonidae* (Joint FAO/WHO Codex Alimentarius Commission 2017) and was sold as a food supplement, packaged in gelatine capsules.

This chromatogram does not include the ${}^1\text{D}$ solvent peak. It is much more complex than the chromatograms of the plant oils shown above. It clearly shows a degree of unsaturation of up to 5, and there is evidence of a peak that represents a degree of unsaturation of 6. Unfortunately the instrument started malfunctioning before this peak could elute completely, and because of a shortage of time and money the

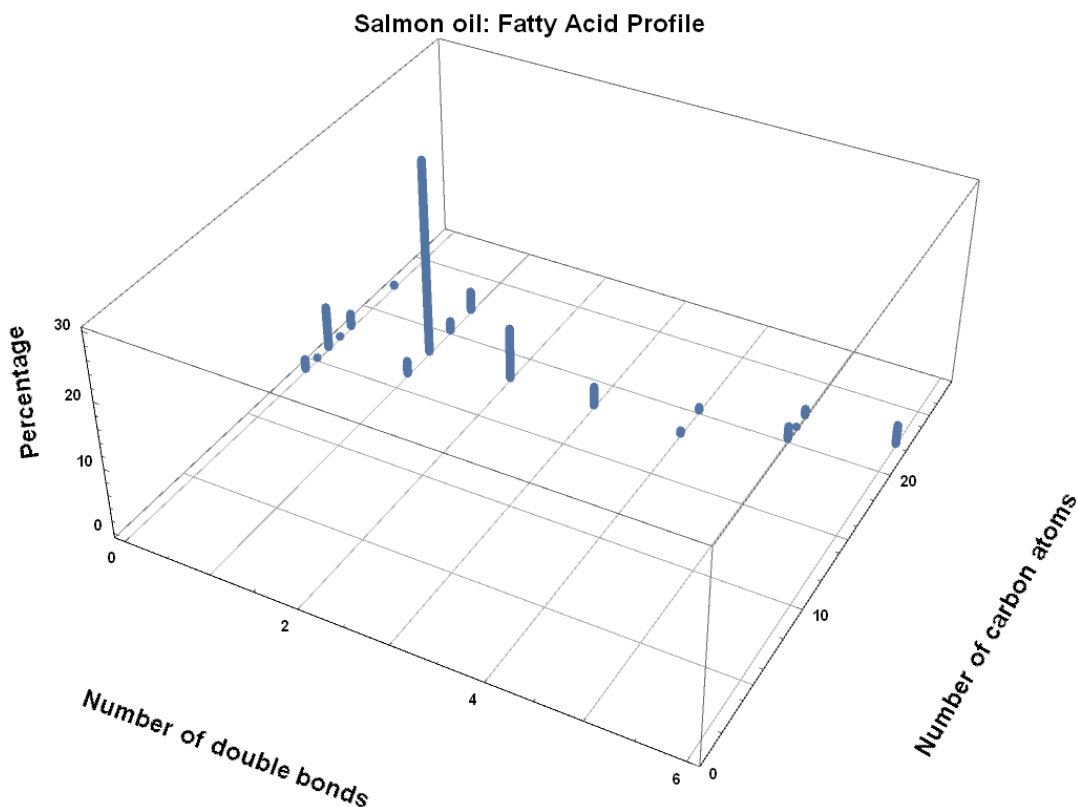


FIGURE 6.8: The fatty acid profile of salmon oil, when plotted on a suitably-scaled bar chart, shows how well the SFC \times GC chromatogram of the same oil (Figure 6.7) represents the same data without any processing.

project could not be extended to repair the instrument, repeat the chromatogram, and confirm the results.

The fatty acid profile of salmon oil given by the Codex Alimentarius (Joint FAO/WHO Codex Alimentarius Commission 2017) is shown in Table D.3. Figure 6.8 shows the bar-chart representation of the fatty acid profile. A comparison of the pattern in chromatogram with the bar chart shows that the chromatogram is consistent with the source of oil being farmed salmon. The chromatogram also suggests that biodiesel made from salmon oil would not be compliant with SANS 1935: the mass fraction of fatty acid methyl esters with four or more double bonds is more than 1 %, which is above the specified limit (see Section 3.9.5).

This complex chromatogram also raises the intriguing possibility of identifying fatty acid isomers by SFC \times GC. This is suggested by the small peaks with a ^1D retention times slightly different from the main peaks. The identification of the isomers fall outside the scope of this project, but initial indications are that, for example, the n-9 isomers of the monounsaturated fatty acids are slightly less retained than the n-7 isomers. Further studies will be needed to compare this suspicion to the separation of *cis/trans* isomers of FAMEs reported by Roger Smith (Smith, Hyytiänen, et al. 2001).

The peak patterns generated in SFC \times GC chromatograms of FAME mixtures are powerful and highly suggestive, but it should be emphasized that patterns are mere guides and cannot be used to positively identify compounds. Mass spectrometry can give additional confirmatory information, and injecting standards is the ultimate

method for identifying peaks with compounds.

6.5 Conclusion

Comprehensively coupled chromatography offers better analytical separations in three ways: improved peak capacity, improved sensitivity, and more structured data. The examples presented here do not pretend to prove improved peak capacity: biodiesel is not normally considered a chromatographically-challenging complex sample. Neither is improved sensitivity relevant: determining biodiesel components is not a trace analysis problem for which high sensitivity is necessary. What these examples do show is that the high orthogonality between SFC and GC provides data that contains a clear and powerful pattern that greatly simplifies interpretation. In contrast, Figure 6.9 shows a GC \times GC chromatogram of a 37-component FAMEs standard. This separation uses a polar column in the first dimension, and a non-polar column in the second dimension (SepSolve Analytical 2018). The coloured bands indicates the 2D retention times of FAMEs with different degrees of unsaturation. The positions of these bands were determined experimentally using TOF-MS, and are not based on a separation mechanism. The lower orthogonality of GC \times GC, compared to SFC \times GC, means that the position of the bands cannot be predicted, and the shapes of the bands are likely to change with changing chromatographic conditions.

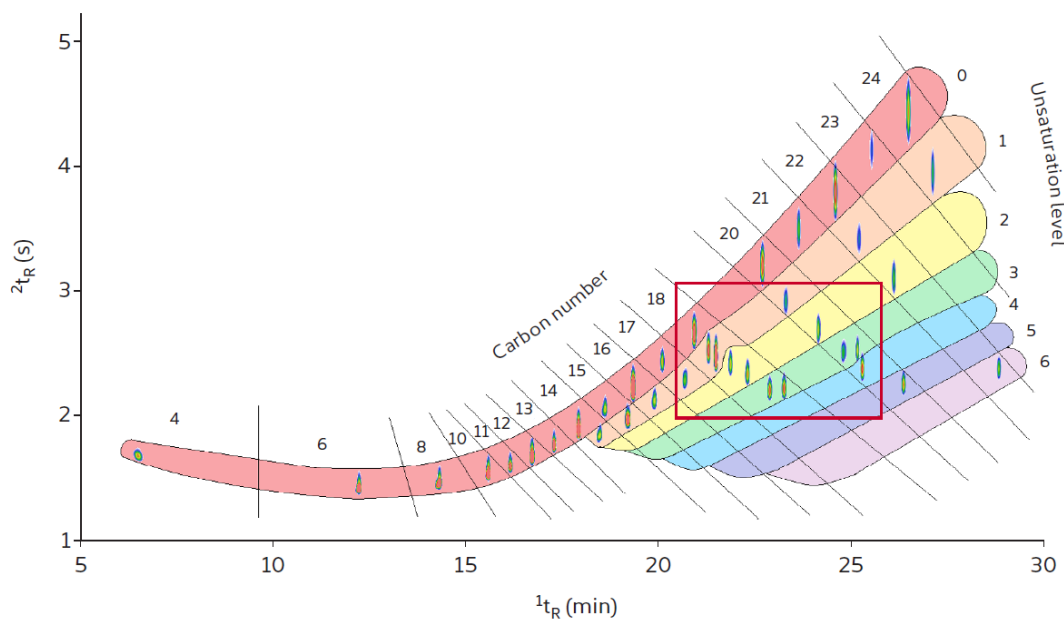


FIGURE 6.9: GC \times GC-FID colour plot of a 37-component FAME standard. The coloured bands indicate successively higher levels of unsaturation, from 0 (red, no double bonds) to 6 (violet, with 6 double bonds) (SepSolve Analytical 2018).

In the example of FAMEs derived from various oils the pattern shows how the separation is based on degree of unsaturation in the first dimension and on volatility in the second dimension. These separations, combined in one 2D chromatogram,

provides intuitive understanding of the chemical composition of the oils which facilitates prediction about the contribution these oils will make to the final biodiesel product.

SFC \times GC can assist with proving compliance: it provides a chromatographic method that combines the determination of total FAMEs and unsaturated FAMEs in a single method. The provided examples also prove that it is possible to design a system that solves the problems of doing practical, rapidly-repeated fast temperature programmed GC, ramping temperatures from below ambient to the limits of the column in hundreds of consecutive, identical runs. This high performance is possible without resorting to expensive technology.

I love the smell of diesel in the morning.

T-shirt slogan, popular with truckers, which reflects the aromatic content of diesel fuels.

7

The determination of FAMEs and PAHs in diesel fuel by SFC \times GC.

7.1 Introduction

In South Africa the quality of biodiesel is regulated by the technical standard SANS 1935, and that of petrodiesel by SANS 342. There is a considerable overlap in the requirements of the two, as discussed in Section 3.10.1 and illustrated in Figure 3.5. Two of the requirements of SANS 342 that are not found in SANS 1935 are the allowed amounts of polycyclic aromatic hydrocarbons (PAHs) and fatty acid methyl esters (FAMEs). This chapter introduces SFC \times GC as a method that can combine these two determinations.

7.1.1 FAMEs in diesel

Biodiesel can be blended in all proportions with diesel obtained from petroleum (**petrodiesel**). To reduce the carbon footprint of diesel fuel, legislators are encouraging the use of blended fuels. Manufacturers might also add biodiesel to their fuel formulations to improve properties such as lubricity (Knothe and Steidley 2005), or for its ability to reduce engine emissions (Wattrus et al. 2016). In South Africa the standard grade of diesel may contain up to 5 % volume fraction biodiesel, and higher fractions of FAMEs are allowed as different grades (South African Government 1977).

The test methods for FAMEs in standard diesel allowed by SANS 342 are EN 14078, ASTM D7806, or ASTM D7371. These are all infrared (IR) absorption methods. The methods described in EN 14078 and ASTM D7806 quantify FAMEs by measuring the absorption of infrared radiation at 1745 cm^{-1} ($5.4\text{ }\mu\text{m}$) in an absorption cell with a path length of 0.5 mm. The stretching vibrations of the carbonyl groups found in the ester functional group of FAMEs resonate with electromagnetic radiation at this wavelength, which causes strong absorption. The amount of radiation absorbed is proportional to the concentration of the FAMEs so a **Beer's law** method is used for calibration and quantitation. The hydrocarbons that constitute the bulk of petrodiesel do not absorb radiation of this wavelength and will not interfere with

the measurement. The method prescribed by ASTM D7371 specifies **attenuated total reflection** (ATR) IR absorption spectrophotometry combined with **partial least squares** (PLS) calibration, which simplifies sample handling but complicates calibration. Both these methods make some assumptions about the sample, and the methods may suffer from inaccuracy if those assumptions do not hold (Pinho et al. 2014).

7.1.2 PAHs in diesel

Polycyclic aromatic hydrocarbons (PAHs) are noxious pollutants and are therefore regulated when possible. The primary source of PAHs that enter the environment is combustion, of which a portion takes place in internal-combustion engines. PAHs are also abundant in fossil fuels, including diesel, and might escape from diesel during normal operations or in leaks and spills. Primarily, however, the higher the proportion of aromatic compounds in diesel fuel, the higher the PAH emissions of the engine it fuels (Souza and Corrêa 2016). These higher emissions are ascribed to the poorer combustion of fuels containing higher amounts of aromatics. For all these reasons regulators aim to reduce the exposure of the population to the harm of PAHs by limiting the amount of PAHs in diesel.

SANS 342 describes two classes of diesel fuel, CF1 and CF2, named after the Department of Energy's Cleaner Fuels programme. For CF1 the standard does not include a requirement for PAHs, but for CF2 an upper limit of 8 % mass fraction is prescribed. At the time of writing the implementation date of the CF2 standard had been indefinitely postponed.

The test methods for determining the amount of PAHs in diesel prescribed by SANS 342 are IP 391, ASTM D2425, or EN 12916. In case of dispute EN 12916 is the referee method. IP 391 and EN 12916 are HPLC methods with **refractive index** (RI) detection. ASTM D2425, although entitled "Standard Test Method for Hydrocarbon Types in Middle Distillates by Mass Spectrometry" requires the chromatographic separation of the aromatics from the saturates by chromatography before the MS measurement. All these methods allow for the presence of FAMEs in diesel. Although these methods undoubtedly provide reliable results when applied intelligently, quantitation by refractive index and mass spectrometric detection have their problems, as reviewed in detail by Kamiński et al. 2005. As an example of one of the challenges for RI detection, there is no correlation between the refractive index of a compound and its chemical structure. Therefore successful quantitation depends on the precise determination of response factors. But in a mixture of petrochemicals from different feedstocks the compounds and their relative quantities are unknown, so the physical meaning of the determined peak areas is unclear (Sarowha et al. 2000).

Although not specified by SANS 342, ASTM D5186 is an SFC-FID method for determining the amount and type of aromatic compounds. In principle it is similar to the prescribed HPLC methods, with three key differences: it uses neat carbon dioxide at high pressure as a mobile phase, it uses bare silica as a stationary phase, and it uses flame ionization as a detector (FID). As discussed in Section 2.3.1, the FID has an unsurpassed dynamic range and responds primarily to the number of carbon atoms in the analyte, which means that its signal reflects the mass of the analyte. This reliable and robust detector excels at the quantitation of hydrocarbons.

7.1.3 SFC \times GC of petrodiesel/biodiesel blends

The elution behaviour of aromatic hydrocarbons during SFC are different from those of FAMEs. Being polar oxygenates, the FAMEs are much more retained on silica than the non-polar aromatic compounds, and the two classes elute separately. But, just as the aromatic hydrocarbon compounds elute in order of their number of rings, the FAMEs elute in order of their number of double bonds (Smith, Hyytiänen, et al. 2001).

Comprehensively coupling GC to SFC to separate fractions of the SFC eluate on a second dimension will then yield further information that correlates with the molecular mass of the compounds. The simplicity of coupling GC to SFC has been recognized and used for the detailed analysis of hydrocarbon groups in diesel (Pál, Juhász, and Stumpf 1998).

7.2 Experimental

7.2.1 Samples

Diesel/biodiesel blend

A sample was prepared by blending 7 % of biodiesel from canola (labelled "rapeseed methyl ester" (RME), provided as a research sample by Sasol Fuels) with a commercial low-sulfur (50 ppm) diesel. (The 7 % blend level was chosen to reflect the amount allowed by EN 590, the European equivalent to SANS 342). In a GC \times GC-MS analysis of the low-sulfur diesel using **electron ionization** (EI) the relative percentages of total ion intensity for different classes of compounds were 68.19 % alkanes, 18.10 % alkenes, 13.69 % aromatics and 0.01 % oxygenates (Smit 2015).

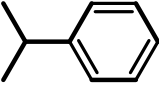
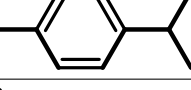
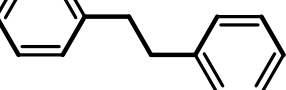
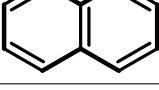
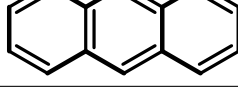
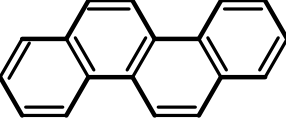
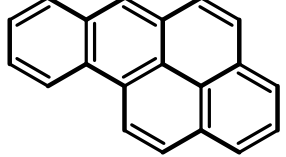
Spiked diesel

To examine the effect different numbers of rings of aromatic compounds have on their retention times, known amounts of selected aromatic compounds were added (**spiked**) to a neat sample of the same low-sulfur diesel as used in the blend described in Section 7.2.1 above. To keep costs low the compounds were selected from standards available in the laboratory, rather than compounds that might be used in standard methods. They were also selected to have high boiling points to ensure that they elute in the second dimension with retention times similar to the majority of the aromatic compounds in the sample. Under other circumstances toluene and tetralin (1,2,3,4-tetrahydronaphthalene) might have been chosen as the monocyclic aromatic hydrocarbon spikes, because these are prescribed for use in a performance mixture by ASTM D5186 and would be more familiar to users of that method. Although chemists might assume that PAHs all have fused rings, ASTM D5186 terminology makes it clear that the rings need not be fused: therefore bibenzyl and naphthalene are both examples of dicyclic aromatic hydrocarbons. The selected compounds and their amounts used in the spike are listed in Table 7.1.

7.2.2 SFC

The injection system described in Section 4.4 was used to inject a 0.5 μ l volume of the samples. The SFC mobile phase was neat carbon dioxide at 200 bar inlet pressure. The column consisted of five HPLC bare silica columns (150 mm \times 4.6 mm, 3 μ m particles) (Restek, Pinnacle DB Silica) connected in series.

TABLE 7.1: Aromatic compounds added to a 1.2819 g low-sulfur diesel sample

Structure	Name	Boiling point (°C)	Mass (mg)
	cumene	153.°C	8.4
	1,4-diisopropylbenzene	210.°C	9.3
	bibenzyl	284.°C	14.2
	naphthalene	218.°C	8.3
	anthracene	340.°C	7.1
	chrysene	448.°C	3.2
	benzo[a]pyrene	495.°C	3.1

7.2.3 Modulation

Two modulation periods were used: For the first portion of the chromatogram 3 s fractions of SFC eluate were collected on the GC column cooled to a temperature of -20°C or below. The inlet vent was held closed for 3 s after the the SFC stop valve closed to allow all of the eluted fraction to be swept onto the column, and then opened for 1 s to release excess pressure. For the second portion of the chromatogram the same trapping temperature was used, but the modulation period was increased to 10 s. This longer trapping period causes a higher increase in inlet pressure by the eluting carbon dioxide, which required a vent time of 3 s to release the excess pressure. Under these conditions all the criteria for comprehensive chromatography (see Section 9.4.2) are still met, so the coupling remains comprehensive throughout the 2D chromatographic run.

7.2.4 GC

The column used in the fast gas chromatograph was a DB-5MS column from J&W Scientific Inc, which had a stationary phase comprised of 5 % diphenyl, 95 % dimethylpolysiloxane. It was 1 m long, with an internal diameter of 0.25 mm. The thickness of the stationary phase was $0.25\text{ }\mu\text{m}$, and had an operational temperature range of -60°C to 325°C for isothermal elution, or up to 350°C when using temperature programming.

For every fast GC run the temperature program ramped from -30°C to 25°C at a rate of $8000\text{ }^{\circ}\text{C min}^{-1}$, and from 25°C to 350°C at a rate of $2000\text{ }^{\circ}\text{C min}^{-1}$, where it was held for 2 s. After the temperature program had ended the column was cooled to -20°C again and the next fraction was collected. Figure 7.1 compares the indicated average temperature of the column with the temperature program.

Fast GC chromatograms were obtained by recording the signal of the FID. The oven temperature of the FID was at 350°C . The amplifier gain was set so that an FID current of $1 \times 10^{-8}\text{ A}$ gave a 10 V output signal. The collected GC chromatograms were used to compile the 2D chromatogram.

7.3 Results and discussion

The chromatogram of the biodiesel/petrodiesel blend (Figure 7.2) shows that the blend was separated into two distinct groups of compounds. At a ${}^1\text{D}$ (SFC) retention time of about 780 s the hydrocarbons from the petrodiesel part of the blend eluted. To those familiar with petrochemical chromatography the characteristic unresolved complex mixture ("hydrocarbon hump") topped by alkane peaks will be instantly recognizable as representing a petroleum product. (See Figure 7.3 for an example.)

At ${}^1t_r \geq 2200\text{ s}$ a series of tall peaks represent the FAMEs, in a pattern that was described in Chapter 6: ${}^1\text{D}$ separation according to the number of double bonds of the fatty acids, and ${}^2\text{D}$ separation according to the chain length of the fatty acids.

7.3.1 Aromatic hydrocarbons

Between 800 s and 1200 s a pattern of small peaks can be seen in the chromatogram. This portion of the chromatogram is shown magnified in Figure 7.4, where individual peaks can clearly be distinguished.

This result can be compared to the results of the SFC-FID method by integrating each ${}^2\text{D}$ GC chromatogram, and plotting these values against their start times.

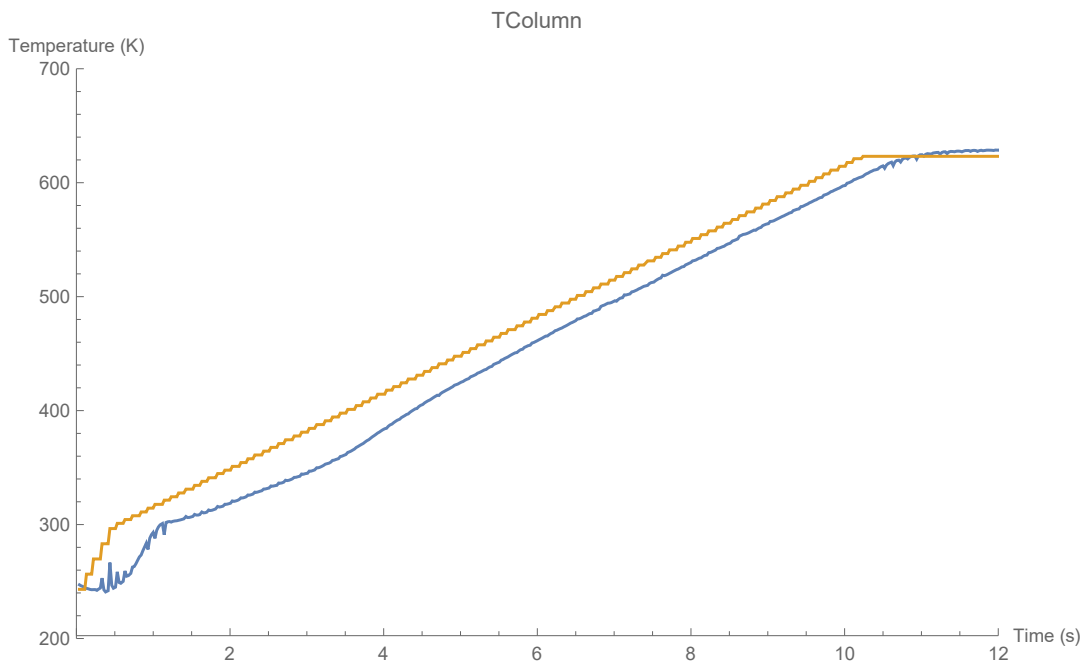


FIGURE 7.1: A comparison of the temperature set point and the indicated coaxial heater temperature during a fast GC run. The orange line shows the intended temperature program and the blue line shows the actual indicated temperature, as recorded. The “steps” in the orange line are caused by the 100 ms period of the control loop.

This creates a virtual SFC chromatogram, which should look similar to 1D SFC chromatograms. The virtual SFC chromatogram corresponding to Figure 7.4 is shown in Figure 7.5, compared to an SFC-GC chromatogram taken from the paper on which ASTM 5186 is based (Di Sanzo and Yoder 1991). The similarity between the virtual and real chromatograms suggest that the compounds that elute shortly after the alkanes are the aromatic hydrocarbons. The virtual chromatogram seems to show that there is incomplete separation between the alkanes and the aromatics, but the 2D chromatogram reveals that there is complete separation between any aromatic compound and its nearest neighbour alkane, but that there is tailing from the SFC column, which can be ascribed to excessive dead volume in the post-column flow path.

Although the identification of peaks of individual aromatic hydrocarbons in the SFC \times GC chromatogram is beyond the scope of this project, injection of the spiked diesel sample confirms that aromatic compounds elute in this region and shows that the PAHs in diesel can be clearly separated from the alkanes and quantified. By comparing the boiling points and relative masses of the spike compounds, a tentative peak assignment could be made, as shown in Figure 7.6.

It should be noted that the 5-ring PAH compound benzo[*a*]pyrene that was included in the spike did not elute in the SFC dimension on this chromatogram. Its ^1D retention time is still unknown, but broad interfering peaks in subsequent chromatograms can be attributed to slowly-eluting benzo[*a*]pyrene shows that it elutes in ^2D without wrap-around, so if the ^1D run was made longer one would expect its peak to appear in the 2D chromatogram.

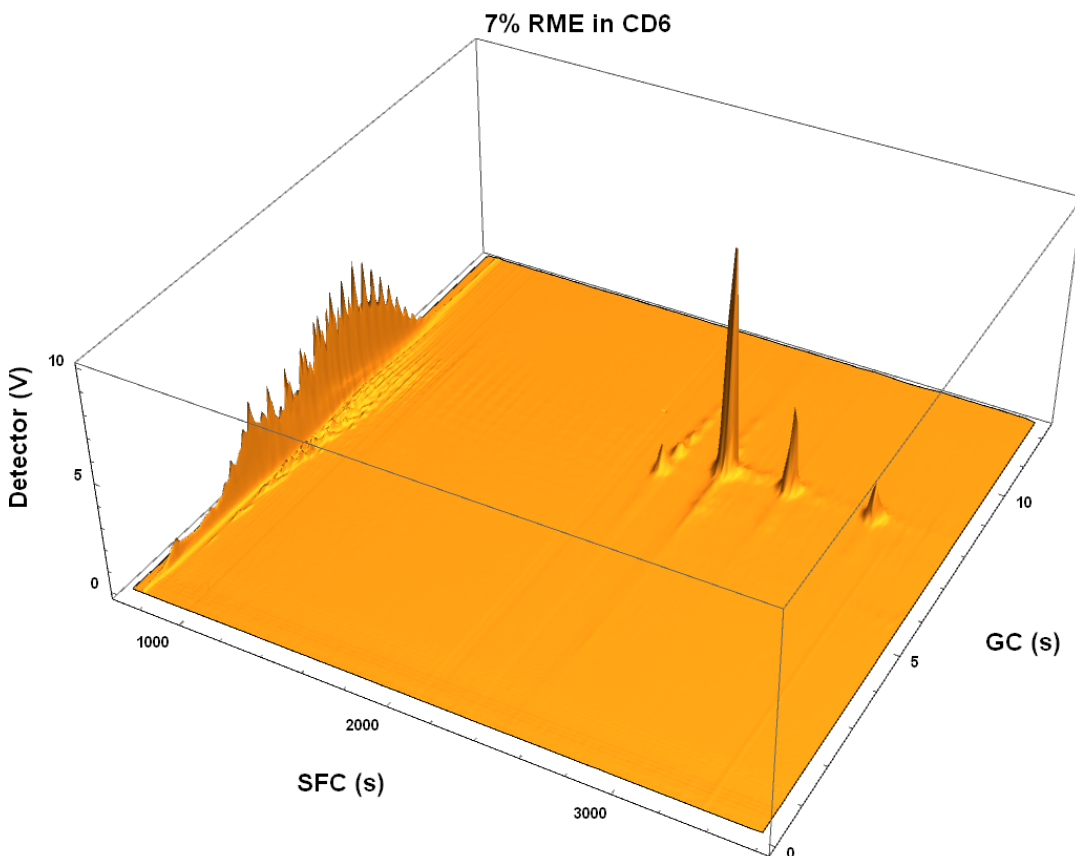


FIGURE 7.2: A 2D chromatogram of biodiesel and petrodiesel in a 7% blend. The hydrocarbons elute completely before the first FAME elutes, offering interference-free determination of both. The chromatogram was compiled from 368 1D fast temperature-programmed GC chromatograms.

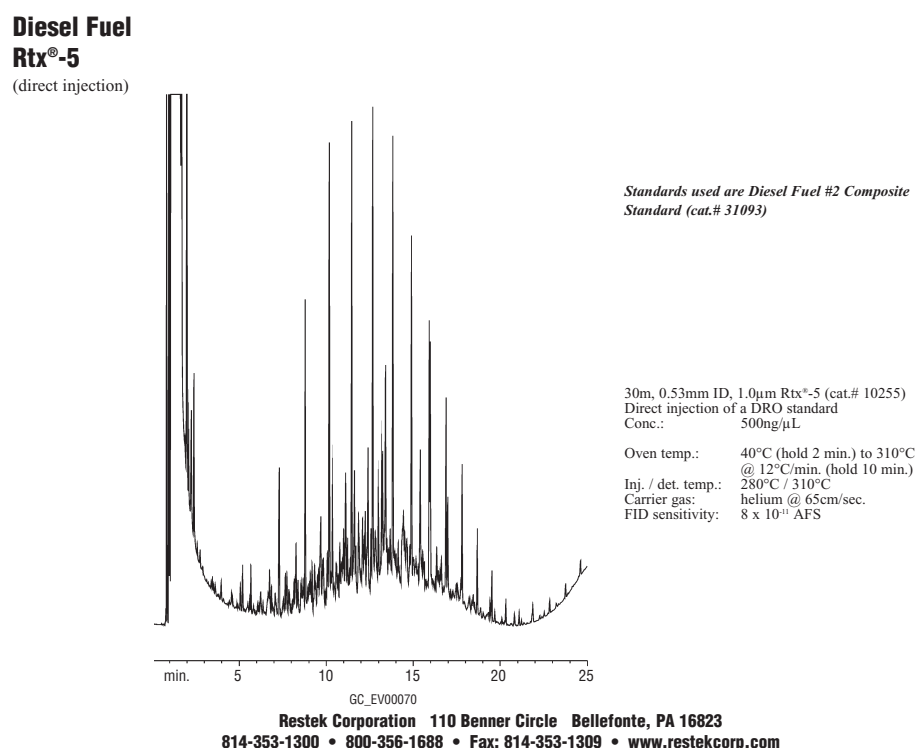


FIGURE 7.3: An example of a GC chromatogram obtained from a petroleum-based diesel fuel sample, showing the unresolved complex mixture topped by alkane peaks. Restek Searchable Chromatogram Library, reproduced with permission of Restek Corporation.

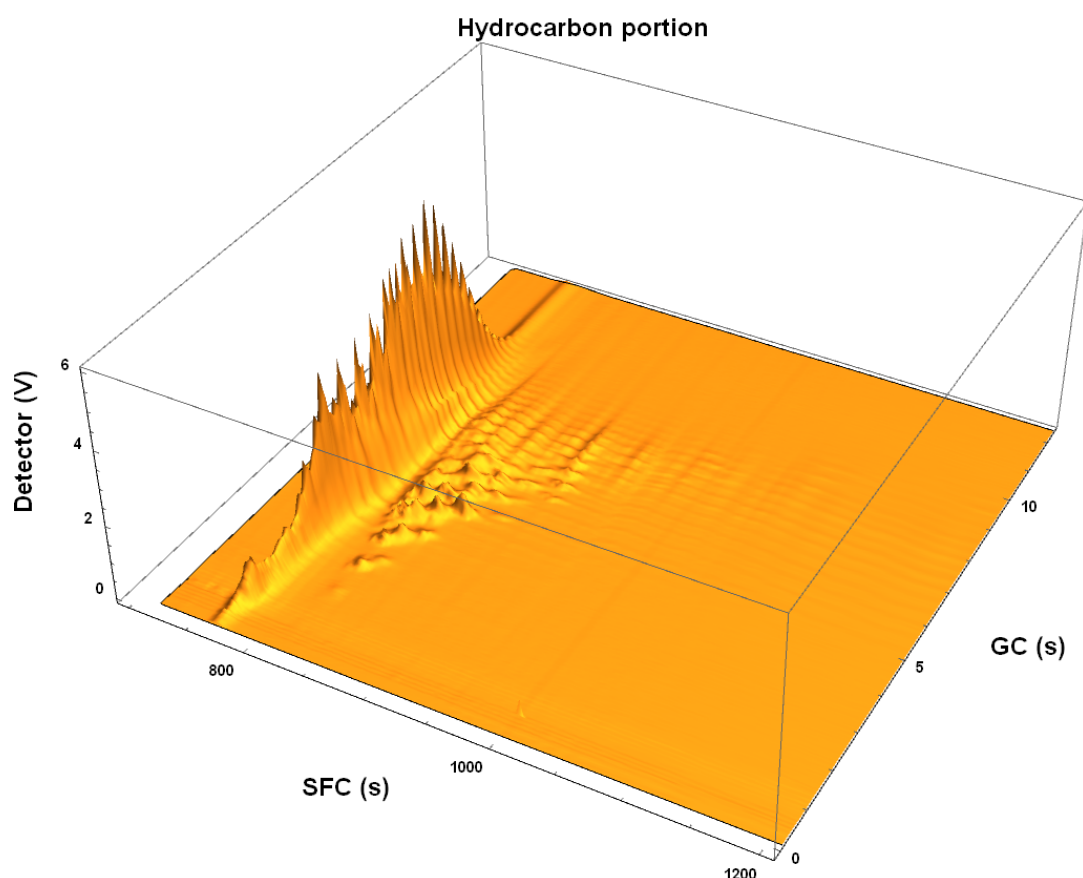


FIGURE 7.4: The portion of the chromatogram of the 7% biodiesel blend that contains the peaks attributed to the hydrocarbons.

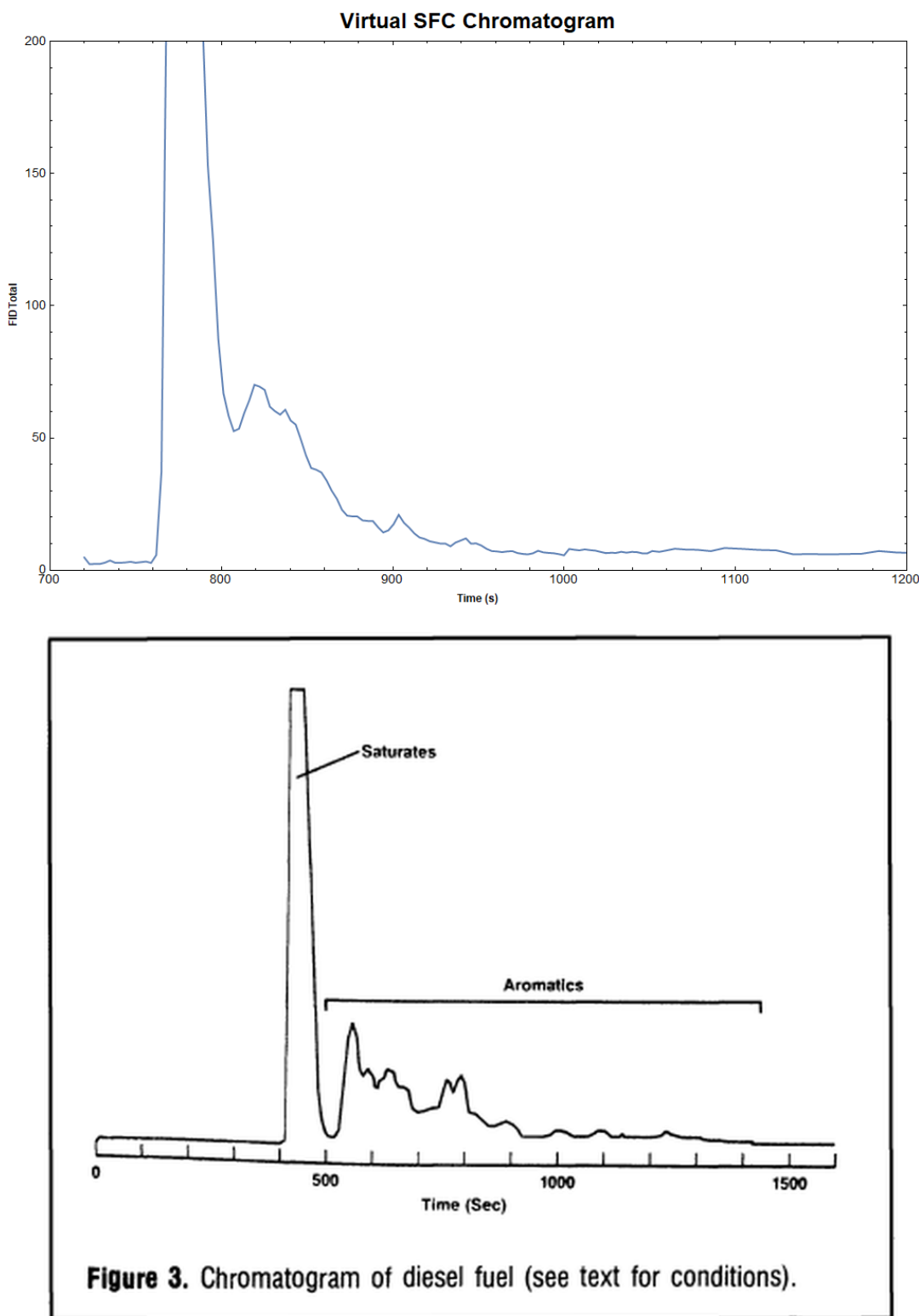


FIGURE 7.5: The virtual SFC chromatogram appears very similar to an SFC-FID chromatogram from literature (Di Sanzo and Yoder 1991).

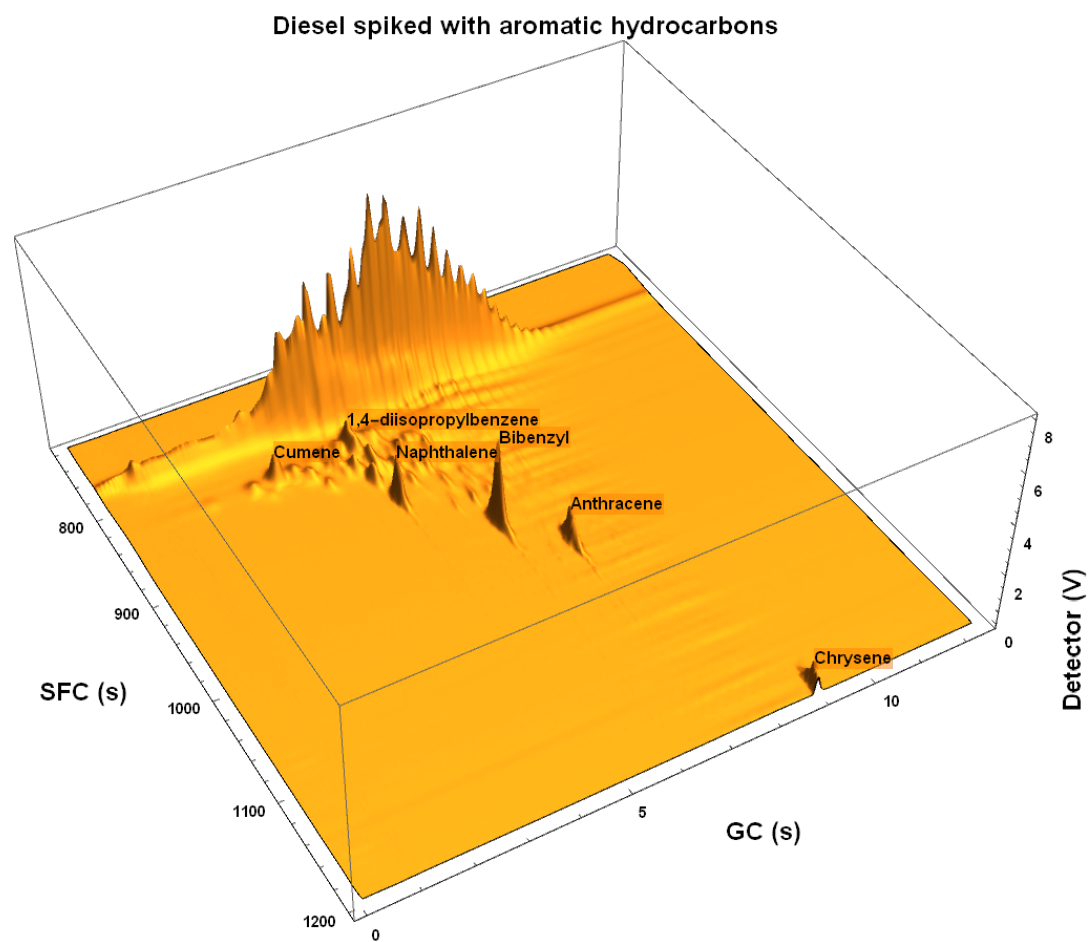


FIGURE 7.6: A 2D chromatogram of a commercial diesel sample spiked with selected aromatic compounds. Tentative peak assignments were made using knowledge of the boiling points and relative masses of the spike compounds.

7.3.2 FAMEs

Between the ${}^1\text{D}$ retention times of 2200 s and 3200 s the peaks of the FAMEs are seen, clearly separated by number of double bonds in the SFC dimension, and by volatility in the GC dimension. When compared to an SFC \times GC chromatogram of FAMEs obtained from canola oil (see Figure 6.2), the pattern is clearly similar, so the label “rapeseed methyl ester” is not incorrect.

7.3.3 Adjustable modulation

Because the SFC is operated in stopped-flow mode, the modulation period is independent of the fast GC run times. This means that the modulation period can be adapted during the SFC \times GC chromatographic run. Short modulation periods might be required to preserve resolution obtained in the ${}^1\text{D}$ separation but in areas of the chromatogram where there is plenty of resolution the modulation period can be increased to decrease the run time.

In the chromatogram of the biodiesel blend (Figure 7.2), the modulation period was 3 s up to a ${}^1\text{D}$ retention time of 1100 s. After that the modulation period was increased to 10 s, which shortened the chromatographic run time. In this instrument this is the upper limit of the modulation period, and is determined by the flow of carbon dioxide that the FID flame can tolerate¹

Suspending SFC fraction trapping

In an extreme version of adjustable modulation, it is also possible to suspend trapping. This is implemented by opening both the SFC stop valve and the GC inlet vent and not performing GC runs. The SFC eluate is then swept out of the GC inlet with no, or minimal, trapping on the GC column. This scheme might be used, for example, between ${}^1t_r = 1200$ and ${}^1t_r = 2200$ of the diesel blend chromatogram (Figure 7.2). No peaks of interest elute during this period, so suspending trapping can save a significant amount of time.

Variable GC temperature programs

Because stopped-flow operation decouples the SFC and the GC, the modulation period is independent of the GC run time as discussed in the previous section. But this implies that, conversely, the GC run time is independent of the modulation period. This means that the GC fast temperature program can be adapted to suit the GC separation of the different classes of compounds as separated by the SFC. For example, in the chromatogram shown in Figure 7.2 it can be seen that the FAMEs elute in a narrower temperature range than the hydrocarbons, which suggests that a different temperature program can be used for optimum separation.

¹If the flow of carbon dioxide through the column during trapping becomes too high, the flame is extinguished and the signal disappears. This limitation can be overcome fairly simply by arranging automatic re-ignition of the flame before the start of the fast GC run. Then the upper limit of the modulation period depends on the pressure limit of the GC inlet. This might be determined by mechanical strength, but experience has also taught that overly high inlet pressures can damage pressure gauges without any other sign of over-pressure. Alternatively, a portion of the SFC flow could be split off before it enters the GC inlet.

7.3.4 Application

The separation of the compounds found in the 7 % diesel/biodiesel blend shows that SFC \times GC can be used to investigate the amount of FAMEs and PAHs in petrodiesel blended with biodiesel without sample pre-treatment or specialized columns. The intrinsic orthogonality of the separations provides structured chromatograms which assist with the identification of components and the ample separation space allows for the addition of suitable internal standards for reliable qualitative and quantitative analysis by exploiting the robustness and reliability of the FID. Expensive mass spectrometric detection is unnecessary.

Being able to determine the biodiesel content of biodiesel blends may prove useful in at least two scenarios:

The first is in monitoring blending. Biodiesel (essentially a mixture of esters) is quite polar compared to petrodiesel (essentially a mixture of hydrocarbons). This means that blending might not be a matter of just pumping the relevant volumes of the respective fuels into a tank and relying on diffusion to complete the mixing. Being able to determine the amount of biodiesel in different samples of a blend will provide assurance that the blend is homogenous and should perform according to expectations. While such monitoring is perhaps better performed using a spectroscopic method, SFC \times GC can provide information for calibration, and will of course be invaluable during trouble shooting.

The second application of SFC \times GC is in regulating biodiesel content. In some political environments fuels might be taxed according to their biologically-derived content, for example to promote agriculture or to meet carbon emissions targets. Sometimes biological content is simply mandated. Such incentives and mandates are of course liable to corruption, and therefore it is necessary to be able to monitor the blending of the fuels. The most reliable way to differentiate between organic matter derived from biological sources and organic matter derived from fossil sources is a radiochemical method, where the content of radioactive ^{14}C is determined. (Organic material from fossil sources contains no ^{14}C .) The technical standard ASTM D6866 provides an approved method. But radiochemical methods require specialized equipment and trained staff, whereas fuel laboratories more often have experience with chromatographic techniques and might find SFC \times GC a useful technique to provide evidence that a diesel fuel blend contains the stated amount of biodiesel.

Apart from demonstrating compliance with regulation, SFC \times GC for the determination of PAHs has potential forensic applications. Oil spills are often followed by litigation, and methods are required to unambiguously identify sources of spills. The ratios between different PAHs species is unique to each crude oil, which transfers to the products distilled from them. Such a ratio pattern, or PAH **fingerprint**, can therefore be used to help establish the source of an oil spill (Wang 2008). As the results of this chapter has shown, SFC \times GC can be used to generate chromatograms with patterns that could be used as PAH fingerprints.

7.4 Future work

Previous work has shown that SFC can also separate the alkenes from the alkanes (Venter, Rohwer, and Laubscher 1999), at least in petrol, and that the resolution can be improved by cooling the SFC column. Further research along these lines might reveal that is possible to separate the alkenes from the alkanes in diesel. While cooling requires more complex instrumentation, the SFC \times GC instrument discussed in this thesis offers two sources of cooling that might be exploited in such a project:

a portion of the coolant used to cool the SFC pump (see Section 4.3) can be diverted to cool the column, or any excess coolant from the cooling cycle of the fast GC can be used to also cool the SFC column. Alternatively, small solid-state Peltier cooling devices used for cooling integrated circuits are readily available on the consumer market.

7.5 Conclusion

In the transition to a low-carbon economy that protects and promotes human dignity and health, the standards set for fuels for internal combustion engines will continue to evolve. This evolution will pose increasingly challenging problems to the analytical chemist. While innovation will undoubtedly produce new analytical instrumentation, the application of SFC \times GC to the analysis of diesel/biodiesel blends shows that it is possible to create new, sophisticated methods of analysis by re-imagining mature, trusted, and reliable analytical chemistry technologies.

It is a bad plan that admits of no modification.

Publilius Syrus

8

Modified CO₂ as mobile phase for SFC×GC

8.1 Introduction

The previous chapters described SFC×GC runs that used neat carbon dioxide as mobile phase for the SFC separation. Carbon dioxide as a mobile phase is compatible with a flame ionization (FID) detector: under the conditions found in the hydrogen-rich portion of the flame the carbon dioxide cannot be reduced to methane, the first step in the process that produces the ions that gives the FID its name. But most modern SFC development involves the use of modifiers and additives¹. These modifiers are usually organic compounds, and in the FID flame they produce ions. When the modifier-containing eluate of an SFC column passes through the detector, the quantity of the modifiers will be much higher than quantity of the analytes. If the detector is an FID, the modifiers will produce many more ions than the analyte will produce, and therefore the the modifier signal will swamp the analyte signal. Mixing organic modifiers and additives with the carbon dioxide mobile phase therefore renders SFC incompatible with flame ionization as a detection method. As a result, most modern SFC chromatographs use optical detectors, most commonly UV spectrophotometry adopted from HPLC.

While the use of optical detectors has not hampered the development of SFC, they do have a few shortcomings, which might be imposing artificial limits on the exploitation of the versatility of carbon dioxide as a mobile phase:

- While SFC is compatible with optical detection (carbon dioxide does not absorb visible or ultraviolet radiation), there is a wide range of potential modifiers that are not compatible with spectrophotometric detection because they absorb strongly in the UV, but might have chemical properties useful for manipulating SFC separations.
- Optical detectors can only detect analytes with chromophores, and the intensity of the signal depends strongly on the species.

¹Nominally, **modifiers** are added to the carbon dioxide to manipulate the solubility of the analytes in the mobile phase, in the same way that mixtures of solvents are used in, say, gradient elution in HPLC. **Additives** are added in small amounts and manipulate the interaction of the analyte with the stationary phase. In reality, the mechanisms of their action are more complex (Berger and Deye 1991).

- Optical detectors have a limited dynamic range, which complicates quantification.
- Expensive 'HPLC-grade' solvents do not provide better chromatography than other grades of solvents: the processes used to purify them are just optimized to reduce the amount of UV-absorbing impurities that can interfere with analysis.

In comparison, the FID can detect practically any organic compound over a wide concentration range, giving an integrated-over-time signal proportional to the mass of the compound.

When GC is comprehensively coupled to SFC, the modulator will focus each fraction of SFC eluate, and then the GC will separate all the compounds in the fraction, be they analytes, modifiers, or additives. If the modifiers are more volatile than the analytes, the modifiers will elute before the analytes, and the analyte can be detected or quantified using an FID while the signal from the modifier is ignored.

Of course it is quite likely that the peak from the modifiers will **overload** the GC. Both the detector and the column may be overloaded. If the *detector* is overloaded, it just means that the detector no longer responds linearly to the amount of material eluting from the column — this might include responding with its maximum output, leaving flat-topped peaks. If the *column* is overloaded, the capacity of the stationary phase is exceeded and the peaks will **front**: they will be asymmetrical, with the side of the peak towards earlier elution times having a slope smaller than the slope of non-overloaded peaks, and the side of the peak towards later elution times having a larger slope.

The requirement that the modifiers added to the SFC mobile phase be volatile (so that they can elute before the analyte) is not too onerous a restriction. Higher volatility correlates with higher diffusivity, so that the preferred high-diffusivity modifiers for SFC would also tend to be volatile enough to elute early on GC.

A practical SFC×GC chromatograph opens up the field for the use of carbon dioxide mixed with modifier as a mobile phase for analysing complex mixtures found in biodiesel production, biodiesel quality control, and compliance monitoring.

8.2 SFC×GC using modified carbon dioxide.

In this section a SFC×GC chromatogram is presented that shows that methanol added as a modifier to the SFC mobile phase does not interfere with the fast GC any more than a sample's solvent interferes in the usual 1D GC. The 2D separation space of SFC×GC therefore gains in control over elution in the SFC dimension at the cost of losing the capability to detect compounds more volatile than methanol on the GC dimension: modifiers can help elute more polar compounds on SFC, but they will co-elute with volatile analytes and saturate the detector.

8.2.1 Sample

The sample was a 1:1 blend of petrodiesel and biodiesel, prepared in the laboratory. The biodiesel sample was donated by a commercial testing laboratory and had been produced from palm oil by an anonymous producer. The petrodiesel (Shell Extra Diesel 500 ppm) was obtained from a commercial filling station.

8.2.2 SFC

The SFC used carbon dioxide at 200 bar inlet pressure and room temperature as mobile phase, into which 0.5 μ l of sample was injected. The flow rate of carbon dioxide at atmospheric pressure was 175 ml min^{-1} , corresponding to a mass flow rate of about 0.3 g min^{-1} . The carbon dioxide mobile phase was modified with 5 % mass fraction of HPLC-grade methanol (Merck LiChrosolv), using the mechanism described in Section 4.3.2. The column consisted of five HPLC bare silica columns (150 mm \times 4.6 mm, 3 μm particles) (Restek, Pinnacle DB Silica) connected in series.

8.2.3 Modulation

A fraction was collected for each 5 s SFC flow time. After the flow from the SFC was stopped, 3 s was allowed for the last vapour in the inlet to be swept into the cold (-20°C) column for trapping, and then the inlet vent valve was opened for 1 s to relieve excess inlet pressure.

8.2.4 GC

The GC column was a Restek Rxi-5Sil MS 0.250 mm \times 0.25 μm \times 1 m.

For each fast GC program the temperature was ramped from -20°C to 320°C in 10.3 s (33°C s^{-1}) and kept there for 10 s before cooling the column down to -20°C to prepare for trapping the next fraction.

A total of 233 fast chromatograms were recorded and combined into a 2D chromatogram.

8.2.5 Results and discussion

The chromatogram obtained for this run is shown in Figure 8.1. Note the unusual orientation of the chromatogram, chosen to best show the data: In the SFC dimension the later elution times are closer to the reader.

The purpose of doing this chromatographic run was to explore the effect of the methanol modifier on the retention behaviour of the biodiesel fraction of the B50 blend. However, the run time was not long enough for the FAMEs to elute and the only peaks on the chromatogram are the group of hydrocarbons from the petrodiesel. Nevertheless, the chromatogram shows the possibilities that arise when a modifier is added to the SFC mobile phase.

The ‘wall’ that appears on the chromatogram is the tailing edge of the peak of the modifier added to the SFC. These peaks are present in all the fractions at equal concentration. The flat top of the peak is caused by **detector overload**. It should be emphasized that this overload is not caused by saturation of the FID response, but by limits imposed by the chosen signal amplifier. The FID has a dynamic range of 10^6 and could comfortably accommodate the modifier peak, but the amplifier gain was chosen to best match the analyte signal with the input range of the 16-bit analog-to-digital converter.

The ‘corrugations’ on the wall can be ascribed to two sources. Firstly, there may be variations in retention time of the modifier peak, which can be caused by variations in GC gas flow and variations in the fast temperature programs. Second, variations in the amount of modifier collected by the modulator will also cause slight changes in the apparent position of the peak. This second reason is probably the major contributor for this run, caused by variations in the timed collection period

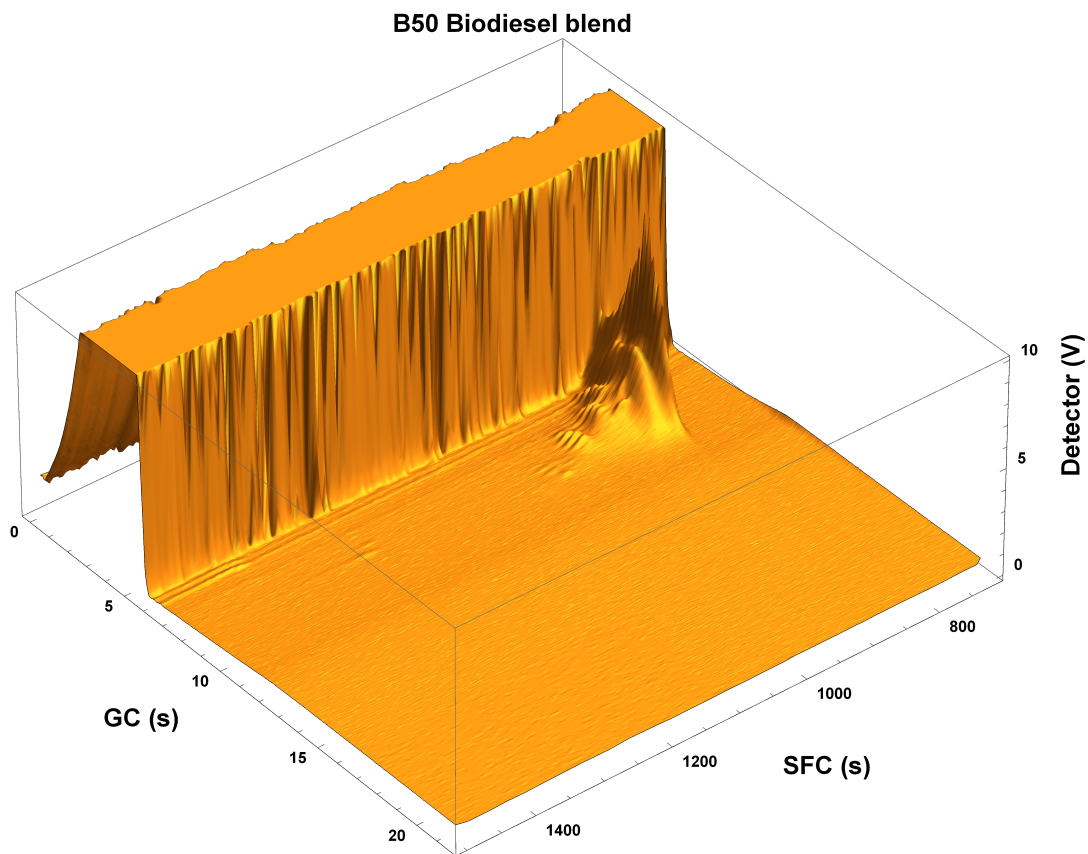


FIGURE 8.1: The modifier used in the SFC dimension elutes as a solvent front on the GC dimension, and does not otherwise affect the separation.

introduced by the imprecision of the electromechanical valve actuator and by variations in the SFC flow.

The chromatogram shows the hydrocarbon “hump” in the GC dimension and the separation of the aromatics in the SFC dimension, as discussed in Section 7. It can be seen that the ‘solvent peak’ of the modifier interferes with the more volatile of the hydrocarbons, but the rest of the separation space is available for separation.

8.2.6 Conclusion

Adding modifiers to SFC expands the versatility of carbon dioxide as a mobile phase, but in 1D SFC the use of modifiers precludes the use of the universal flame ionization detector (FID), because the modifier signal will swamp the analyte signal. Adding GC-FID as a ²D separation allows the use of any volatile modifier to manipulate retention in the SFC dimension, including modifiers that might not be UV-transparent. Modifiers present in the fraction collected by the modulator elute like the customary solvent peak in the GC dimension, which means that the signal from the modifier does not interfere with the signal of the analyte, if it is given that the analyte is less volatile than the modifier.

The example above shows that SFC \times GC will reliably separate methanol used as an SFC modifier from the less-volatile analytes found in a biodiesel blend sample, promising the use of FID as a detector for gradient-elution SFC \times GC separations of biodiesel and biodiesel blends.

"Begin at the beginning," the King said, very gravely,
"and go on till you come to the end: then stop".

Lewis Carroll, *Alice in Wonderland*

9

Conclusion

In this thesis the research conducted on the practical implementation of SFC \times GC as a chromatographic technique is discussed. In this final chapter an overview of the project is provided and some of the lessons learned are discussed.

9.1 Synopsis

The molecular basis of sustainability (Anastas and Zimmerman 2016) demands that chemists discuss sustainability in terms of chemical compounds. Chapter 1 of this thesis opens with the idea that energy is an essential component of industrialized societies, but that choosing fossil fuels as our source of energy causes pollution, which threatens to nullify the benefits they bring. It describes the thermodynamic realities and the economic forces that cause carbon dioxide to be emitted in large quantities, and how its interaction with planetary radiation makes it a pollutant. The concept of a "carbon footprint" is introduced, which allows the comparison of activities in terms of their carbon pollution, enabling decision makers to select the least polluting option. The discussion then focuses on internal-combustion engines, a major source of carbon and noxious pollution, and shows that higher-efficiency engines have lower carbon footprints. A discussion of ways to reduce the carbon footprint of internal combustion engines shows that, in the cases where they cannot be replaced by electric motors, a reduction of carbon footprint can be obtained by preferring large, high-performance diesel engines fuelled by biodiesel. The discussion concludes with the idea that the success of such engines will demand high quality biodiesel and that chromatography will play a central role in ensuring that quality.

Chapter 2 starts with a discussion of the chemical industry and the need to move towards "green" chemistry. It introduces carbon dioxide as a renewable resource, discusses its various uses in industry, and then focuses on its application in extraction and chromatography. It describes how carbon dioxide becomes a solvent at high pressures and densities, and then introduces supercritical fluid chromatography (SFC). Fractions of eluate from SFC can be analysed by gas chromatography (GC), and if a suitable set of criteria is met the combination is called SFC \times GC.

As discussed in Chapter 1, a reliable high-performance engine requires a reliable fuel. Chapter 3 discusses the concepts of technical standards, which establish requirements fuels must comply with to be considered reliable. The discussion then focuses on the technical standard SANS 1935, which contains the requirements of South African commercial biodiesel, concluding with the role chromatography plays in the process of ensuring compliance.

Chapter 4 explains the experimental equipment used for chromatography using high-pressure carbon dioxide as a mobile phase. It starts with describing the mobile phase, how it is stored and pumped, how modifier is added, and how the sample is injected. It describes problems with designing the restrictor that maintains the pressure, and concludes with remarks about using a gas chromatograph as a detector for SFC.

Chapter 5 opens with a discussion of run times of comprehensive SFC \times GC chromatography and shows that for practical analysis the GC dimension must be *fast*. The theory of fast GC is discussed, which introduces the need for fast temperature programming. The design of a resistively heated coaxial heater for short GC columns is described, including its temperature calibration and -control. The discussion then covers how a cold GC column acts as a chromatographic trap, and the design of coaxial cooling using boiling liquid carbon dioxide is described. Next, the discussion covers the design of hardware to mount the coaxial heater of the fast GC in a conventional GC oven. The chapter concludes with a description of the flame ionization detector (FID) and the data flow from signal to final chromatogram.

Chapter 6 discusses the application of the developed SFC \times GC instrument to the study of fatty acid profiles of various potential biodiesel feedstocks, and shows that the pattern of peaks generated by SFC \times GC can be used to evaluate the suitability of feedstock for biodiesel production.

Chapter 7 demonstrates that SFC \times GC can be used to determine the aromatic hydrocarbon and fatty acid methyl ester content of standard grades of diesel.

Chapter 8 demonstrates that the use of SFC with organic modifiers does not preclude the use of the flame ionization detector when GC is used as a second dimension.

Chapter 9 is this concluding chapter, which provides a summary of the thesis and the lessons learned.

Appendix A provides an index to **keywords**. Appendix B contains the accepted manuscript of a paper published in the journal *Review of Scientific Instruments* which reflects some of the experimental work done for this thesis. Appendix C contains technical drawings used for parts of the fast GC system. Appendix D contains fatty acid profiles of some of the feedstocks referred to in Chapter 6.

9.2 Contributions of this study

The research presented in this thesis contributes to the field of chromatography in the following aspects, in order of decreasing novelty.

The most significant new contribution to chromatography of this project is proving the concept of active cooling of short gas chromatography columns by precisely-applied liquid carbon dioxide. To the best of our knowledge there are no other fast temperature-programmed chromatographs with sub-ambient ramp start temperatures or higher repetition rates.

In previous work in our laboratories the concept of SFC \times GC with resistively-heated fast temperature programming (Venter and Rohwer 2004; Venter, Makgwane,

and Rohwer 2006) was proven, but the repeatability of the gas chromatography was not good enough for practical implementation. The implementation of the coaxial heater made the heating of the column highly reliable and repeatable, enabling of hundreds of consecutive fast GC runs to be registered with supreme retention time stability.

Resistive heating has been used in chromatography before, but to the best of our knowledge this is the first time a coaxial heater simultaneously serves as temperature sensing element.

Modern 1D SFC mostly uses carbon dioxide as a mobile phase, with modifiers added. This precludes the use of the flame ionization detector (SFC-FID), because the signal from the organic modifier will swamp the signal from the analyte. But when a fraction collected from a modified-SFC separation is subjected to a GC separation the modifiers and the analytes are separated, and the signal from the analyte can be captured while the signal from the organic modifier is ignored. It was demonstrated that modified-SFC comprehensively coupled to GC yields a chromatographic space that can be used for novel separations, and the possibility of exploiting the advantages of the FID promises reliable quantitation.

The low viscosity of carbon dioxide allows the use of very long packed columns without excessively high pressure. It was possible to run SFC separations on five columns packed with 3 µm particles in series. There were no problems in obtaining adequate flow using an inlet pressure of 200 bar. As was shown in Chapter 7, this long column provided sufficient retention to separate the poorly-retained aromatic hydrocarbons from the alkanes in a diesel sample.

9.3 Special challenges

The fact that the study came to a successful conclusion does not mean that success was ever guaranteed. A few problems brought the project close to failure and tested perseverance.

The persistent blocking of the Guthrie restrictor (Section 4.5) came as a surprise. No previous work in our laboratories prepared us for it, and our colleagues in industry who used them have also not experienced it. Identifying the true root of the problem took patience and persistence, and lead to the first measurement of the size of the Guthrie restrictor orifice. In the end a linear restrictor was used, which means that there might be some degree of volatility discrimination.

The resistive heater initially worked as expected at low applied power, but at higher powers inexplicable deviations appeared. At first the problem was handled by restricting the applied power to the range where it behaved as expected, but that limited the heating rate of the coaxial heater. Persistent study of the problem eventually revealed that a voltage exceeded the safe operating range of the analog-to-digital converter (ADC) device. Under these conditions safety circuits were activated, resulting in the ADC providing unexpected values. The problem was solved by installing an **isolation amplifier**.

9.4 Design

Although this was a 'scientific' project, with an emphasis on demonstrating theoretical ideas, over time it became apparent that using proper design principles when building scientific apparatus saves time and energy in the long run.

9.4.1 Design weaknesses

Energy efficiency

The design of the SFC \times GC is not particularly energy-efficient, and two elements of the design can be greatly improved. Firstly, the heated T-piece blocks are probably not the best solution to the problem. Together they demand up to 800 W of electrical power, for which there is no significant scientific return. Secondly, the power supply to the coaxial heater is a **linear power supply**. In practical terms this means that the excess power of the voltage drop between the DC power supply and the coaxial heater input is dissipated as heat. A future design for a resistively, coaxially heated fast gas chromatograph would be more efficient if it was powered by a **switched-mode power supply**.

Two-wire resistance measurement

The resistive heater had a design that depended on measuring the electrical resistance of the thin-walled stainless steel tube. The resistance was measured by comparing the potential difference between the terminals of the coaxial heater with the potential difference between the terminals of a reference resistor in series with the coaxial heater. The circuit that carried the current also measured the potential difference. Because the current was high, the circuit had to be constructed in such a way that the coaxial heater was the only significant resistor and also the only resistance that changed, which meant that care had to be taken to use heavy-gauge cable and to only use soldered joints.

A future design could relieve some of these problems if the current circuit and the measuring circuit were separated, using **four wire resistance measurement**. In such a design the potential difference between the terminals of the coaxial heater is measured using a circuit that connects directly to the voltmeter, and the current through the coaxial heater is carried by a separate circuit. The voltmeter has a high input impedance, which means that the current the circuit carries is low and stray resistances will only have a small effect on the measurement. A four-wire design also makes it possible to use bolted or plugged connectors on the current-carrying circuit, which would simplify operations.

Cooling control

The fast GC temperature was poorly controlled in the -20°C to 50°C region of the temperature ramps, because the coaxial heater was not thermally isolated. It was mounted in a GC oven together with the heated T-piece blocks. The heat leaking from these uninsulated blocks accumulated in the oven, until the oven reached a temperature of about 50°C . Once the coolant flow stopped the temperature of the coaxial heater would immediate rise to the temperature of the oven. Also, the coolant flow was only on/off controlled. If a future design uses variable orifice control or **pulse width modulation control** (PWM), the actual cooling power can be controlled and with it the trapping temperature of the column.

Intertwined operation

The system, as built, does not allow for the separate operation of the SFC and the GC: the SFC needs the fast GC as a detector, and the fast GC can only inject fractions collected from the SFC. This means that it is not possible to trial a 1D separation on

SFC before engaging the ^2D GC, or to optimize the GC independently of running the SFC. Adding an optical detector to the SFC, or writing code that will allow the manual injection of samples into the GC will make optimizing more flexible.

General-purpose computer operating system

The software ran on a general-purpose operating system (Microsoft Windows XP or Microsoft Windows 7), designed for interactive use by a human operator. In such a system there are many computing tasks running in parallel. The user is usually not aware that many tasks are running, because the operating system (usually) switches between tasks in less time than it takes a human to notice. The operating system decides which task gets priority. To most humans it is at most an irritating experience if the task they are working on gets lower priority than another task, but when the task is controlling a machine and it doesn't get priority, then accidents can happen. As an example of what can go wrong, a heater was left switched on for too long because the heater control task was not given any processor time: the operating system had given priority to a non-critical software-updating task. This resulted in overheating and the risk of fire. On other occasions data got corrupted because data collection tasks got lower priority. Future designs of SFC \times GC instruments can benefit from the use of **real-time operating systems** that offer deterministic timing to critical tasks.

9.4.2 Design strengths

Metal protection for column

Sheathing a capillary GC column in a stainless steel tube proved to be a good design choice. Combining the multiple roles of heating element, temperature sensing element, conduit for cryogenic coolant, and column protector into a single object makes for a robust, efficient design element that could find multiple applications.

Time decoupling

The use of stopped-flow SFC decouples ^1D times from ^2D times. This means that (unlike in GC \times GC) the ^2D run time can be longer than the modulation period and can be varied, but it also means that it is possible to vary the modulation period during an SFC \times GC run. Provided that the criteria for comprehensive coupling continues to be met (see), this allows the chromatographer to reduce times by collecting fewer fractions where less information would be expected, or to get more detail in interesting portions of the ^1D chromatogram.

9.5 Aspects to be addressed

Since the focus of this study was the development of practical instrumentation, some aspects of good chromatography and good design were deferred.

None of the flow rates or heating rates were optimized, so the results merely prove that it is possible to do chromatography using SFC \times GC but do not provide any figures of merit.

Although it was demonstrated that modifiers can be added to the SFC mobile phase when running SFC \times GC-FID, no separations that require or would be improved by using modifiers were demonstrated.

It was demonstrated that the SFC \times GC can separate compounds, but not that they can be quantified, for example by setting up calibration curves. But the FID excels at quantification and the technology for quantification from 2D chromatograms is mature, so major obstacles to quantification by SFC \times GC-FID are not expected.

When the coaxial heater power electronics and control system was designed, the choice of material, its dimensions and the required power matched well with the chosen analog-to-digital converter and made it possible to use a remarkably simple electronic control circuit. A different resistive heater system might require more complex circuitry to match all the components. Such a circuit could be designed by an experienced electronic engineer using the principles established by this project.

9.6 Future work

On the successful operation of the SFC \times GC we look forward to applications that can benefit from the increased separation space and highly structured information provided by SFC \times GC.

SFC \times GC was shown to be able to separate the main components of biodiesel and diesel fuel blends. Future work can include the determination of impurities, in particular free glycerol, glycerides and free fatty acids. Such work will exploit the possibilities of SFC \times GC-FID using modified carbon dioxide as a mobile phase.

Knowing that the strength of SFG \times GC lies in the orthogonality of the two separations, it would be worth doing an exhaustive literature search to find novel or forgotten normal-phase LC separations that effectively separate compounds by functional group. Such methods could be adapted to SFC \times GC to expand the analysis of complex mixtures.

9.7 Concluding comments

The high repeatability of fast temperature ramps afforded by a resistively-heated coaxial heating of short GC columns, combined with the high repetition rate afforded by coaxial cooling of column, applied to the analysis of fractions of compounds separated by the selective group-type separation of SFC, creates a powerful chromatograph that can find a use in many different aspects of quality control in the biodiesel industry.

A

Index

Index

- acid rain, 13
- adopt, 38
- aerosol, 2
- attenuated total reflection, 113
- auto-ignition temperature, 10
- autocatalytic, 44
- azeotropic mixture, 18
- back pressure regulator, 62
- beer's law, 113
- biodiesel, 19
- biofuels, 16
- boiling point, 28
- caffeine, 27
- calibration, 84
- carbon footprint, 6
- carbon pollution, 7
- carbonated water, 26
- cetane number, 42
- chromatographic rate theory, 69
- chromatography, 31
- coal, 1
- coefficient of thermal expansion, 100
- cold filter plugging point, 45
- column bleed, 100
- combined cycle gas turbine, 20
- comprehensively coupled chromatography, 34
- comprehensive, 67
- compression ratio, 9
- condenses, 28
- constraints, 69
- coulometric, 47
- criterion, 69
- critical point, 29
- crude oil, 1
- cryo-focusing, 88
- cryo-trapping, 88
- current, 75
- cut-off ratio, 11
- decaffeinated coffee, 27
- degree of unsaturation, 47
- derivatization reagent, 50
- detector overload, 129
- dielectric heating, 75
- dip tube, 89
- discrimination, 62
- drying oil, 109
- efficiency optimized velocity, 70
- efficiency-optimized flow, 70
- efficiency, 7, 70
- electrometer, 32
- electron capture detector, 71
- electron-impact, 115
- emissivity, 78, 79
- error, 57
- exhaust gas recirculation, 14
- fast chromatography, 68
- fast, 35
- fingerprint, 124
- first dimension, 34
- flame ionization detector, 32
- flash point, 43
- fly ash, 2
- four wire resistance measurement, 136
- fracture toughness, 98
- front, 128
- fuel cell, 15
- gas chromatography, 31
- gas turbine, 11
- general elution problem, 72
- goal, 69
- gradient elution, 72
- green chemistry, 18, 25
- heart-cutting, 34
- high performance liquid chromatography, 31
- holds, 73
- hydrogen, 16
- ignition delay, 43
- induction period, 44
- inductive heating, 75
- injector, 42
- input power, 7
- internal-combustion engines, 6
- iodine value, 47
- isolation amplifier, 135
- kinetic optimization, 69
- knocking, 11

- lean-burn, 14
life cycle analysis, 6
linear power supply, 136
linseed oil, 107
liquid chromatography, 31
lubricity, 53
manipulated variable, 57
modifier, 30
modulation period, 68
modulation rate, 68
modulators, 67
natural gas, 1
noxious pollution, 7
number of plates, 60, 70
ocean acidification, 4
octane number, 11
optimization, 68
optimizing parameters, 69
orthogonal, 34
output power, 7
overload, 128
ozone, 12
partial least squares, 114
payload, 15
peak resolution, 60
peak tailing, 60
peak width, 70
petrodiesel, 38, 113
photochemical smog, 13
photovoltaic, 16
plate height, 70
pollution, 2
polycyclic aromatic hydrocarbons, 51
polyimide resin, 98
polyunsaturated fatty acids, 51
porous layer open tubular, 51
power, 75
process variable, 57
property, 40
pulse width modulation control, 136
pulse width modulation, 87
pyro-synthesis, 12
pyrometry, 81
radiative heating, 75
ramp rate, 73
ramps, 73
rancid, 44
real-time operating systems, 137
refractive index, 114
requirement, 40
resistance, 75
resistive heating, 75
restrictor, 62
retention factor, 60, 72
retention times, 57
retention time, 70
retention volumes, 57
run time, 68
sample cleanup, 71
sample throughput, 68
second dimension, 34
seebeck effect, 81
selectivity optimization, 69
selective detection, 71
selective, 28
selectivity, 60
separation, 31
set value, 57
silicon mica, 90
single ion monitoring, 72
soaps, 48
solar methanol, 16
solid phase extraction, 72
speed-optimized flow, 71
spiked, 115
standards organizations, 38
standard, 37
storage battery, 15
stratified charge, 14
supercritical fluid chromatography, 31
supercritical fluid extraction, 28
switched-mode power supply, 136
technical committees, 38
technical standards, 37
temperature programming, 72
tensile strength, 98
test method, 40
thermal fatigue, 101
thermal imaging, 79
thermal shock, 100
thermocouple, 81
thin-film case, 70
thin-layer chromatography, 34
total contamination, 46
transesterification, 19
triple point, 29
tunable, 28
tuning, 90
van deemter equation, 70
virtual instruments, 92
visual programming language, 92
void time, 70

voltage, 75
wear scar, 53
wrap-around, 73

B

Published paper

This appendix contains the accepted manuscript of a paper published in the journal *Review of Scientific Instruments* which reflects some of the experimental work done for this thesis.

D. Malan, S. J. van der Walt, and E. R. Rohwer (Mar. 2020). "A high-repetition-rate, fast temperature-programmed gas chromatograph and its online coupling to a supercritical fluid chromatograph (SFC × GC)". in: *Review of Scientific Instruments* 91.3, p. 034101. DOI: [10.1063/1.5125060](https://doi.org/10.1063/1.5125060)

82.80.Bg

A high-repetition-rate, fast temperature-programmed gas chromatograph and its on-line coupling to a supercritical fluid chromatograph (SFC×GC)

D Malan,^{a)} SJ van der Walt,^{b)} and ER Rohwer^{c)}

*Department of Chemistry, University of Pretoria, Pretoria, 0002,
South Africa*

(Dated: 3 February 2020)

We present a fast gas chromatographic system that can be used as a second dimension in comprehensive two-dimensional (supercritical fluid \times gas) chromatography (SFC \times GC). The temperature of the short (1 metre long) capillary column is controlled by a resistively heated coaxial stainless-steel tube. The electrical resistance and therefore temperature of the stainless-steel tube is measured by continuous monitoring of the current/voltage ratio. Highly repeatable heating rates of up to $2100\text{ }^{\circ}\text{C min}^{-1}$ ($35\text{ }^{\circ}\text{Cs}^{-1}$) are obtained, which should be high enough for the most demanding fast chromatograms. To reduce the cooling time between temperature programs the column is cooled by injecting evaporating carbon dioxide into the space between the coaxial heater and the column. This gives cooling rates of $5100\text{ }^{\circ}\text{C min}^{-1}$ ($85\text{ }^{\circ}\text{Cs}^{-1}$) which allows quick succession of temperature programs. More repeatable heating profiles with stable GC retention times together with faster cooling are significant improvements on previous SFC \times GC systems. Cycle times of four gas chromatograms per minute could readily be achieved, which allows efficient coupling to high-resolution stop-flow SFC in the first dimension. We demonstrate the fast chromatograph by separating fatty acid methyl esters, yielding information which would be useful in the food and biodiesel industries.

Keywords: high speed temperature programmed GC, sub-ambient GC, fast process GC

^{a)}niel.malan@tuks.co.za; www.scidat.co.za

^{b)}sjvdwalt@lantic.co.za

^{c)}egmont.rohwer@up.ac.za

I. INTRODUCTION

Speed of analysis is a most important criterion for any analytical system. Chromatography as an analytical technique is notoriously slow, compared to, say, some spectroscopic techniques. While it is of interest to (especially high-throughput) laboratories to reduce run times, at some point the faster chromatography starts outstripping the sample preparation capacity. Once the chromatographic run duration approaches the time it takes to prepare the sample, faster chromatography will not improve the sample throughput. Technology development in fast chromatography is therefore driven not by conventional injection-based chromatography, but by applications where no sample preparation is necessary and rapid results are needed.

Examples of these would be headspace analysis for detecting explosives¹, drugs² and fuel adulteration³, monitoring anaesthetic agents in the breath of sedated patients^{4,5}, and in ‘electronic noses’ that can distinguish between frozen and chill-stored meat⁶. Another application for fast gas chromatography is industrial process monitoring⁷.

However, in the past two decades the major application for fast gas chromatography has not been in direct sample analysis, but in the analysis of fractions of eluate from chromatographic separations. This concept is called *comprehensive two-dimensional chromatography*. For example, in comprehensive two-dimensional gas chromatography (GC×GC), fractions of a conventional gas chromatographic run are collected by a *modulator* and then admitted to a second, fast gas chromatograph⁸. GC×GC has become well established: the annual GC×GC Symposium is in its 15th year, and major reviews are published regularly^{9,10}.

In comprehensive 2D chromatography the second-dimension chromatography must be *fast*. The theory and practice of improving the speed of GC is well developed^{11,12}. Typically, short columns and high carrier flows rates are used, which reduce retention times by reducing void times. Resolution can be maintained at even higher gas flows by using narrow-bore columns and thin films: these improve the mass transfer rate between the mobile and stationary phases, which reduces peak broadening by bringing the analyte exchange between the phases closer to equilibrium at higher-than-optimum carrier gas velocities.

Comprehensive two-dimensional chromatography depends on *orthogonality*: the second dimension (²D) separation must have a different mechanism than that of the first dimension (¹D) separation^{13,14}. The higher the orthogonality, the better the *separation space* offered by

the system. In GC \times GC the different separation mechanisms that determine orthogonality are usually provided by the different stationary phases offered by column manufacturers, but it is also possible to use a different form of chromatography as a first dimension: liquid chromatography has been used as a first dimension in LC \times GC¹⁵, and in our laboratory we are developing SFC \times GC instrumentation¹⁶.

If a chromatographic 2 D separation is highly orthogonal to the 1 D separation, then the 2 D separation will run into the *general elution problem*¹⁷: the higher the orthogonality, the more diverse the compounds found in each 1 D fraction, and it becomes increasingly unlikely that one set of acceptable operating conditions (temperature, flow and stationary phase) will give an acceptable (fast enough and with adequate resolution) 2 D separation. In GC \times GC as it is practised today this has become a real problem, known as *wraparound*, a well-known phenomenon¹⁸. Wraparound happens when a peak or peaks elute ‘late’ on the second dimension, so late that the next modulation period has already started before its elution and the peak only appears on the next 2 D chromatogram. Careful interpretation of 2D chromatograms can identify which peaks can be attributed to wraparound, and adjusting some parameters might mitigate the problem.

If the general elution problem causes the phenomenon of wraparound in GC \times GC, where the compounds found in 1 D fractions have a relatively narrow boiling point range, it will cause much greater problems in SFC \times GC, since the first dimension (SFC) does not normally separate compounds in a way that correlates with vapour pressure. Indeed, SFC is particularly good in performing group-type separations¹⁹, where compounds with a wide range of boiling points elute together. Therefore, in SFC \times GC we can expect compounds with a wide range of boiling points in each 1 D (SFC) fraction, and the general elution problem makes it unlikely that an isothermal 2 D (GC) run will provide an acceptable separation. This is why successful SFC \times GC demands temperature programming in the GC dimension.

A. Fast column heating for GC

In GC the usual solution to the general elution problem is temperature programming, *i.e.* increasing the temperature of the column throughout the duration of the chromatographic run. Temperature programming decreases the retention times of late-eluting analytes without sacrificing the resolution of early-eluting analytes. Instrument manufacturers

have mastered the art of temperature programming, and today the vast majority of 1D gas chromatography uses temperature programming.

However, implementing temperature programming in the fast ²D GC poses some challenges. Since the recommended heating rate for temperature programmed chromatography is around 10 °C per void time²⁰, the short void times of fast chromatography imply that high heating rates are required. Conventional air-bath GC ovens cannot attain these high heating rates, and therefore specialized column heating is required. Resistive heating by electric current offers a simple method, as reviewed^{21,22}, and a recent paper²³ describes the elimination of wraparound in GC×GC of diesel samples using resistive heating to implement a simple temperature program in the ²D column.

Of the three broad classes of resistive heating of capillary columns identified²¹ (*i.e.* (1) direct heating of a metal column or conductive coating on the column, (2) coaxial heating by a conductive tube around the column, (3) collinear heating by a heating element parallel to the column), we have experience with direct heating and coaxial heating.

In previous work in our laboratories^{16,24} a resistively heated metal column was used. The temperature of the column was controlled by following the temperature of a thermocouple glued to the column, but this method had some shortcomings, like uncertainty about the absolute temperature along the length of the column and stationary phase limitations: metal columns are often developed for high-temperature applications, and are not available with all the stationary phases offered in fused silica columns.

In this work we used a coaxial heater, in the form of a thin-walled stainless-steel tube that surrounds the capillary column. This tube is resistively heated by controlled direct current. Due to the low thermal mass the heating is rapid, and since the resistance of the tube indicates its temperature there is no need for external temperature measuring devices. The benefit of this design is that it allows the use of commercially-available fused silica columns with their wide range of internal diameters and selectivities. Columns can be exchanged without altering the temperature feedback system and therefore the rapid heating characteristics. Additionally, the co-axial space between the capillary column and the stainless steel tube can be filled with coolant to rapidly cool the column.

B. Fast column cooling for GC

At the end of temperature-programmed chromatographic run, GC columns are usually cooled to the starting temperature by ambient air. This cooling is slow and inefficient because of the poor conductivity and low heat capacity of air. Fast chromatography usually implies analysis at high repetition rates, so cool-down times also need to be shortened.

There have been attempts to improve the cooling rate of air baths. AgilentTM markets a ‘low thermal mass’ column, which includes a collinear heating wire and a collinear sensing element bundled with a short silica column. These units cool down faster than normal air-baths, but only to ambient temperature. For short columns a cooling time of 1.3 min has been reported²⁵. These columns are available with only a limited range of stationary phases. The Zip ScientificTM solution operates by forced convection. Their ‘GC-Chaser’ system uses a blast of (chilled) room air to the GC oven to cool it down after each GC run, allowing the use of conventional fused silica columns. In an example²⁶ it reduces cooling time from 16 min to 7 min. Although this can significantly decrease the cost per analysis in a high-throughput laboratory, the cooling is not fast enough for 2D chromatography. The EZ FlashTM system uses a coaxial resistive heating system, which allows the column to cool down ballistically. Reports from the literature claims cool-down periods of 30 s²⁷. The Valco FTP-200 fast temperature programmer²⁸ (Valco Instruments Co. Inc.) uses a small, optional fan to cool down the columns.

Cryogenic coolers for GC ovens are available but are intended to cool the oven to low temperatures for the analysis of volatile compounds and not necessarily to improve cycle times. In previous SFC×GC work in our laboratories^{16,24} the cryogenic function of a Varian 3300 gas chromatograph was used to cool down the column oven at the beginning of each run, using large quantities of coolant in the process. The resistively heated column cooling required 30 s to get back to the starting temperature in this cool environment. We estimate that a single SFC×GC run consumed an unacceptable 15 kg of carbon dioxide coolant.

Recognizing that the precise application of coolant will require less coolant and permit faster cooling, we developed a system that injects liquid carbon dioxide into the space between the column and the coaxial heater. The evaporating carbon dioxide rapidly absorbs heat from the column and coaxial heater, achieving a high cooling rate to sub-ambient temperatures at a minimal expense of coolant.

At the same time, the cold GC column acts as a focusing trap for the subsequent sample, and thus forms an integral part of the modulator of the SFC \times GC system.

C. Application

The fast GC system described in this paper can be used in any application where fast chromatograms are needed in rapid succession, for example in process control. In our case we applied it as a fast second dimension separation, comprehensively coupled to a supercritical fluid chromatograph.

We applied our fast GC system to the evaluation of fatty acid profiles of potential biodiesel feedstock. The fast GC separation was highly orthogonal to the ^1D separation on SFC, showcasing this type of comprehensive two-dimensional chromatography. An easily interpretable 2D separation was obtained, with run times similar to the total run times required by official GC methods for the determination of fatty acid profiles.

II. EXPERIMENTAL

A. Introduction

For better understanding of subsequent detail, a description of the cycle of the SFC \times GC is appropriate. The SFC subsystem runs in stop-flow mode. The eluate of the SFC passes through a stop valve and a static linear capillary restrictor. The end of the restrictor is inserted through the septum into the hot inlet of the GC. After the sample is injected, the SFC runs for an optional uninterrupted period, usually briefer than the void time. No data is collected during this time. Then the stop valve closes, and the cooling system activates to cool the GC column. Once the column is at the set temperature, the stop valve opens and the SFC eluate exits the restrictor into the hot splitless inlet of the GC, where it evaporates instantly. The vapour-phase material is swept from the inlet onto the column where it is trapped in the cold stationary phase. Once the desired amount of the SFC eluate has been collected, the stop valve closes and some time is allowed to elapse so that the last of the evaporated SFC eluate can be flushed into the column. Then the split vent of the GC inlet opens for a short period to vent excess carbon dioxide to the atmosphere. This normalizes the pressure in the inlet (having been raised by the high flow rate of CO₂ from the SFC)

and allows the carbon dioxide to be replaced by the pressure-controlled hydrogen carrier gas. The closing of the split vent marks the start of the GC run, which of course means the start of the temperature program. Under control of the temperature program the analytes trapped on the head of the cold column desorb, migrate, separate, elute, and are detected. The end of the temperature program marks the end of the GC run, and the GC column is cooled to prepare for trapping the next fraction.

B. Hardware

The short-cycle fast gas chromatograph was built into a modified VarianTM 3300 gas chromatograph. The inlet was a VarianTM 1075 split/splitless inlet. The temperature control of the inlet was by the original electronics, controlled from the Varian 3300 front panel. The split vent valve was disconnected from the gas chromatograph control and connected to the control computer described below.

The detector was an unmodified VarianTM 3300 flame ionization detector (FID). The temperature of the detector was regulated by the original electronics, controlled from the front panel. The detector bias voltage was supplied by the original electronics, but a stand-alone high-speed electrometer (V.G. Micromass Ltd, Model M406-H) captured the signal, which was then conditioned by a bench-top amplifier (V.G. Micromass Ltd, Model M406) before it was sent to the computer.

The coaxial heater was made of a 940 mm length of stainless steel (SAE 304 grade), obtained from MIFAM (Milanówek, Poland). It had an outside diameter of 1.06 mm and an inside diameter of 0.80 mm. The ends of the coaxial heater tube terminated in two identical, specially designed T-piece blocks, machined from brass (see Figure 1). These blocks fulfilled three roles: They (1) sealed the coaxial tube to contain coolant, (2) allowed electrical connection to the coaxial heater, and (3) acted as a heated transfer line between the column and the detector and inlet. Each end of the stainless-steel tube of the coaxial heater was brazed onto a block. The CO₂ coolant passed through one side, and on the opposite side a thermocouple probe inserted into a blind hole measured the temperature of the block. An electrical contact was added, to which an electrical conductor could be soft-soldered. Four holes through the width of the block allowed the fitting of four 220 V, 100 W heater cartridges (Hotset), providing each of the two blocks 400 W of heating. The

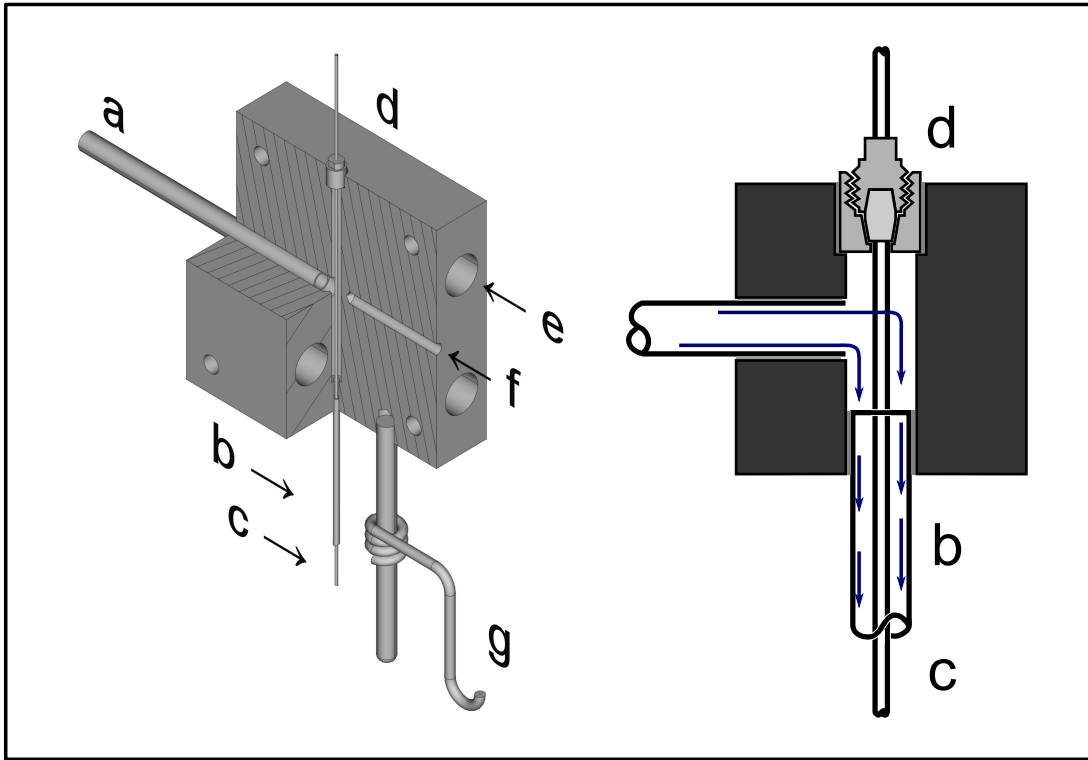


FIG. 1. Left: A cutaway diagram of the inlet/outlet T-piece blocks with all the parts to scale, showing (a) the cryogenic coolant inlet/outlet, (b) the coaxial heater, (c) the capillary column, (d) the micro-union seal, (e) the cartridge heater socket, (f) the thermocouple socket, and (g) the connector to which the power feed conductor was soft-soldered. Right: A schematic diagram showing the flow of the coolant through the T-piece block into the coaxial heater.

chromatographic capillary column entered the T-piece block via the bottom port with the coaxial heater tube and passed out through the top port, where a micro-union using a metal ferrule (Restek™ SilTite μ -Union Connectors) brazed to the block created a seal to contain the coolant. From the top port the column crossed a small, electrically isolating air gap before entering the inlet or detector.

The T-piece blocks were mounted on ‘cars’ that slid up and down twin round-bar rails on brass bushes. The cars carried the weight of the inlet and outlet T-piece blocks and rigidly aligned the column with the inlet and detector of the gas chromatograph. The cars were isolated electrically from the rails by a sandwich construction that included silicone-

impregnated mica as insulating material. The whole of the inlet and outlet T-piece blocks were at the electrical potential of the coaxial heater ends.

The cryogenic carbon dioxide (Afrox, Tec (Wet)) was supplied from a cylinder equipped with a dip tube. It flowed to a coil heat exchanger mounted on top of the Varian GC from where the carbon dioxide flowed down to the cryo shut-off valve (ASCO, RedHat brand). (The heat exchanger was bathed in a cold (-5°C) propylene glycol heat transfer fluid.) This arrangement ensured a supply of liquid CO₂ at the shut-off valve, without which some gaseous CO₂ might have to vent through the coaxial heater before the liquid CO₂ coolant could reach it. Downstream of the shut-off valve a 10-turn metering valve controlled the flow of carbon dioxide into the coaxial heater. At the outlet end of the coaxial heater the carbon dioxide escaped through the T-piece block into the atmosphere.

The SFC subsystem consisted of five packed silica columns (150 mm \times 4.6 mm, 3 μm particles) (Restek, Pinnacle DB Silica) in series, a sample valve (VICI), and a stop valve (VICI). Carbon dioxide, (99.995 % purity, Air Products) was supplied to a Varian 8500 piston pump. The inlet pressure of the SFC columns was controlled by a software proportional controller driving the stepper motor of the piston pump. The high pressure at the column exit was maintained by a linear fused silica capillary restrictor with an internal diameter of 0.050 mm, 800 mm long.

C. Electronics

The electronics for controlling the fast temperature programmed gas chromatograph and the SFC front-end was developed in-house. A controlled direct current was used to heat the coaxial heater. The heating circuit consisted of the coaxial heater in series with a reference resistor and a ballast resistor. The reference and ballast resistors were constructed from stainless steel wire with a diameter of 1.0 mm. The reference resistor had multiple, parallel conductors, the ballast resistor had a bifilar winding, and both had air cores. These designs (see Figure 2) minimized electromagnetic interference and encouraged heat dissipation. Since the coaxial heater resistance measurement used a two-wire technique, the current-carrying circuit was made entirely of soldered joints to minimize stray resistance from developing in electrical connections.

The resistance of the reference resistor (R_{ref}) was about 0.005 Ω , the resistance of the

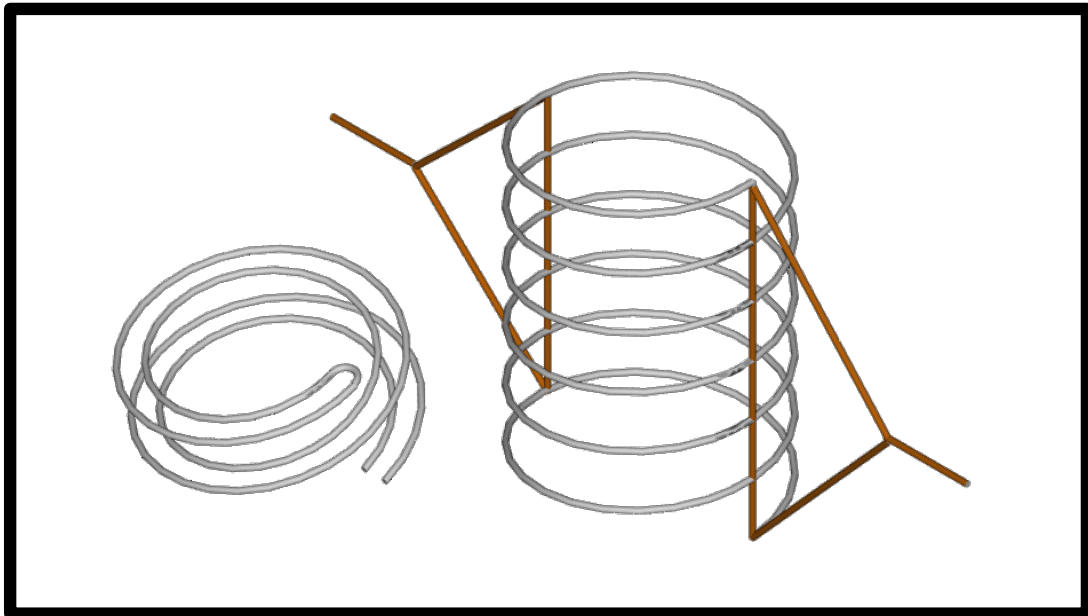


FIG. 2. An illustration of the designs of the ballast (left) and reference (right) resistors. The outside diameters of the coils are about 25 mm and 50 mm respectively. The designs emphasize heat dissipation by air convection and mitigation of electromagnetic interference by using parallel conductors.

coaxial heater (R_{col}) was about 0.3Ω , and the resistance of the ballast resistor was about 0.01Ω , so that most of the heat in the circuit was dissipated by the coaxial heater. The potential differences across the coaxial heater (V_{col}) and the reference resistor (V_{ref}) were measured (see Figure 3). If the resistances of the coaxial heater and the reference resistor were both constant, the ratio V_{col}/V_{ref} would be constant, independent of the current. But metals have positive coefficients of resistivity so the resistance of the coaxial heater will increase with temperature. If the assumption is made that the temperature of the reference resistor does not change, then the ratio V_{col}/V_{ref} will be proportional to R_{col} . If the resistance R_{col} is assumed to be a monotonically rising function of the temperature ($R_{col} = f(T)$), then the inverse function will provide the temperature ($T = f^{-1}(R_{col})$). In practice the voltage V_{ref} is too small to be digitized directly and needs to be amplified to V_b , but it can be shown that R_{col} is a function of $\left(\frac{dV}{V_b}\right)$, where dV is the difference between the supply voltage and V_b . dV and V_b are of magnitudes that can be conveniently digitized.

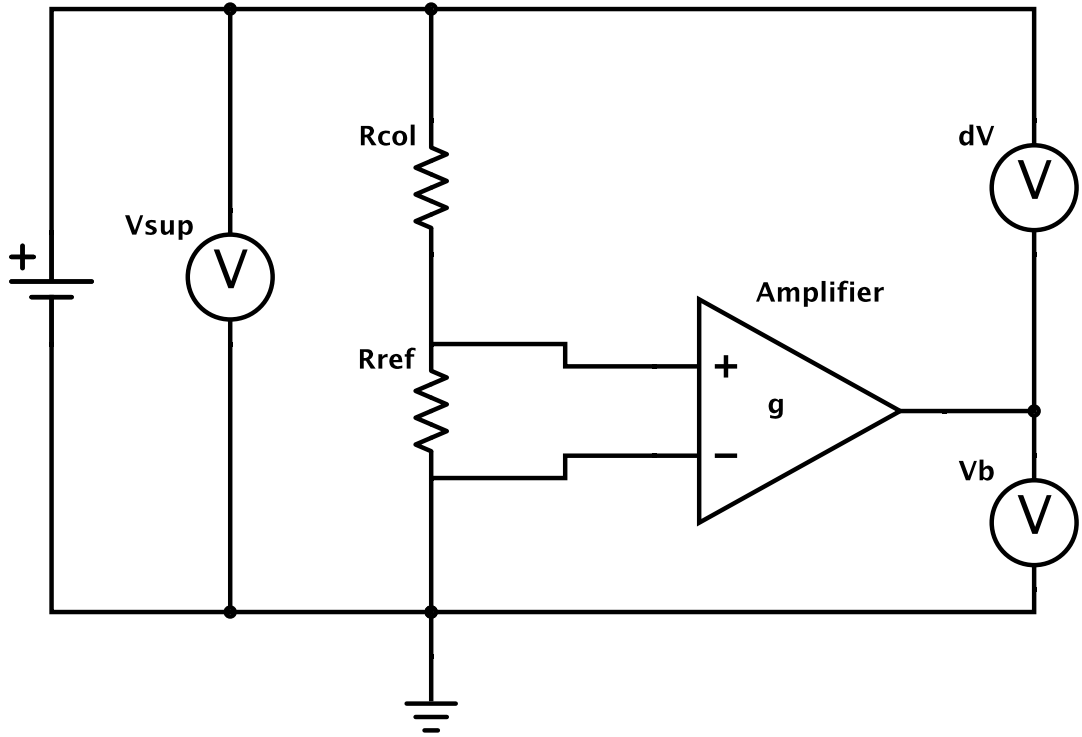


FIG. 3. A simplified circuit diagram of the resistance measuring circuit.

A bank of six PNP 2N2955 bipolar transistors mounted in parallel on an aluminium plate air-cooled by two 4-inch fans controlled a current of up to 20 A at 20 V through the coaxial heater. A two-stage control system controlled the current. The first stage of the control system was a PID controller implemented in LabVIEW 7.1™ (National Instruments). The process variable was the temperature of the coaxial heater, as calculated from its electrical resistance, and the set value was determined by the desired chromatographic temperature program. The manipulated variable was the voltage of the digital-to-analog converter (DAC) of the data acquisition board. The final stage was an electronic system, where the voltage applied to the coaxial heater was the process variable, and the set value was a voltage provided by the DAC. The manipulated variable was the base current of the power transistors. In summary, the software set a voltage, which set the power of the coaxial heater. This two-stage design allows for switching of the control of the coaxial heater from computer control to manual control by a potentiometer on the instrument front panel. Being able to

control the power of the coaxial heater manually is extremely useful during development and fault-finding.

AD595 monolithic thermocouple amplifiers (Analog Devices) with integral cold junction compensation were used to condition the signal of the K-type thermocouples that were used for temperature monitoring and calibration. Solid state relays (Opto 22, Model 240D3) were used to switch the inlet and outlet T-piece block cartridge heaters (described above) on and off. Pulse width modulation, implemented in software, was used to control the amount of heat produced by the cartridge heaters, and hence the temperature of the T-piece blocks. A PCI-6014 multifunction data acquisition board (National InstrumentsTM) was used to interface the electronics with the computer.

D. Coaxial heater temperature calibration

The temperature of the coaxial heater was calibrated by constructing a thermocouple probe from 0.025 mm diameter thermocouple alloy wire (T1 and T2 alloys, Goodfellow) threaded inside a 1000 mm length of 0.25 mm i.d. fused silica capillary. This thermocouple probe was then threaded inside the coaxial heater (just like the capillary column during GC operation) to record the temperature of the heater. The recorded temperature could then be used to calibrate the coaxial heater resistance.

E. Heating uniformity

To determine whether the coaxial heater was heating the column with acceptable uniformity, we used two methods. Firstly, we acquired thermographic videos of the coaxial heater, using a FLIR T660 infrared camera. Secondly, for experiments in determining temperature gradients, a thermocouple probe was constructed as described above, except that the probe contained two thermocouples, 330 mm apart, equidistant from the ends.

F. Software

1. *Instrument Control*

The software for controlling the instrument and collecting data was written in LabVIEW. Two main loops were used. One controlled the various aspects of the instrument, in particular the temperature control, and ran with a period of 200 ms. The second main loop collected the data and ran as often as the hardware allowed.

The coaxial heater temperature was controlled by proportional-integral-derivative (PID) controllers implemented in LabVIEW. In practice it was found that only proportional and integral control was needed. We used a privately published²⁹ step-by-step implementation of the Cohen-Coon loop tuning method. Subsidiary PID controllers controlled the T-piece block temperatures and the CO₂ pump pressure.

2. *Data structure*

In GC×GC, 2D data is recorded as a continuous detector output stream, as if it were a 1D GC chromatogram, and later converted into a 2D chromatogram, using knowledge of the modulation period. For two reasons we could not use this approach. Firstly, in our instrument the first (SFC) dimension runs in a stop-flow mode making continuous data recording inappropriate. Secondly, the duration of the cooling cycle can vary slightly, which could introduce unacceptable variation in ²D retention times. We therefore started detector output recording at the start of each GC fast temperature program, using the GC start time as the elution time of the first (SFC) dimension.

3. *Data visualization*

For data visualization we used the technical computing system Mathematica 11.3TM (Wolfram). The collected data was first converted to a list of three-element lists, with ¹D retention time, ²D retention time, and detector signal as the elements of the inner lists. The Mathematica functions `List3DPlot[]` and `ContourPlot[]` was then used to plot 3D chromatograms or contour plots respectively.

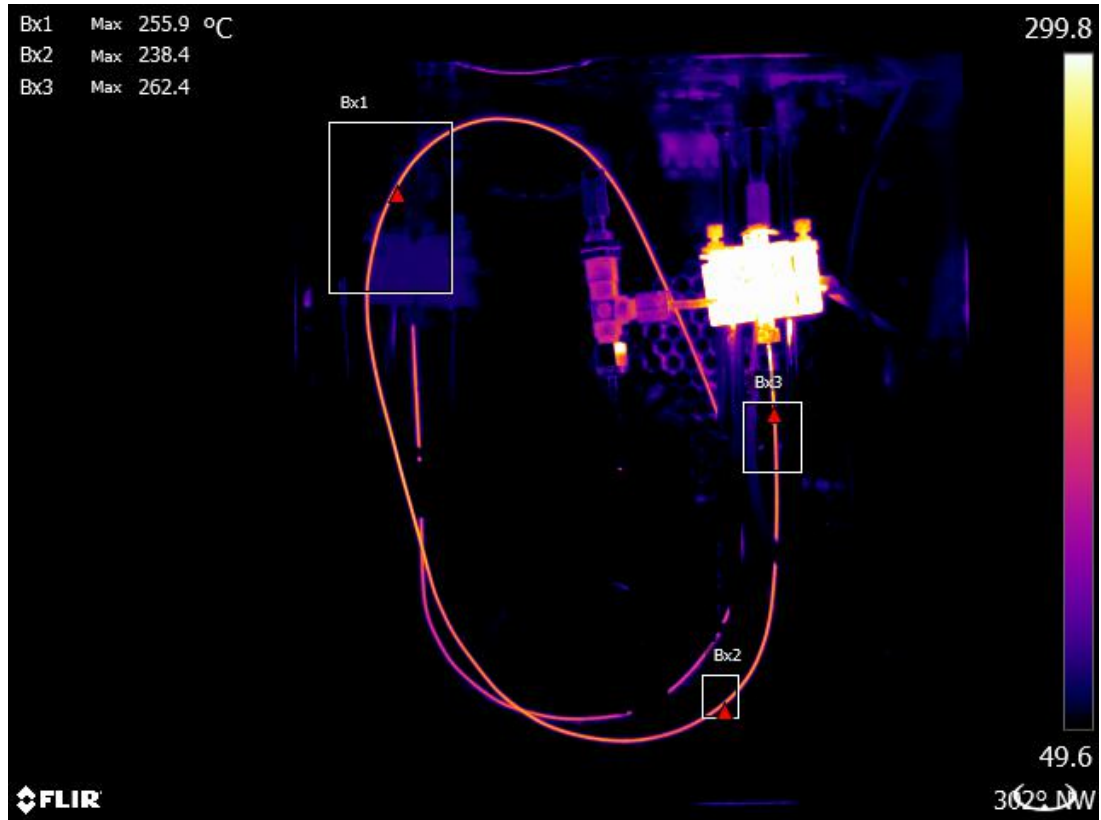


FIG. 4. A frame from the thermographic video of the coaxial heater. There are no evident run-away hot spots. (Multimedia view)

III. RESULTS AND DISCUSSION

A. Heating uniformity

As a first step in developing the coaxial heater, we tried to answer the question about its temperature uniformity. Because the temperature coefficient of resistivity of metals is positive, in the absence of equalizing heat flow along the length of conductor the resistive heating process in a long, thin tube is inherently unstable. To monitor the temperature profile along its length we acquired a thermographic video of the coaxial heater. The video shows that the coaxial heater heats and cools smoothly with no run-away hot spots, as shown in Figure 4 (Multimedia view).

To quantify the non-uniformity of the coaxial heater, a dual thermocouple probe was

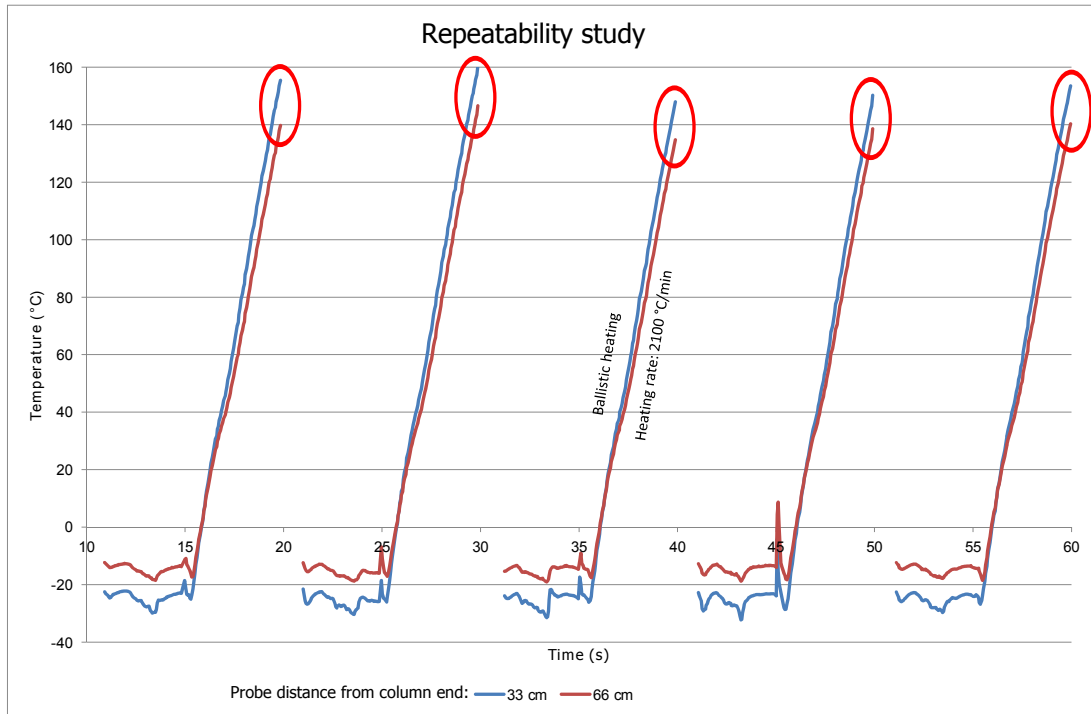


FIG. 5. The temperature difference between two points in the coaxial heater. The temperature difference established during cooling is reversed during heating, which shows that gradients exist, but they are small and repeatable.

inserted into the coaxial heater. The two thermocouples in the probe were 330 mm apart and positioned in the central third of the coaxial heater. The coaxial heater was submitted to a repeated program of cooling and ballistic heating. The recorded data (see Figure 5) shows that the two thermocouples reported different temperatures and that the difference changed during the heating, implying that the coaxial heater did not cool or heat perfectly uniformly. But the temperature differences between the two points were small (approximately 10 °C at most), stable, and repeatable and should not prevent good chromatography. In fact, a small longitudinal gradient, with the lower temperature nearer the detector, will produce sharper peaks³⁰. These data also show that ballistic heating is not repeatable enough for gas chromatography, as can be seen in the variation in temperatures at the end of the heating runs.

B. Temperature calibration

While it is conceptually possible to have a fast temperature program by using the voltage/current ratio alone as a temperature indicator and controlled variable, it would be hard to design chromatographic methods or translate methods without a knowledge of the real temperature. Therefore, we went to some effort to calibrate the coaxial heater.

To calibrate a thermometer, the thermometer under test and its calibration environment must be in equilibrium. This requirement is hard to meet in our calibration, because a single point (the junction of the thermocouple) needs to be in equilibrium with the length of the coaxial heater during the full fast heating cycle. This equilibrium would be very difficult to maintain, especially because the uniformity of heating cannot be guaranteed, and is additionally influenced by the presence of the hot T-piece blocks — for a totally uniform heating of the coaxial heater the T-piece blocks would have to be at the same temperature as the coaxial heater. Acknowledging these limitations, we performed a calibration procedure assuming that the thermocouple junction was in equilibrium with the coaxial heater, which was assumed to be of uniform temperature over its length. Because these assumptions are simplifications, or for other overlooked reasons, the calibration curve (see Figure 6) is oddly curved, and we arbitrarily fitted a B-spline to the data points. This procedure can be automated³¹. Points from this B-spline curve were then extracted to create a calibration curve, from which an estimate of the temperature can be calculated by linear interpolation³².

C. Heating rate

To achieve good resolution in temperature-programmed chromatography, a good rule of thumb for the heating rate is 10 °C per void time²⁰. With hydrogen as carrier gas in a 0.25 mm i.d. column the efficiency-optimized linear velocity is 40 cm s^{-1} . Then the void time of a 1 m column is 2.5 s, so the recommended heating rate is 10 °C per 2.5 s, which is 4 °C s^{-1} , or 240 °C min^{-1} . Since in fast chromatography excess peak resolution is traded for shorter run times, higher-than-optimum flow rates will be used, so higher heating rates will be required. For narrower columns the flow will be even higher so that heating rates of more than 1000 °C min^{-1} will be required.

The attainable heating rate is a function of power to the heater and of the temperature

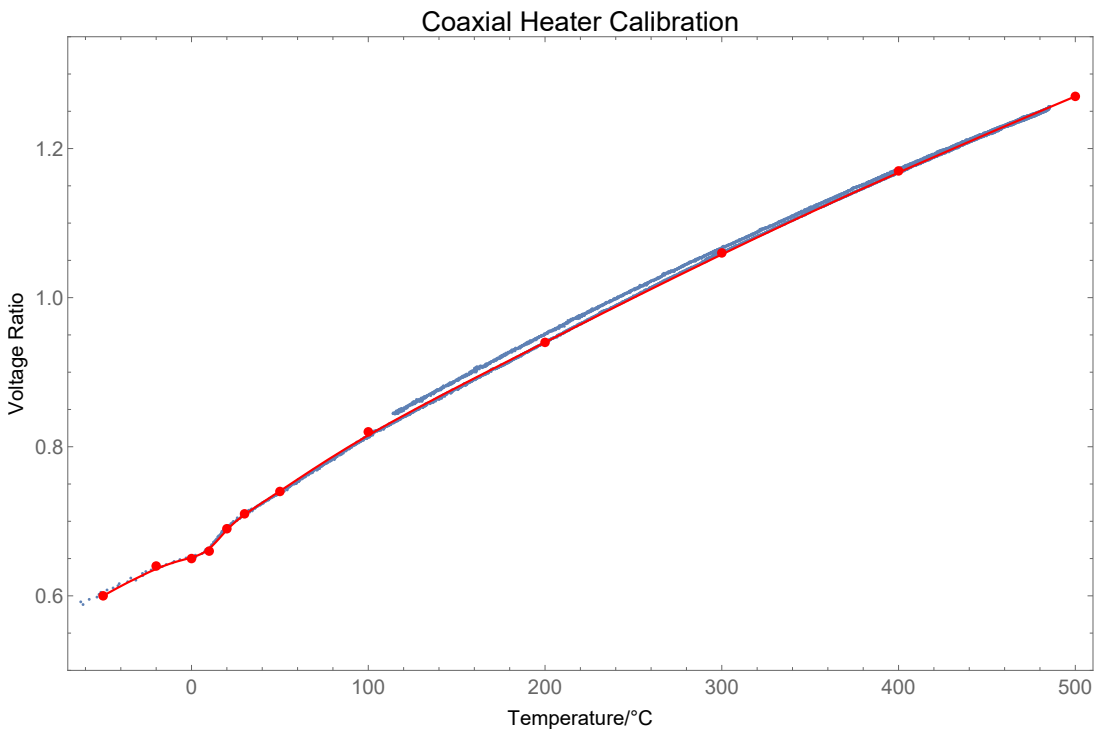


FIG. 6. A calibration curve of the coaxial heater. The blue points represent the experimental data, and the red line is a B-spline fitted manually to the data. The red markers are points extracted from the B-spline. The temperature is obtained by linear interpolation between markers.

required. (In the instrument presented here the power was limited by the voltage output range of the DAC of the data acquisition board, and not by the power of the heater.) We were able to maintain controlled heating rates of $2500\text{ }^{\circ}\text{C min}^{-1}$ up to $400\text{ }^{\circ}\text{C}$, or up to $4000\text{ }^{\circ}\text{C min}^{-1}$ up to $350\text{ }^{\circ}\text{C}$ (see Figure 7). The heating rates attainable seem to be high enough for the most demanding fast gas chromatography.

D. Cooling rate

Using evaporating carbon dioxide as a powerful coolant, it was possible to cool down the column at a rate of $5100\text{ }^{\circ}\text{C min}^{-1}$. The cooling rate depends on the setting of the metering valve, with the lowest coaxial heater temperatures and smallest gradients achieved at an intermediate flow of about 30 g min^{-1} .

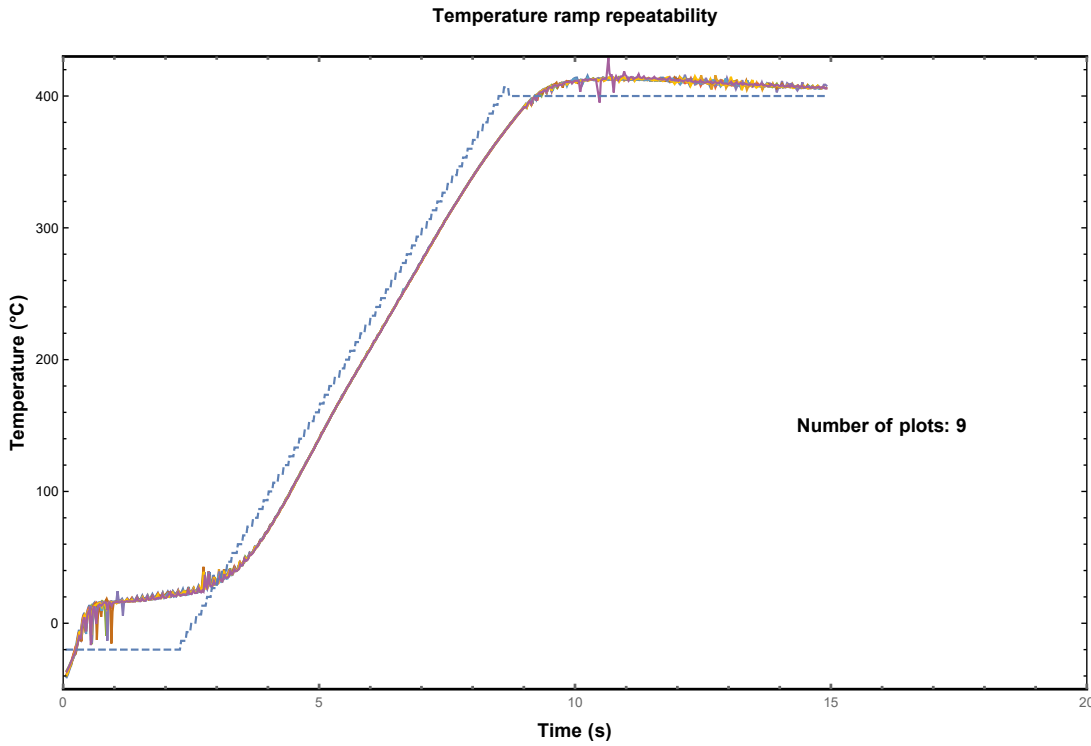


FIG. 7. A graph of 9 identical, consecutive temperature ramps overlaid. The heating rate is $4000\text{ }^{\circ}\text{C min}^{-1}$. The temperature follows the setpoint faithfully up to $350\text{ }^{\circ}\text{C}$

E. Repeatability

Comprehensive two-dimensional chromatography depends heavily on repeatable 2D separations. To test for chromatographic repeatability, we added small amounts of hydrocarbons to the 1D mobile phase. They are unretained on the silica stationary phase and are therefore present in every fraction of the SFC eluate in equal amounts and should yield identical 2D chromatograms. Results obtained from creating a 2D blank chromatogram with two alkanes in the mobile phase are summarized in Table I. The peak widths were about 500 ms, so the 20 ms standard deviation for hexadecane means that the variation in retention time is only about 10% of the peak width. The relative standard deviations (RSD) of retention times were similar to those obtained in GC \times GC³³.

TABLE I. A summary of retention time repeatability of alkanes separated on the fast temperature programmed chromatograph.

Compound	n	t _r (s)	S.D. of t _r (s)	R.S.D. of t _r (%)
Dodecane	73	5.07	0.023	0.46
Hexadecane	73	6.58	0.052	0.78

F. Chromatography

Comprehensive two-dimensional chromatography is made possible by having different retention mechanisms in the columns of the two dimensions. When fatty acid methyl esters (FAMEs) are chromatographically separated on bare silica with neat carbon dioxide as a mobile phase, they are separated according to the number of double bonds, independent of chain length³⁴. On a GC column, FAMEs are separated according to volatility or, equivalently, chain length. Therefore, when SFC and GC are comprehensively coupled, we can expect FAMEs to have a highly orthogonal separation.

We prepared FAMEs by esterifying oil samples, following an official method³⁵. Of these samples, 0.2 μ l was injected into the pure carbon dioxide mobile phase at 200 bar and room temperature and eluted through bare silica. We collected 10 s fractions of SFC eluate on the cold GC column. The fast temperature program ramped the GC column temperature from -20°C to 350°C in 10 s ($2200\text{ }^{\circ}\text{Cs}^{-1}$), then maintaining 350°C for 2 s. Then the cooling system would activate and cool the column to -20°C or below, ready to trap the next SFC fraction. In this way a series of GC chromatograms of SFC fractions were recorded to build up a 2D chromatogram. Figure 8 shows a 2D chromatogram of a sample of FAME prepared from canola oil. This 2D chromatogram consists of 132 fast GC chromatograms collected in approximately 90 min.

IV. CONCLUSION

To our knowledge, the cycle time of this new temperature programmed GC is unmatched in the literature, and it allows for the improved performance of SFC \times GC instruments. The fast GC will be of interest to all GC analyses of highly dynamic chemical systems, including on-line monitoring and control of fast laboratory or industrial reactions.

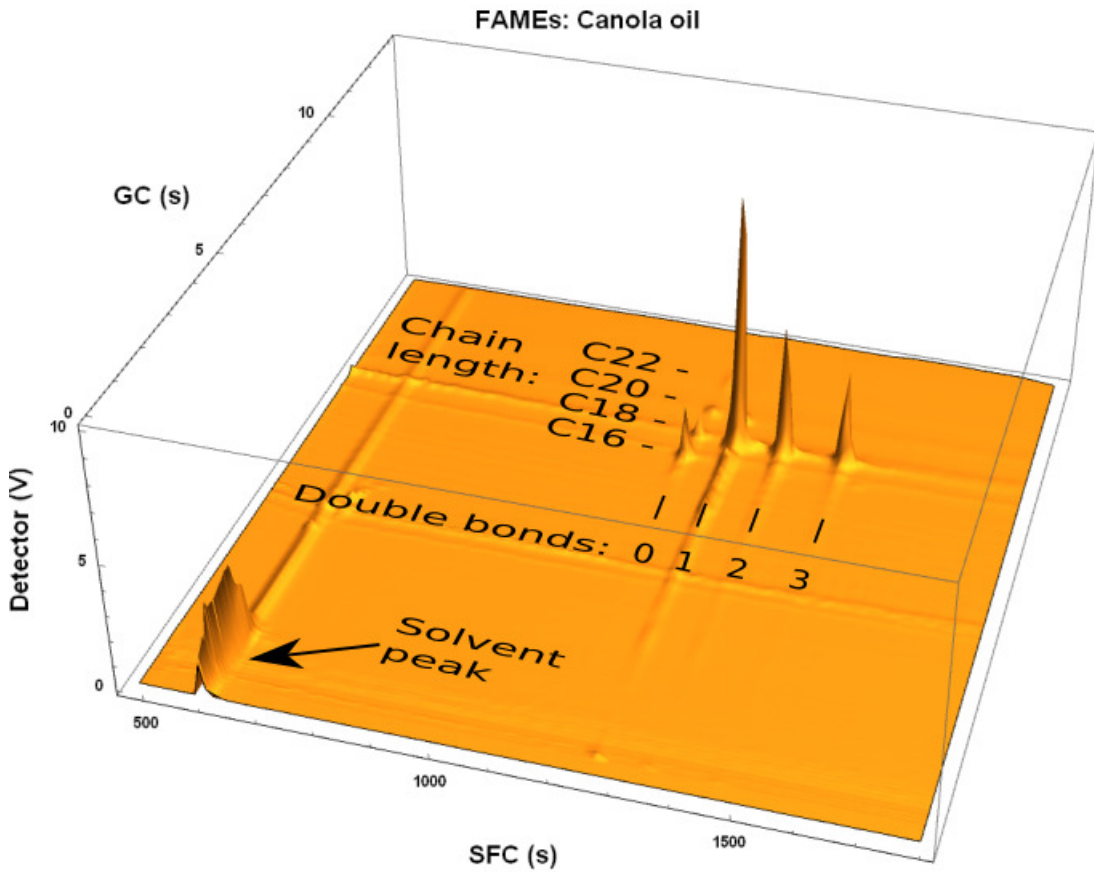


FIG. 8. A 2D chromatogram of FAMEs derived from canola oil. It is clear that the oil consists mostly of unsaturated fatty acids.

The low thermal mass of the heater and column simplifies heating and cooling of a portable fast GC, reducing electrical and carbon dioxide coolant requirements. When sub-ambient temperatures and extreme cycle times are not essential, compressed air could also serve to cool the column.

ACKNOWLEDGMENTS

Prof. Walter Meyer of the Department of Physics at the University of Pretoria supplied the idea for the resistance-measuring electronic circuit. Nico van Vuuren machined the T-piece blocks and their mounting rails. We thank Restek for the generous donation of the packed silica columns. Reinhardt Heymans from FLIR Systems recorded the thermographic

REFERENCES

- ¹G. Watson, W. Horton, and E. Staples, "Gas chromatography utilizing SAW sensors," in *IEEE 1991 Ultrasonics Symposium*, Vol. 1 (1991) pp. 305–309.
- ²S. He, J. Liu, and M. Liu, "Research progress of SAW gas chromatography," in *Proceedings of the 2014 Symposium on Piezoelectricity, Acoustic Waves, and Device Applications* (2014) pp. 59–64.
- ³A. M. Hupp, J. Perron, N. Roques, J. Crandall, S. Ramos, and B. Rohrback, "Analysis of biodiesel-diesel blends using ultrafast gas chromatography (UFGC) and chemometric methods: Extending ASTM D7798 to biodiesel," *Fuel* **231**, 264 – 270 (2018).
- ⁴X. Chen, X. L. Zhang, L. Liu, Y. Chen, M. Y. Piao, F. J. Zhang, W. D. Wu, Y. B. Zhong, K. Sun, Y. C. Zou, X. Zhang, D. Wan, P. Wang, and M. Yan, "Gas chromatograph-surface acoustic wave for quick real-time assessment of blood/exhaled gas ratio of propofol in humans," *British Journal of Anaesthesia* **113**, 807–814 (2014).
- ⁵H. Dong, F. J. Zhang, F. Y. Wang, Y. Y. Wang, J. Guo, G. M. Kanhar, J. Chen, J. Liu, C. Zhou, M. Yan, and X. Chen, "Simultaneous on-line monitoring of propofol and sevoflurane in balanced anesthesia by direct resistive heating gas chromatography," *Journal of Chromatography A* **1506**, 93–100 (2017).
- ⁶E. Górska-Horczyczak, I. Wojtasik-Kalinowska, D. Guzek, D.-W. Sun, and A. Wierzbicka, "Differentiation of chill-stored and frozen pork necks using electronic nose with ultra-fast gas chromatography," *Journal of Food Process Engineering* **40**, e12540 (2017), <https://onlinelibrary.wiley.com/doi/pdf/10.1111/jfpe.12540>.
- ⁷R. L. White, "Evolved gas composition monitoring by repetitive injection gas chromatography," *Journal of Chromatography A* **1421**, 129–136 (2015).
- ⁸Z. Liu and J. B. Phillips, "Comprehensive two-dimensional gas chromatography using an on-column thermal modulator interface," *Journal of Chromatographic Science* **29**, 227–231 (1991).
- ⁹J. V. Seeley and S. K. Seeley, "Multidimensional gas chromatography: Fundamental advances and new applications," *Anal. Chem.* **85**, 557–578 (2013).
- ¹⁰S. E. Prebihalo, K. L. Berrier, C. E. Freye, H. D. Bahaghightat, N. R. Moore, D. K. Pinker-

- ton, and R. E. Synovec, "Multidimensional gas chromatography: Advances in instrumentation, chemometrics, and applications," *Analytical Chemistry* **90**, 505–532 (2018).
- ¹¹C. A. Cramers, H. G. Janssen, M. M. Van Deursen, and P. A. Leclercq, "High-speed gas chromatography: An overview of various concepts," *Journal of Chromatography A* **856**, 315–329 (1999).
- ¹²P. Korytár, H.-G. Janssen, E. Matisová, and U. A. T. Brinkman, "Practical fast gas chromatography: methods, instrumentation and applications," *TrAC Trends in Analytical Chemistry* **21**, 558 – 572 (2002).
- ¹³J. C. Giddings, "Sample dimensionality: A predictor of order-disorder in component peak distribution in multidimensional separation," *Journal of Chromatography A* **703**, 3–15 (1995).
- ¹⁴M. Camenzuli and P. J. Schoenmakers, "A new measure of orthogonality for multi-dimensional chromatography," *Analytica Chimica Acta* **838**, 93–101 (2014).
- ¹⁵S. de Koning, H.-G. Janssen, M. van Deursen, and U. A. T. Brinkman, "Automated on-line comprehensive two-dimensional LC×GC and LC×GC-ToF MS: Instrument design and application to edible oil and fat analysis," *Journal of Separation Science* **27**, 397–409 (2004).
- ¹⁶A. Venter and E. R. Rohwer, "Comprehensive two-dimensional supercritical fluid and gas chromatography with independent fast programmed heating of the gas chromatographic column," *Analytical chemistry* **76**, 3699–706 (2004).
- ¹⁷D. A. Skoog, F. J. Holler, and S. R. Crouch, *Principles of instrumental analysis*, sixth edition. ed. (Thomson Brooks/Cole, Belmont, CA, 2007).
- ¹⁸J. Dalluge, J. Beens, and U. A. T. Brinkman, "Comprehensive two-dimensional gas chromatography: a powerful and versatile analytical tool," *Journal of Chromatography A* **1000**, 69–108 (2003).
- ¹⁹A. Venter, E. R. Rohwer, and A. E. Laubscher, "Analysis of alkane, alkene, aromatic and oxygenated groups in petrochemical mixtures by supercritical fluid chromatography on silica gel," *Journal of Chromatography A* **847**, 309–321 (1999).
- ²⁰L. M. Blumberg and M. S. Klee, "Optimal heating rate in gas chromatography," *Journal of Microcolumn Separations* **12**, 508–514 (2000).
- ²¹A. Wang, H. D. Tolley, and M. L. Lee, "Gas chromatography using resistive heating technology," *Journal of Chromatography A* **1261**, 46–57 (2012).

- ²²M. R. Jacobs, E. F. Hilder, and R. A. Shellie, "Applications of resistive heating in gas chromatography: A review," *Analytica Chimica Acta* **803**, 2–14 (2013).
- ²³H.-Y. J. Chow and T. Górecki, "Temperature programming of the second dimension in comprehensive two-dimensional gas chromatography," *Analytical Chemistry* **89**, 8207–8211 (2017).
- ²⁴A. Venter, P. R. Makgware, and E. R. Rohwer, "Group-type analysis of oxygenated compounds with a silica gel porous layer open tubular column and comprehensive two-dimensional supercritical fluid and gas chromatography," *Analytical Chemistry* **78**, 2051–2054 (2006).
- ²⁵J. Luong, R. Gras, R. Mustacich, and H. Cortes, "Low thermal mass gas chromatography: Principles and applications," *Journal of Chromatographic Science* **44**, 253–261 (2006).
- ²⁶Zip Scientific, "Fast cooling performance," (2008).
- ²⁷J. Dalluge, R. Ou-Aissa, J. J. Vreuls, U. A. T. Brinkman, and J. R. Veraart, "Fast temperature programming in gas chromatography using resistive heating," *Journal of High Resolution Chromatography* **22**, 459–464 (1999).
- ²⁸VICI AG International, "Multichannel fast temperature programmer," (2019).
- ²⁹F. Peacock, "PID tuning blueprint," Internet (2008).
- ³⁰J. A. Contreras, A. L. Rockwood, H. D. Tolley, and M. L. Lee, "Peak sweeping and gating using thermal gradient gas chromatography," *Journal of Chromatography A* **1278**, 160–165 (2013).
- ³¹W. Zheng, P. Bo, Y. Liu, and W. Wang, "Fast B-spline curve fitting by l-BFGS," *Computer Aided Geometric Design* **29**, 448–462 (2012).
- ³²A. Possolo and H. K. Iyer, "Invited article: Concepts and tools for the evaluation of measurement uncertainty," *Review of Scientific Instruments* **88**, 011301 (2017).
- ³³R. A. Shellie, L.-L. Xie, and P. J. Marriott, "Retention time reproducibility in comprehensive two-dimensional gas chromatography using cryogenic modulation," *Journal of Chromatography A* **968**, 161–170 (2002).
- ³⁴R. M. Smith, M. Hyytiänen, A. V. Felipe, and P. M. Morris, "High resolution packed column supercritical fluid chromatography of fatty acid methyl esters," *Journal of Separation Science* **24**, 208–212 (2001).
- ³⁵AOCS, "AOCS official method Ce 2-66," in *Official Methods and Recommended Practices of the AOCS* (American Oil Chemists' Society, 2017) 7th ed.

C

Technical drawings

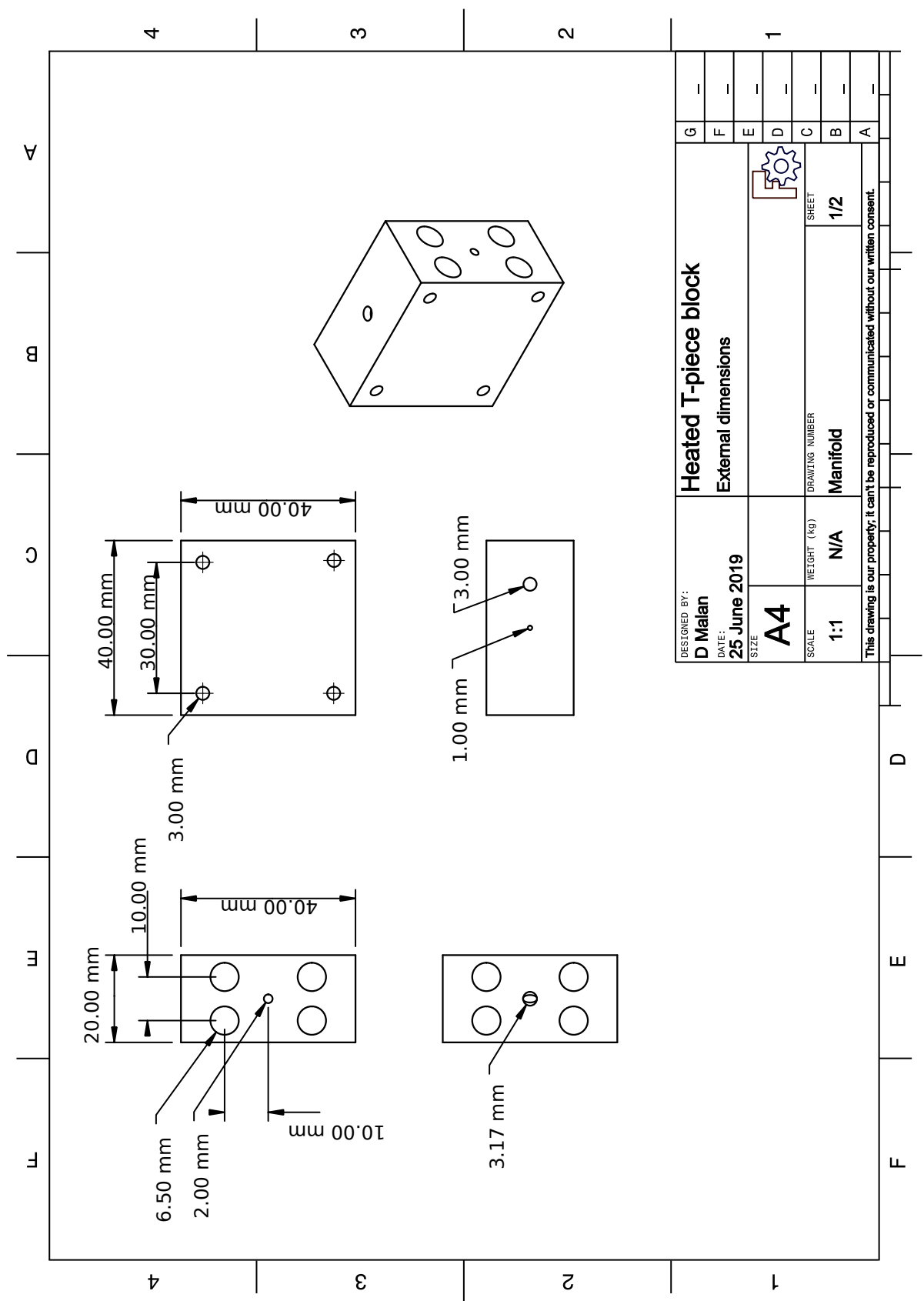


FIGURE C.1: A technical drawing showing the dimensions of the heated T-piece blocks.

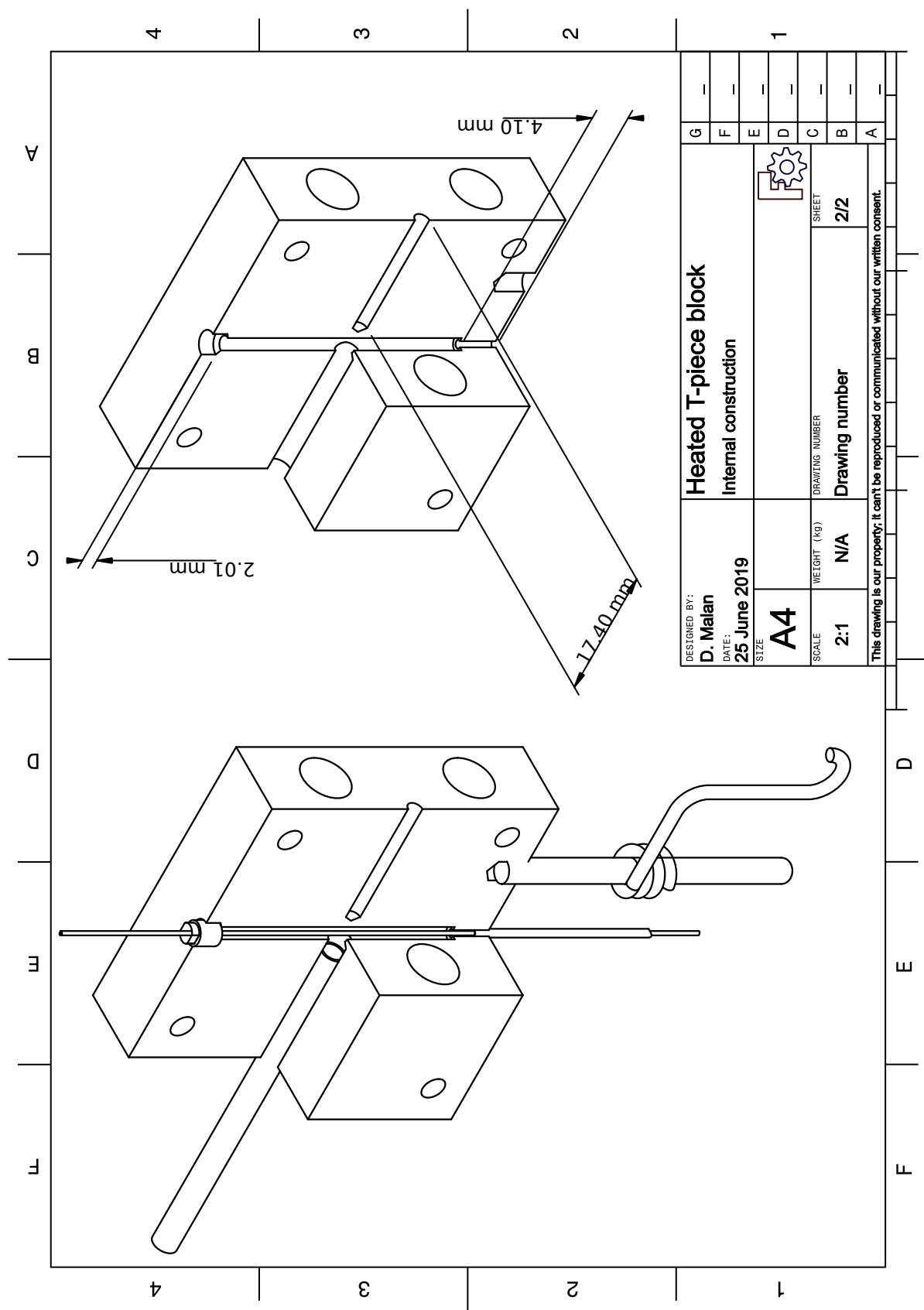


FIGURE C.2: A technical drawing of the internal construction and assembly of the heated T-piece blocks.

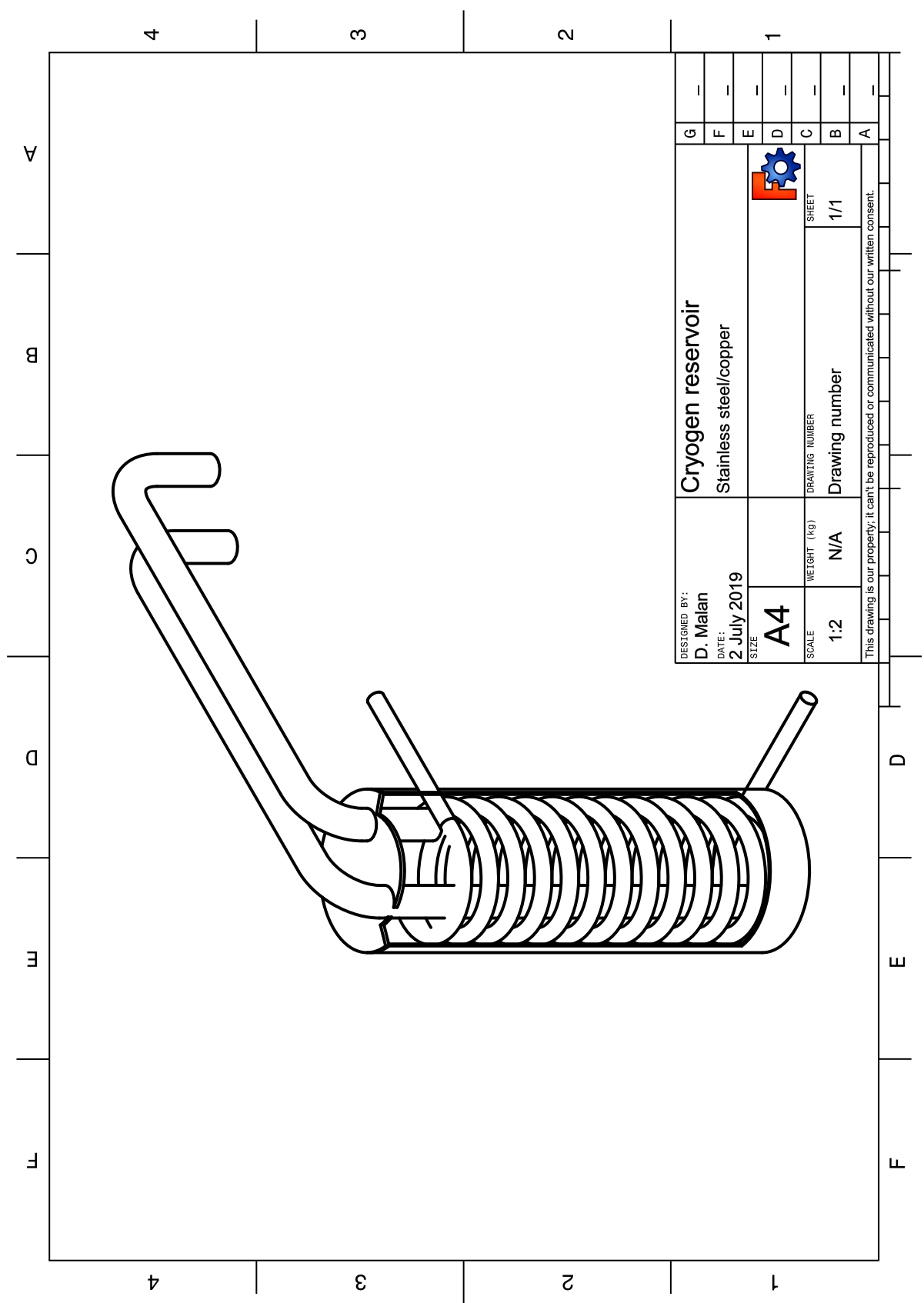


FIGURE C.3: Cut-away technical drawing of coolant reservoir.

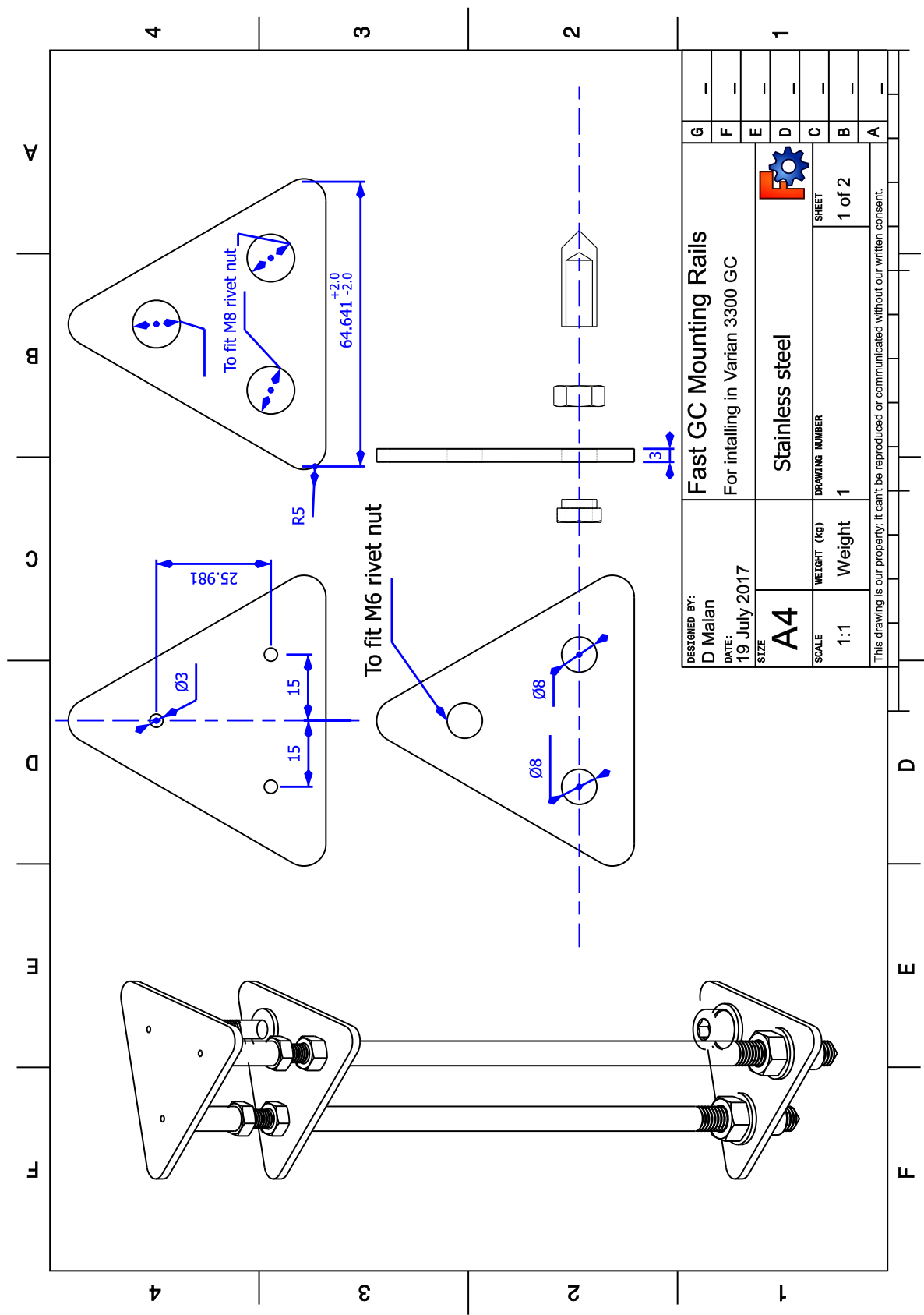


FIGURE C.4: A technical drawing of the rails carrying the T-piece mounting block.

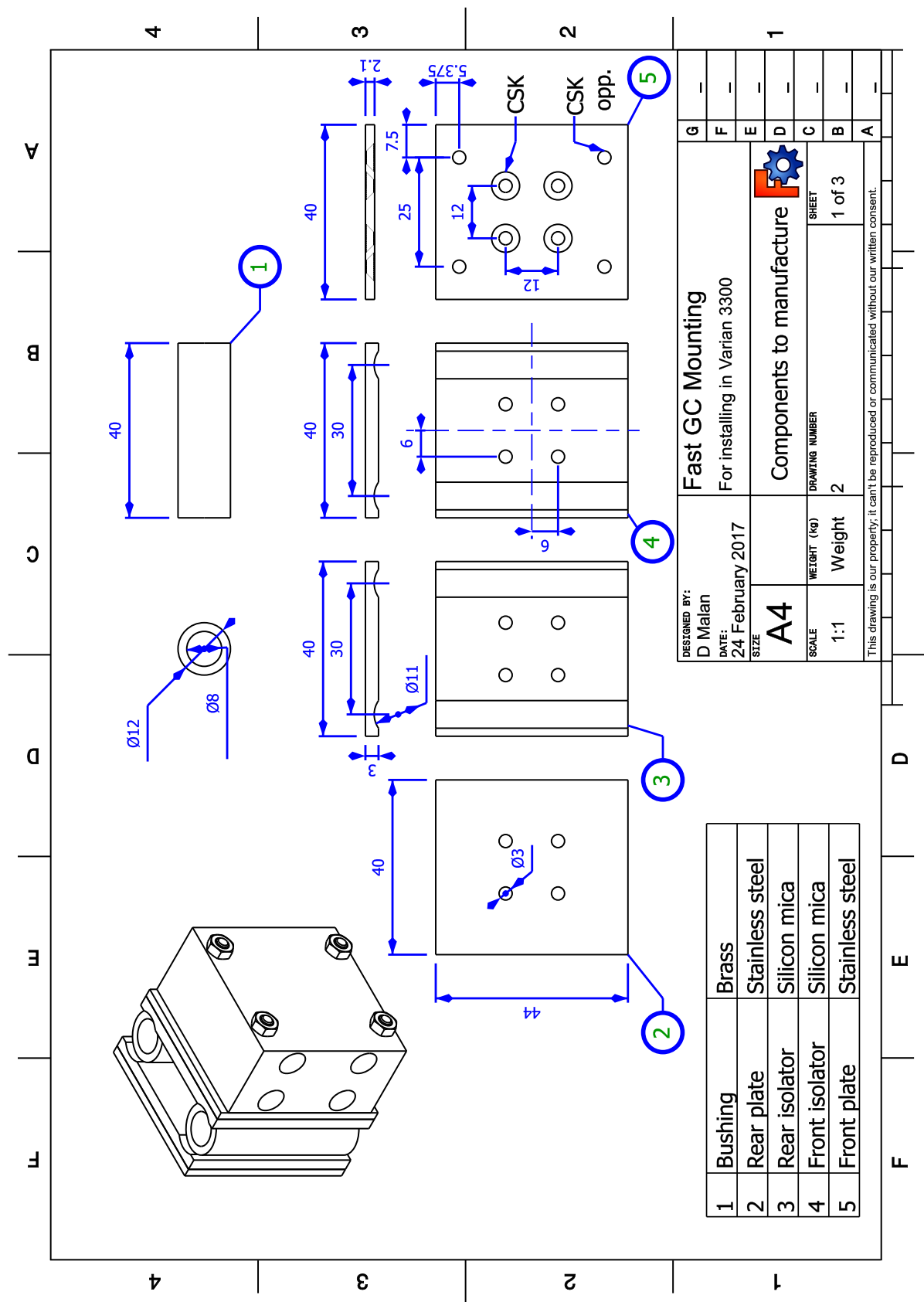


FIGURE C.5: A technical drawing of the T-piece block mounting, showing parts and dimensions.

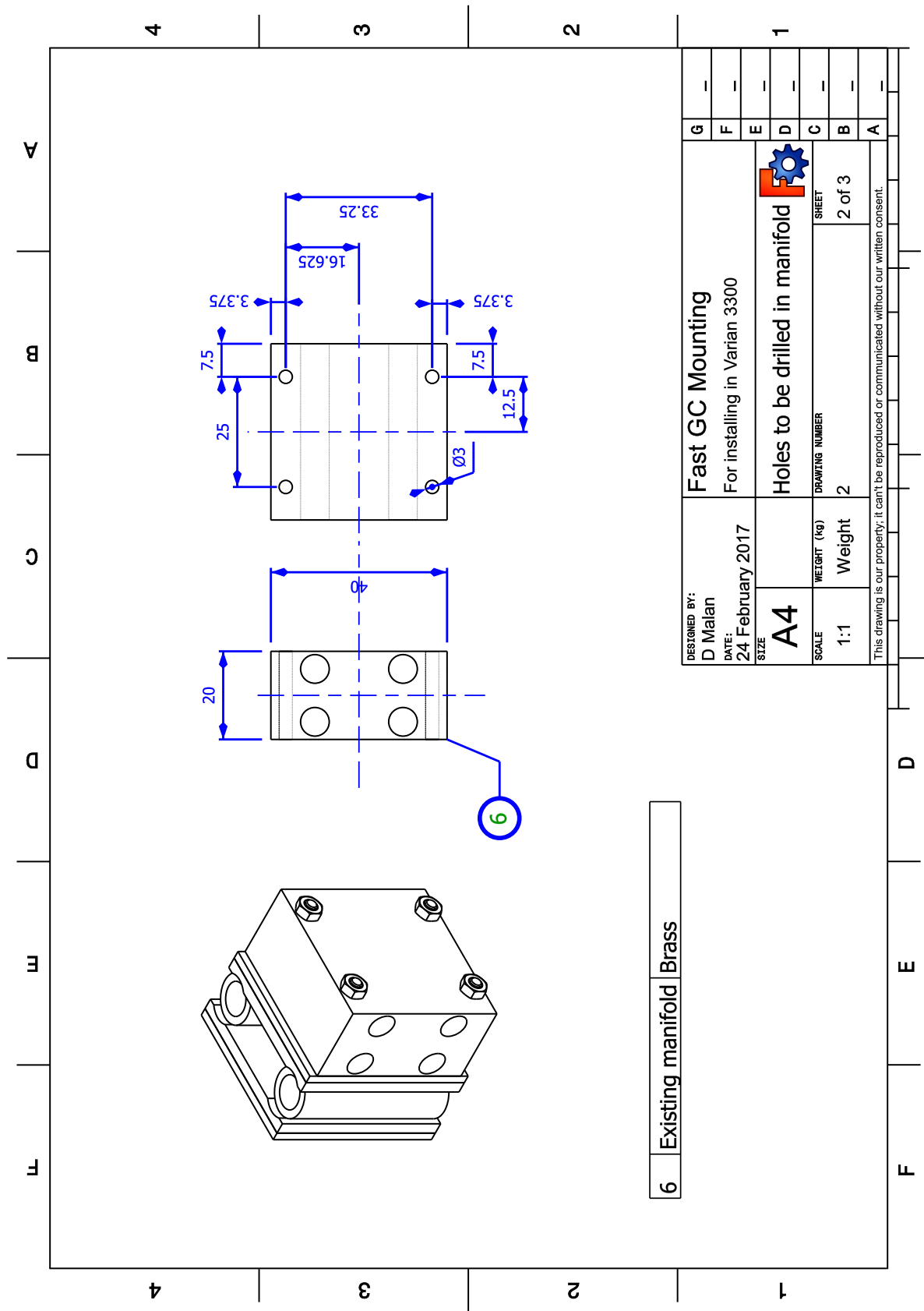


FIGURE C.5: (continued) A technical drawing of the T-piece block mounting, showing final assembly and dimensions.

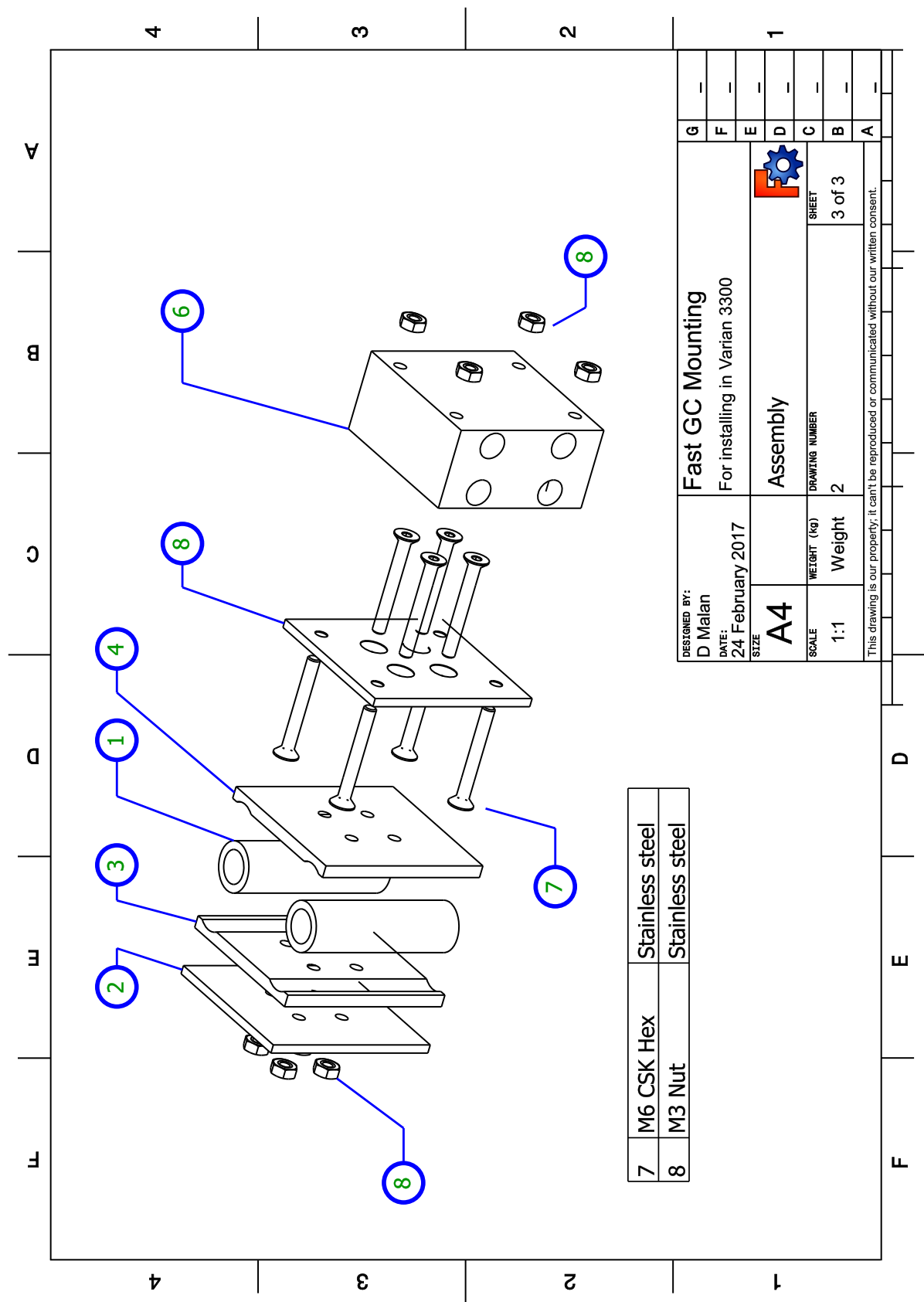


FIGURE C.5: (continued) A technical drawing of the T-piece block mounting, showing assembly method.

D

Fatty acid profiles

TABLE D.1: The fatty acid profile of a sunflower oil sample as determined by a commercial oil analysis laboratory.

Fatty acid	Fraction
C14:0	0.05
C16:0	6.14
C16:1	0.04
C17:0	0.05
C17:1	0
C18:0	5.77
C18:1 t	0
C18:1 c	21.21
C18:2 t	0
C18:2 c	63.91
C18:3n6	0.11
C18:3n3	1.04
C20:0	0.47
C20:1	0.24
C20:2	0
C21:0	0
C22:0	0.77
C22:1	0
C24:0	0.19
C24:1	0

TABLE D.2: Fatty acid profile of coconut oil according to the Codex Alimentarius, a collection of internationally adopted food standards (Joint FAO/WHO Codex Alimentarius Commission 2019).

Fatty acid	Lower	Upper
C6:0	ND	0.7
C8:0	4.6	10
C10:0	5	8
C12:0	45.1	53.2
C14:0	16.8	21
C16:0	7.5	10.2
C16:1	ND	
C17:0	ND	
C17:1	ND	
C18:0	2	4
C18:1	5	10
C18:2	1	2.5
C18:3	ND	0.2
C20:0	ND	0.2
C20:1	ND	0.2
C20:2	ND	
C22:0	ND	
C22:1	ND	
C22:2	ND	
C24:0	ND	
C24:1	ND	

TABLE D.3: The fatty acid profile of salmon oil according to the Codex Alimentarius, a collection of internationally adopted food standards (Joint FAO/WHO Codex Alimentarius Commission 2017).

N:D	n-	Fatty acids	Salmon (Wild)		Salmon (Farmed)	
			Limits		Low	High
C14:0		myristic acid	2.	5.	1.5	5.5
C15:0		pentadecanoic acid	ND	1.	ND	0.5
C16:0	(n-7)	palmitic acid	10.	16.	6.5	12.
C17:0		palmitoleic acid	4.	6.	2.	5.
C18:0		heptadecanoic acid	ND	1.	ND	0.5
C18:1	(n-7)	stearic acid	2.	5.	2.	5.
C18:1	(n-9)	vaccenic acid	2.5	NA	2.0	7.0
C18:2	(n-6)	oleic acid	8.	16.	30.	47.
C18:3	(n-3)	linoleic acid	1.5	2.5	8.	15.
C18:3	(n-6)	linolenic acid	ND	2.	3.	6.
C18:4	(n-3)	γ -linolenic acid	ND	2.	ND	0.5
C20:0		stearidonic acid	1.	4.	0.5	1.5
C20:1	(n-9)	arachidic acid	ND	0.5	0.1	0.5
C20:1	(n-11)	eicosenoic acid	2.	10.	1.5	7.
C20:4	(n-6)	arachidonic acid	NA	NA	NA	NA
C20:4	(n-3)	eicosatetraenoic acid	0.5	2.5	ND	1.2
C20:5	(n-3)	eicosapentaenoic acid	1.	3.	0.5	1.
C21:5	(n-3)	heneicosapentaenoic acid	6.5	11.5	2.	6.
C22:1	(n-9)	erucic acid	ND	4.	NA	NA
C22:1	(n-11)	cetoleic acid	1.	1.5	3.	7.
C22:5	(n-3)	docosapentaenoic acid	1.5	3.	1.	2.5
C22:6	(n-3)	docosahexaenoic acid	6.	14.	3.	10.

Bibliography

- Abebe, Mimi (Oct. 2008). "History of Ethanol". In: *Journalism & Mass Communications: Student Media*.
- Agence France-Presse (Sept. 17, 2018). "Germany launches world's first hydrogen-powered train". In: *The Guardian*.
- Agilent Technologies (2019). *Agilent 7890B gas chromatography data sheet*.
- Allen, Myles et al. (Nov. 2014). *IPCC fifth assessment synthesis report - Climate Change 2014 synthesis report*. Intergovernmental Panel on Climate Change (IPCC), pp. -- 116.
- Analog Devices (1999). *Monolithic Thermocouple Amplifiers with Cold Junction Compensation*. AD594/AD595. Rev. C. Analog Devices.
- Anastas, Paul T. and John Charles. Warner (1998). *Green chemistry : theory and practice*. English. Oxford [England]; New York: Oxford University Press.
- Anastas, Paul T. and Julie B. Zimmerman (July 2016). "The Molecular Basis of Sustainability". In: *Chem* 1.1, pp. 10–12. DOI: [10.1016/j.chempr.2016.06.016](https://doi.org/10.1016/j.chempr.2016.06.016).
- Angelis, Vanda De et al. (June 2007). "Multiperiod integrated routing and scheduling of World Food Programme cargo planes in Angola". In: *Computers & Operations Research* 34.6, pp. 1601–1615. DOI: [10.1016/j.cor.2005.07.012](https://doi.org/10.1016/j.cor.2005.07.012).
- AOCS, ed. (2017). *AOCS Official Method Ce* 2-66.
- Arrhenius, S. (1897). "On the Influence of Carbonic Acid in the Air upon the Temperature of the Earth". In: *Publications of the Astronomical Society of the Pacific* 9.54, p. 14.
- Atadashi, I. M. et al. (Dec. 2011). "Refining technologies for the purification of crude biodiesel". In: *Applied Energy* 88.12, pp. 4239–4251. DOI: [10.1016/j.apenergy.2011.05.029](https://doi.org/10.1016/j.apenergy.2011.05.029).
- Bainbridge, Lisanne (Nov. 1983). "Ironies of automation". In: *Automatica* 19.6, pp. 775–779. DOI: [10.1016/0005-1098\(83\)90046-8](https://doi.org/10.1016/0005-1098(83)90046-8).
- Ball, William T. et al. (Feb. 2018). "Evidence for a continuous decline in lower stratospheric ozone offsetting ozone layer recovery". In: *Atmospheric Chemistry and Physics* 18.2, pp. 1379–1394. DOI: [10.5194/acp-18-1379-2018](https://doi.org/10.5194/acp-18-1379-2018).
- Barnett, James A. (2000). "A history of research on yeasts 2: Louis Pasteur and his contemporaries, 1850-1880". In: *Yeast* 16.8, pp. 755–771. DOI: [10.1002/1097-0061\(20000615\)16:8<755::aid-yea587>3.0.co;2-4](https://doi.org/10.1002/1097-0061(20000615)16:8<755::aid-yea587>3.0.co;2-4).
- Berche, Bertrand, Malte Henkel, and Ralph Kenna (June 2009). "Fenômenos críticos: 150 anos desde Cagniard de la Tour". In: *Revista Brasileira de Ensino de Física* 31.2, pp. 26021–26024. DOI: [10.1590/s1806-11172009000200015](https://doi.org/10.1590/s1806-11172009000200015).
- Berdick, Murray (July 1972). "The role of fats and oils in cosmetics". In: *Journal of the American Oil Chemists' Society* 49.7, pp. 406–408. DOI: [10.1007/bf02582522](https://doi.org/10.1007/bf02582522).
- Berger, Terry A. and Jerome F. Deye (June 1991). "Role of additives in packed column supercritical fluid chromatography: suppression of solute ionization". In: *Journal of Chromatography A* 547, pp. 377–392. DOI: [10.1016/s0021-9673\(01\)88661-1](https://doi.org/10.1016/s0021-9673(01)88661-1).
- Blumberg, L. M. and M. S. Klee (2000). "Optimal Heating Rate in Gas Chromatography". In: *Journal of Microcolumn Separations* 12.9, pp. 508–514.

- Blumberg, Leonid M. (Nov. 1997). "Theory of fast capillary gas chromatography. Part 1: Column efficiency". In: *Journal of High Resolution Chromatography* 20.11, pp. 597–604. DOI: [10.1002/jhrc.1240201106](https://doi.org/10.1002/jhrc.1240201106).
- (July 1999). "Theory of Fast Capillary Gas Chromatography - Part 3: Column Performance vs. Gas Flow Rate". In: *Journal of High Resolution Chromatography* 22.7, pp. 403–413. DOI: [10.1002/\(sici\)1521-4168\(19990701\)22:7<403::aid-jhrc403>3.0.co;2-r](https://doi.org/10.1002/(sici)1521-4168(19990701)22:7<403::aid-jhrc403>3.0.co;2-r).
- (Feb. 2018). "Flow optimization in one-dimensional and comprehensive two-dimensional gas chromatography". In: *Journal of Chromatography A* 1536, pp. 27–38. DOI: [10.1016/j.chroma.2017.08.040](https://doi.org/10.1016/j.chroma.2017.08.040).
- Braun, Peter et al. (May 2018). "Potential Technical Approaches for Improving Low-Temperature NO_x Conversion of Exhaust Aftertreatment Systems". In: *Chemie Ingenieur Technik* 90.6, pp. 762–773. DOI: [10.1002/cite.201700122](https://doi.org/10.1002/cite.201700122).
- Brown, S., S. Menon, and C. Hagen (Oct. 5, 2015). "Investigation of scaling laws for combustion engine performance." In: Fall Technical Meeting of the Western States Section of the Combustion Institute (WSS/CI 2015 Fall Meeting) (Provo, Utah, USA).
- BSI (2016). *A standard for standards – Principles of standardization*. BSI Standards Limited. ISBN: 978-0-580-94429-1.
- Burke-Kennedy, Eoin (Feb. 16, 2018). "Ireland 2040: €22bn to turn State into low-carbon economy". In: *The Irish Times*.
- Cardona, C. A. and O. J. Sánchez (2007). "Fuel ethanol production: Process design trends and integration opportunities". English. In: *Bioresource technology* 98.12, pp. 2415–2457. DOI: [10.1016/j.biortech.2007.01.002](https://doi.org/10.1016/j.biortech.2007.01.002).
- Carson, Rachel (Oct. 23, 2003). *Silent Spring*. Houghton Mifflin. 400 pp. ISBN: 9780618249060.
- CEN (2008). *Automotive fuels – Fatty acid methyl esters (FAME) for diesel engines – Requirements and test methods*. Tech. rep. European Committee for Standardization.
- Chiaramonti, David et al. (Dec. 2014). "Sustainable bio kerosene: Process routes and industrial demonstration activities in aviation biofuels". In: *Applied Energy* 136, pp. 767–774. DOI: [10.1016/j.apenergy.2014.08.065](https://doi.org/10.1016/j.apenergy.2014.08.065).
- Clarke, Coby J. et al. (Jan. 2018). "Green and Sustainable Solvents in Chemical Processes". In: *Chemical Reviews* 118.2, pp. 747–800. DOI: [10.1021/acs.chemrev.7b00571](https://doi.org/10.1021/acs.chemrev.7b00571).
- Coffee Market Report December 2018* (2018). Tech. rep. International Coffee Organization.
- Cummins Jr., C. Lyle (1989). *Internal Fire*. Society of Automotive Engineers. ISBN: 978-0898837650.
- Davidson, Arthur (1998). "Photochemical oxidant air pollution: A historical perspective". In: *Air pollution in the 21st century - Priority issues and policy*. Elsevier, pp. 393–405. DOI: [10.1016/s0166-1116\(98\)80024-1](https://doi.org/10.1016/s0166-1116(98)80024-1).
- Day, G. M. et al. (Mar. 2003). "Thermally Stable Siloxane Polymers for Gas Chromatography". In: *ACS Symposium Series*. American Chemical Society, pp. 127–136. DOI: [10.1021/bk-2003-0838.ch012](https://doi.org/10.1021/bk-2003-0838.ch012).
- Department of Defence (1996). *MIL-STD-883E Test method standard: microcircuits*.
- Desty, D. H. and B. H. F. Whyman (Mar. 1957). "Application of Gas-Liquid Chromatography to Analysis of Liquid Petroleum Fractions". In: *Analytical Chemistry* 29.3, pp. 320–329. DOI: [10.1021/ac60123a001](https://doi.org/10.1021/ac60123a001).
- Di Sanzo, F. P. and R. E. Yoder (Jan. 1, 1991). "Determination of Aromatics in Jet and Diesel Fuels by Supercritical Fluid Chromatography with Flame Ionization Detection (SFC-FID): A Quantitative Study". In: *Journal of Chromatographic Science* 29.1, pp. 4–7. DOI: [10.1093/chromsci/29.1.4](https://doi.org/10.1093/chromsci/29.1.4).

- Diamond, Jared M. (June 30, 2011). *Collapse : how societies choose to fail or succeed.* English. New York: Penguin. 608 pp. ISBN: 978-0-241-95868-1.
- Doucette, Reed T. and Malcolm D. McCulloch (Feb. 2011). "Modeling the CO₂ emissions from battery electric vehicles given the power generation mixes of different countries". In: *Energy Policy* 39.2, pp. 803–811. DOI: [10.1016/j.enpol.2010.10.054](https://doi.org/10.1016/j.enpol.2010.10.054).
- Duncan, Bryan N. et al. (Jan. 2016). "A space-based, high-resolution view of notable changes in urban NO_x pollution around the world (2005–2014)". In: *Journal of Geophysical Research: Atmospheres* 121.2, pp. 976–996. DOI: [10.1002/2015jd024121](https://doi.org/10.1002/2015jd024121).
- Dunn, Robert O. (Dec. 2009). "Effects of minor constituents on cold flow properties and performance of biodiesel". In: *Progress in Energy and Combustion Science* 35.6, pp. 481–489. DOI: [10.1016/j.pecs.2009.07.002](https://doi.org/10.1016/j.pecs.2009.07.002).
- Dyos, G. (2012). "Handbook of Electrical Resistivity - New Materials and Pressure Effects - 2.1 Introduction". In: *Handbook of Electrical Resistivity - New Materials and Pressure Effects*. Institution of Engineering and Technology, p. 11. ISBN: 978-1-84919-149-4.
- Eggertsen, F. T., H. S. Knight, and Sigurd Groennings (Mar. 1956). "Gas Chromatography Use of Liquid-Modified Solid Adsorbent to Resolve C₅ and C₆ Saturates". In: *Analytical Chemistry* 28.3, pp. 303–306. DOI: [10.1021/ac60111a004](https://doi.org/10.1021/ac60111a004).
- Eisenmenger, Michael et al. (Oct. 2006). "Pilot-scale supercritical carbon dioxide extraction and fractionation of wheat germ oil". In: *Journal of the American Oil Chemists' Society* 83.10, pp. 863–868. ISSN: 1558-9331. DOI: [10.1007/s11746-006-5038-6](https://doi.org/10.1007/s11746-006-5038-6).
- Ettre, L. S. (Jan. 1993). "Nomenclature for chromatography (IUPAC Recommendations 1993)". In: *Pure and Applied Chemistry* 65.4, pp. 819–872. DOI: [10.1351/pac199365040819](https://doi.org/10.1351/pac199365040819).
- (June 2008). "The Invention, Development, and Triumph of the Flame-Ionization Detector". In: *Chapters in the Evolution of Chromatography*. PUBLISHED BY IMPERIAL COLLEGE PRESS AND DISTRIBUTED BY WORLD SCIENTIFIC PUBLISHING CO., pp. 303–320. DOI: [10.1142/9781860949449_0023](https://doi.org/10.1142/9781860949449_0023).
- Ettre, L. S. and K. I. Sakodynzkii (Feb. 1993a). "M. S. Tswett and the discovery of chromatography I: Early work (1899–1903)". In: *Chromatographia* 35.3-4, pp. 223–231. DOI: [10.1007/bf02269707](https://doi.org/10.1007/bf02269707).
- (Mar. 1993b). "M. S. Tswett and the discovery of chromatography II: Completion of the development of chromatography (1903–1910)". In: *Chromatographia* 35.5-6, pp. 329–338. DOI: [10.1007/bf02277520](https://doi.org/10.1007/bf02277520).
- Ferguson, Paul (Nov. 1, 2013). "Meeting Review: Advances in GC IV". In: *Chromatography Today*.
- Flick, Carlos (1980). "The Movement for Smoke Abatement in 19th-Century Britain". In: *Technology and Culture* 21.1, pp. 29–50. ISSN: 0040-165X. DOI: [10.2307/3103986](https://doi.org/10.2307/3103986).
- Frauhammer, Jörg, Alexander Schenck zu Schweinsberg, and Klaus Winkler (July 2014). "Catalytic emission control". In: *Gasoline Engine Management*. Springer Fachmedien Wiesbaden, pp. 268–283. DOI: [10.1007/978-3-658-03964-6_18](https://doi.org/10.1007/978-3-658-03964-6_18).
- Gabbatiss, Josh (Oct. 19, 2018). "Ban new petrol and diesel cars by 2032 instead of current 'unambitious' target, MPs say". In: *The Independent*.
- Gertler, Alan W. et al. (Nov. 1999). "The Impact of California Phase 2 Reformulated Gasoline on Real-World Vehicle Emissions". In: *Journal of the Air & Waste Management Association* 49.11, pp. 1339–1346. DOI: [10.1080/10473289.1999.10463965](https://doi.org/10.1080/10473289.1999.10463965).
- Gibson, Jennifer et al. (Jan. 2016). "Levels and trends of contaminants in humans of the Arctic". In: *International Journal of Circumpolar Health* 75.1, p. 33804. DOI: [10.3402/ijch.v75.33804](https://doi.org/10.3402/ijch.v75.33804).

- Giddings, J. C. (May 1987). "Concepts and comparisons in multidimensional separation". In: *Journal of High Resolution Chromatography* 10.5, pp. 319–323. DOI: [10.1002/jhrc.1240100517](https://doi.org/10.1002/jhrc.1240100517).
- Grażyna, Wejnerowska and Ciaciuch Anna (Feb. 2018). "Optimisation of oil extraction from quinoa seeds with supercritical carbon dioxide with co-solvents". In: *Czech Journal of Food Sciences* 36.No. 1, pp. 81–87. DOI: [10.17221/122/2017-cjfs](https://doi.org/10.17221/122/2017-cjfs).
- Green, Martin A. et al. (Nov. 12, 2019). "Solar cell efficiency tables (Version 55)". In: *Progress in Photovoltaics: Research and Applications* 28.1, pp. 3–15. DOI: [10.1002/pip.3228](https://doi.org/10.1002/pip.3228).
- Greenberg, Jon (May 17, 2017). *No, coffee is not the second-most traded commodity after oil*. URL: <https://www.politifact.com/global-news/statements/2017/may/08/starbucks/no-coffee-not-second-most-traded-commodity-after-o/> (visited on 01/31/2019).
- Griffin, John Joseph (Jan. 1, 1838). *Chemical Recreations: A Compendium of Experimental Chemistry, Part 1*. R. Griffin and Company.
- Gritti, Fabrice and Georges Guiochon (Aug. 2006). "General HETP Equation for the Study of Mass-Transfer Mechanisms in RPLC". In: *Analytical Chemistry* 78.15, pp. 5329–5347. DOI: [10.1021/ac060203r](https://doi.org/10.1021/ac060203r).
- Gumm, Brian (Oct. 22, 2015). *Blowing Smoke: Chemical Companies Say 'Trust Us,' But Environmental and Workplace Safety Violations Belie Their Rhetoric*. Tech. rep. Center for Effective Government.
- Guthrie, E. J. and H. E. Schwartz (1986). "Integral Pressure Restrictor for Capillary SFC". In: *Journal of Chromatographic Science* 24.6, pp. 236–241. ISSN: 0021-9665.
- Halliday, Stephen (2001). "Death and miasma in Victorian London: an obstinate belief". In: *BMJ: British Medical Journal* 323.7327, pp. 1469–1471. ISSN: 0959-8138. DOI: [10.1136/bmj.323.7327.1469](https://doi.org/10.1136/bmj.323.7327.1469). eprint: <https://www.bmjjournals.org/content/323/7327/1469.full.pdf>.
- Hanmer, Clare and Simone Abram (Dec. 2017). "Actors, networks, and translation hubs: Gas central heating as a rapid socio-technical transition in the United Kingdom". In: *Energy Research & Social Science* 34, pp. 176–183. DOI: [10.1016/j.erss.2017.03.017](https://doi.org/10.1016/j.erss.2017.03.017).
- Harris, Daniel C. (Oct. 2010). "Charles David Keeling and the Story of Atmospheric CO₂ Measurements". In: *Analytical Chemistry* 82.19, pp. 7865–7870. ISSN: 0003-2700. DOI: [10.1021/ac1001492](https://doi.org/10.1021/ac1001492).
- Hatto, Peter (2010). *Standards and Standardization Handbook*. European Commission Directorate-General for Research Industrial Technologies.
- Hayes, John G. et al. (Sept. 2011). "Simplified electric vehicle power train models and range estimation". In: *2011 IEEE Vehicle Power and Propulsion Conference*. IEEE. DOI: [10.1109/vppc.2011.6043163](https://doi.org/10.1109/vppc.2011.6043163).
- Herrero, Miguel et al. (Apr. 2010). "Supercritical fluid extraction: Recent advances and applications". In: *Journal of Chromatography A* 1217.16, pp. 2495–2511. DOI: [10.1016/j.chroma.2009.12.019](https://doi.org/10.1016/j.chroma.2009.12.019).
- Hoffmann, Karl Heinz (Feb. 2008). "An introduction to endoreversible thermodynamics". In: *Atti della Accademia Peloritana dei Pericolanti - Classe di Scienze Fisiche, Matematiche e Naturali* 1, pp. 1–18. ISSN: 1825-1242. DOI: [10.1478/C1S0801011](https://doi.org/10.1478/C1S0801011).
- Holm, Torkil and Jørgen Øgaard Madsen (Jan. 1996). "Methane Formation by Flame-Generated Hydrogen Atoms in the Flame Ionization Detector". In: *Analytical Chemistry* 68.20, pp. 3607–3611. DOI: [10.1021/ac960556y](https://doi.org/10.1021/ac960556y).
- Hunt, Andrew J. et al. (Jan. 2010). "Generation, Capture, and Utilization of Industrial Carbon Dioxide". In: *ChemSusChem* 3.3, pp. 306–322. DOI: [10.1002/cssc.200900169](https://doi.org/10.1002/cssc.200900169).

- International vocabulary of metrology – Basic and general concepts and associated terms (VIM)* (2019). 3rd ed. Joint Committee for Guides in Metrology, International Bureau of Weights and Measures.
- IPCC (2014). "2014: Summary for policymakers". In: *Climate Change 2014: Impacts, Adaptation, and Vulnerability. Part A: Global and Sectoral Aspects. Contribution of Working Group II to the Fifth Assessment Report of the Intergovernmental Panel on Climate Change*. Ed. by C. B. Field et al. IPCC.
- ISO (2015). *BS EN ISO 18134-3:2015 Solid biofuels. Determination of moisture content. Oven dry method. Moisture in general analysis sample*.
- (2017). *ISO/IEC 17025:2017: GENERAL REQUIREMENTS FOR THE COMPETENCE OF TESTING AND CALIBRATION LABORATORIES*.
- (2019). *ISO 14708-2: IMPLANTS FOR SURGERY – ACTIVE IMPLANTABLE MEDICAL DEVICES – PART 2: CARDIAC PACEMAKERS*.
- Jacobs, Matthew R., Emily F. Hilder, and Robert A. Shellie (Nov. 2013). "Applications of resistive heating in gas chromatography: A review". In: *Analytica Chimica Acta* 803, pp. 2–14. DOI: [10.1016/j.aca.2013.04.063](https://doi.org/10.1016/j.aca.2013.04.063).
- Jacobsen, M. and G. Bertelsen (June 2002). "The use of CO₂ in packaging of fresh red meats and its effect on chemical quality changes in the meat: a review". In: *Journal of Muscle Foods* 13.2, pp. 143–168. DOI: [10.1111/j.1745-4573.2002.tb00326.x](https://doi.org/10.1111/j.1745-4573.2002.tb00326.x).
- Joint FAO/WHO Codex Alimentarius Commission (2017). *Codex Alimentarius: STANDARD FOR FISH OILS CXS 329-2017*. World Health Organization : Food and Agriculture Organization of the United Nations.
- (2019). *Codex Alimentarius: STANDARD FOR NAMED VEGETABLE OILS CXS 210-1999*. World Health Organization : Food and Agriculture Organization of the United Nations. ISBN: 92-5-104682-4.
- Kamiński, Marian et al. (July 2005). "High-Performance Liquid Chromatography in Group-Type Separation and Technical or Process Analytics of Petroleum Products". In: *Critical Reviews in Analytical Chemistry* 35.3, pp. 193–216. DOI: [10.1080/10408340500304024](https://doi.org/10.1080/10408340500304024).
- Keulemans, A. I. M., A. Kwanten, and P. Zaal (1955). "The selectivity of the stationary liquid in vapour phase chromatography". In: *Analytica Chimica Acta* 13, pp. 357–372. DOI: [10.1016/s0003-2670\(00\)87957-x](https://doi.org/10.1016/s0003-2670(00)87957-x).
- Kimpe, K., P. A. Jacobs, and M. Waelkens (Dec. 2001). "Analysis of oil used in late Roman oil lamps with different mass spectrometric techniques revealed the presence of predominantly olive oil together with traces of animal fat". In: *Journal of Chromatography A* 937.1-2, pp. 87–95. DOI: [10.1016/s0021-9673\(01\)01304-8](https://doi.org/10.1016/s0021-9673(01)01304-8).
- Kitessa, Soressa et al. (May 2014). "DHA-Containing Oilseed: A Timely Solution for the Sustainability Issues Surrounding Fish Oil Sources of the Health-Benefiting Long-Chain Omega-3 Oils". In: *Nutrients* 6.5, pp. 2035–2058. DOI: [10.3390/nu6052035](https://doi.org/10.3390/nu6052035).
- Klass, Donald (1998). *Biomass for renewable energy, fuels, and chemicals*. San Diego: Academic Press. ISBN: 9780080528052.
- Klee, M. S. and L. M. Blumberg (May 2002). "Theoretical and Practical Aspects of Fast Gas Chromatography and Method Translation". In: *Journal of Chromatographic Science* 40.5, pp. 234–247. DOI: [10.1093/chromsci/40.5.234](https://doi.org/10.1093/chromsci/40.5.234).
- Knothe, Gerhard (Sept. 2002). "Structure indices in FA chemistry. How relevant is the iodine value?" In: *Journal of the American Oil Chemists' Society* 79.9, pp. 847–854. DOI: [10.1007/s11746-002-0569-4](https://doi.org/10.1007/s11746-002-0569-4).
- (Feb. 2007). "Arthur von Hübl and the iodine value". English. In: *INFORM* 18.2. Copyright - Copyright AOCS Press Feb 2007; Document feature - Photographs; Equations; Last updated - 2010-07-17, pp. 136–138.

- Knothe, Gerhard (2010). "History of Vegetable Oil-Based Diesel Fuels". In: *The Biodiesel Handbook*. Elsevier, pp. 5–19. DOI: [10.1016/b978-1-893997-62-2.50007-3](https://doi.org/10.1016/b978-1-893997-62-2.50007-3).
- Knothe, Gerhard and Kevin R. Steidley (May 2005). "Lubricity of Components of Biodiesel and Petrodiesel. The Origin of Biodiesel Lubricity". In: *Energy & Fuels* 19.3, pp. 1192–1200. DOI: [10.1021/ef049684c](https://doi.org/10.1021/ef049684c).
- Koenig, David M. (Jan. 11, 2009). *Practical Control Engineering: A Guide for Engineers, Managers, and Practitioners*. MCGRaw HILL BOOK CO. 474 pp. ISBN: 0071606130.
- Kornblut, Phil (Mar. 1, 2019). "Helium Shortage 3.0". In: *Gasworld*.
- Kumar, Santosh, Neetu Singh, and Ram Prasad (Sept. 2010). "Anhydrous ethanol: A renewable source of energy". In: *Renewable and Sustainable Energy Reviews* 14.7, pp. 1830–1844. DOI: [10.1016/j.rser.2010.03.015](https://doi.org/10.1016/j.rser.2010.03.015).
- Kyoto Protocol to the United Nations Framework Convention on Climate Change*. (Dec. 11, 1997).
- Lauer, Henk H., Douglass. McManigill, and Robert D. Board (July 1983). "Mobile-phase transport properties of liquefied gases in near critical and supercritical fluid chromatography". In: *Analytical Chemistry* 55.8, pp. 1370–1375. DOI: [10.1021/ac00259a041](https://doi.org/10.1021/ac00259a041).
- Li, Harry and Radu Curiac (Jan. 2012). "Energy Conservation: Motor Efficiency, Efficiency Tolerances, and the Factors That Influence Them". In: *IEEE Industry Applications Magazine* 18.1, pp. 62–68. DOI: [10.1109/mias.2011.943105](https://doi.org/10.1109/mias.2011.943105).
- Linseed (1911). In: *Encyclopædia Britannica*. 11th ed. Cambridge University Press, pp. 734–735.
- Linthorst, J. A. (Apr. 2010). "An overview: origins and development of green chemistry". In: *Foundations of Chemistry* 12.1, pp. 55–68. ISSN: 1572-8463. DOI: [10.1007/s10698-009-9079-4](https://doi.org/10.1007/s10698-009-9079-4).
- Luque de Castro, Maria D., Miguel Valcárcel, and María T. Tena (1994). *Analytical Supercritical Fluid Extraction*. Springer. ISBN: 3-540-57495-6.
- Malan, D., S. J. van der Walt, and E. R. Rohwer (Mar. 2020). "A high-repetition-rate, fast temperature-programmed gas chromatograph and its online coupling to a supercritical fluid chromatograph (SFC × GC)". In: *Review of Scientific Instruments* 91.3, p. 034101. DOI: [10.1063/1.5125060](https://doi.org/10.1063/1.5125060).
- Mansouri, Nazanin (2016). "A Case Study of Volkswagen Unethical Practice in Diesel Emission Test". In: *International Journal of Science and Engineering Applications* 5.4, pp. 211–216.
- Marriott, Philip J., Peter Schoenmakers, and Ze-ying Wu (2012). "Nomenclature and conventions in comprehensive multidimensional chromatography — an update". In: *LC-GC Europe*.
- McCurry, James D. and Wesley Norman (May 2009). "5-in-1 biodiesel: an approach to combining five biodiesel gas chromatographic methods on a single instrument". In: *Biofuels, Bioproducts and Biorefining* 3.3, pp. 296–298. DOI: [10.1002/bbb.155](https://doi.org/10.1002/bbb.155).
- McGee, Thomas D. (1988). *Principles and methods of temperature measurement*. Wiley-Interscience.
- McNair, Harold M., James M. Miller, and Nicholas H. Snow (Sept. 11, 2019). *Basic Gas Chromatography*. WILEY. 284 pp. ISBN: 1119450756.
- Mekonnen, Mesfin M. et al. (2018). "Water, Energy, and Carbon Footprints of Bioethanol from the U.S. and Brazil". In: *Environmental Science & Technology* 52.24, pp. 14508–14518. DOI: [10.1021/acs.est.8b03359](https://doi.org/10.1021/acs.est.8b03359).
- Ministere de la santé (2018). *Strategic response plan for the ebola virus disease outbreak*. Democratic Republic of Congo. World Health Organization.

- Miranda, Jesse Alberto Contreras (2010). "Axial Temperature Gradients in Gas Chromatography". PhD thesis. Brigham Young University.
- Modanlou, H. D. (2008). "A tribute to Zakariya Razi (865 - 925 AD), an Iranian pioneer scholar." In: *Archives of Iranian medicine* 11.6, pp. 673–7. ISSN: 1029-2977.
- Mohankumar, S. and P. Senthilkumar (2017). "Particulate matter formation and its control methodologies for diesel engine: A comprehensive review". In: *Renewable and Sustainable Energy Reviews* 80, pp. 1227–1238. DOI: [10.1016/j.rser.2017.05.133](https://doi.org/10.1016/j.rser.2017.05.133).
- Morris, Hugh (Aug. 16, 2017). "How many planes are there in the world right now?" In: *The Telegraph*.
- Morris, L. J. (1966). "Separations of lipids by silver ion chromatography". In: *Journal of Lipid Research* 7.6, pp. 717–732. eprint: <http://www.jlr.org/content/7/6/717.full.pdf+html>.
- Murphy, Robert E., Mark R. Schure, and Joe P. Foley (Apr. 1998). "Effect of Sampling Rate on Resolution in Comprehensive Two-Dimensional Liquid Chromatography". In: *Analytical Chemistry* 70.8, pp. 1585–1594. DOI: [10.1021/ac971184b](https://doi.org/10.1021/ac971184b).
- Needleman, Herbert L. (Sept. 2000). "The Removal of Lead from Gasoline: Historical and Personal Reflections". In: *Environmental Research* 84.1, pp. 20–35. DOI: [10.1006/enrs.2000.4069](https://doi.org/10.1006/enrs.2000.4069).
- Nič, Miloslav et al., eds. (June 2009). *IUPAC Compendium of Chemical Terminology*. IUPAC. DOI: [10.1351/goldbook](https://doi.org/10.1351/goldbook).
- Nikolova-Damyanova, Boryana (Sept. 10, 2019). *Multiple Interactions in Silver Ion Chromatography of Lipids*. URL: <https://lipidlibrary.aocs.org/lipid-analysis/silver-ion-chromatography-of-lipids/multiple-interactions-in-silver-ion-chromatography-of-lipids>.
- O'Dell, John (June 12, 2000). "Harley-Davidson quits trying to hog sound". In: *Los Angeles Times*.
- Oxford University Press (2019). *Optimization*. In: *Lexico*.
- Pál, Róbert, Miklós Juhász, and Árpád Stumpf (Sept. 1998). "Detailed analysis of hydrocarbon groups in diesel range petroleum fractions with on-line coupled supercritical fluid chromatography–gas chromatography–mass spectrometry". In: *Journal of Chromatography A* 819.1-2, pp. 249–257. DOI: [10.1016/s0021-9673\(98\)00505-6](https://doi.org/10.1016/s0021-9673(98)00505-6).
- Paris Agreement (Dec. 12, 2015). UNTC XXVII 7.d.
- Peacock, Finn (2008). *PID Tuning Blueprint*. URL: <http://www.pidtuning.net>.
- Pearson, Andy (Dec. 2005). "Carbon dioxide—new uses for an old refrigerant". In: *International Journal of Refrigeration* 28.8, pp. 1140–1148. DOI: [10.1016/j.ijrefrig.2005.09.005](https://doi.org/10.1016/j.ijrefrig.2005.09.005).
- Perrenoud, Alexandre Grand-Guillaume, Jean-Luc Veuthey, and Davy Guillarme (Nov. 30, 2012). "Comparison of ultra-high performance supercritical fluid chromatography and ultra-high performance liquid chromatography for the analysis of pharmaceutical compounds". In: *Journal of Chromatography A* 1266, pp. 158–167. DOI: [10.1016/j.chroma.2012.10.005](https://doi.org/10.1016/j.chroma.2012.10.005).
- Petit, J. R. et al. (June 1999). "Climate and atmospheric history of the past 420,000 years from the Vostok ice core, Antarctica". English. In: *Nature* 399.6735. Copyright - Copyright Macmillan Journals Ltd. Jun 3, 1999; Last updated - 2017-10-31; CODEN - NATUAS; SubjectsTermNotLitGenreText - Antarctica, pp. 429–436.
- Pinho, David M. M. et al. (Nov. 2014). "Evaluating the use of EN 14078 for determination of biodiesel in diesel blends sold in the Brazilian market". In: *Fuel* 136, pp. 136–142. DOI: [10.1016/j.fuel.2014.07.043](https://doi.org/10.1016/j.fuel.2014.07.043).

- Pischinger, Rudolf, Stefan Schlag, and Martin Mittelbach (2000). *Chemische und mortechnische Untersuchungen der Ursachen der Einspritzpumpenverklebung bei Biodiesel*. Endbericht zum Forschungsauftrag. Research rep.
- Plata, Vladimir, Paola Gauthier-Maradei, and Viatcheslav Kafarov (Mar. 2015). "Influence of minor components on precipitate formation and filterability of palm oil biodiesel". In: *Fuel* 144, pp. 130–136. DOI: [10.1016/j.fuel.2014.12.043](https://doi.org/10.1016/j.fuel.2014.12.043).
- Poole, Colin F. (2003). "Supercritical Fluid Chromatography". In: *The Essence of Chromatography*. Elsevier, pp. 569–617. DOI: [10.1016/b978-044450198-1/50020-3](https://doi.org/10.1016/b978-044450198-1/50020-3).
- Potgieter, H. et al. (June 2013). "Hyphenation of supercritical fluid chromatography and two-dimensional gas chromatography–mass spectrometry for group type separations". In: *Journal of Chromatography A* 1294, pp. 137–144. DOI: [10.1016/j.chroma.2013.04.020](https://doi.org/10.1016/j.chroma.2013.04.020).
- Ramalakshmi, K. and B. Raghavan (July 1999). "Caffeine in Coffee: Its Removal. Why and How?" In: *Critical Reviews in Food Science and Nutrition* 39.5, pp. 441–456. DOI: [10.1080/1040869991279231](https://doi.org/10.1080/1040869991279231).
- Randall, L. G. (1982). "The Present Status of Dense (Supercritical) Gas Extraction and Dense Gas Chromatography: Impetus for DGC/MS Development". In: *Separation Science and Technology* 17.1, pp. 1–118. ISSN: 0149-6395.
- Rao, K. Bhanu Sankara and B. Raj (2001). "Fatigue Testing: Thermal and Thermomechanical". In: *Encyclopedia of Materials: Science and Technology*. Elsevier, pp. 2999–3001. DOI: [10.1016/b0-08-043152-6/00534-9](https://doi.org/10.1016/b0-08-043152-6/00534-9).
- Raveendran, Poovathinthodiyil, Yutaka Ikushima, and Scott L. Wallen (June 2005). "Polar Attributes of Supercritical Carbon Dioxide". In: *Accounts of Chemical Research* 38.6, pp. 478–485. DOI: [10.1021/ar040082m](https://doi.org/10.1021/ar040082m).
- Reed, Gail L. (Sept. 15, 1999). "Fast GC: applications and theoretical studies". PhD thesis. Virginia Polytechnic.
- Reif, Konrad, ed. (2015). *Gasoline Engine Management*. Springer Fachmedien Wiesbaden. DOI: [10.1007/978-3-658-03964-6](https://doi.org/10.1007/978-3-658-03964-6).
- Restek Corporation (2014). *Restek EZGC Method Translator and Flow Calculator*. Restek Corporation, Bellefonte, PA. URL: <https://www.restek.com/ezgc-mtfc> (visited on 11/20/2019).
- Reumuth, Georg et al. (Aug. 2018). "Carbon monoxide intoxication: What we know". In: *Burns*. DOI: [10.1016/j.burns.2018.07.006](https://doi.org/10.1016/j.burns.2018.07.006).
- Reuters (Nov. 13, 2018). "Spain to propose ban on sale of petrol and diesel cars from 2040". In: *Sunday Times*.
- Ripple, D. C. (1995). *ITS-90 Thermocouple Database, NIST Standard Reference Database 60*. eng. DOI: [10.18434/t4s888](https://doi.org/10.18434/t4s888).
- Robertson, Alan M. et al. (1991). "Research and development topics in Analytical Chemistry". In: *Analytical Proceedings* 28.1, p. 8. DOI: [10.1039/ap9912800008](https://doi.org/10.1039/ap9912800008).
- Rohwer, E. R., V. Pretorius, and G. A. Hulse (Jan. 1986). "Deactivation, coating and performance of nickel capillary columns for GLC". In: *Journal of High Resolution Chromatography* 9.1, pp. 30–34. DOI: [10.1002/jhrc.1240090105](https://doi.org/10.1002/jhrc.1240090105).
- Rosen, William (Mar. 11, 2012). *The Most Powerful Idea in the World: A Story of Steam, Industry, and Invention*. UNIV OF CHICAGO PR. 370 pp. ISBN: 0226726347.
- SABS (1993). CKS 440: Coffins and caskets.
- (2008). *Automotive biodiesel — Fatty Acid Methyl Esters (FAME) for diesel engines — Requirements and test methods*. Standard. South African Bureau of Standards.
- Sandra, P. (May 1989a). "Resolution: Column efficiency". In: *Journal of High Resolution Chromatography* 12.5, pp. 273–277. DOI: [10.1002/jhrc.1240120503](https://doi.org/10.1002/jhrc.1240120503).
- (Feb. 1989b). "Resolution: Definition and nomenclature". In: *Journal of High Resolution Chromatography* 12.2, pp. 82–86. DOI: [10.1002/jhrc.1240120204](https://doi.org/10.1002/jhrc.1240120204).

- Sandra, P. et al. (Oct. 2002). "Characterization of triglycerides in vegetable oils by silver-ion packed-column supercritical fluid chromatography coupled to mass spectroscopy with atmospheric pressure chemical ionization and coordination ion spray". In: *Journal of Chromatography A* 974.1-2, pp. 231–241. DOI: [10.1016/s0021-9673\(02\)01311-0](https://doi.org/10.1016/s0021-9673(02)01311-0).
- Sarowha, S. L. S. et al. (Apr. 22, 2000). "Determination of hydrocarbon group types in middle distillates: A modification proposed for method IP 391/95". In: *Petroleum Science and Technology* 18.9-10, pp. 1089–1106. DOI: [10.1080/10916460008949893](https://doi.org/10.1080/10916460008949893).
- Schönberger, C. and T. Kostelecky (2011). "125th Anniversary Review: The Role of Hops in Brewing". In: *Journal of the Institute of Brewing* 117.3, pp. 259–267. DOI: [10.1002/j.2050-0416.2011.tb00471.x](https://doi.org/10.1002/j.2050-0416.2011.tb00471.x).
- SepSolve Analytical (Mar. 1, 2018). *Reliable speciation of fatty acidmethyl esters (FAMEs) by flow-modulated GC \times GC-TOF MS/FID with Tandem Ionisation*. Tech. rep. SepSolve Analytical Ltd.
- Shabecoff, Philip (June 24, 1988). "Global Warming Has Begun, Expert Tells Senate". In: *New York Times*, p. 1.
- Shamsul, N. S. et al. (May 2014). "An overview on the production of bio-methanol as potential renewable energy". In: *Renewable and Sustainable Energy Reviews* 33, pp. 578–588. DOI: [10.1016/j.rser.2014.02.024](https://doi.org/10.1016/j.rser.2014.02.024).
- Shellie, Robert A., Li-Ling Xie, and Philip J. Marriott (Aug. 2002). "Retention time reproducibility in comprehensive two-dimensional gas chromatography using cryogenic modulation". In: *Journal of Chromatography A* 968.1-2, pp. 161–170. DOI: [10.1016/s0021-9673\(02\)00961-5](https://doi.org/10.1016/s0021-9673(02)00961-5).
- Simkin, Andrew J., Patricia E. López-Calcagno, and Christine A. Raines (Feb. 16, 2019). "Feeding the world: improving photosynthetic efficiency for sustainable crop production". In: *Journal of Experimental Botany* 70.4, pp. 1119–1140. DOI: [10.1093/jxb/ery445](https://doi.org/10.1093/jxb/ery445).
- Skoog, Douglas A., F. James Holler, and Stanley R. Crouch (2007). *Principles of instrumental analysis*. Sixth edition. Belmont, CA: Thomson Brooks/Cole.
- Smeets, Edward et al. (Aug. 1, 2006). *Sustainability of Brazilian bio-ethanol*. Research rep. Universiteit Utrecht, Copernicus Institute, Department of Science, Technology and Society.
- Smit, Elize (June 1, 2015). "High resolution mass spectrometry and other methods for diesel and surface chemical analysis to investigate the tribology in automotive fuel injection systems." University of Pretoria.
- Smith, David Abbott (Sept. 3, 2002). "Surface modification of solid supports through the thermal decomposition and functionalization of silanes." US 6,444,326 B1.
- Smith, Roger M. and Simon Cocks (1994). "Separation of saturated and unsaturated fatty acid methyl esters by supercritical fluid chromatography on a silica column". In: *The Analyst* 119.5, p. 921. DOI: [10.1039/an9941900921](https://doi.org/10.1039/an9941900921).
- Smith, Roger M., Minna Hytylänen, et al. (2001). "High resolution packed column supercritical fluid chromatography of fatty acid methyl esters". In: *Journal of Separation Science* 24, pp. 208–212. DOI: [https://doi.org/10.1002/1615-9314\(20010301\)24:3%3C208::AID-JSSC208%3E3.0.CO;2-P](https://doi.org/10.1002/1615-9314(20010301)24:3%3C208::AID-JSSC208%3E3.0.CO;2-P).
- South Africa's Intended Nationally Determined Contribution (INDC)* (Nov. 1, 2016). English. UNFCCC.
- South African Government (1977). *Petroleum Products Act, 1977 (Act No. 120 of 1977)*. — (2008). *Standards Act 2008*.
- Souza, Carolina Vieira de and Sergio Machado Corrêa (Dec. 2016). "Polycyclic aromatic hydrocarbons in diesel emission, diesel fuel and lubricant oil". In: *Fuel* 185, pp. 925–931. DOI: [10.1016/j.fuel.2016.08.054](https://doi.org/10.1016/j.fuel.2016.08.054).

- Spur, G., E. Uhlmann, and F. Elbing (Dec. 1999). "Dry-ice blasting for cleaning: process, optimization and application". In: *Wear* 233-235, pp. 402–411. DOI: [10.1016/s0043-1648\(99\)00204-5](https://doi.org/10.1016/s0043-1648(99)00204-5).
- Strauch, Barry (Oct. 2018). "Ironies of Automation: Still Unresolved After All These Years". In: *IEEE Transactions on Human-Machine Systems* 48.5, pp. 419–433. DOI: [10.1109/thms.2017.2732506](https://doi.org/10.1109/thms.2017.2732506).
- Szreter, Simon (Mar. 2003). "The population health approach in historical perspective". In: *American journal of public health* 93.12604486, pp. 421–431. ISSN: 1541-0048.
- Taylor, Larry T. (Nov. 1, 2013). "Analytical Supercritical Fluid Extraction Goes Back to the Future". In: *LCGC* 31 (11). ISSN: 1527-5949.
- Van der Walt, A. N. and F. J. C. Hugo (Jan. 1982). "Attempts to prevent injector coking with sunflower oil by engine modifications and fuel additives". In: *PROCEEDINGS OF THE INTERNATIONAL CONFERENCE ON PLANT AND VEGETABLE OILS AS FUELS, ASAE (VEGETABLE OIL FUELS)*.
- Van Niekerk, P. S. (1980). *Doenlikheidstudie ; die gebruik van sonneblomolie as plaasvervanger vir diesel in die R S A*. Die outeur.
- Varma, Roli and Daya R. Varma (Feb. 2005). "The Bhopal Disaster of 1984". In: *Bulletin of Science, Technology & Society* 25.1, pp. 37–45. DOI: [10.1177/0270467604273822](https://doi.org/10.1177/0270467604273822).
- Velasco, J., C. Dobarganes, and G. Márquez-Ruiz (2010). "Oxidative rancidity in foods and food quality". In: *Chemical deterioration and physical instability of food and beverages*. Elsevier.
- Venter, A., E. R. Rohwer, and A. E. Laubscher (June 1999). "Analysis of alkane, alkene, aromatic and oxygenated groups in petrochemical mixtures by supercritical fluid chromatography on silica gel". In: *Journal of Chromatography A* 847.1-2, pp. 309–321. DOI: [10.1016/s0021-9673\(99\)00137-5](https://doi.org/10.1016/s0021-9673(99)00137-5).
- Venter, Andre (2003). "Comprehensive two-dimensional supercritical fluid and gas chromatography (SFC×GC)". PhD thesis. University of Pretoria.
- Venter, Andre, Peter R. Makgwane, and Egmont R. Rohwer (Mar. 2006). "Group-type analysis of oxygenated compounds with a silica gel porous layer open tubular column and comprehensive two-dimensional supercritical fluid and gas chromatography." In: *Analytical chemistry* 78.6, pp. 2051–4. ISSN: 0003-2700. DOI: [10.1021/ac051693a](https://doi.org/10.1021/ac051693a).
- Venter, Andre and Egmont R. Rohwer (July 2004). "Comprehensive two-dimensional supercritical fluid and gas chromatography with independent fast programmed heating of the gas chromatographic column." In: *Analytical chemistry* 76.13, pp. 3699–706. ISSN: 0003-2700. DOI: [10.1021/ac035538c](https://doi.org/10.1021/ac035538c).
- Venter, Irma (Oct. 29, 2014). "Renewable energy project set to power BMW's Rosslyn plant". In: *Engineering News*.
- Vincenti, Walter G. (1990). *What engineers know and how they know it : analytical studies from aeronautical history*. English. Baltimore: Johns Hopkins University Press.
- Wang, Anzi, H. Dennis Tolley, and Milton L. Lee (2012). "Gas chromatography using resistive heating technology". In: *Journal of Chromatography A* 1261, pp. 46–57.
- Wang, Z. (2008). "Oil Fingerprinting and Spill Source Identification". In: *NATO Science for Peace and Security Series C: Environmental Security*. Springer Netherlands, pp. 191–192. DOI: [10.1007/978-1-4020-8565-9_23](https://doi.org/10.1007/978-1-4020-8565-9_23).
- Watrus, M. C. et al. (Sept. 1, 2016). "An evaluation of fuels and retrofit diesel particulate filters to reduce diesel particulate matter emissions in an underground mine". In: *MVSSA Annual Conference 2016: Increasing the relevance of the Mine Ventilation Profession*.

- Watts, Steven (2005). *The People's Tycoon: Henry Ford and the American Century*. Knopf. ISBN: 978-0-375-40735-2.
- Wells, P. S., S. Zhou, and J. F. Parcher (Jan. 2003). "Unified Chromatography with CO₂-Based Binary Mobile Phases". In: *Analytical Chemistry* 75.1, 18 A–24 A. DOI: 10.1021/ac031212s.
- Wentz, Dennis A. et al. (2014). *Mercury in the nation's streams - Levels, trends, and implications. U.S. Geological Survey Circular 1395*. Tech. rep. DOI: 10.3133/cir1395.
- Williams, William Henry. (1965). *The Commons, Open Spaces & Footpaths Preservation Society, 1865-1965 : a short history of the society and its work*. English. [London]: [The Society]. ISBN: 978-0-375-40735-2.
- Wolfram|Alpha (2019a). URL: <https://www.wolframalpha.com/input/?i=otto+cycle> (visited on 07/09/2019).
- (2019b). URL: <https://www.wolframalpha.com/input/?i=diesel+cycle> (visited on 07/09/2019).
- (2019c). URL: <https://www.wolframalpha.com/input/?i=brayton+cycle> (visited on 07/09/2019).
- (2019d). URL: <https://www.wolframalpha.com/input/?i=carbon%20dioxide%20phase%20diagram> (visited on 07/09/2019).
- Woodall, L. C. et al. (Dec. 2014). "The deep sea is a major sink for microplastic debris". In: *Royal Society Open Science* 1.4, pp. 140317–140317. DOI: 10.1098/rsos.140317.
- World Resource Institute (2004). *The Greenhouse Gas Protocol: A Corporate Accounting and Reporting Standard*. World Resources Inst. ISBN: 1-56973-568-9.
- Worldwide Fuel Charter Committee (2009). *Biodiesel guidelines*. Worldwide Fuel Charter Committee.
- Wright, J. (Sept. 2002). "Chronic and occult carbon monoxide poisoning: we don't know what we're missing". In: *Emergency Medicine Journal* 19.5, pp. 386–390. DOI: 10.1136/emj.19.5.386.
- Xu, Ming et al. (June 2010). "Gigaton Problems Need Gigaton Solutions". In: *Environmental Science & Technology* 44.11, pp. 4037–4041. DOI: 10.1021/es903306e.
- Young, I. S. and J. McEneny (May 2001). "Lipoprotein oxidation and atherosclerosis". In: *Biochemical Society Transactions* 29.2, pp. 358–362. DOI: 10.1042/bst0290358.